THE INFLUENCE OF WATER CIRCULATION PATTERNS IN BASS STRAIT ON RECRUITMENT SUCCESS AND STOCK DIFFERENCES IN SCALLOPS

FINAL REPORT TO FRDC COMMITTEE
ON PROJECT 87/117

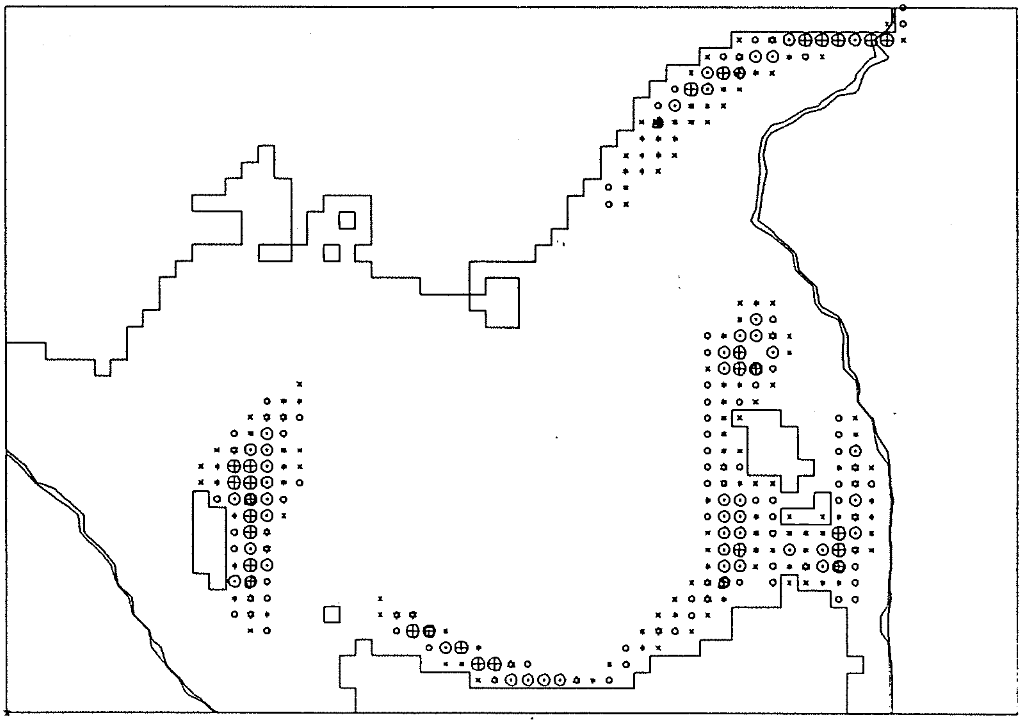

L.S. Hammond, K.P. Black, G.P. Jenkins and R.S. Hodgkinson

VICTORIAN INSTITUTE OF MARINE SCIENCES

October, 1994

EXECUTIVE SUMMARY

Management of the Bass Strait scallop fishery hitherto has assumed no relationship between stock and recruitment and, therefore, that fished populations could be replenished by low numbers of individuals spawning in distant areas from which water currents would supply larvae. Thus, a relatively high connectedness between Bass Strait scallop beds was assumed.

Recruitment failure in the Bass Strait fishery in recent years and in other scallop fisheries under this type of management regime has led to proposals that scallop beds may be self-sustaining entities with little transfer of propagules to other beds. If so, the replenishment of an individual bed will be highly dependent on the spawning stock remaining in the bed. The relative degree of self-seeding versus cross-seeding of scallop beds is critical to management of the resource.

A numerical model of Bass Strait circulation was used to simulate larval dispersal over periods of 14 to 28 days, assuming continuous reproduction, between September and March of 1985/86, 1986/87 and 1987/88. Simulations were run separately for eight beds which were extant in the mid 1980s, and also for these beds together with historical beds (those known to have been fished before the 1980s). The numerical hydrodynamic model provided good spatial resolution of currents throughout Bass Strait. Calibrated by data from field studies and particular weather events, and interfaced with a larval dispersal model, it provided a means to quantify the potential for self-seeding of scallop beds around Bass Strait. The model was vertically averaged due to a lack of information on vertical distribution of scallop larvae and vertical stratification of the water column.

The major finding of the study was that, for extant scallop beds, self-seeding at most sites was common whilst cross-seeding was rare. Cross-seeding was more common when historical beds were included, because the density of beds in the Strait was higher, corresponding to less distance between beds. The orientation of the historical beds appears related to the dominant flow directions and recruitment to them is a mixture of self- and cross-seeding. As the number of viable scallop beds is reduced by overfishing the importance of self-seeding versus cross-seeding increases.

Few larvae were lost from the Bass Strait system through transport into deeper, off-shelf water, but many were dispersed to areas where scallop beds have not previously been known to exist, and where hydrodynamic conditions or benthic substrates may not be suitable for settlement.

Certain beds showed greater tendency to cross-seeding because another bed was relatively close-by and prevailing currents tended to carry larvae from this point. Cross-seeding in these situations was essentially one-way. There also were interannual differences, with calmer conditions in 1985/86 resulting in greater self-seeding compared with subsequent years.

The pattern of larval dispersal varied greatly depending on the climatic conditions at the time of larval release. Further information on the periodicity of spawning, environmental cues for spawning, and the subsequent vertical distribution of larvae in the water column, would improve the accuracy of model predictions. The major conclusion that scallop beds are primarily self-seeding, however, would be unlikely to change.

The primary relevance of the findings to fishery managers is that traditional views on the dynamics of scallop fisheries are probably wrong. Independence of stock and recruitment cannot be assumed and there should not be a reliance on colonisation and recruitment from other areas to re-populate overfished beds. Management should treat widely separated scallop beds as individual stocks and ensure that an adequate spawning stock remains after fishing. In the past, fishing practices have tended to cause a large mortality induced by gear damage and have removed large numbers of scallops before reproduction had occurred. Future management of scallop stocks must take into account the closed dynamics of scallop populations and regulate accordingly.

TABLE OF CONTENTS

APPENDICES

LIST OF TABLES

LIST OF FIGURES

CHAPTER 1: INTRODUCTION

1.1 PROJECT DEFINITION AND AIMS

Declining catches in the Bass Strait scallop fishery in the 1980's raised concerns about its sustainability. Management of the fishery apparently, was based on assumptions of no relationship between stock and recruitment, whereby fished populations could be replenished by low numbers of individuals spawning in areas from which water currents would supply larvae. Thus a relatively high connectedness between Bass Strait scallop beds was assumed. However, an alternative view, supported by research on other scallop fisheries, is that scallop beds may be self-sustaining entities with little transfer of propogules to other beds. The replenishment of an individual bed will be highly dependent on the spawning stock remaining in the bed. The question of the degree of self-seeding versus cross-seeding of scallop beds is a critical one to the management of this resource.

Research done at the Victorian Institute of Marine Sciences (VIMS) during the 1980's to develop numerical hydrodynamic models of Bass Strait provides a powerful tool to address this biological question, by analysing the dispersal of scallop larvae under a variety of climatic and environmental conditions, times of spawning, locations of spawning, and durations of larval life. Modelling can define the scope for retention of larvae within the parent beds, transport between beds or from beds to unsuitable areas elsewhere within or outside Bass Strait.

Using numerical modelling techniques, this study aimed to provide insight into stock relationships and recruitment success by:

a) defining conditions (spawning times, locations, weather, tides etc.) that facilitate dispersal of larvae between existing commercial beds;

b) defining conditions under which existing beds may be self-seeding, providing their own recruits; and,

c) defining conditions under which scallop larvae are transported out of Bass Strait or to areas in Bass Strait unsuitable for establishment of scallop beds.

1.2 SCALLOP FISHERY IN BASS STRAIT

The Bass Strait fishery was once among the largest non-crustacean fisheries in Australia. The fishery started in 1970 when large concentrations of the commercial scallop, *Pecten fumatus*, were located for the first time in Bass Strait off Lakes Entrance in eastern Victoria (Fig. 1.1) (Young, 1994). Further discoveries of beds throughout the Strait and off Tasmania stimulated a rapid increase in fishing with highest landings occurring in 1982-83 (Fig. 1.2). By 1985-86, however, the numbers declined and southern Bass Strait was closed to fishing in 1987.

Martin *et al.*, (1989) concluded that there had been widespread recruitment failure following the 1985-87 spawning seasons and as a result, commercial scallop stocks in Bass Strait were at an extremely low level. Surveys have since shown no significant recruitment to the Bass Strait region (McLoughlin *et al.*, 1988; Zacharin, 1990). The situation in Bass Strait may be linked to current fishing practices which target areas of high scallop density and harvest scallops before or during the spawning season. While this practice results in higher meat yields it also effectively eliminates the reproductive contribution of whole year classes by taking scallops before they spawn. The direct mortality due to fishing is apparently exacerbated by mortality due to dredge-induced damage and viral infection related to large numbers of decomposing scallops left on the beds (Young, 1994). It may also reduce the populations of scallops to densities below that required for successful spawning. A study conducted by Zacharin (1991) reported little scallop spat settlement. He suggested that the Tasmanian scallop stocks had been overfished to a level at which reproduction and the likelihood of recruitment were severely depressed.

The high recruitment variability observed in the *Pecten* scallops of Bass Strait, and the general depletion of scallop beds is common throughout south-eastern Australia. The marked interannual variability in catches in Bass Strait has been linked to the sequential discovery and exploitation of new beds, and recruitment failure on previously fished beds (Young *et al.* 1992). Scallop fisheries throughout the world similarly show major fluctuations in recruitment and commercial catches from year to year. These fluctuations have been described as erratic and unrelated to stock size (Hancock, 1973, 1979), and management has been based on assumptions of a negligible relationship between stock and recruitment and significant replenishment from low stock levels (Young, 1994).

Recently, evidence has begun to accumulate which contradicts the assumption of independence of recruitment from parental stocks. Sinclair *et al.* (1985) examined historical fishery data on the scallops, *P. magellanicus*, *P. maximus*, and *Chlamys opercularis* and suggested that widely separated beds of scallops had characteristic abundances in precise geographical locations, strongly implying that the aggregations were self-sustaining. These may be related to hydrodynamic factors as many populations are coincident with tidally induced physical-oceanographic features such as gyres and two-layered circulation (Young, 1994).

The Bass Strait fishery was characterised by similar isolated, high-density beds. If their existence is linked to the types of factors described by Sinclair *et al.* (1985), the impact of the fishery on these beds may have been primarily one of reducing stock density to non-sustaining levels. The possibility that recruitment is dependent on stock size and that local populations are self seeding would imply that the management of scallop stocks must include conservation of some spawning stock at high densities (Caddy, 1989; Young and Martin, 1989).

This self-sustaining hypothesis may be tested by assessing the likelihood of self-seeding to the natal bed. The project to be described below uses numerical modelling to address this fundamental question.

1.3 · REPRODUCTIVE BIOLOGY OF SCALLOPS IN BASS STRAIT

Information on reproduction of Bass Strait scallops has been reviewed most recently by Young (1994). The exact spawning time of scallops is variable; *P. fumatus* individuals mature in their second year of life and gonad indices indicate the spawning period is protracted, extending from mid-winter to late Autumn, with strong geographic variation. Spat collections confirm this pattern, but major spatfalls often occur over limited periods and the timing of such settlement events shows significant geographic variation. A correlation between numbers of settling spat and local catch-rates of adults adds to the suggestion that larvae may not disperse widely.

The fertilized eggs of *P. meridionalis* (synonymous with *P.alba* and *P.fumatus* (Woodburn, 1988)) developed through the trochophore stage to straight-hinged veligers after three days (Dix and Sjardin 1975). Metamorphosing larvae were observed in cultures after 31 days when reared at a temperature between 13-15°C. The pediveliger stage, when larvae begin searching the substrate for a suitable settlement area, was reached approximately mid-way through this period (Dix and Sjardin 1975).

Nothing is known of the vertical distribution, swimming ability and behaviour of larval *P. fumatus*. Diurnal variation, with more larvae near the surface by night than by day, has been suggested for *P. maximus* (Kaartveldt *et al.* 1987). Cragg (1980) suggests that early larvae of *P. maximus* swim near the surface but later larvae become gradually more associated with the substrate. The finding that spat in Bass Strait were most numerous on deeper collectors in the earlier part of the settlement season (Young *et al.* 1992) may be consistent with close association with the substrate in the late larval stage; however, spat falls later in the season showed no pattern with depth (Young *et al.* 1992). It is possible that vertical variation in spat distribution is simply related to vertical variation in current strength and turbulence of water carrying the larvae.

1.4 INPUTS TO MODELLING

This project considered the potential dispersal of larvae from historical and extant scallop beds in Bass Strait over a spawning period of September to March in three consecutive years, 1985/86 to 1987/88 inclusive. The larval period was set between 2 and 4 weeks, taking into account the beginning of searching for suitable substrate once the pediveliger stage is reached and variation in larval duration due to temperature. In the mid-1980s, currents in the Strait at the relevant larval dispersal time scales of 2-4 weeks between October and April, when the larvae were in the plankton, were unknown. Instead, well calibrated and validated numerical models of Bass Strait (e.g. Black *et al.*, 1990; Black, 1992c; Middleton and Black, 1994) were used to infer the state of water currents.

The numerical hydrodynamic model provides good spatial resolution of currents throughout the Strait and accepts measured inputs (e.g. tides, currents) and particular weather events. Together with a larval dispersal model, it provides the means to quantify the potential for self-seeding and the connectedness of scallop beds around Bass Strait. Rather than adopting a schematic approach, three particular spawning seasons were modelled and actual dispersal distances were then identified for a wide range of weather conditions.

There were some limitations in the knowledge at the time of the study, some of which still remain. In particular, no information about vertical distribution of the larvae in the water column was available. In the absence of data defining the vertical distribution of larvae, the present study treats the larvae as vertically well-mixed and neutrally buoyant. Consequently, the results are relevant to any organism whose larvae have these characteristics. Though focussing on scallops in this study, the model simulations depict typical excursions throughout

Bass Strait over 2-4 week periods of any pollutant, larva or other material which is neutrally-buoyant.

Since completing this study, a parallel research program conducted by Dr John Middleton (University of New South Wales, Mathematics Department) in collaboration with K.P. Black has numerically and analytically treated the passage of coastal-trapped waves through Bass Strait. These oscillations with typically 10-14 day periods are responsible for low-frequency currents which simultaneously act throughout the Strait and up the New South Wales coast (Middleton and Black, 1994; Appendix 1). When the scallop study was undertaken, the methods to incorporate coastal-trapped waves in the model had not been completed and so these oscillations have been neglected. While this remains a deficiency in the modelling presented here, given that instantaneous currents may be significant (around 10 $cm.s^{-1}$), the net circulation due to coastal-trapped waves within Bass Strait is relatively small and the effect on scallop larval excursions over 14-28 day periods may be similarly small. However, any future studies of larval dispersal in Bass Strait should incorporate these currents.

The model had been fully calibrated for tidal currents but, due to the very short periods of the tides (12-24 hours) relative to the long pelagic period of the scallops (14-28 days), the tidal influence is relatively unimportant, particularly as the residual tidal circulation within the Strait is very small.

Because the spawning period of *P. fumatus* is protracted and episodic, a long (7-month) spawning period was simulated to indicate the potential excursions before, during and after the most likely spawning times.

For completeness, both the "extant" and "historical" scallop beds in Bass Strait during the mid 1980's were considered.

1.5 NUMERICAL MODELLING

Advection and diffusion of water bodies has been well studied theoretically (e.g. Joseph and Sendner, 1958; Monin and Yaglom, 1971; Okubo, 1971; Talbot and Talbot, 1974; Bowden, 1983). However, in complex environments where the bathymetry is variable and the currents are non-stationary, numerical techniques are needed to treat the advection and dispersal of water-borne material satisfactorily.

In the design of the program, we considered the need to concentrate on the likely dispersal ranges over Bass Strait as no previous study had determined the natural excursion distances. Thus, we needed to consider the regional dispersal, including the possible "losses" of larvae off the edge of the continental shelf. The study uses two distinctly different categories of model: the water flow (hydrodynamic) model and the dispersal (advection/diffusion) model. Relevant numerical hydrodynamic models at the Victorian Institute of Marine Sciences are:

- South-east Australian Model of Bass Strait.
- Central Victorian Model of Port Phillip/Western Port Bay and adjacent Bass Strait.
- Fine-scale models within Port Phillip Bay.

In this study, we used the south-east Australian hydrodynamic model of Bass Strait and environs. While the hydrodynamic model has the capacity to simulate density-stratified circulation, a lack of input data prevented such an undertaking. This level of modelling, however, may be warranted in future studies if the vertical distribution of the larvae is better understood.

1.5.1 Model Code Selection

For this project, we chose the hydrodynamic model 3DD, a coupled 3-dimensional hydrodynamic and advection/diffusion numerical model (Black, 1983; 1992a). The code is general and has been applied to vertically-stratified and homogeneous ocean, continental shelf and shallow water environments. It contains a Eulerian scheme hydrodynamic model coupled with both a Eulerian and a Lagrangian advection/diffusion scheme. The Lagrangian model is very useful in cases with sharp density interfaces which occur around a freshwater or hot water outfall.

The model equations are given in Appendix 2, while a general description of the output and features of the model is given in Appendix 3. Model support software is presented in Appendix 4. The particle advection scheme is described in Appendix 5. The operation of the model is presented in the 3DD User's Guide (Black, 1992a).

1.6 STRUCTURE OF THE REPORT

This report describes the local and regional circulation in Chapter 2. The models are defined and calibrated in Chapters 3 and larval dispersal results are presented in Chapter 4. Discussion and conclusions are presented in Chapter 5. Background to the techniques, models and methods is presented in the Appendices.

1.7 ACKNOWLEDGMENTS

Peter Young, Dick Martin and Richard O'Loughlin of the CSIRO Fisheries Division and Chris Fandry of the CSIRO Oceanography Division, and David Gwyther of Dames & Moore are thanked for their advice during the program.

CHAPTER 2: REGIONAL CIRCULATION

2.1 UNDERSTANDING THE REGIONAL CIRCULATION

To successfully model a region, the forces responsible for the currents need to be known in order to properly set the boundary conditions. Prior studies made this task easier (e.g. Black *et al.*, 1993; Middleton and Black, 1994). The region is characterised by complex circulation patterns modified by the two entrances to the Strait.

2.1.1 Tidal

The tidal current component of the circulation in Bass Strait is shown in Figs. 2.1a-e for the 5 largest tidal constituents. The Bass Strait model tidal calibration for these constituents is shown in Figs. 2.2a-e and 2.3a-e. For the semi-diurnal constituents, the currents are fastest in the two entrances to the Strait. These fast streams meet in the central Strait where the current intensities diminish. Black (1992c) showed that when the surficial sediment grain sizes in Bass Strait were compared to the calibrated numerical model of the M_2 tidal circulation, this grain size variation was found to correspond with tidal current intensity. In particular, a correspondence between the sediment entrainment threshold velocity and the maximum tidal current was observed. The results demonstrate that current strength is the dominant factor determining the nature of the modern sea bed throughout Bass Strait. Wave processes become successively more important as the depth decreases.

The net tidal currents in Bass Strait are small except near the entrances to the major bays. In Central Victoria, the local tidal dynamics are elaborately influenced by the two large bays, Port Phillip and Western Port (Fig 2.4a). The model depicts a classical ebb-tidal jet structure in the net circulation patterns (Fig. 2.4b). The jet is bounded by two counter-rotating eddies with the strongest occurring to the left of the jet due to the Coriolis force. The jet is also deflected to the left. A second clockwise-rotating residual cell is evident off Cape Schanck, with residual currents as large as 10 $cm.s^{-1}$ (Fig. 2.4b).

While the tidal currents are fast in the Strait and near the entrances to the Bays, the net tidal circulation in open water where the scallop beds are found is relatively small. Consequently, the tides are expected to have very little influence on the net long-term (14-28 day) pelagic dispersal of the larvae throughout the deeper exposed sections of the Strait. This is contrary to findings on the continental shelf of Queensland, where tidal currents play a very significant role around the more complex topography of the reef matrix (e.g. Black, 1993). For the Bass Strait modelling of scallop larval dispersal, the tidal currents were neglected.

2.1.2 Wind-driven (locally-forced)

Winds along the Victorian coast and throughout Bass Strait are spatially highly variable. Thus, to successfully model the region, the spatial wind variability needs to be included in the model. To attempt to incorporate this variability, winds from Currie, Eddystone Point and Kingfish B (Fig. 2.5) were utilised.

In addition, the wind roses for the chosen sites vary significantly from month to month and between the years (Fig. 2.6a-i). For this reason, three different years, 1985/86 to 1987/88, were modelled to enable a broader range of conditions to be treated. However, the results still remain indicative only of likely excursions.

2.1.3 Remotely-forced Coastal-trapped Waves

Residual water level oscillations due to coastal-trapped waves and coastal surge with a range of approximately 0.3 m characterise the non-tidal sea levels at Portland outside the western entrance to Bass Strait (Fig. 2.7). These waves perturb the waters of Bass Strait and continue through the Strait up the New South Wales coast and therefore should be represented in the model (Middleton and Black, 1994).

The Bass Strait model depicts this important non-tidal circulation throughout Bass Strait, and around much of Tasmania and the New South Wales Coast. As an example, Fig. 2.8a-d shows the currents at 00:00 hours on March 16-19, 1992 inclusive. Circulation patterns are complex, and spatially and temporally variable. For example, the figures show a large-scale eddy migrating across central Bass Strait, while currents change in intensity and direction west of Cape Otway during the 4-day period.

On March 19, 1992 (Fig. 2.8d), the currents moving up the western Tasmanian coast bifurcate around King Island to travel west on the Portland continental shelf and east through Bass Strait. At this time, the currents near Central Victoria and east of Cape Otway are slow between the bifurcation. The orientation of the Victorian coastline changes from 135°T between Cape Otway and Port Phillip Bay, to around 225°T along the eastern central Victorian coast. These changes in coastal orientation and the large-scale "sheltering" provided by Cape Otway and Wilson's Promontory strongly affect the regional circulation patterns with the result that the currents around Central Victoria are modified by the regional morphology.

When the scallop larval dispersal study was initiated, the coastal-trapped wave modelling techniques had not been developed and so coastal-trapped waves were not included.

2.1.4 Inertial Oscillations

Sharp changes in the wind or any other sudden relaxation in forcing can cause inertial current oscillations to develop. The inertial period T is dependent on latitude,

$$T = 2\pi / f$$

where f is the Coriolis parameter. For latitude 38°S, the inertial period is 19.4 hours. The Fourier spectrum of currents measured on the central Victorian coast indicate very little energy at this period. Thus, inertial oscillations are relatively unimportant and, as the period is short relative to the dispersal period of the scallops, they may be neglected.

2.1.5 Density-driven Circulation and Stratification

Density structure in Bass Strait varies between winter and summer (Baines and Fandry, 1983) with strongest stratification occurring during the spring and summer. Sea temperature is primarily determined by the level of incident solar radiation, total water depth, advection and mixing. Black *et al.* (in press) recorded significant natural temperature stratification at sites in eastern Bass Strait in the East Gippsland region (Fig. 2.9). The stratification was eliminated every 10-14 days with the arrival of strong storm winds. Similarly, thermal stratification has been recorded in nearby Port Phillip Bay (e.g. Rosenberg *et al.*, 1992; Black *et al.*, 1993).

Stratification may substantially alter the local dynamics, particularly in the upper part of the water column. Unfortunately, no measurements of the density structure across Bass Strait are available so the stratification could not be simulated. However, in view of the lack of information about the vertical distribution of scallop larvae in the water column, the hydrodynamic approximation of a vertically homogeneous water body remains the most appropriate.

CHAPTER 3: ESTABLISHING THE MODEL

3.1 MODEL GRID, BATHYMETRY AND BOUNDARY CONDITIONS

The model grid used in this study had a grid-cell resolution of 10 km and a regional extent shown in Fig. 3.1. Depths for the Bass Strait model were taken from the detailed NATMAP charts which map Australia's continental shelf. These were digitised at VIMS at a 5 minute resolution and interpolated to form the 10,000 m Bass Strait grid of 83 by 116 cells.

The model boundaries were clamped to zero sea level with a sponge to absorb outgoing waves. The boundaries were mostly in deep water and this condition proved to be very reliable and gave the model long-term stability. More recent simulations (Middleton and Black, 1994) have confirmed the robustness of this condition. The model was driven by wind only.

3.2 MODEL CALIBRATION

An example of the model calibration in eastern Bass Strait is shown in Fig. 3.2. The model currents are being compared to the measured non-tidal currents. The measurements include all components, and the good comparison with the model suggests that the wind has a dominant influence in this region. The model was less skilful in western Bass Strait where coastal-trapped waves are relatively more important. However, the model is expected to be effectively predicting the wind-driven circulation (Black *et al.*, 1990), which is the dominant factor causing net advection of larvae in the Strait.

3.3 MODEL SIMULATIONS AND OUTPUT

Three 7-month periods were simulated. These were 1985/86, 1986/87 and 1987/88 over the period from the beginning of September to the end of March. The model output is presented as excursions and integrated abundances. The "larvae" are treated as single "particles" released at selected sites in the dispersal model. The advection of the particles is determined by the currents hindcast using the hydrodynamic model. Horizontal diffusion was neglected.

The excursion diagrams (Figs. 4.1a - 4.4x) show the locations of the larvae at daily intervals in the 14-28 period after a single release at a selected time and at multiple sites. Integrated abundance diagrams show the accumulated numbers of visits by larvae (particles) in each model cell over prescribed time intervals. Larvae were typically released daily and their positions 14-28 days after release were recorded. Both the modern scallop beds (Figs. 4.1a - 4.3x) and the historical sites (Figs. 4.4a-x) were considered in separate sets of simulations.

CHAPTER 4: SCALLOP LARVAL DISPERSAL

4.1 LARVAL EXCURSIONS

4.1.1 Modern Beds

Larval excursions for releases at the 8 extant scallop beds at 1-week intervals are shown for the three periods simulated in Figs. 4.1a-x for 1985/86, Figs. 4.2a-x for 1986/87 and Figs. 4.3a-x for 1987/88. In each case, the large crossed circle shows the release point and the straight line shows the excursion over the first non-viable 14 days. The small circles then show the positions at daily intervals in the 14-28 day interval, while the star shows the final position at the end of the 28 day pelagic period.

The results are characterised by both spatial and temporal variability. Fig. 4.1a, for example, shows a case when the larvae remained very close to the initial release point at the end of the 14 day non-viable period. This occurred at all sites across Bass Strait in response to a period of universally light winds. This means that competent larvae could have settled on the natal site after 14 days. The excursions were much bigger in the full 28 day period.

Fig. 4.1j shows a similar result except that the initial excursions over the first 14 day period were relatively large on the East Gippsland and northern Tasmanian coasts while remaining excursions were small near King and Flinders Island. A wind reversal in the 14-28 day period brought the larvae back towards the natal beds.

Fig. 4.1m is an example where initial excursions were very large in the first 14 days. Excursions of up to 90 km were achieved along the East Gippsland and northern Tasmanian coasts. Larvae near King Island were washed out of the Strait onto the western Tasmanian continental shelf. However, excursions north of Flinders Island remained small, even though currents were fast elsewhere.

Fig. 4.1o shows the case of westerly winds which carry the larvae to the east. In this case, the larvae in the lee of King Island and to the north of Flinders Island remain near the natal bed. Once again, the larvae move furthest along the Gippsland coast. Self-seeding occurs during the 14-28 day period at 7 of the 8 release sites.

Figs. 4.1u and 4.1v show additional cases of relatively high self-seeding. The sites most prone to self-seeding appear to be those around King and Flinders Island and the site on the north-west coast of Tasmania.

Similar variability was obtained for the other years. For example, Fig. 4.2a shows relatively large excursions of up to 100 km on the Gippsland coast, while Fig. 4.2b exhibits a high level of self-seeding. Fig. 4.2e is interesting because it exhibits self-seeding as well as wide-ranging dispersal over the 14-28 day period.

Fig. 4.2g shows a general northerly drift of the particles. Cross-seeding of the sites on the east of King Island is evident, and larvae from the north-east of Tasmania move towards the north of Flinders Island. Excursions in East Gippsland remain large with larvae moving onto the southern New South Wales coast. Fig. 4.2i shows another example of cross-seeding of the King Island sites. Due to current steering by the coast in East Gippsland, cross-seeding of the two release sites is relatively common (e.g. Figs. 4.2k and 4.2q).

In 1987/88, Figs. 4.3b and 4.3c show cross-seeding around King and Flinders Island when currents are directed north. Fig. 4.3d shows both self-seeding and cross-seeding on the east of King Island.

4.1.2 Historical Beds

Releases from the historical beds are depicted for the 1986/87 season in Figs. 4.4a-x. The patterns remain similar with the same tendency for self-seeding. However, with the higher density of beds, cross-seeding becomes far more common. Indeed, the beds appear to be mostly aligned along the dominant flow directions, with the result that cross-seeding is relatively likely (e.g. Fig. 4.4d, 4.4e and 4.4f). Self-seeding is also common (Fig. 4.4k and 4.4o). The results suggest that the orientation of the historical beds are determined by dominant flow directions, and that the recruitment to the beds is a mixture of self- and cross-seeding.

4.1.3 Source Locations

To examine the source of larvae which recruited on the modern beds, reverse larval tracking was undertaken. In this procedure, the larvae are released on the modern beds, and then tracked backwards in time to determine where they would have come from in order to reach the bed in question. A selection of cases from the three seasons are shown in Figs. 4.5a-l.

Figs. 4.5a and 4.5b show a mixtures of self-seeding and cross-seeding sites. Fig. 4.5c interestingly shows the source of larvae on the north-east Tasmanian coast as coming from the west side of Flinders Island. Fig. 4.5g shows larvae on the east side of King Island coming from the continental shelf off western Tasmania. Cross-seeding is also evident off King Island. The largest excursion is seen in Fig. 4.5j which shows larvae for the East Gippsland region coming from as far south as Wilsons Promontory. A poor recruitment at most of the sites should have resulted if spawning coincided with this period.

In Fig. 4.5k, the larvae appear to have come from distant and natal sites.

4.1.4 Integrated Larval Abundances

Integrated larval abundances are shown in Figs. 4.6a-r at monthly intervals. These show the abundances in 1-month periods with larvae being released every 40 minutes and tracked for 28 days. Their positions are noted in each model cell 14-28 days after release, and the total numbers in each cell are accumulated. The integrated abundances show the cells which receive the most/least visits by viable larvae.

In general, the integrated "clouds" centre on the release sites which coincide with the modern beds (Fig. 4.6a and 4.6g). Fig. 4.6b shows larvae spreading uniformly around the east side of

King Island, the north of Flinders Island and along much of the Gippsland and north-east Tasmanian coasts. This pattern is relatively common (e.g. Figs. 4.6c, 4.6d and 4.6e). As noted above, cross-seeding is common along the Gippsland coast and near King Island (e.g. Fig. 4.6n). The typical size of the larval clouds is 30-60 km, although much more dispersed cases occur commonly along the Gippsland coast.

Figs. 4.7a-c show integrated larval abundances for the three seasons to summarise the larval excursions over the full season from both the modern and historical beds. First, it is evident that, given the initial locations of the scallop beds, the flow streamlines tend to carry the larvae around the outskirts of the Strait. This results in a high level of cross-seeding because the beds are aligned on these flow streamlines. There is considerable interaction between the beds around King Island, Flinders Island and the north of Tasmania. However, these is very little cross-fertilisation between the Tasmanian and Victorian coasts, when larvae are viable for a maximum of 28 days.

Currents are slower in 1985/86 (Fig. 4.7a) than in the subsequent years (Figs. 4.7b and 4.7c) with the result that self-seeding is much more common and cross-fertilisation between the southern and northern regions is much less likely. There appears to be some transfer of larvae from the Flinders Island beds to the East Gippsland beds in 1987/88.

The highest probability of recruitment (largest dots) occurs off Cape Otway and in a large region north of Flinders Island. It should be noted however that tidal currents are very fast in the latter region and the sea bed sediment is coarser than in other locations. This bed may be unsuitable for scallop recruitment, or the fast currents may prevent larvae from settling.

4.2 PROBABILITY OF CROSS- AND SELF-SEEDING

By counting each simulated event, a table of the number of self-seeding, cross-seeding, and lost larvae events for extant beds was constructed (Table 4.1). The results are graphically summarised in Figs. 4.8a-d.

Table 4.1 indicates that self-seeding is by far the most likely outcome. All of the beds are regularly self-seeded. Sites 4, 3 and 1 (Fig. 2.5) are most likely to self-seed. These are the beds to the north-east of King Island and along the northern Tasmanian coast.

Cross-seeding occurs from Sites 2 and 8, respectively south-east of King Island and on the Gippsland coast. These seed Sites 1 and 7 (Fig. 2.5).

Losses from the region off the edge of the continental shelf are rare. However, advection of larvae into regions where beds have previously not been noted is the most common outcome ("Nothing" option in Figs. 4.8a-c).

Table 4.1 Frequency (%) of cross-seeding and self-seeding of beds and loss of scallop larvae from Bass Strait system. Data are from simulations of the September-February period in 1985/86, 1986/87 and 1987/88, but are incomplete at some sites in some years

	Site							
	1	**2**	**3**	**4**	**5**	**6**	**7**	**8**
Self-seeding	22	17	38	43	11	15	9	17
Cross-seeding	0	25	0	0	0	0	0	32*
Loss from System	0	0	0	0	2	0	32	15

* Site 8 cross-seeds Site 7, but the reverse phenomenon has not been observed in the simulations.

CHAPTER 5: DISCUSSION AND CONCLUSIONS

The major finding of this study is that over a range of sites and spawning times, with associated variation in climate and hydrology, self-seeding at most sites was relatively common whilst cross-seeding was rare.

This strongly suggests that management based on assumptions of independence of stock and recruitment, and of high probability of new recruitment from distant sources, will be inappropriate. This result is analogous to that in the abalone fishery, where research has demonstrated that individual reefs are largely self-seeding (McShane *et al.*, 1988) and management is now based on the assumption of localised independent stocks where possible. Our results suggest that individual scallop beds should probably be managed as individual stock units.

The problems of management are compounded by the fact that mortality of scallops caused by fishing is not limited to the catch removed. There is apparently also high mortality due to dredge-induced damage and possible viral infections associated with decaying scallops remaining on the substrate after dredging (Young, 1994). Less damaging fishing methods and the maintenance of a significant spawning stock should be a priority.

Whilst self-seeding was relatively common at all extant sites, some cross-seeding did occur at a few sites. This cross-seeding occurred between sites that were relatively close together and tended to be a one-way process. Thus, the bed to the southeast of King Island tended to seed the bed to the north-east of King Island and there was seeding from west to east along the Gippsland coast. These cross-seeding events occurred between beds along contours of relatively strong and consistent current flow. When historical beds are also considered, cross-seeding becomes much more common. The major implication is that reduction in the number of viable scallop beds will inevitably lead to greater importance of self-seeding in those remaining.

Very few larvae were lost from the Bass Strait system, but a large number were dispersed to areas where there are no known historical or extant scallop beds. The question remains open as to why scallop beds have not developed in these areas. It is possible that suitable substrate for settlement of pediveligers occurs only in specific areas (Culliney, 1974). Such habitat selection, however, may only be possible where average current velocities are low enough to allow pediveligers to remain in close proximity to the bottom (Young, 1994). It is possible, therefore, that suitable substrate may be available over a wide area of Bass Strait (Fig. 5.1), but only in certain areas is current flow altered by local conditions to allow larvae to be passively accumulated and deposited on the sea bed (Young, 1994). This hypothesis is supported by the association of Bass Strait scallop beds with topographic features, such as headlands or islands, that may modify or inhibit currents.

We have examined the vertically-averaged case for larval transport in Bass Strait. Patterns will be modified by vertical distributions other than the well-mixed case. Although *Placopecten magellanicus* was found to concentrate near the pycnocline when stratification occurred and there was evidence of weak diurnal migration, the capacity for depth regulation in this species appeared to be limited (Tremblay and Sinclair, 1990 a,b). Cragg (1980) suggests that *Pecten maximus* initially swims upwards in the initial trochophore stage of a few days, then alternately swims upwards and sinks in the veliger stage, and finally is closely associated with the substrate in the pediveliger stage. It seems likely that our modelling would overestimate the dispersal of pediveligers because currents near the bottom would be slower than the vertically averaged case. Thus, dispersal of scallop larvae may be even more limited than our modelling suggests. Simulation of dispersal of scallop larvae could be refined greatly if information on vertical distribution of larvae, together with vertical stratification of the water column, could be made available for incorporation into the three-dimensional model.

Interannual differences were observed in scallop dispersal and may be related to the generally calmer conditions of 1985/6 compared with subsequent years. This effect was not strong when only existing sites were considered, perhaps because the greater dispersal distances were still not enough to bridge the gaps between beds. The biggest effect was observed for the most eastern site along the Gippsland coast where self-seeding was more common in 1985/86 and cross-seeding was particularly prevalent in 1987/88. Consideration of integrated larval abundances for historical and extant beds together shows a stronger pattern with much greater cross-seeding in later years, and potential transfer from the Flinders Island region to the East Gippsland region in 1987/88. A similar conclusion was reached by Young *et al.* (1992) who modelled dispersal to a number of spat collection sites in Bass Strait and found that dispersal distances were much greater in 1986/87 compared with 1985/86. Notwithstanding the interannual differences, self-seeding was still common, and dominated when only extant beds were considered.

Within years, the dispersal of larvae varied greatly depending on the climatic conditions (mainly wind) at the time of spawning. The model assumed that spawning was constant over the seven-month period; however, evidence from gonad indices and spat collections indicate that while spawning is protracted, it is probably episodic and geographically variable over this period (Young, 1994). Thus, the pattern of larval dispersal will depend greatly on the prevailing environmental conditions when spawning episodes occur. This relationship is unlikely to be random, but rather spawning will be triggered by certain environmental events; for example, by cold water intrusions as in the case of *Argopecten gibbus* (Miller *et al.*, 1981). It is possible that spawning may be cued by specific environmental conditions which enhance either cross-seeding or self-seeding. More information on spawning periodicity and spawning cues would considerably enhance the realism of the modelling process.

The results suggest that viability of a scallop bed may be lost if fished too heavily, as larval inputs from remote sites cannot be guaranteed. Settlement at the natal site is far more common. Local recruitment becomes even more important as the number of viable beds that can supply a larval input diminishes.

REFERENCES

Baines, P.G. and Fandry, C.B. (1983) Annual cycle of the density field in Bass Strait, *Aust. J. Mar. Freshw. Res.* 34: 143-153.

Black, K.P. (1983) *Sediment transport and tidal inlet hydraulics.* PhD Thesis. University of Waikato. New Zealand. Volume 1, Text, 331 pp. Volume 2, Figures and Tables.

Black, K.P. (1992a) *The hydrodynamic model 3DD and support software.* Victorian Institute of Marine Sciences 35 pp.

Black, K.P. (1992b) *The Lagrangian advection/diffusion model 3AD and support software.* Victorian Institute of Marine Sciences 25 pp.

Black, K.P. (1992c) Evidence of the importance of deposition and winnowing of surficial sediments at a continental shelf scale. *Journal of Coastal Research.* **8**(2): 319-331.

Black, K.P. (1993) The relative importance of local retention and inter-reef dispersal of neutrally buoyant materials on coral reefs, *Coral Reefs,* 12: 43-53.

Black, K.P., Hatton, D.N. and Colman, R.S. (1990). *Prediction of extreme sea-levels in northern Port Phillip Bay and the possible effects of a rise in mean sea level.* Report to the Board of Works Melbourne. Victorian Institute of Marine Sciences. 48 pp.

Black, K.P., Hatton, D. and Rosenberg, M. (1993) Locally and externally-driven dynamics of a large semi-enclosed bay in Southern Australia. *Journal of Coastal Research,* **9**(2), 509-538.

Bowden, K.F. (1983). *Physical oceanography of coastal waters.* Ellis Horwood Ltd.

Caddy, J.F. (1989) *A perspective on the population dynamics and assessment of scallop fisheries, with special reference to the sea scallop, Pecten magellanicus Gmelin.* In J.F. Caddy (ed.) Marine Invertebrate Fisheries. Their Assessment and Management. John Wiley and Sons, New York. pp. 559-589.

Cragg, S.M. (1980). Swimming behaviour of the larvae of *Pecten maximus* (L.) (Bivalvia). *Journal of the Marine Biological Association UK* 60: 551-564

Culliney, J. L. (1974). Larval development of the giant scallop Placopecten magellanicus (Gmelin). *Biol. Bull. Mar. Biol. Lab. Woods Hole* 147: 321-332.

Dix, T.G. and Sjardin, M.J. (1975). Larvae of the commercial scallop, *Pecten meridionalis* from Tasmania, Australia. *Australian Journal of Marine and Freshwater Research* 26: 109-112

Hancock, D.A. (1973) The relationship between stock and recruitment in exploited invertebrates. *Rapp. P-v. Rèun. Cons. Int. Explor. Mer.* 164: 113-131.

Hancock, D.A. (1979) Population dynamics and management of shellfish stocks. *Rapp. P-v. Réun. Cons. Int. Explor. Mer.* 175: 8-19.

Jones , H.A. and Davies, P.J. (1983) Superficial sediments of the Tasmanian continental shelf and part of Bass Strait. Bureau of Mineral Resources, Geology and Geophysics Bulletin 218 Australian Government Publication ACT 25 pp.

Joseph, J. and Sendner, H. (1958). Über die horizontale Diffusion im Meere. *Dt. Hydrogr. Z.*, **11,** 49-77.

Kaartvedt, S., Aksnes, D.L. and Egge, J.K. (1987). Effect of light on the vertical distribution of *Pecten maximus* larvae. *Marine Ecology - Progress Series* 40: 195-197

Leendertse, J.J. and Liu, S-K. (1975) Modelling of the three dimensional flows in estuaries. 2nd Annual Symposium on Modelling Techniques. Waterways, Harbours and Coastal Engineering (ASCE). pp. 625-642.

Marsden M.A.H. and Sternberg. R.V. (1976). Sea bed drifter studies of bottom currents in Western Port Bay and nearby Bass Strait. Western Port Bay Environmental Study (Ministry of Conservation) Geology Department, Melbourne University. 41 pp

Martin, R.B., Young, P.C., McLoughlin, R.J. and West, G.J. (1989). Bad news in Bass Strait. *Australian Fisheries* 48: 18-19

McLoughlin, R.J., Young, P.C. and Martin, R.B. (1988) The growth and mortality of *Pecten fumatus* spat in collectors in Bass Strait: a preliminary study. In: Dredge, M.L.C., Zacharin, W.F. & Joll, L.M.s (eds) Proceedings of the Australasian Scallop Workshop.

McShane, P.E., Black, K.P. and Smith, M.G. (1988) Recruitment processes in *Haliotus rubra* (Mollusca: Gastropoda) and regional hydrodynamics in southeastern Australia imply localized dispersal of larvae. *J. Exp. Mar. Biol. Ecol.* 124: 175-203.

Middleton, J.F. and Black, K.P. (1994). The low frequency circulation in and around Bass Strait: a numerical study. *Continental Shelf Research.* In press.

Miller, G.C., Allen, D.M., and Costello, T.J. (1981). Spawning of the calico scallop *Argopecten gibbus* in relation to season and temperature. J. Shellfish Res. 1: 17-21

Monin, A.S. and Yaglom, A.M. (1971). *Statistical Fluid Mechanics: Mechanics of Turbulence,* Vol. **1,** M.I.T. Press, Cambridge, Massachusetts.

Okubo, A. (1971). Oceanic diffusion diagrams. *Deep-Sea Res.,* **18,** 789-802.

Perrels, P.A.J and Karelse, M. (1981) A two-dimensional laterally-averaged model for salt intrusion in estuaries. *Delft Hydraulics Laboratory No. 262*, 52 pp.

Rosenberg, M., Hodgkinson, R. Black, K. and Colman, R. (1992) *Hydrodynamics of Port Phillip Bay. Vol. 1: Field data collection and data reduction.* Working Paper No. 23, Victorian Institute of Marine Sciences.

Sinclair, M., Mohn, R.K., Robert, G. and Roddick, D.L. (1985) Considerations for the effective management of Atlantic Scallops, *Can. Tech. Rep. Fish. Aquatic Sci.* 1328: 1-113.

Talbot, J.W. and Talbot, G.A. (1974). Diffusion in shallow seas and in English coastal and estuarine waters. *Rapp. Proc. Verb., Cons. Int. Explor. Mer.*, **167,** 93-110.

Tremblay, M.J. and Sinclair, M. (1990a). Diel vertical migration of sea scallop larvae *Placopecten magellanicus* in a shallow embayment. Marine Ecology - Progress Series 67: 19-25

Tremblay, M.J. and Sinclair, M. (1990b). Sea scallop larvae *Placopecten magellanicus* on Georges Bank: vertical distribution in relation to water column stratification and food. *Marine Ecology - Progress Series* 61: 1-15

Woodburn, L. (1988) Genetic variation in Southern Australasian Pecten. In: Dredge, M.L.C., Zacharin, W.F. & Joll, L.M.s (eds) Proceedings of the Australasian Scallop Workshop.

Young, P.C. (1994) Recruitment variability in scallops: potential causes for the loss of Bass Strait populations. In: Sammarco, P.W. & Heron, M.L.s (eds) Coastal and Estuarine Studies, the bio-physics of marine larval dispersal. American Geophysical Union, Washington,DC, 327-342

Young, P.C. and Martin, R.B. (1989) The scallop fisheries of Australia and their management. *Rev. Aquat. Sci.* 1(4): 615-638.

Young, P.C., McLoughlin, R.J. and Martin, R.B. (1992) Scallop (*Pecten fumatus*) settlement in Bass Strait, Australia. *Journal of Shellfish Research,* 11(2): 315-323.

Zacharin, W. (1990). Tasmanian Zone Scallop Survey, 1989. Department of Primary Industry, Tasmania. Division of Sea Fisheries. Technical Report 41: 1-13

Zacharin, W. (1991). Tasmanian Zone Scallop Survey, 1990. Department of Primary Industry, Tasmania. Division of Sea Fisheries. Technical Report 43: 1-11

FIGURES

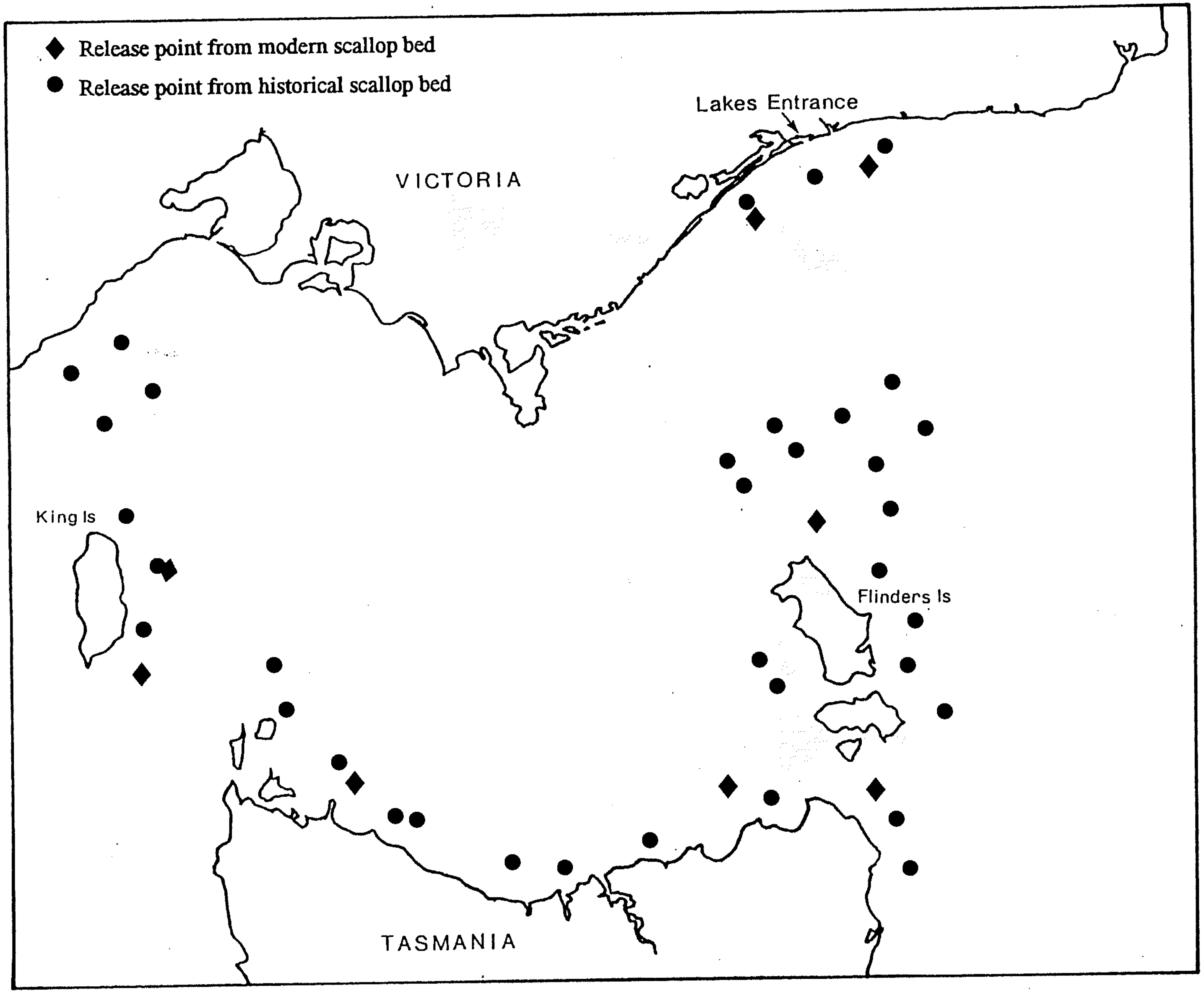

Fig. 1.1 Location of release points for larvae from modern and historical scallop beds in Bass Strait.

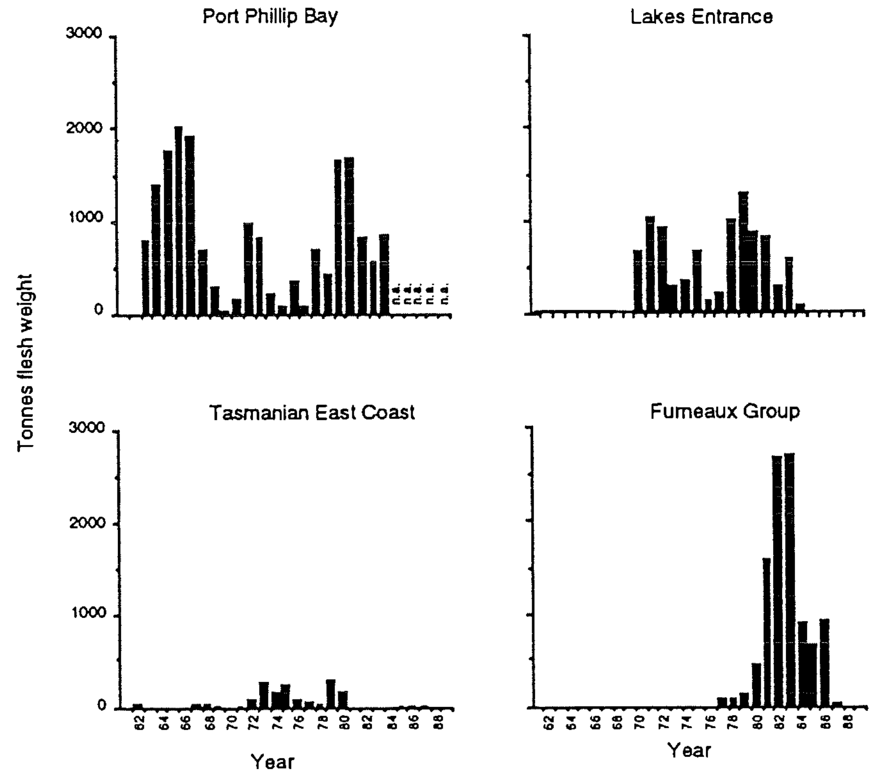

n.a. = information not yet available

Fig. 1.2 Annual scallop catches (in tonnes meat weight) from the major regions fished in Bass Strait (from Young, 1994).

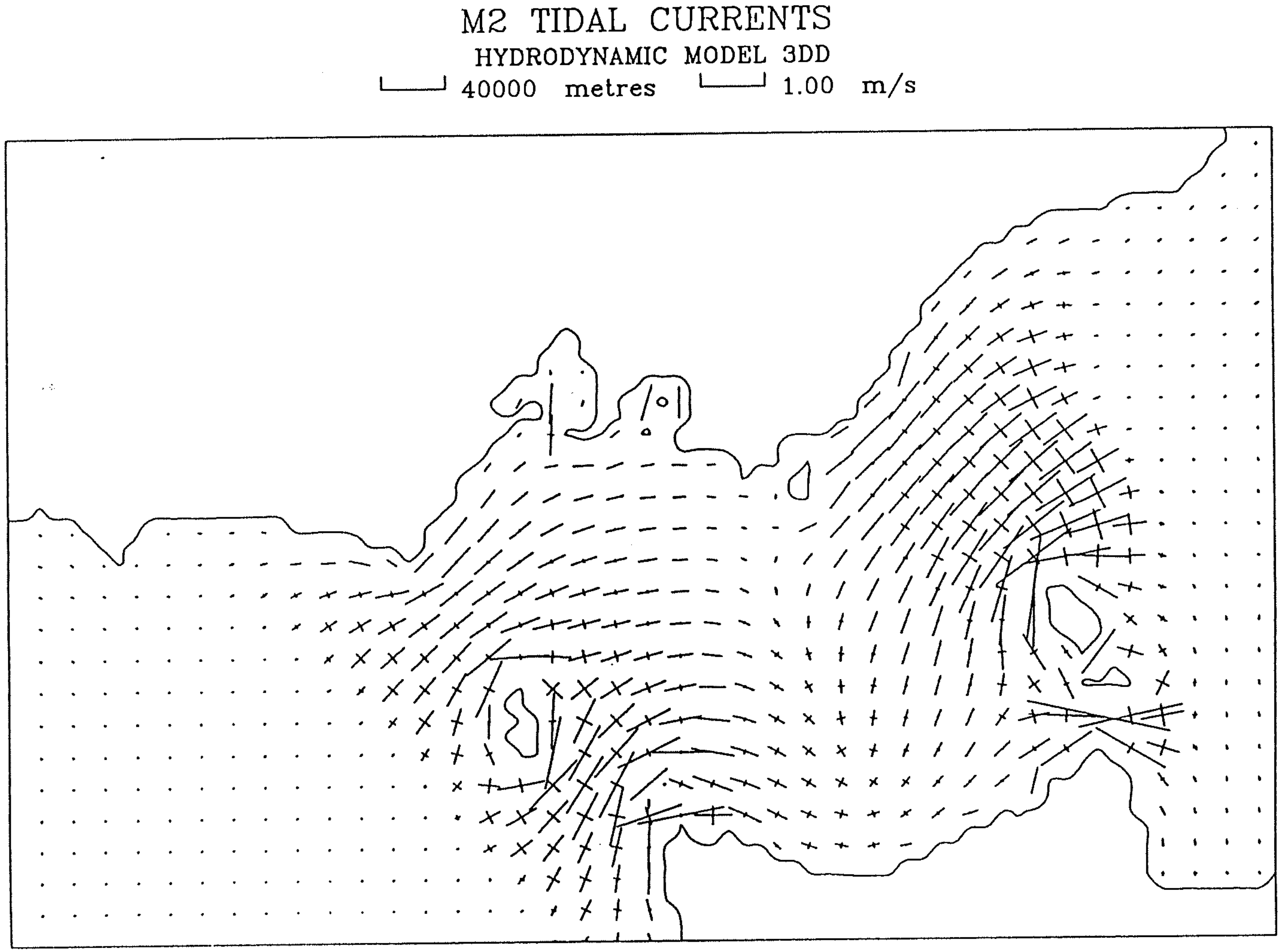

Fig. 2.1a M$_2$ tidal current orbits showing the major and minor axes and the inclination of the ellipse.

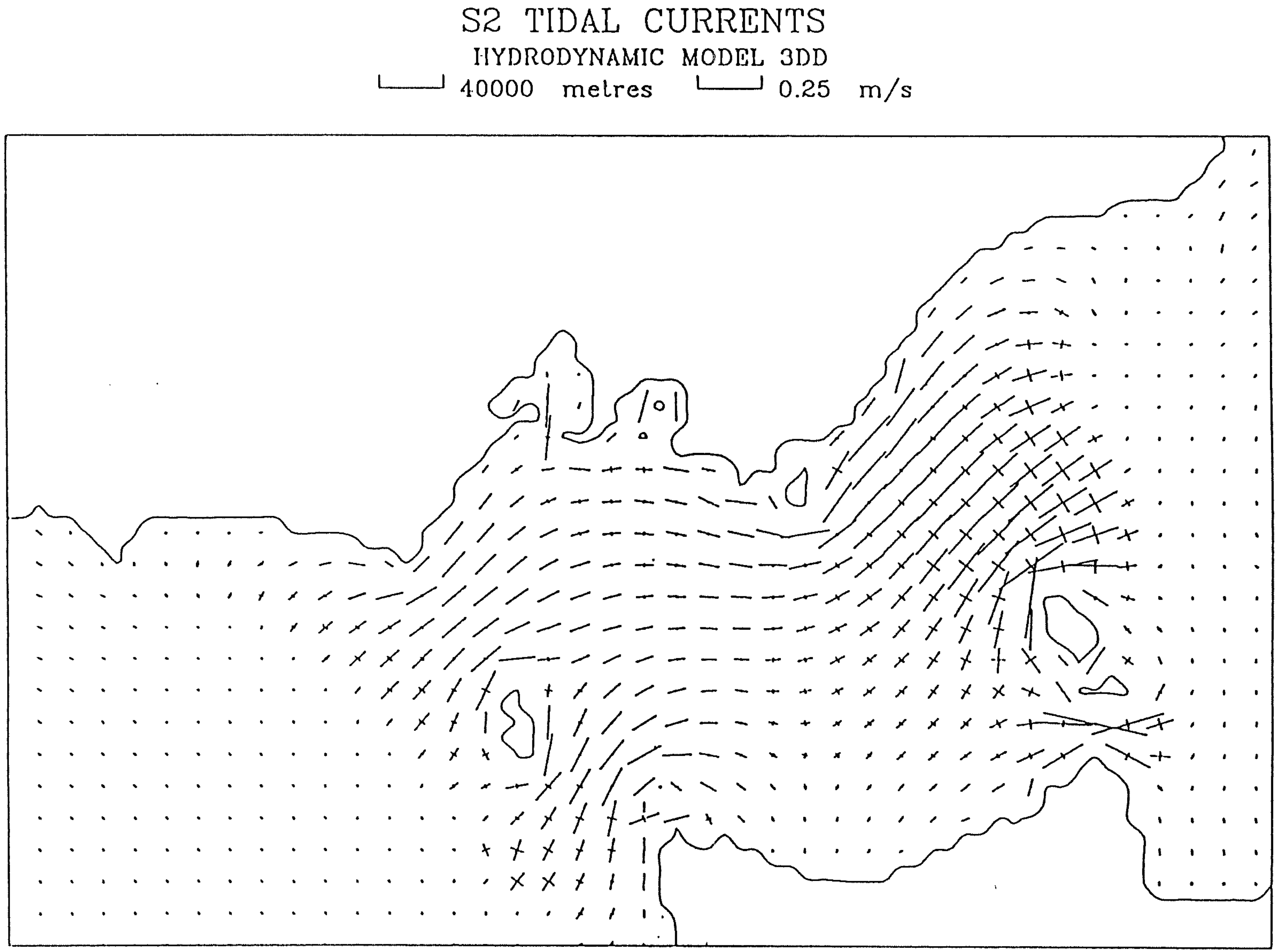

Fig. 2.1b S$_2$ tidal orbits showing the major and minor axes and the inclination of the tidal ellipse.

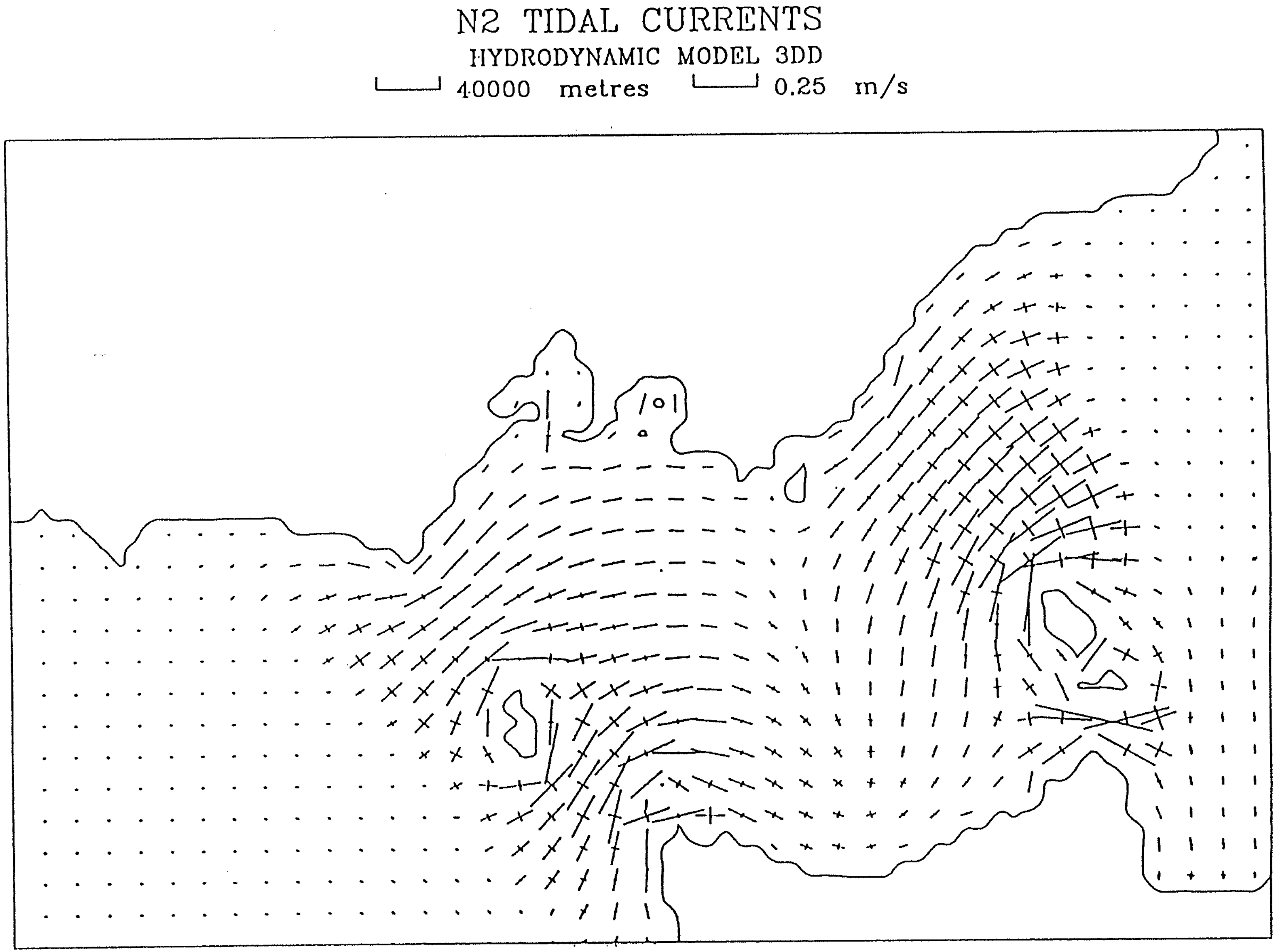

Fig. 2.1c N_2 tidal orbits showing the major and minor axes and the inclination of the tidal ellipse.

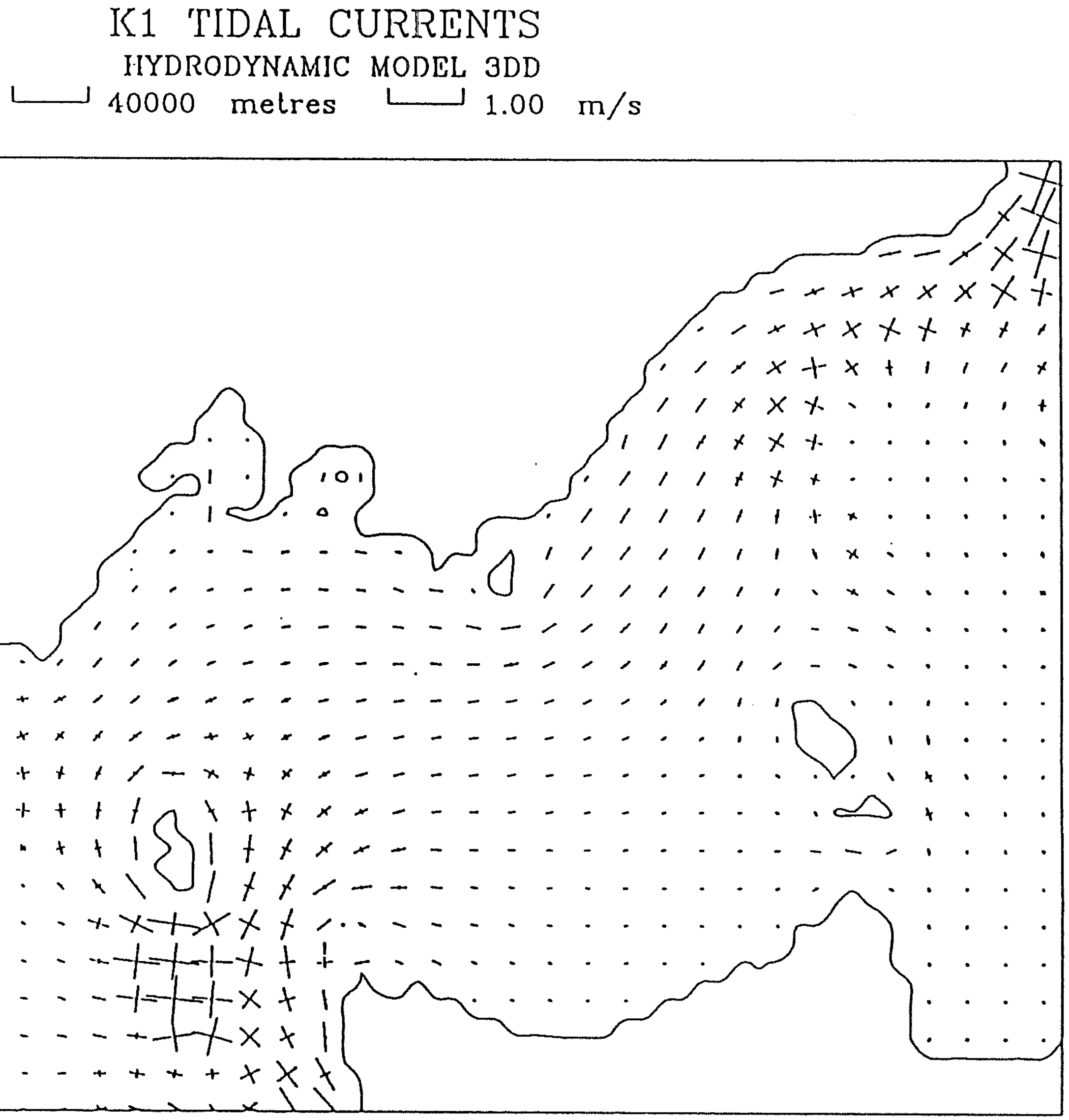

Fig. 2.1d K$_1$ tidal orbits showing the major and minor axes and the inclination of the tidal ellipse.

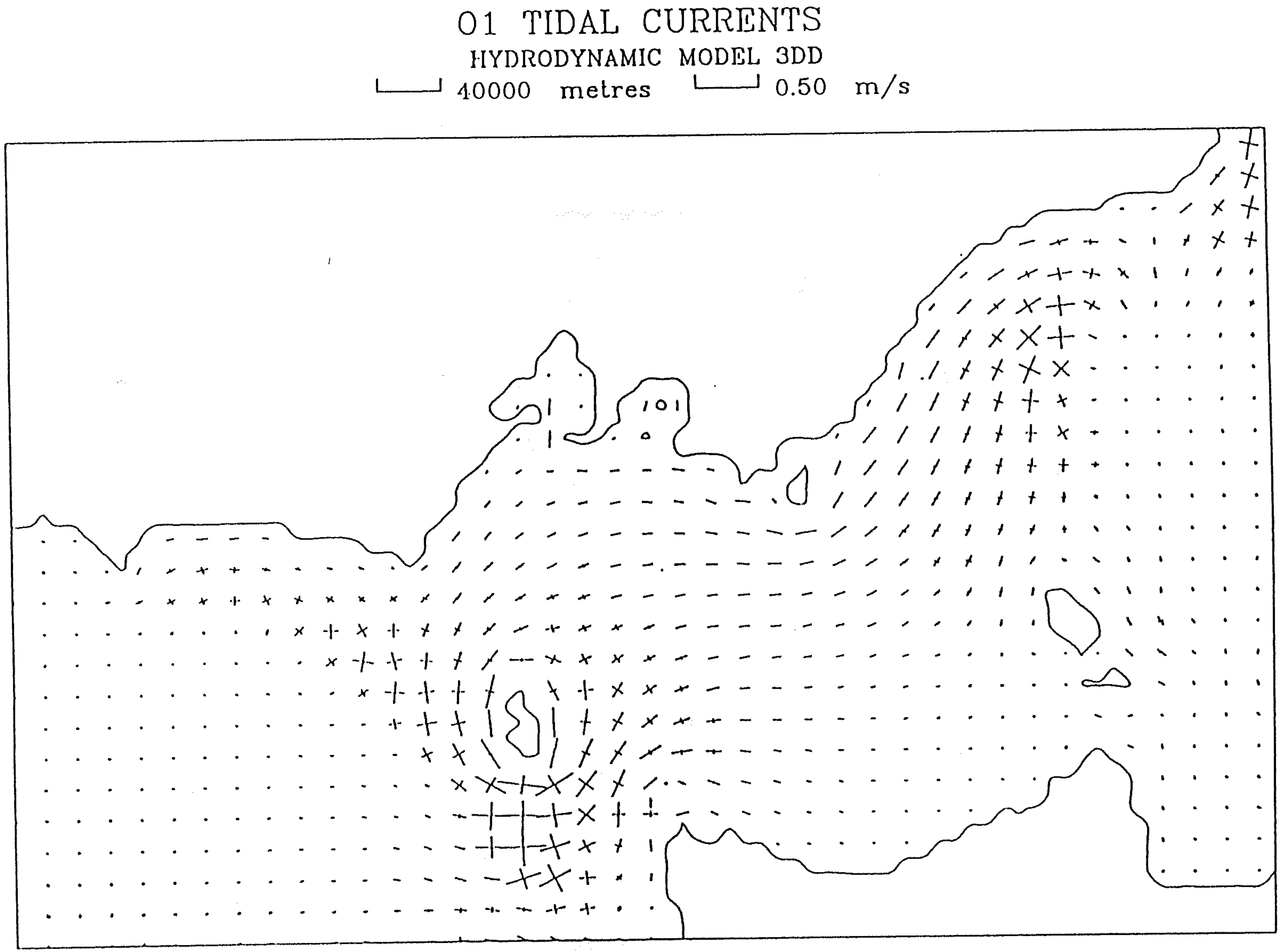

Fig. 2.1e O$_1$ tidal orbits showing the major and minor axes and the inclination of the tidal ellipse.

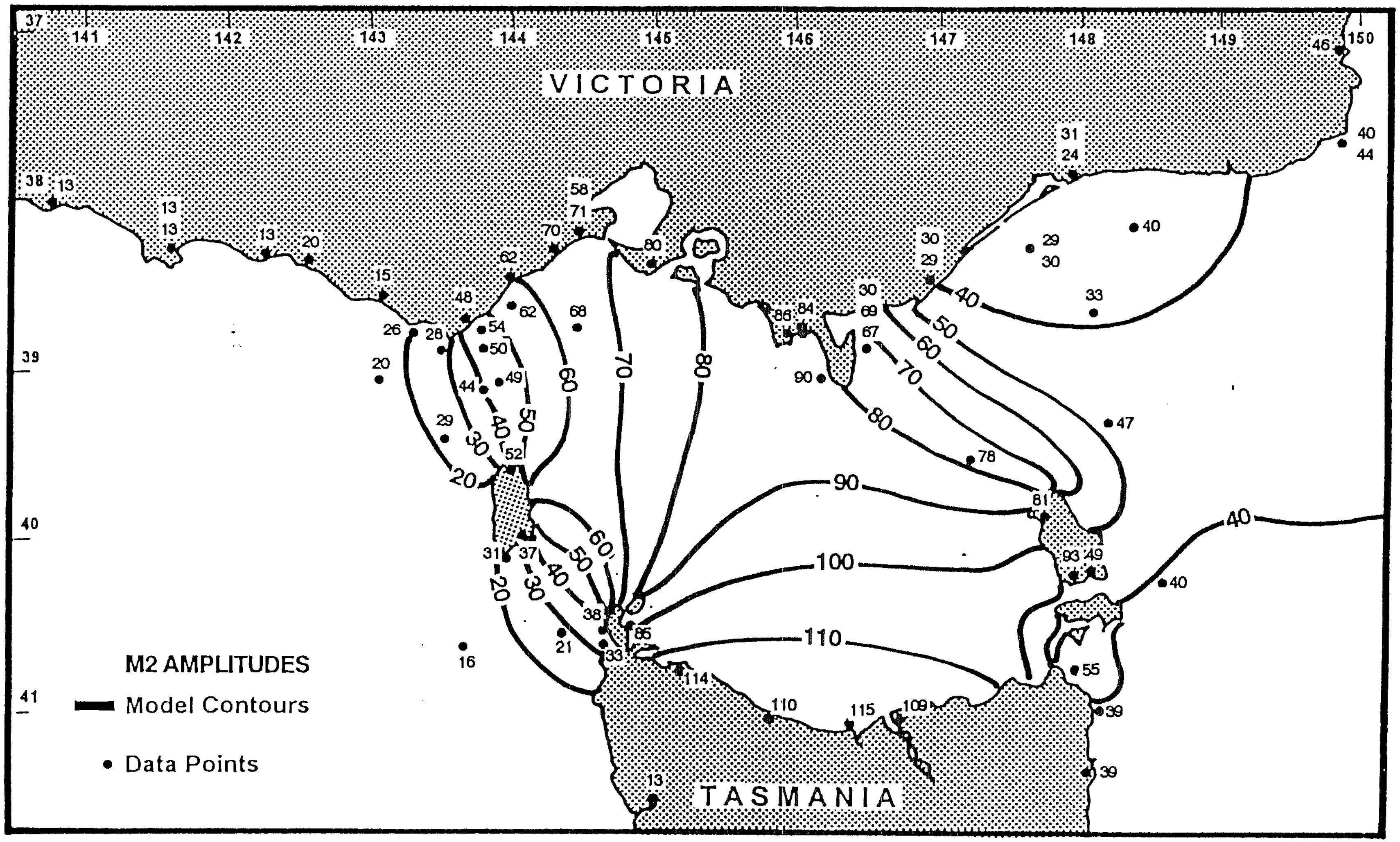

Fig. 2.2a M$_2$ tidal amplitude contours from the numerical model with the measured data.

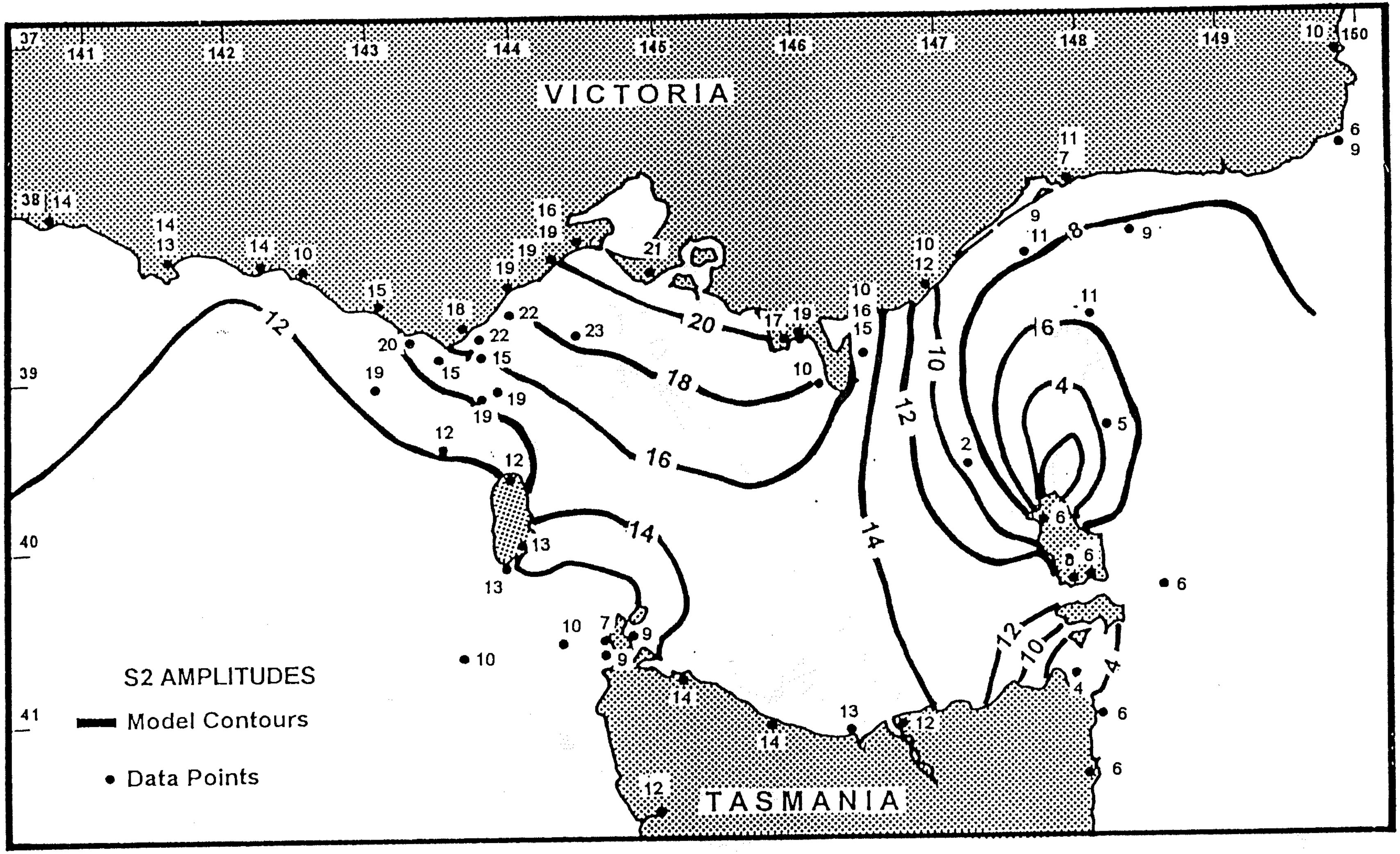

Fig. 2.2b S_2 tidal amplitude contours from the numerical model with the measured data.

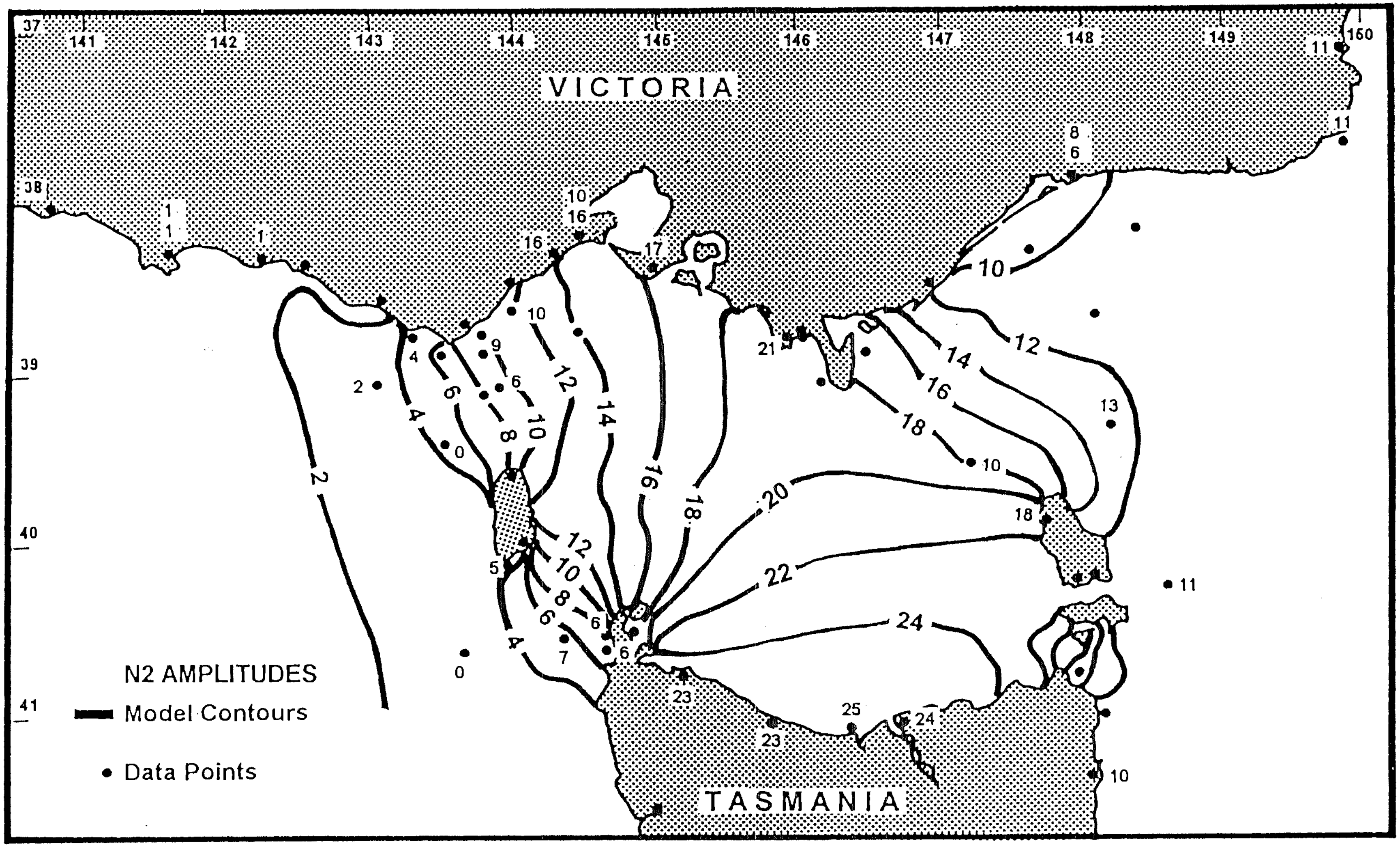

Fig. 2.2c N_2 tidal amplitude contours from the numerical model with the measured data.

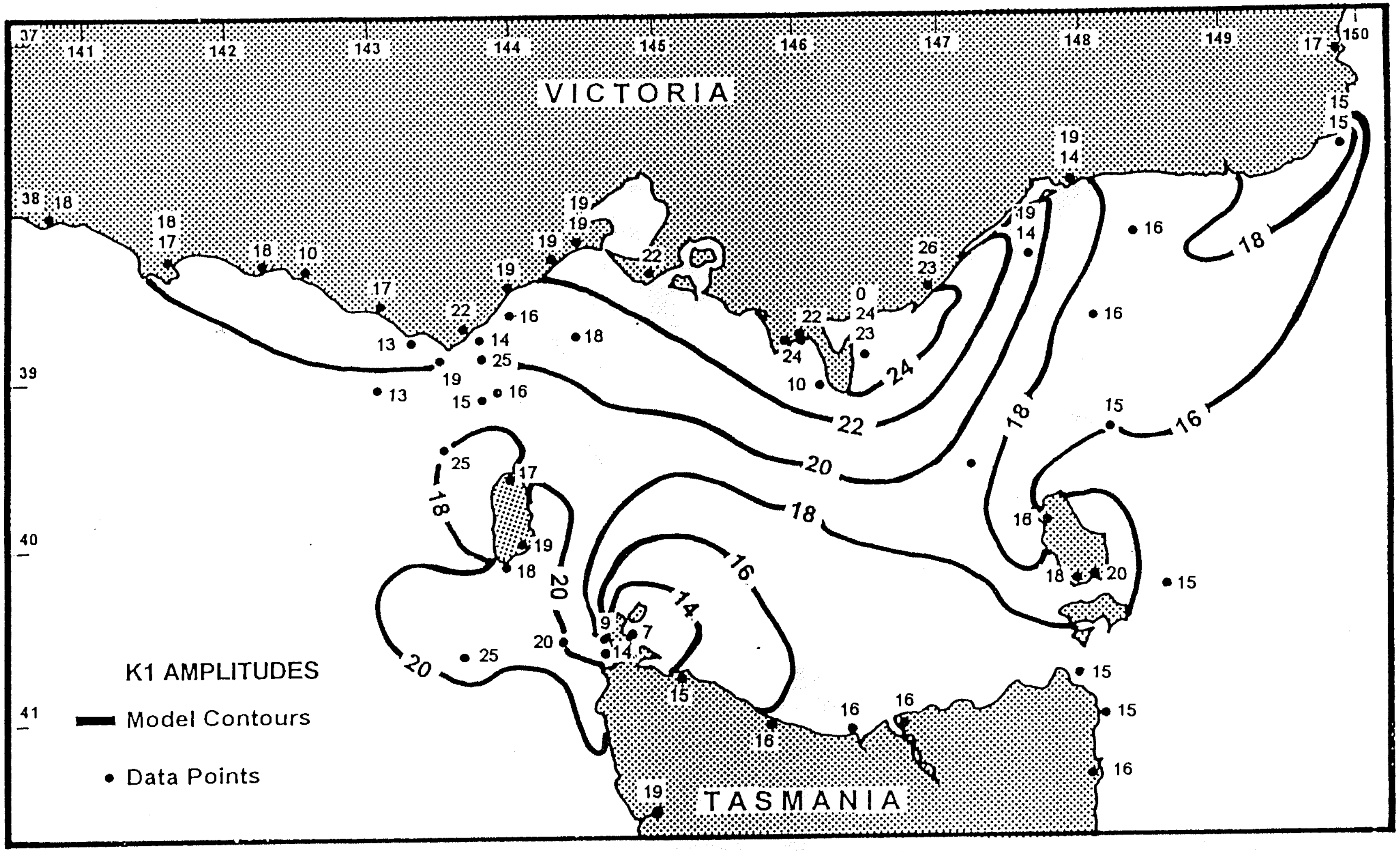

Fig. 2.2d K$_1$ tidal amplitude contours from the numerical model with the measured data.

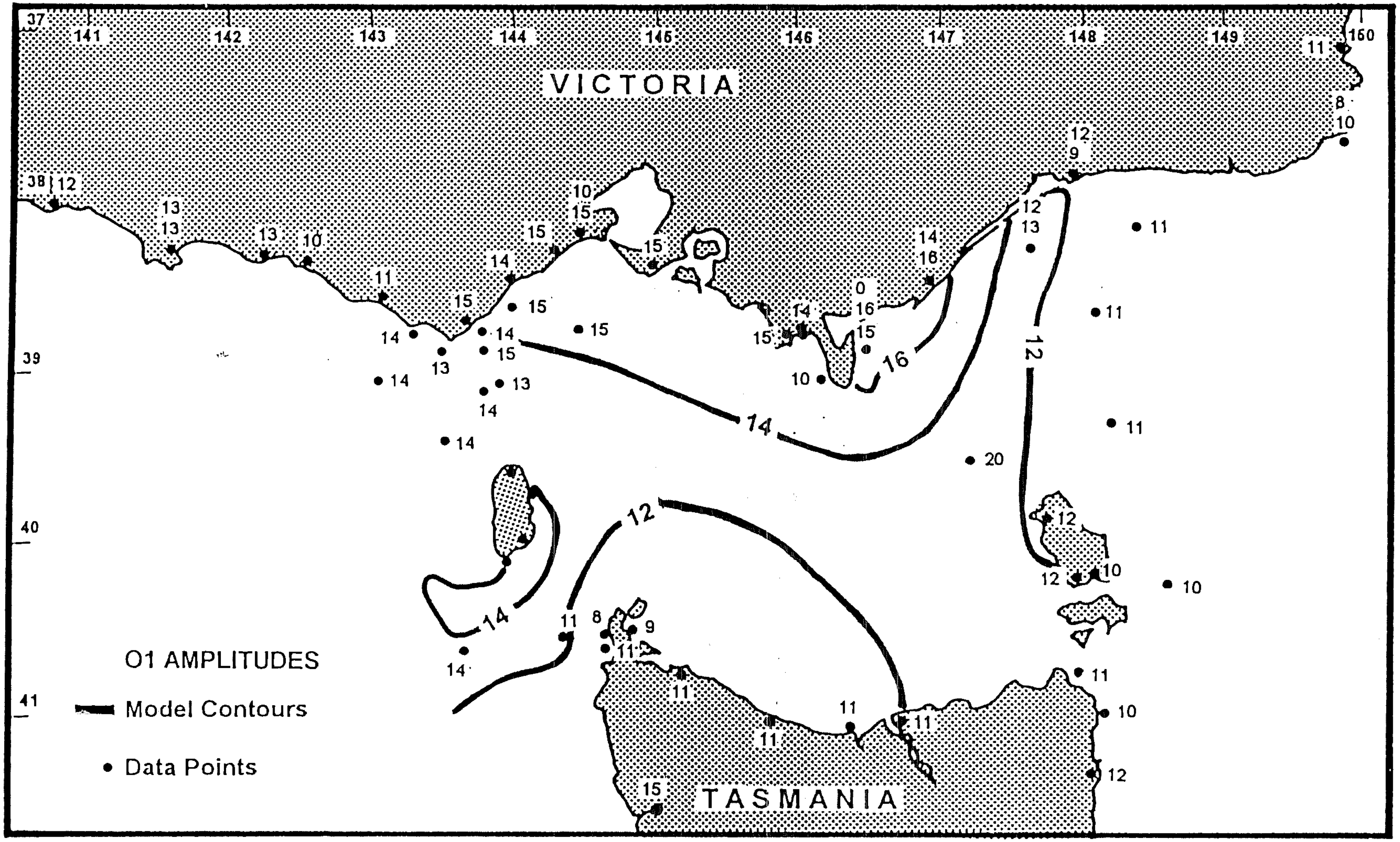

Fig. 2.2e O_1 tidal amplitude contours from the numerical model with the measured data.

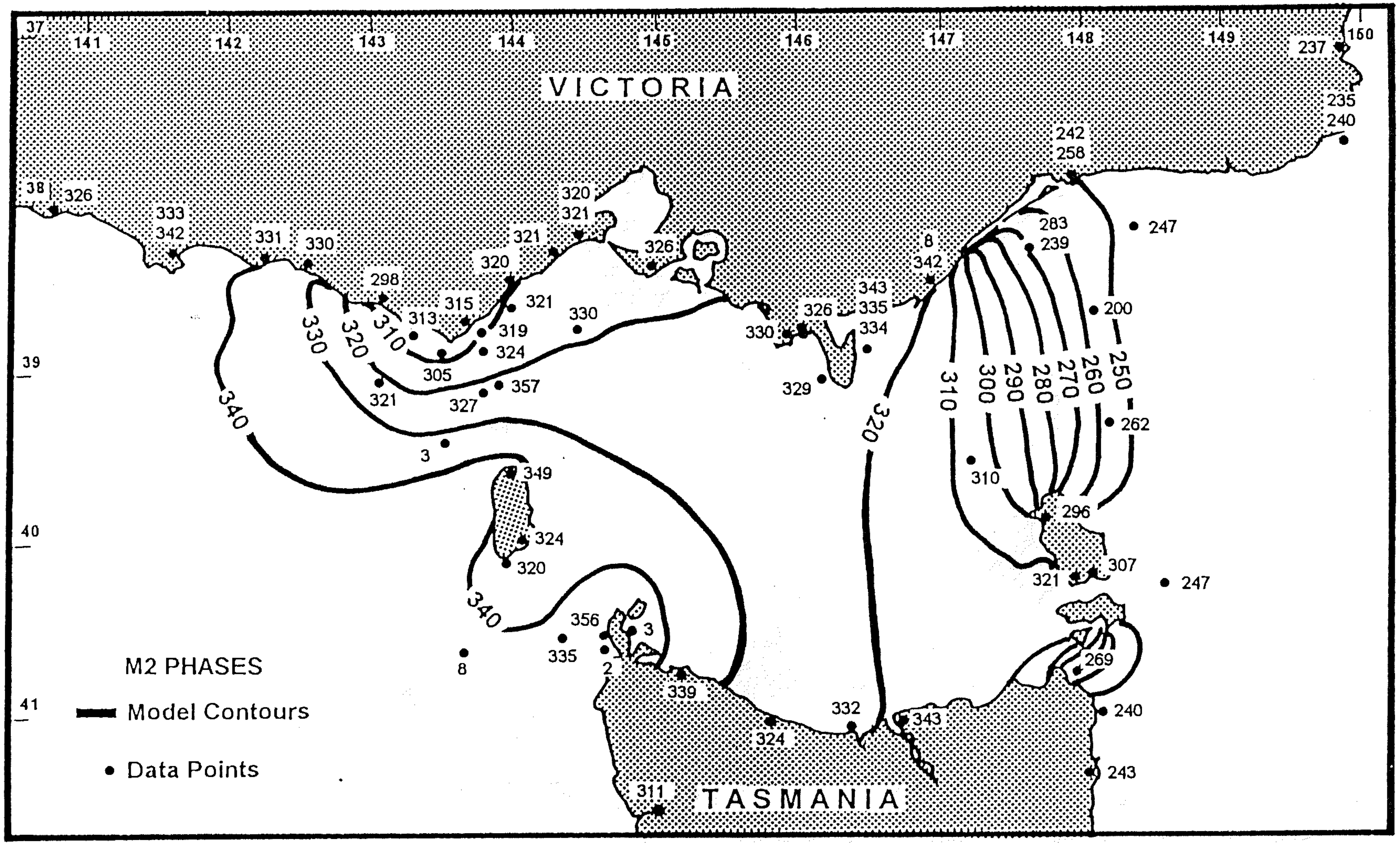

Fig. 2.3a M$_2$ tidal phase contours from the numerical model with the measured data.

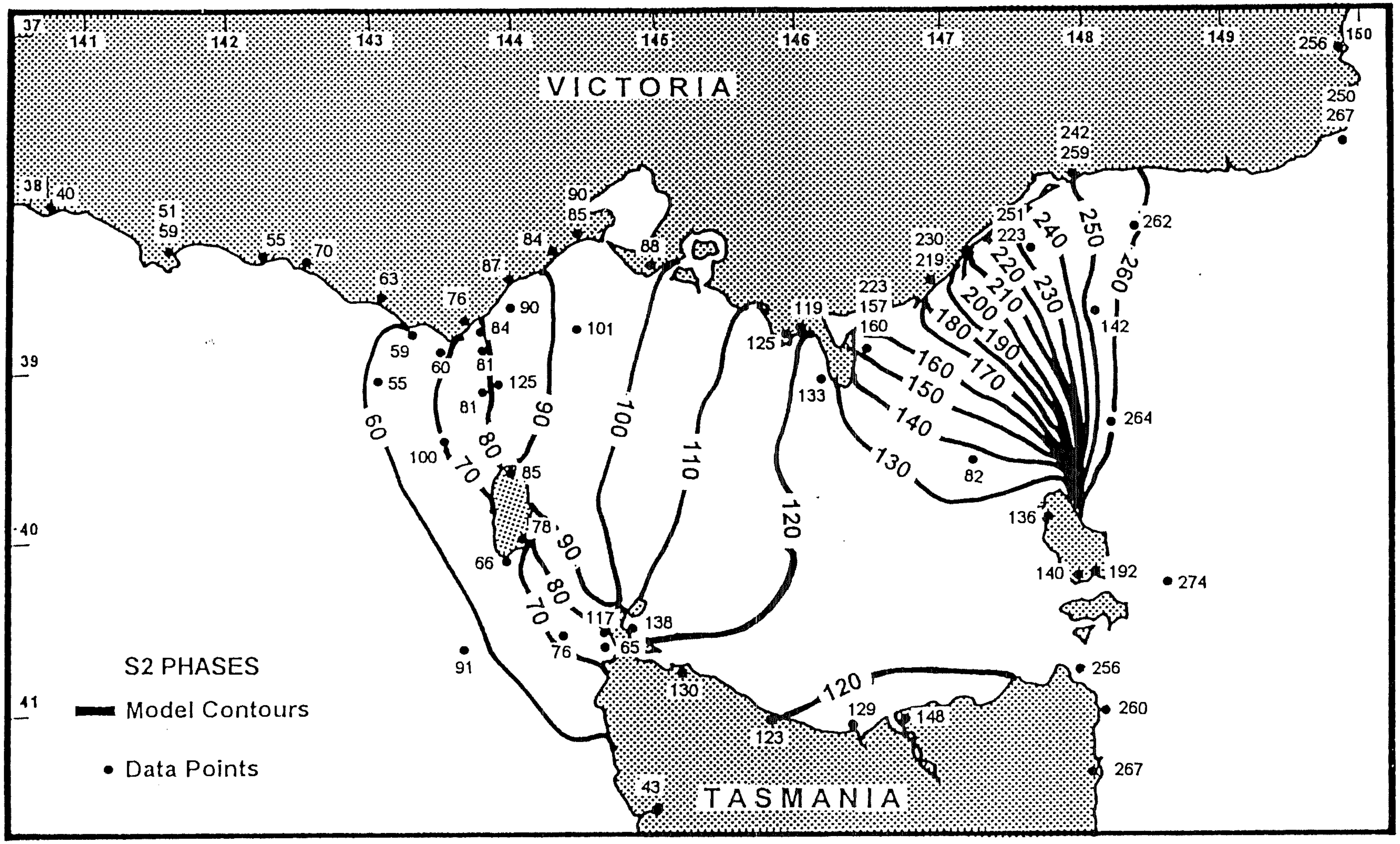

Fig. 2.3b S$_2$ tidal phase contours from the numerical model with the measured data.

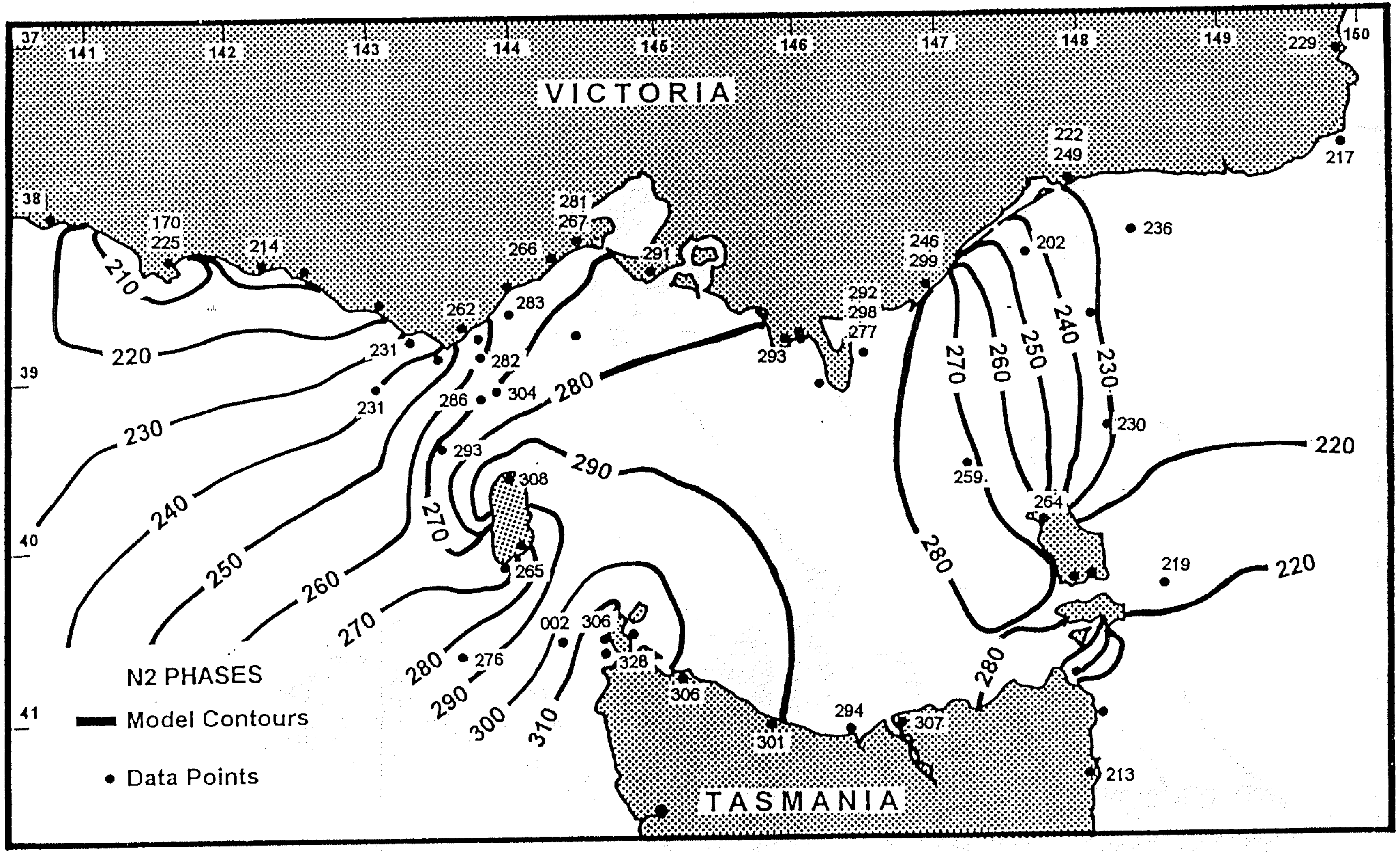

Fig. 2.3c N$_2$ tidal phase contours from the numerical model with the measured data.

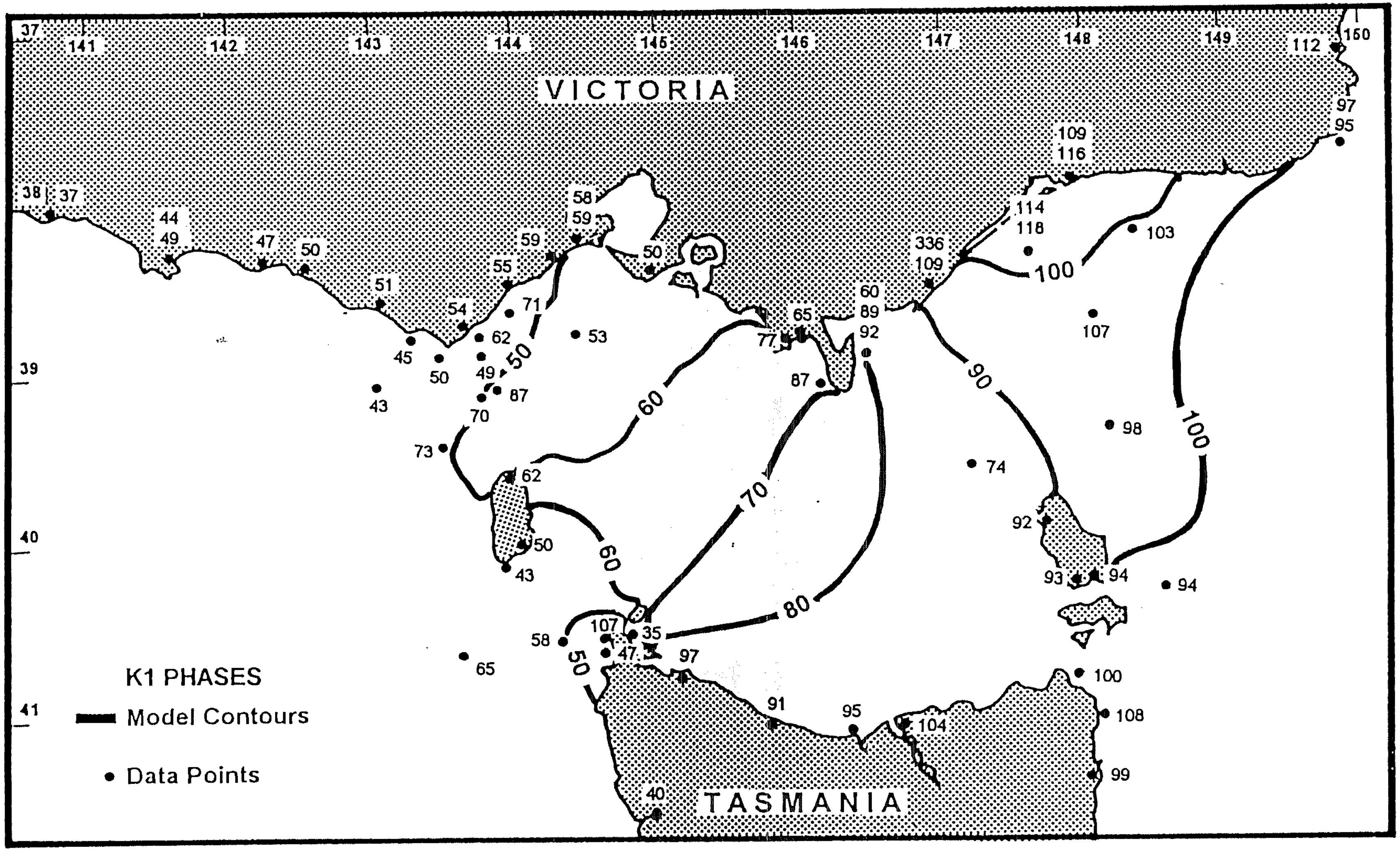

Fig. 2.3d K$_1$ tidal phase contours from the numerical model with the measured data.

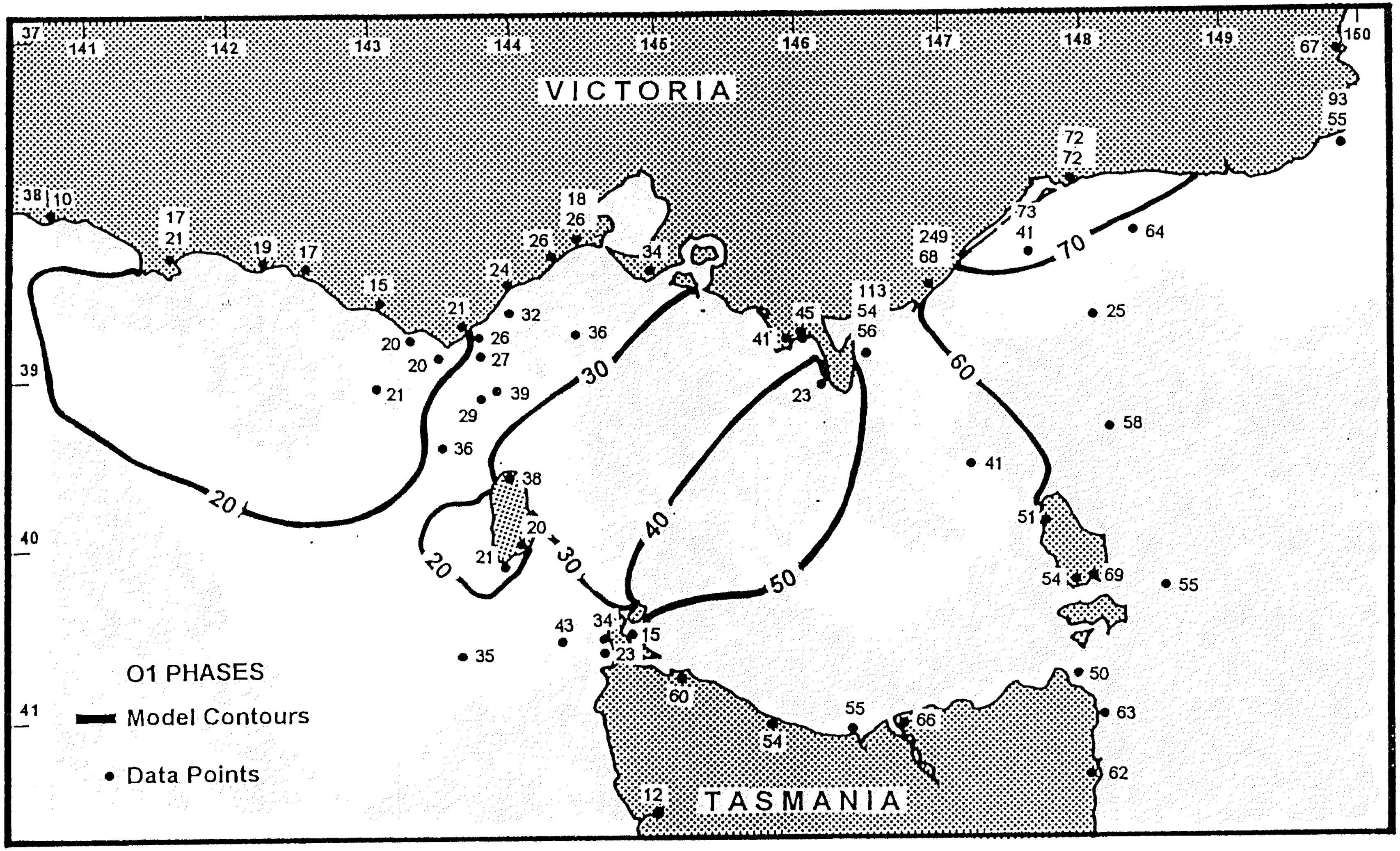

Fig. 2.3e O$_1$ tidal phase contours from the numerical model with the measured data.

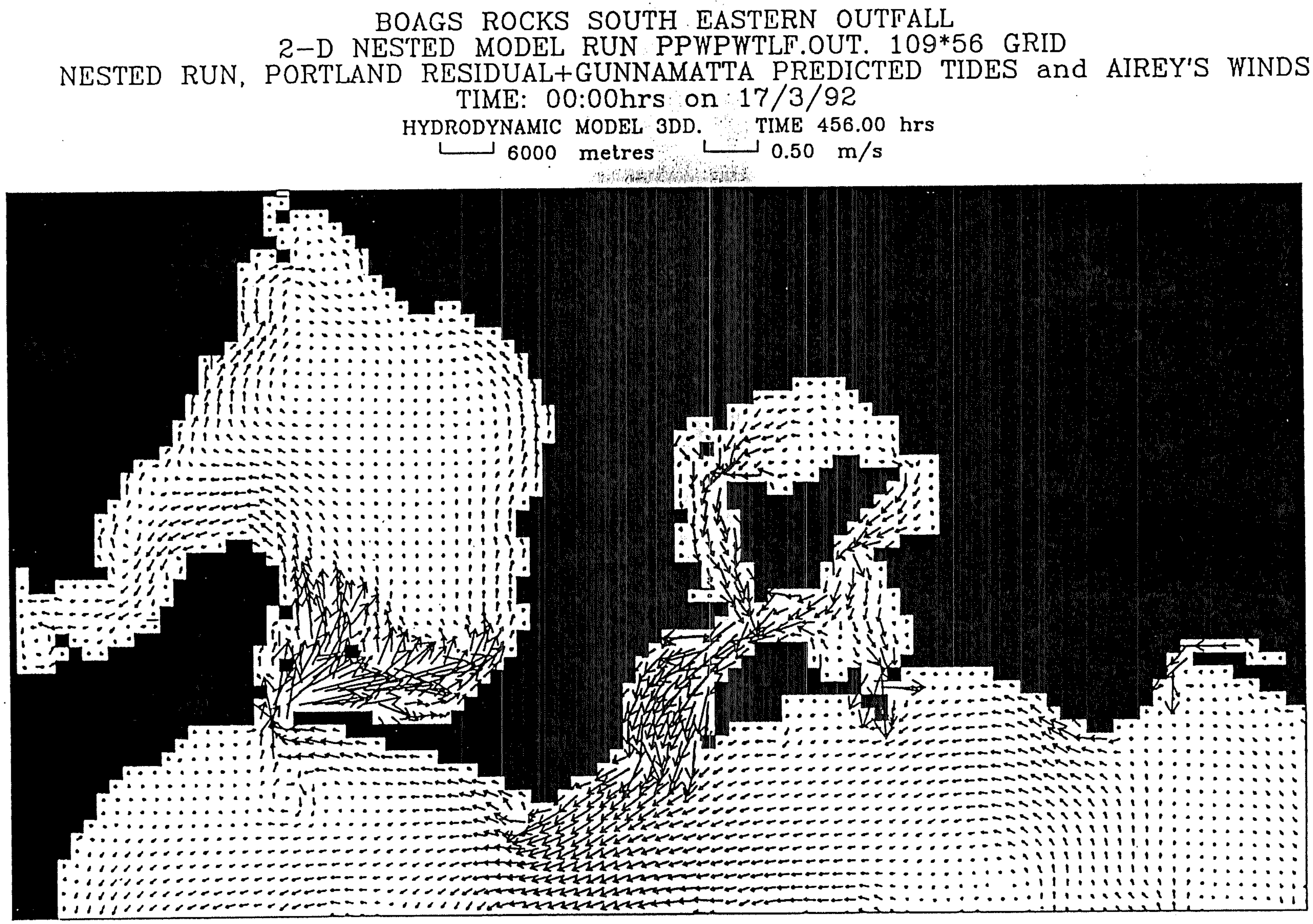

Fig. 2.4a Currents in the Central Victorian region during flood tide at the entrance to Port Phillip Bay. The model is driven by tides, winds and coastal-trapped waves.

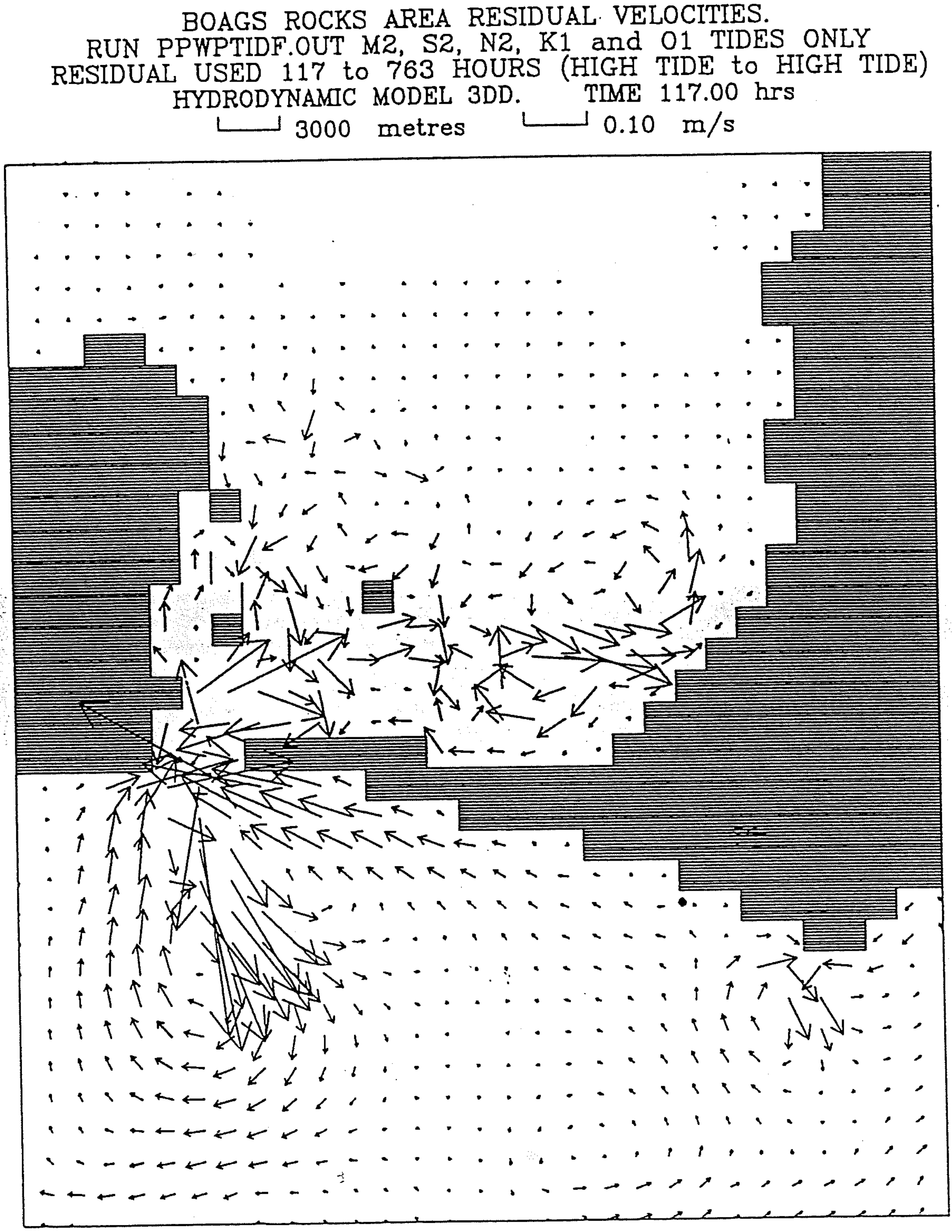

Fig. 2.4b Residual tidal currents near the entrance to Port Phillip Bay on Victoria's central coast.

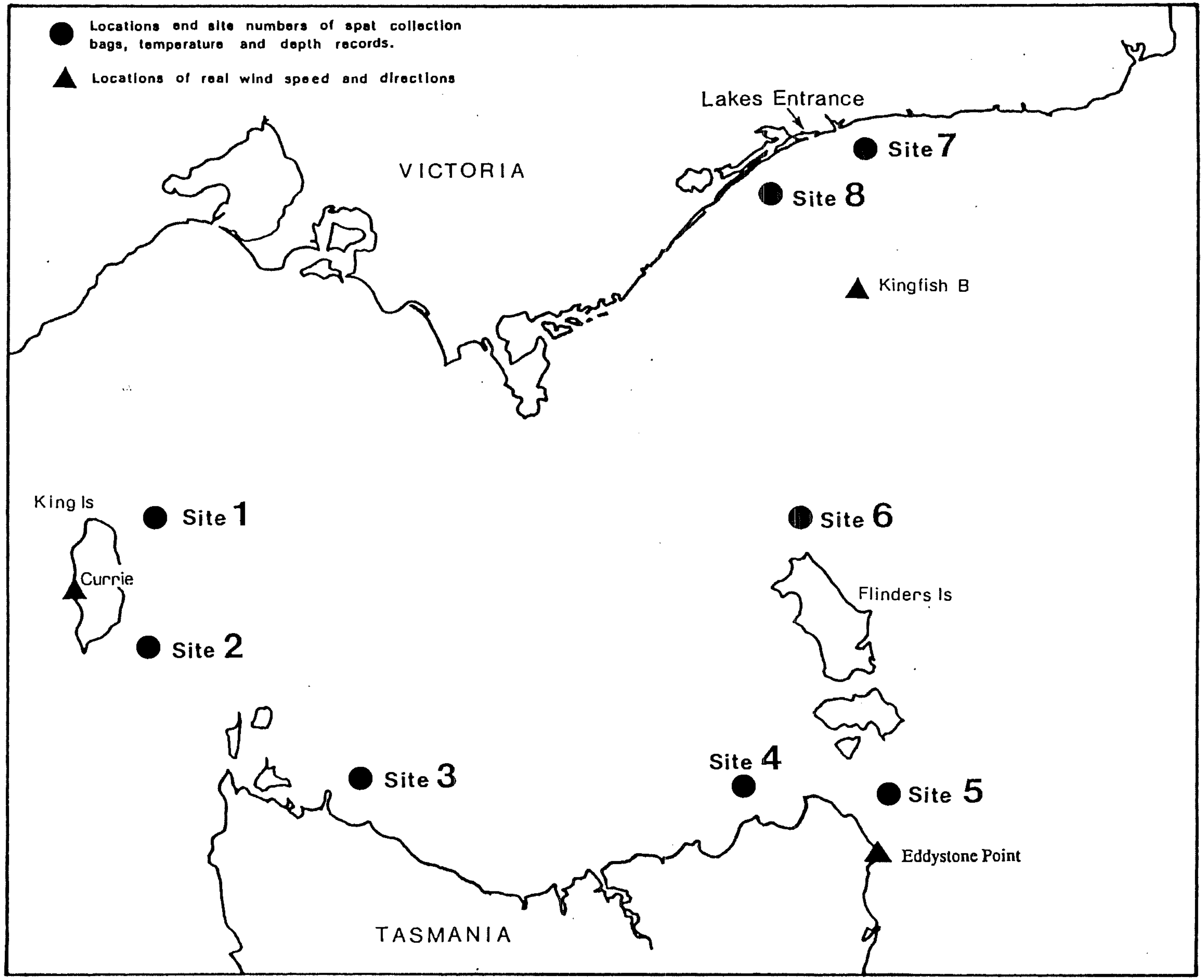

Fig. 2.5 Anemometer and spat collection sites around Bass Strait.

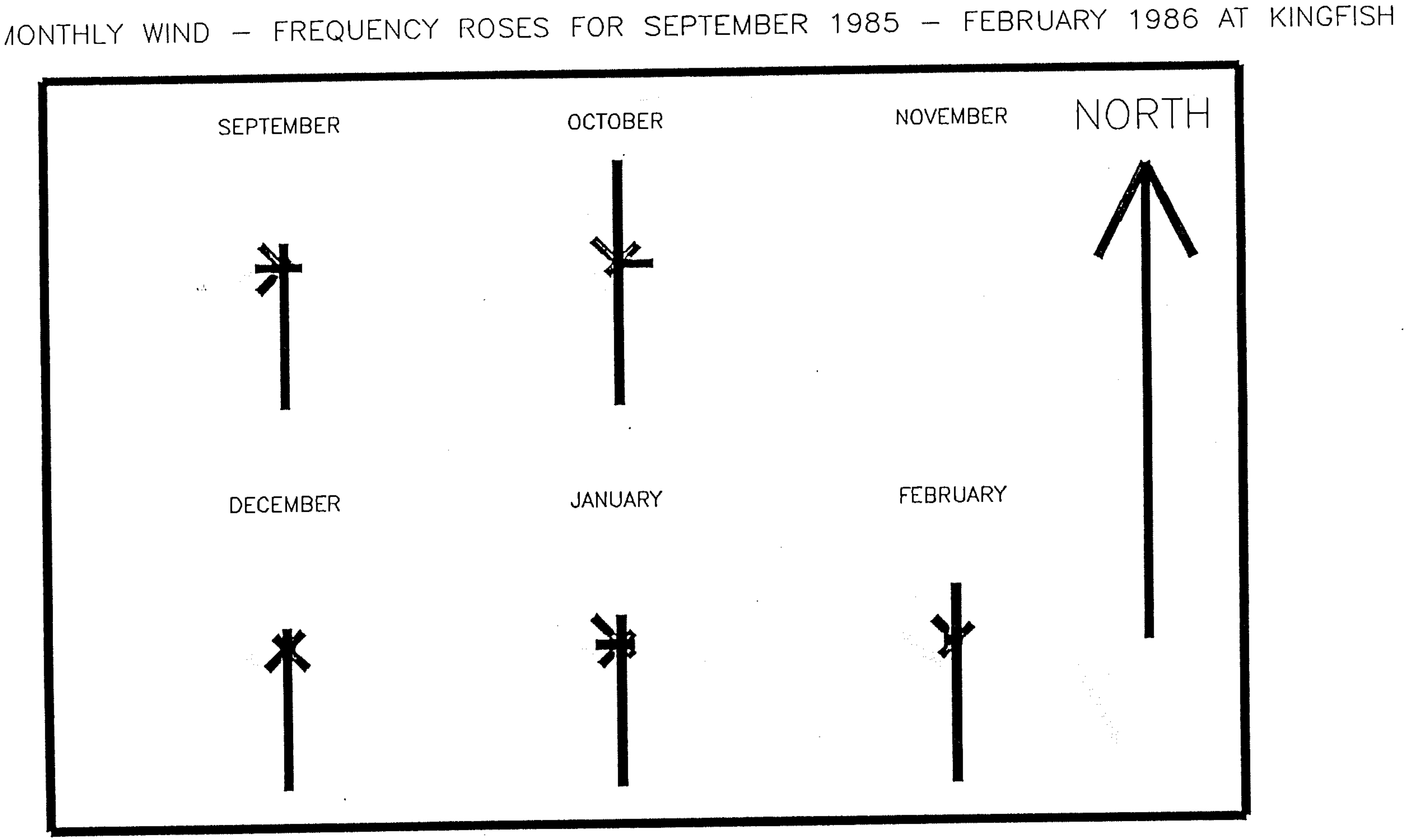

Fig. 2.6a Monthly wind frequency roses for September, 1985 to February 1986 at Kingfish B.

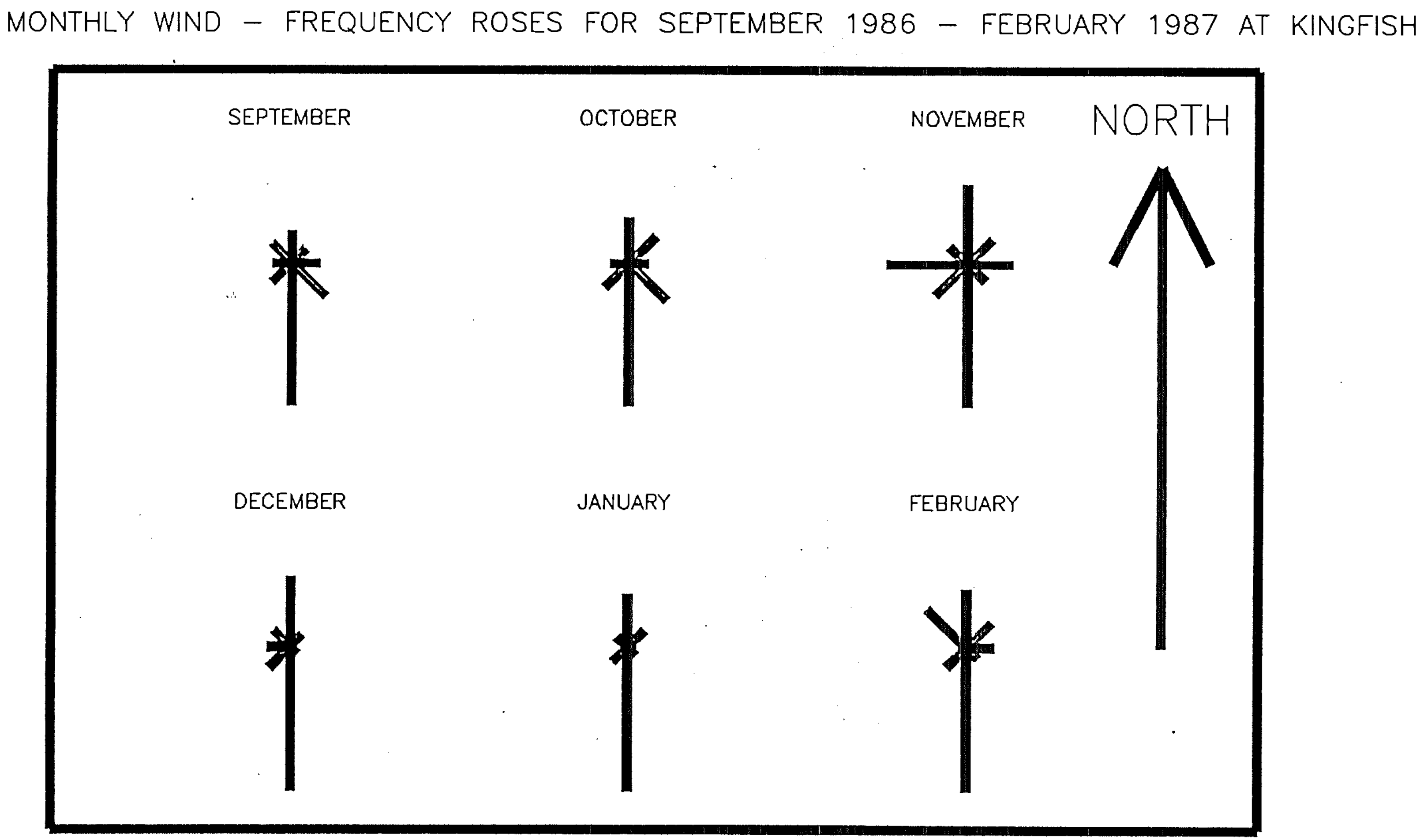

Fig. 2.6b Monthly wind frequency roses for September, 1986 to February 1987 at Kingfish B.

MONTHLY WIND – FREQUENCY ROSES FOR SEPTEMBER 1987 – FEBRUARY 1988 AT KINGFISH

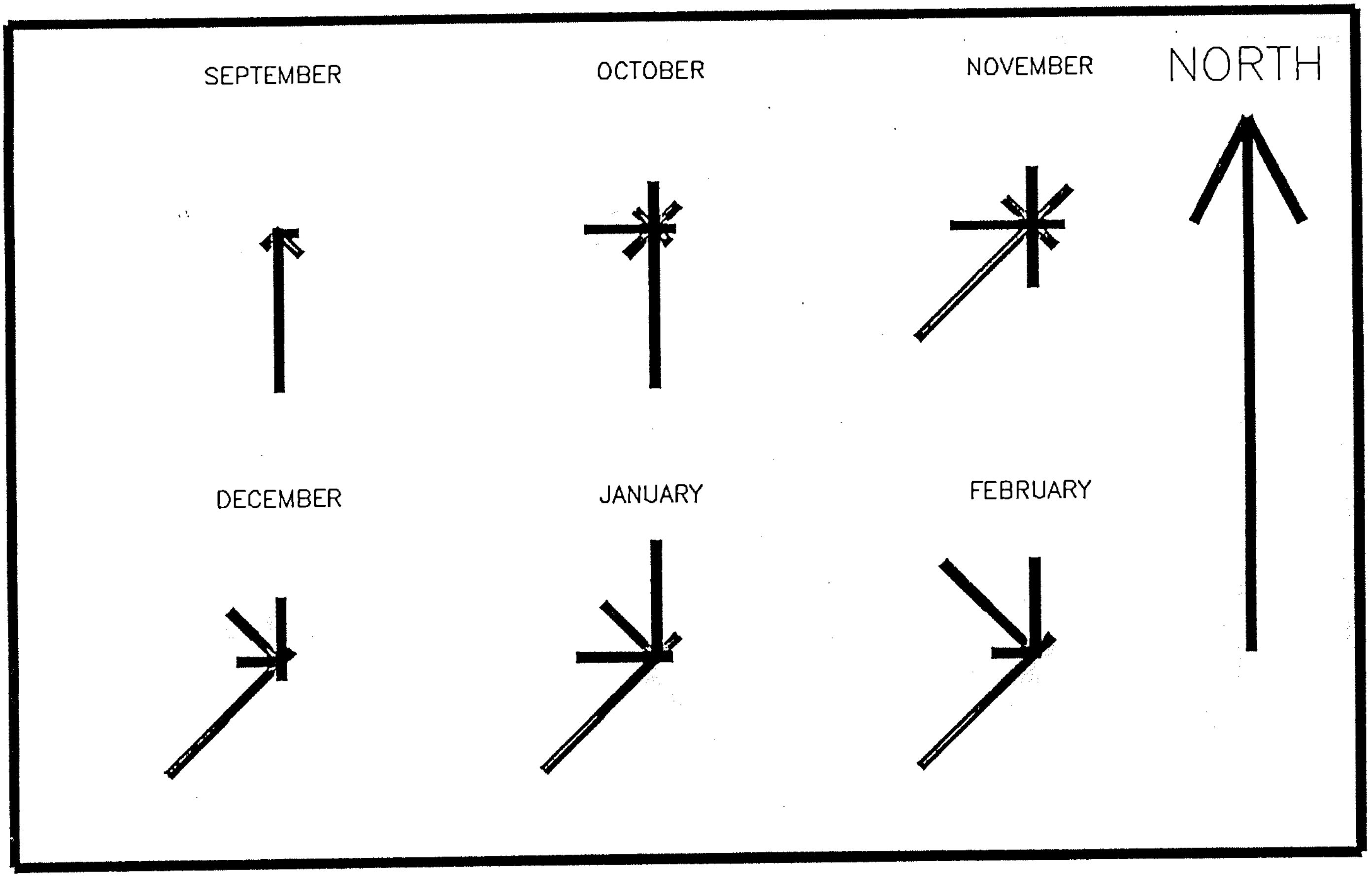

Fig. 2.6c Monthly wind frequency roses for September, 1987 to February 1988 at Kingfish B.

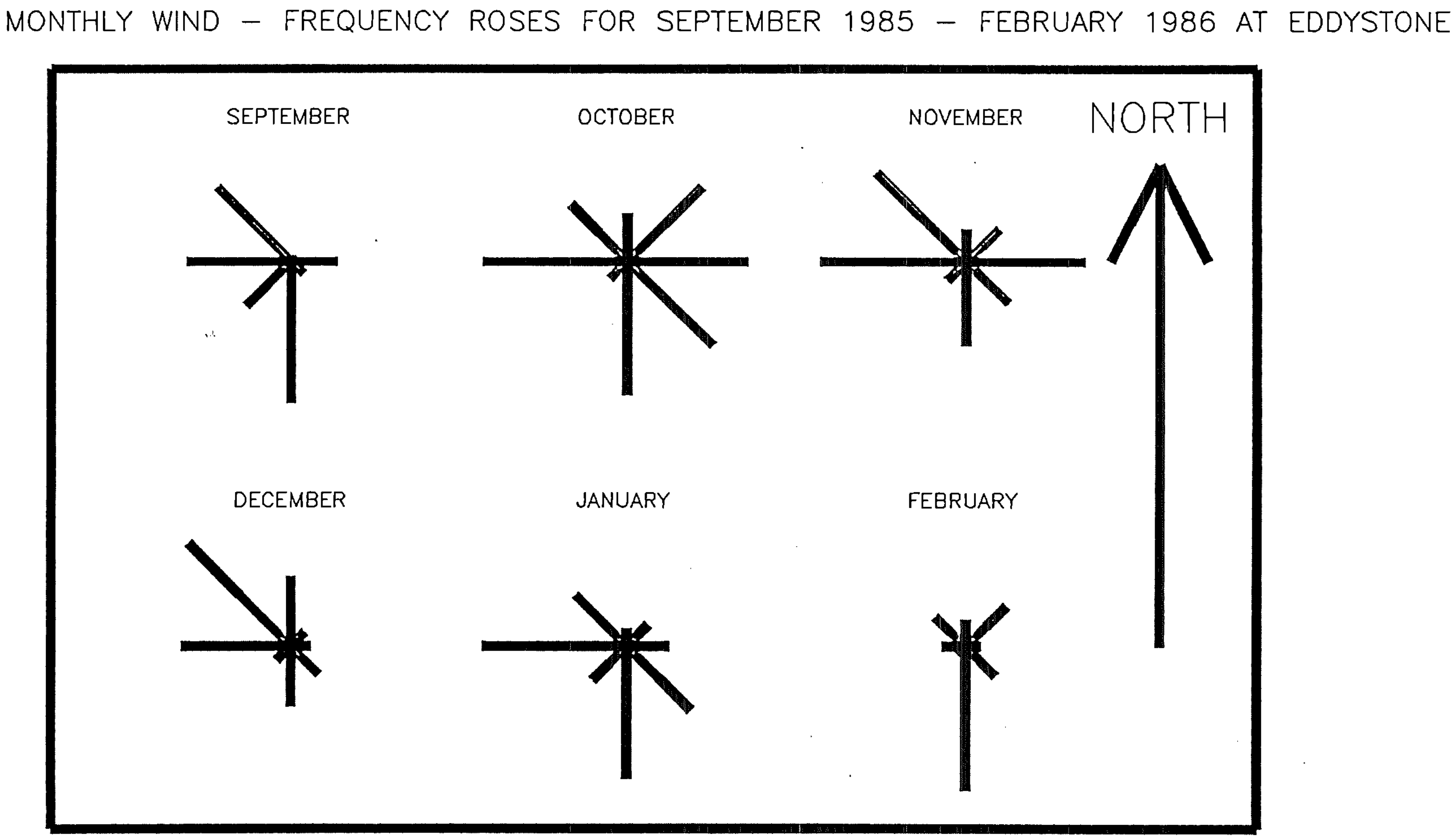

Fig. 2.6d Monthly wind frequency roses for September, 1985 to February 1986 at Eddystone.

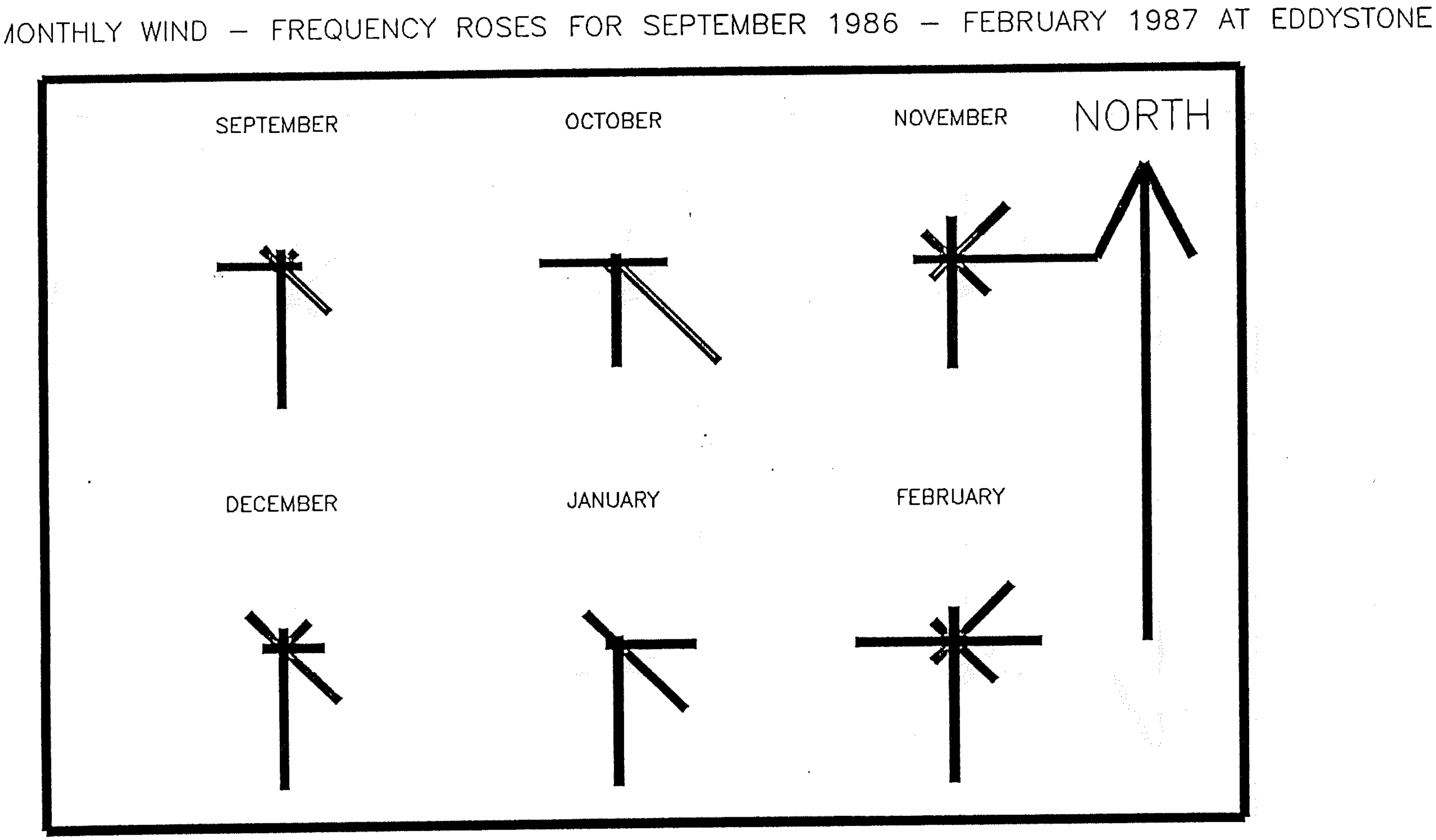

Fig. 2.6e Monthly wind frequency roses for September, 1986 to February 1987 at Eddystone.

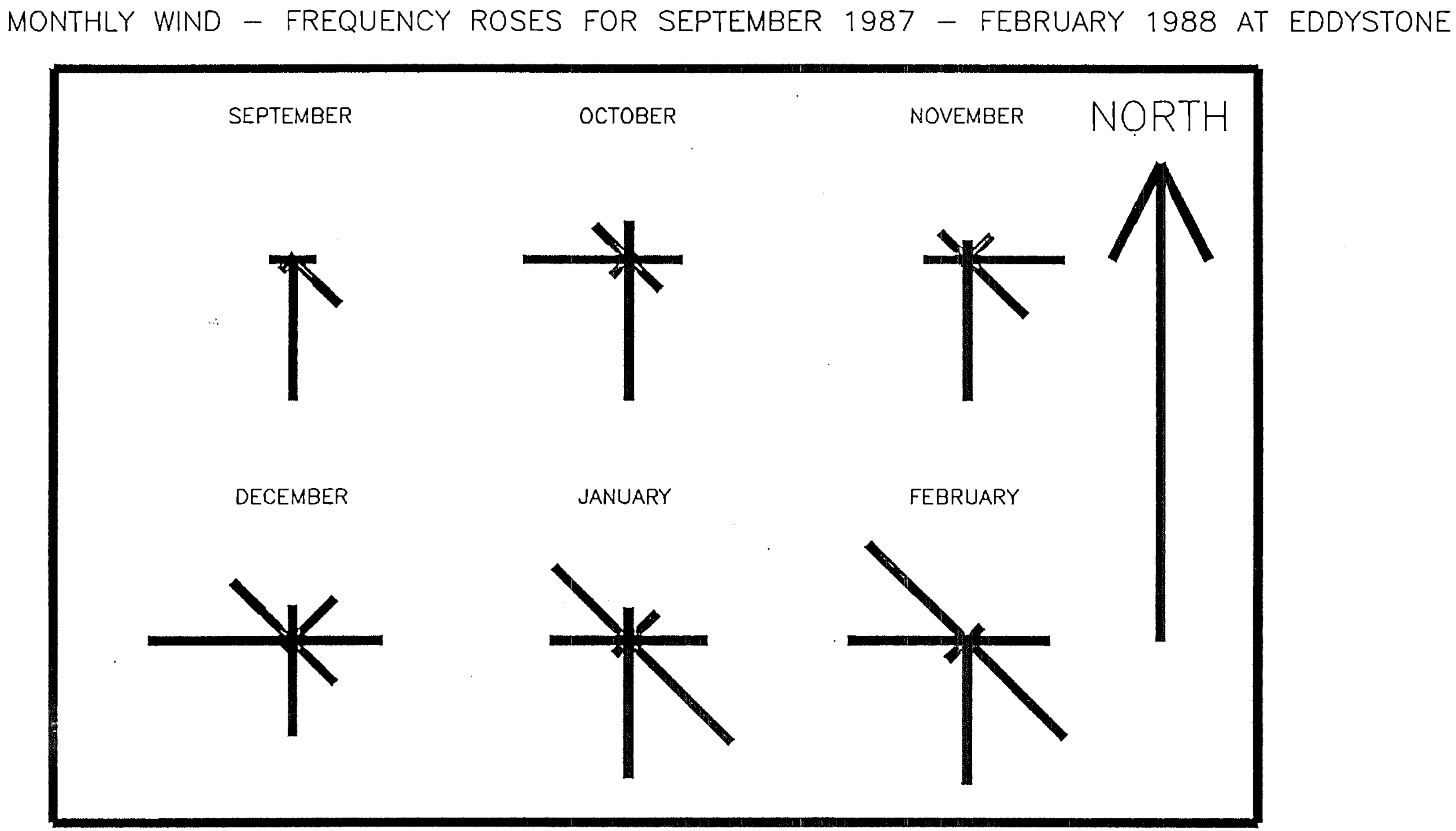

Fig. 2.6f Monthly wind frequency roses for September, 1987 to February 1988 at Eddystone.

MONTHLY WIND – FREQUENCY ROSES FOR SEPTEMBER 1985 – FEBRUARY 1986 AT CURRIE

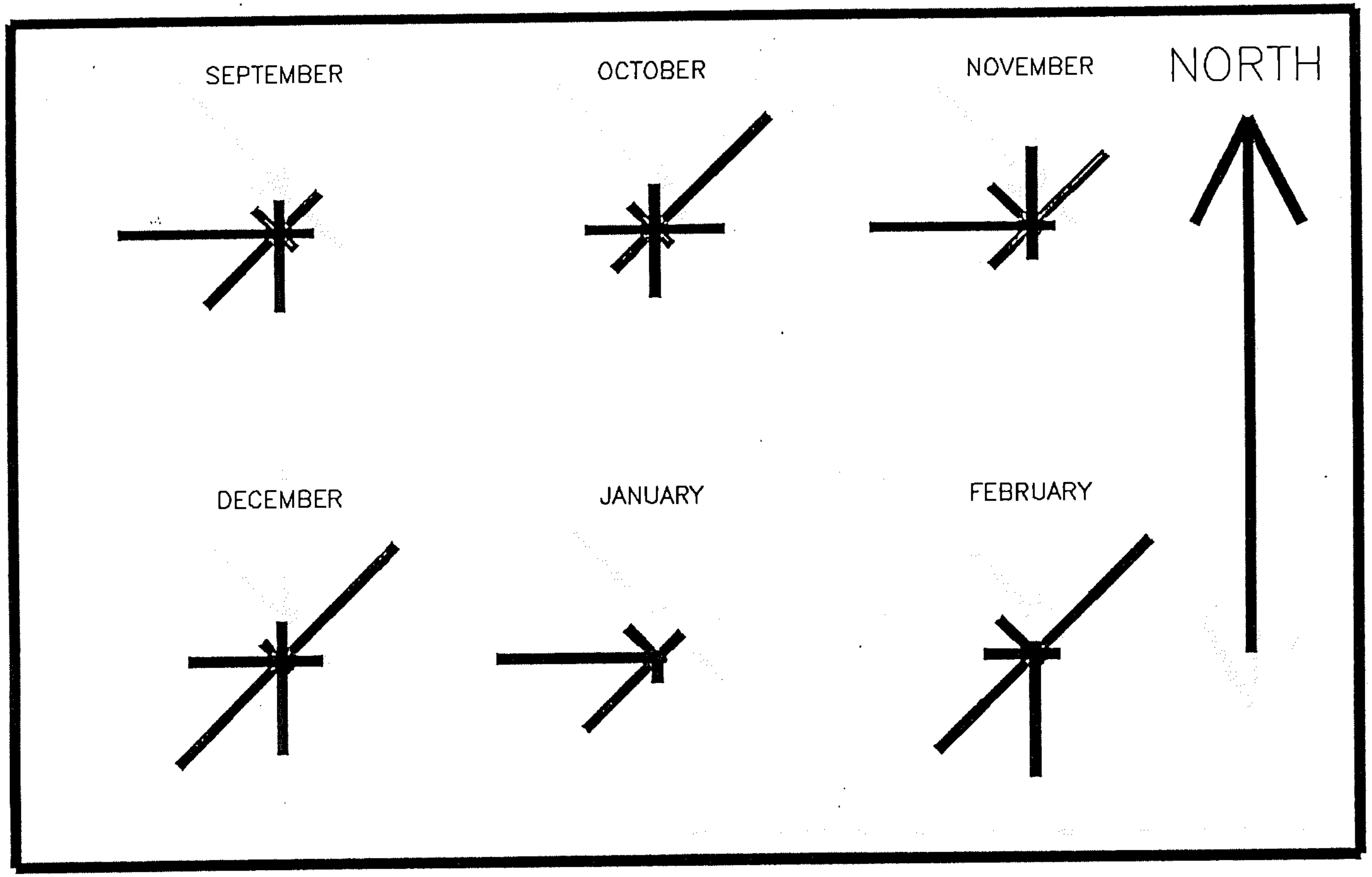

Fig. 2.6g Monthly wind frequency roses for September, 1985 to February 1986 at Currie.

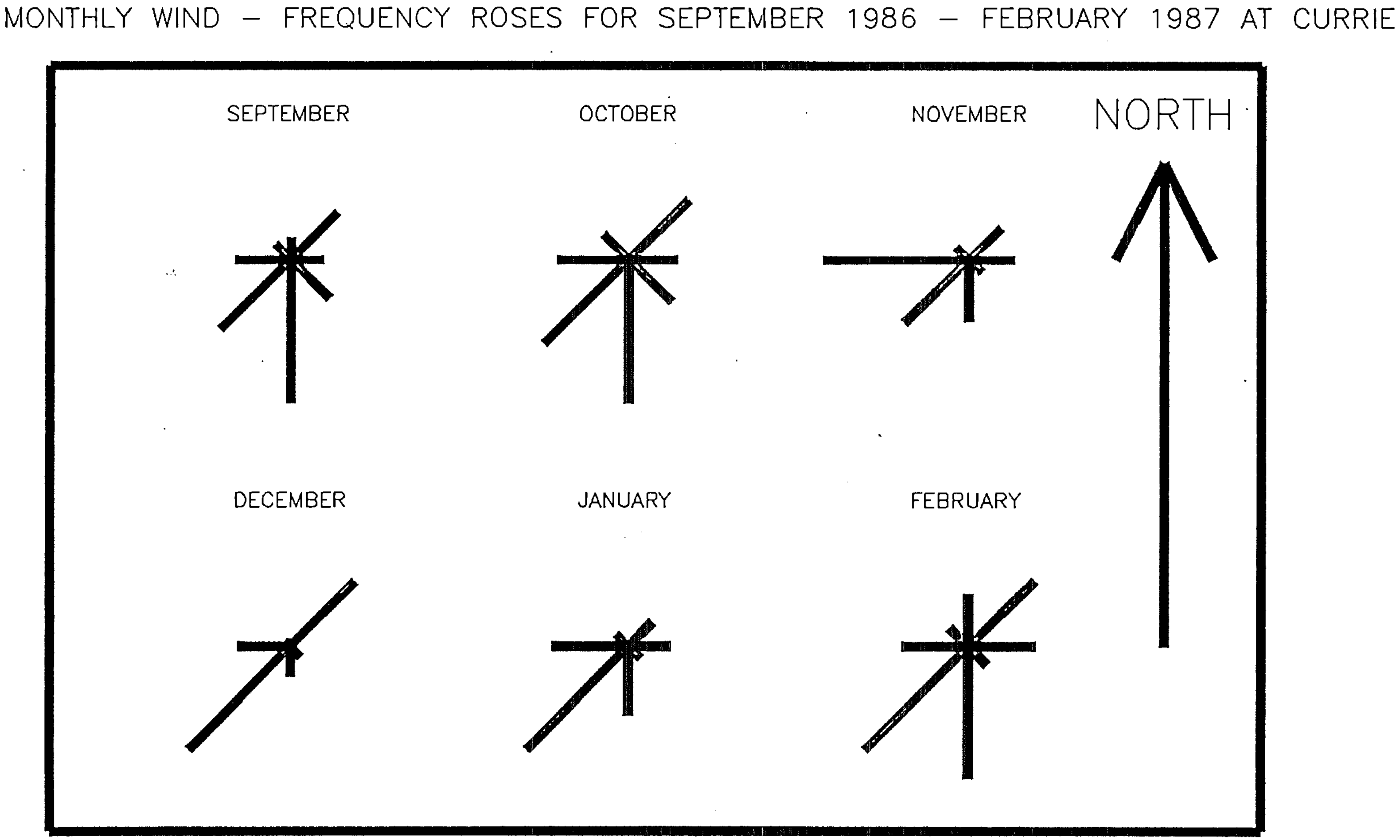

Fig. 2.6h Monthly wind frequency roses for September, 1986 to February 1987 at Currie.

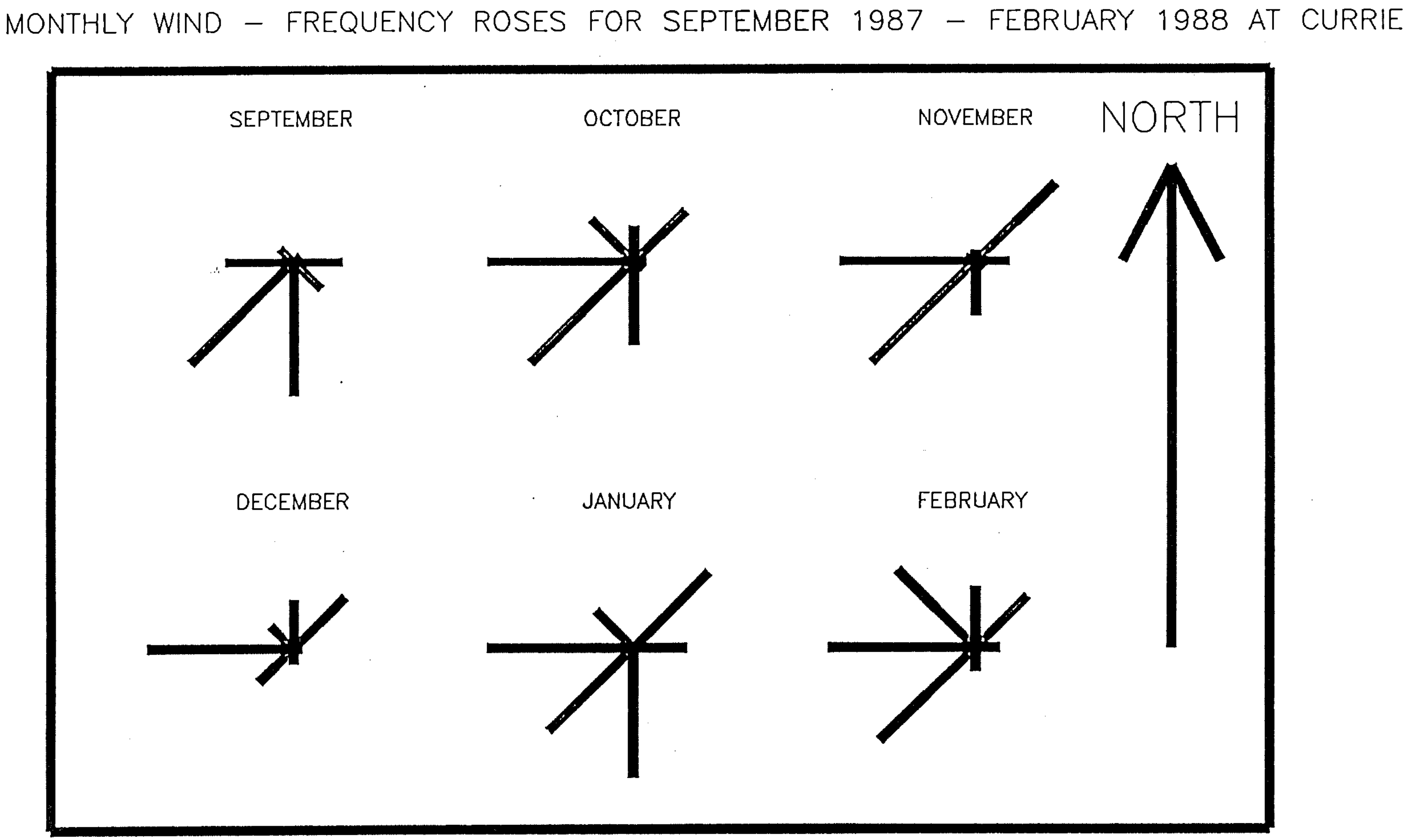

Fig. 2.6i Monthly wind frequency roses for September, 1987 to February 1988 at Currie.

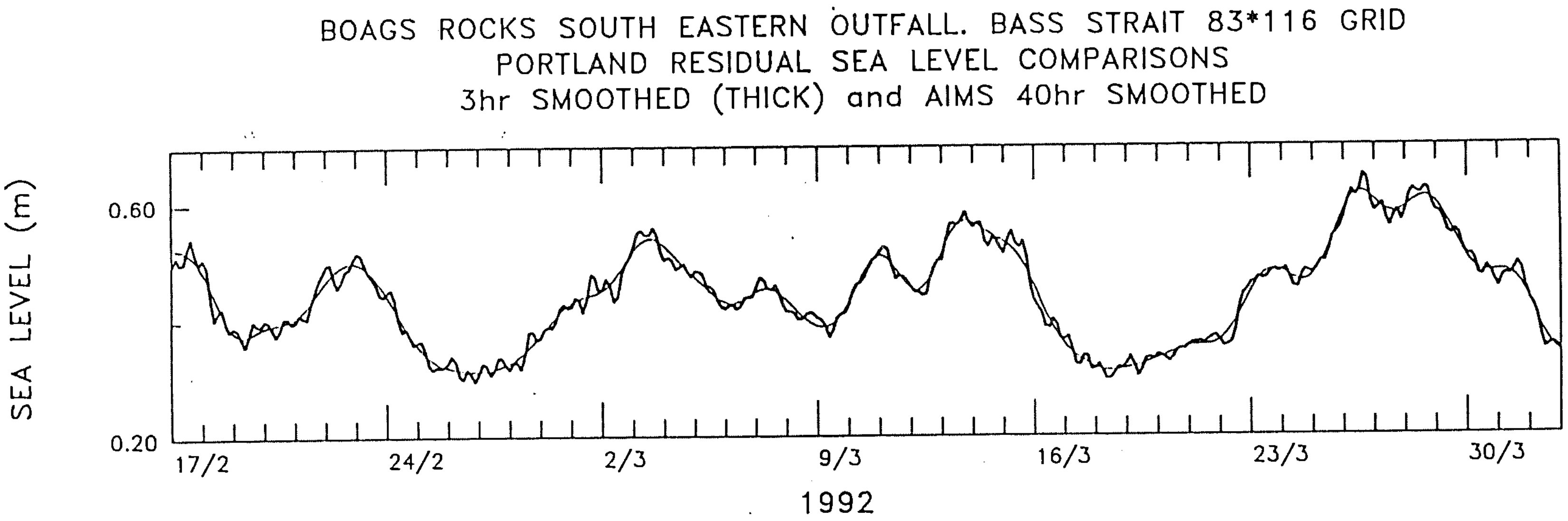

Fig. 2.7 Non-tidal sea levels (smoothed and unsmoothed) at Portland near the western entrance to Bass Strait.

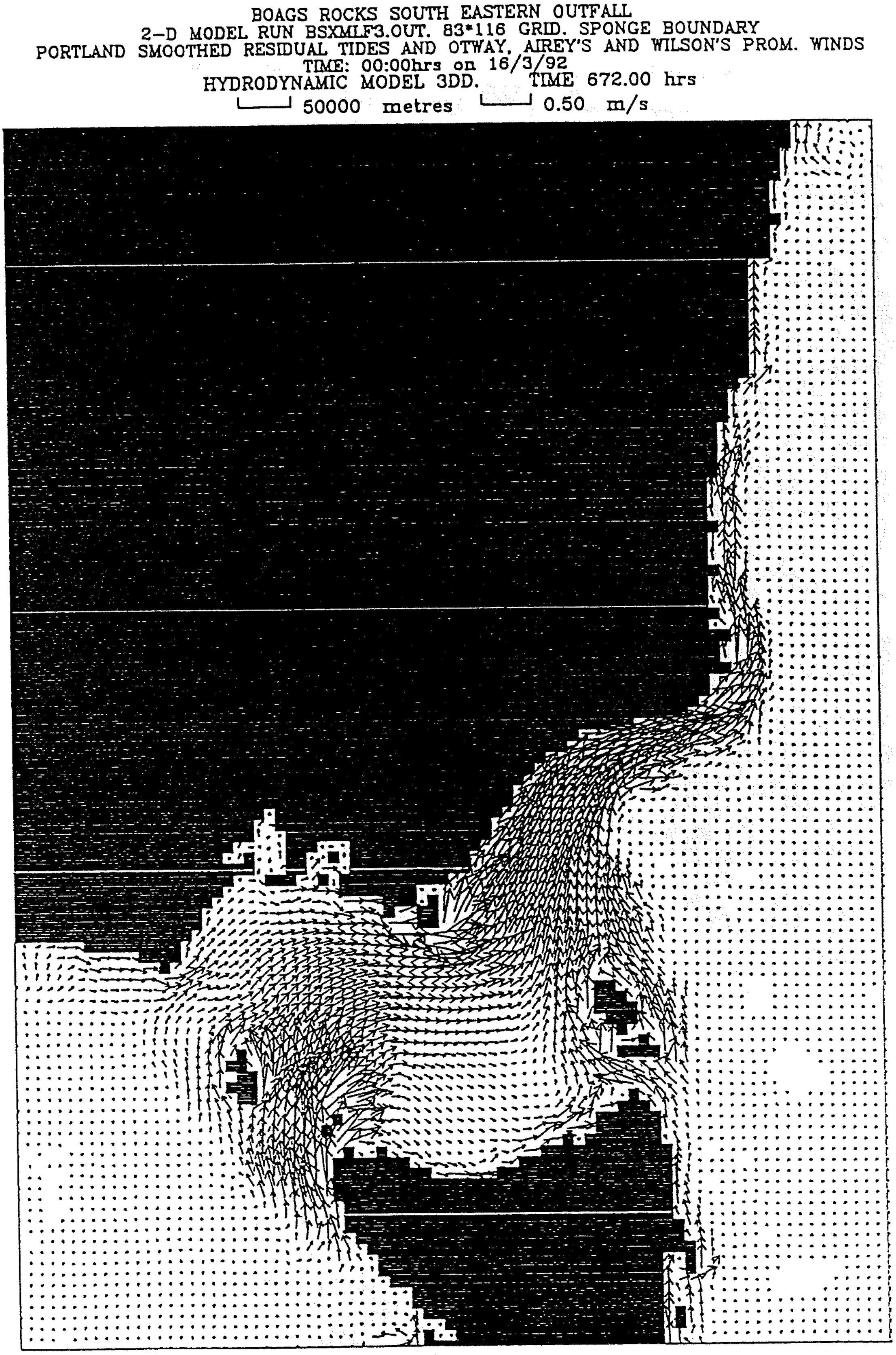

Fig. 2.8a Coastal-trapped wave and wind-driven circulation on March 16, 1992 in Bass Strait and environs.

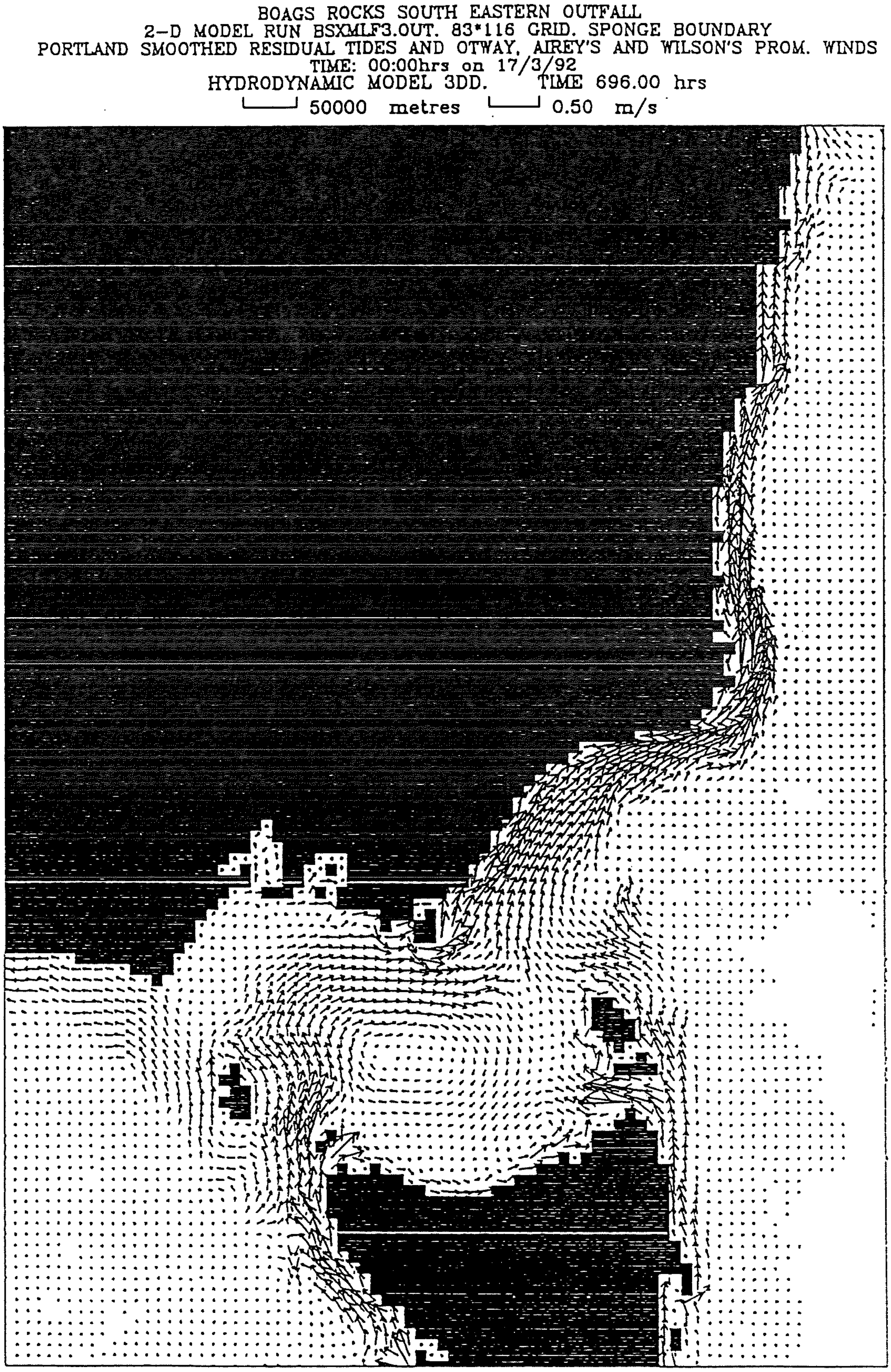

Fig. 2.8b Coastal-trapped wave and wind-driven circulation on March 17, 1992 in Bass Strait and environs.

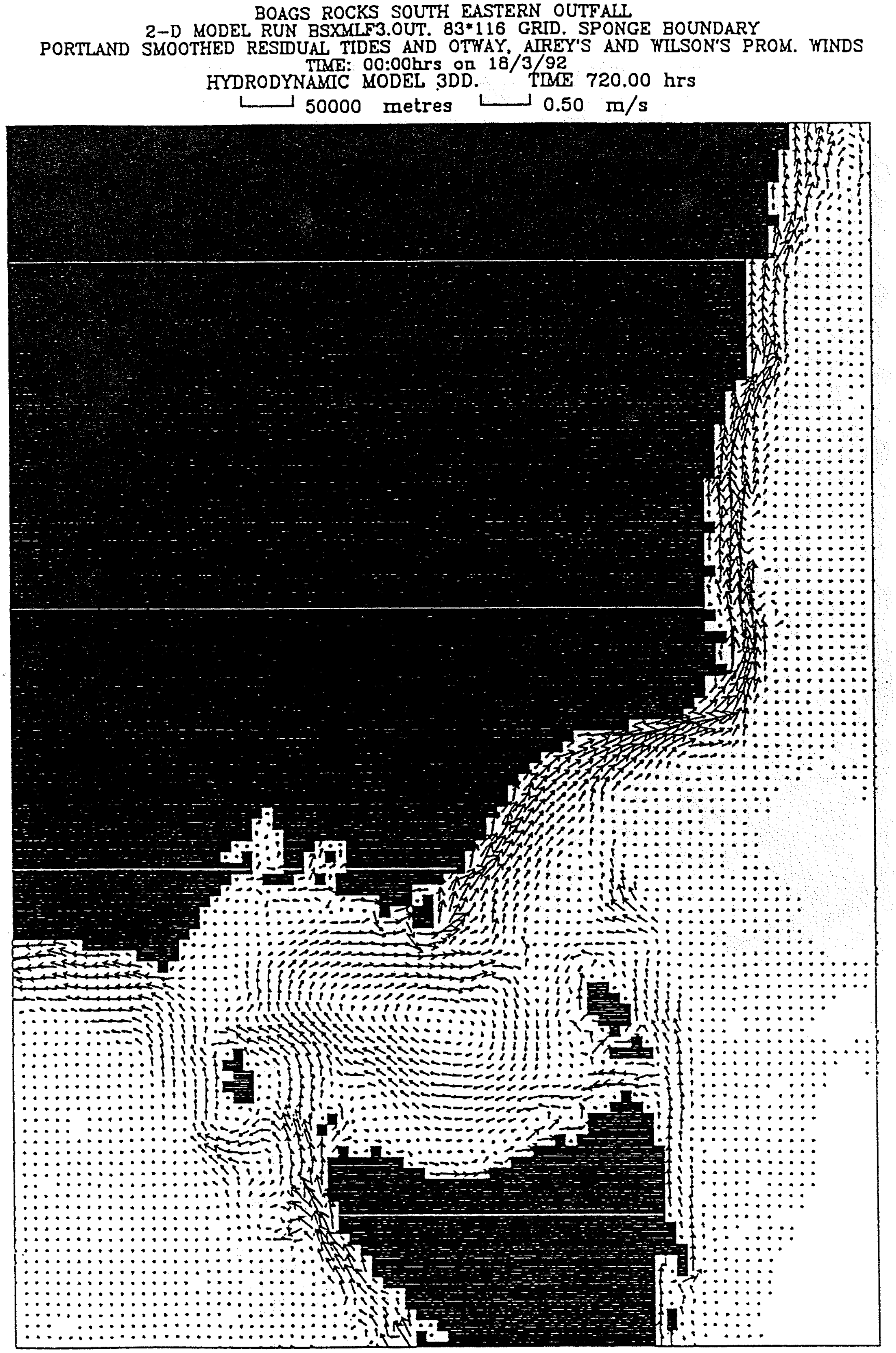

Fig. 2.8c Coastal-trapped wave and wind-driven circulation on March 18, 1992 in Bass Strait and environs.

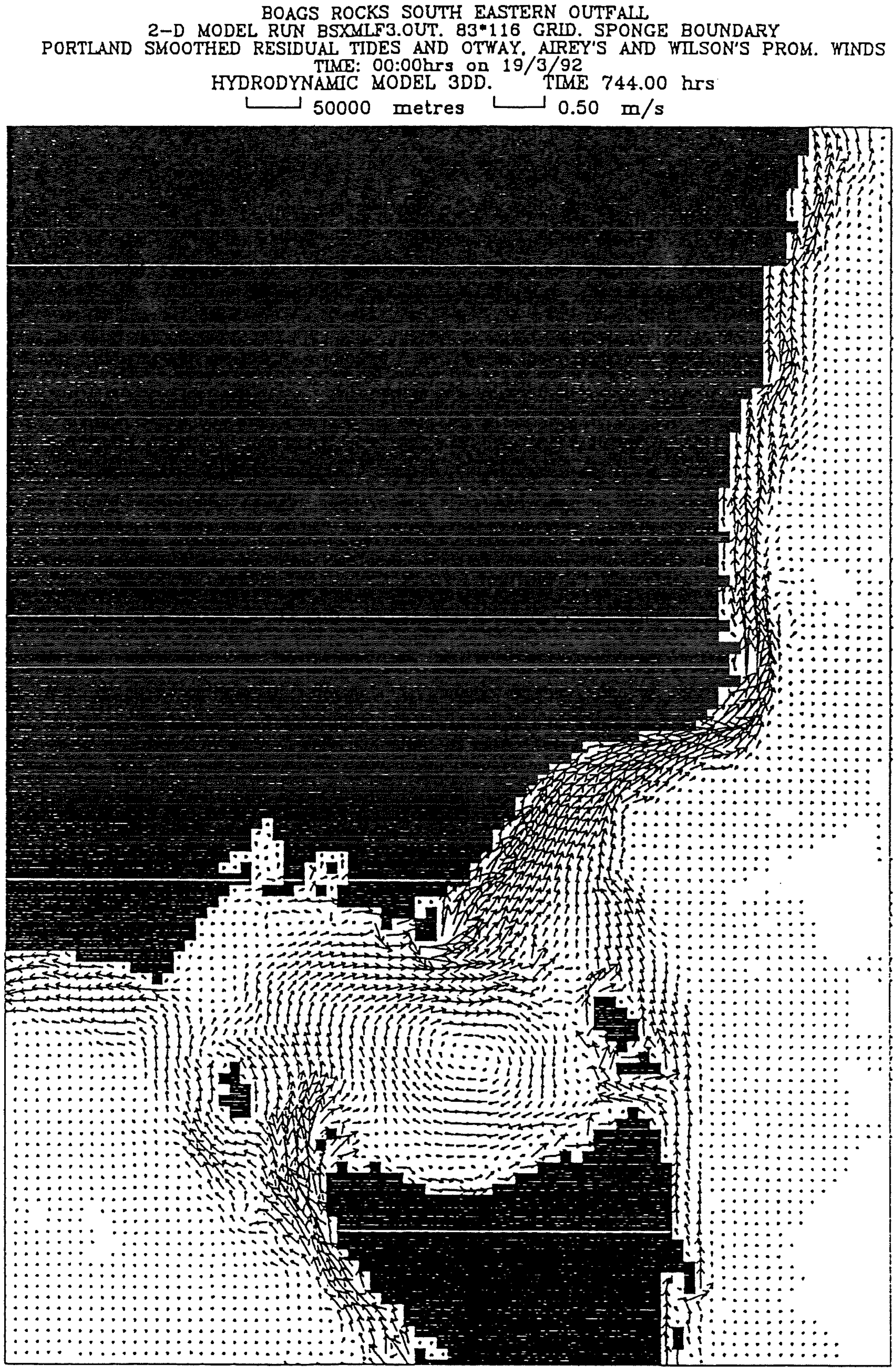

Fig. 2.8d Coastal-trapped wave and wind-driven circulation on March 19, 1992 in Bass Strait and environs.

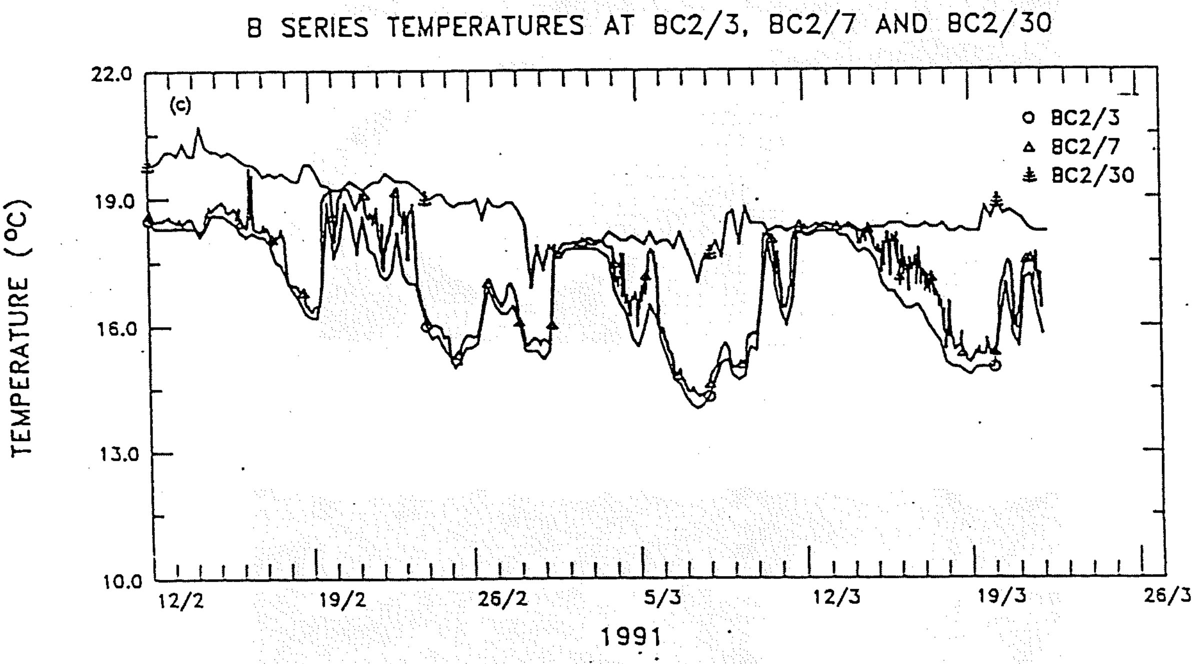

Fig. 2.9 Sea temperatures recorded at 3, 7 and 30 m above the bed in 40 m depth in summer at an East Gippsland site.

BASS STRAIT GRID

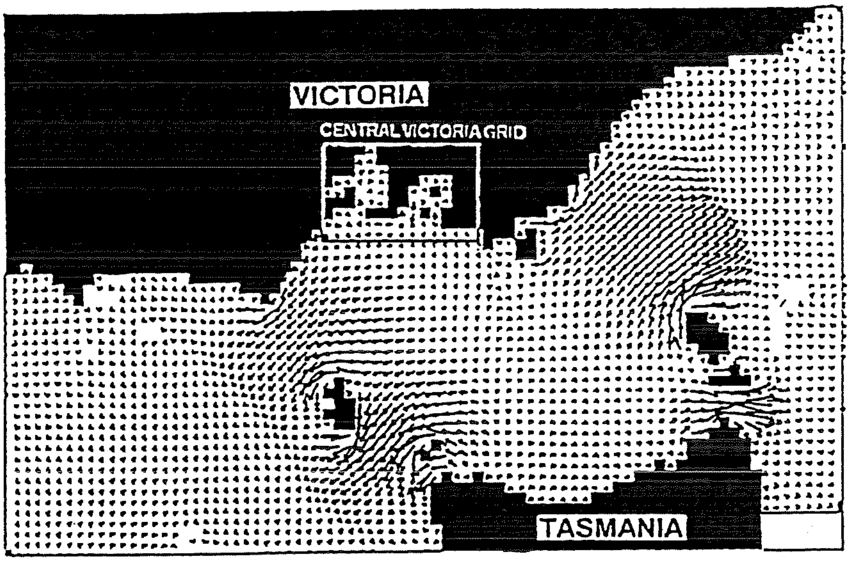

CENTRAL VICTORIA GRID

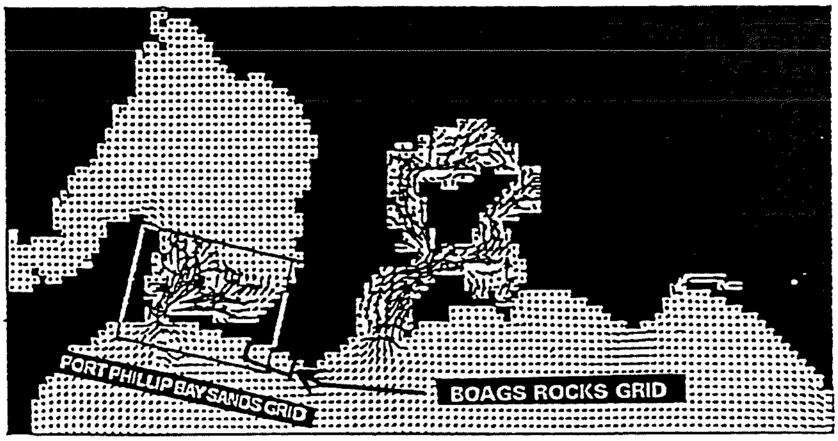

Fig. 3.1 The relationship between the nested numerical model grids

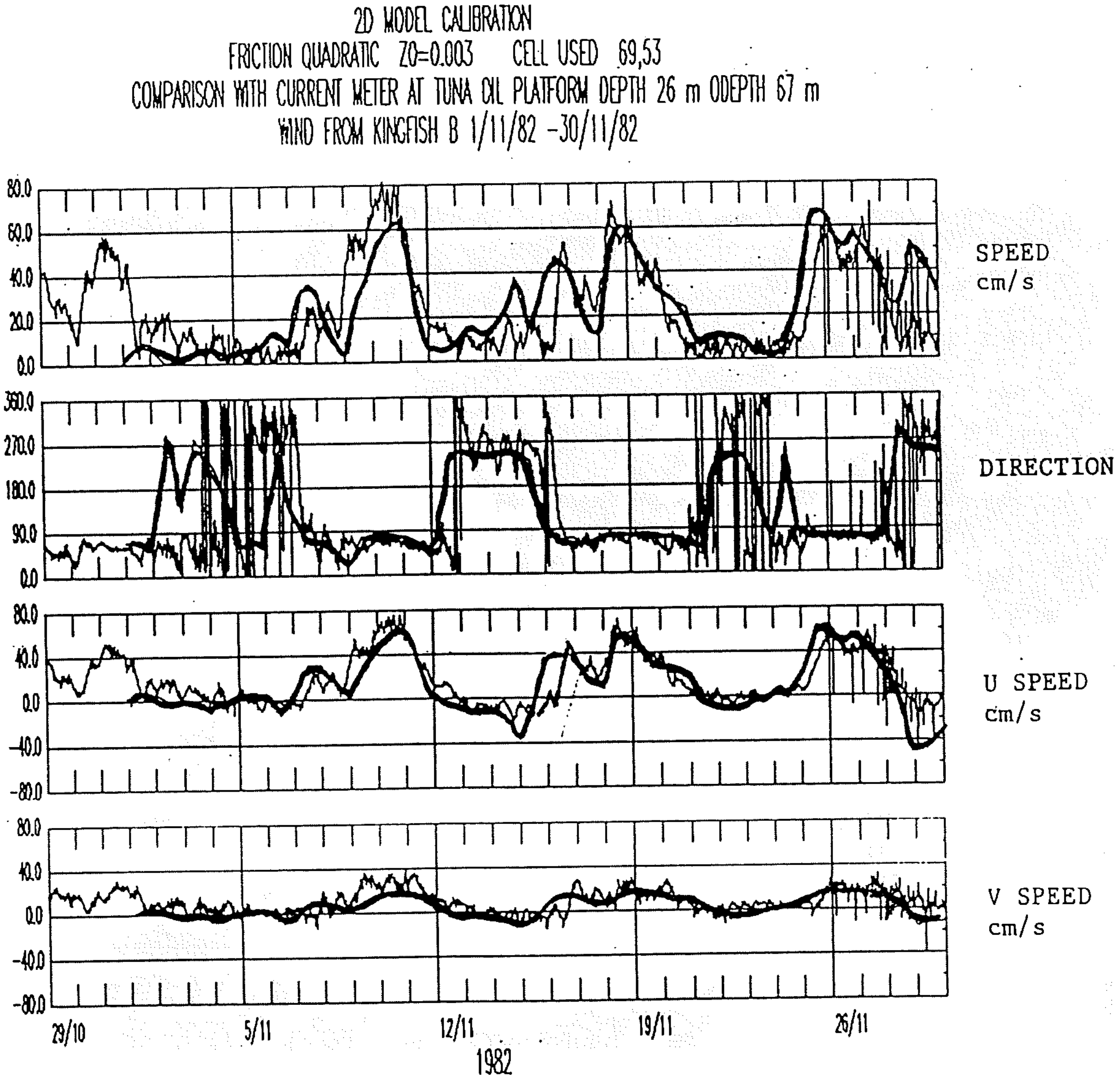

Fig. 3.2 Calibration of the Bass Strait model showing measured and modelled (thick line) currents recorded at Kingfish B.

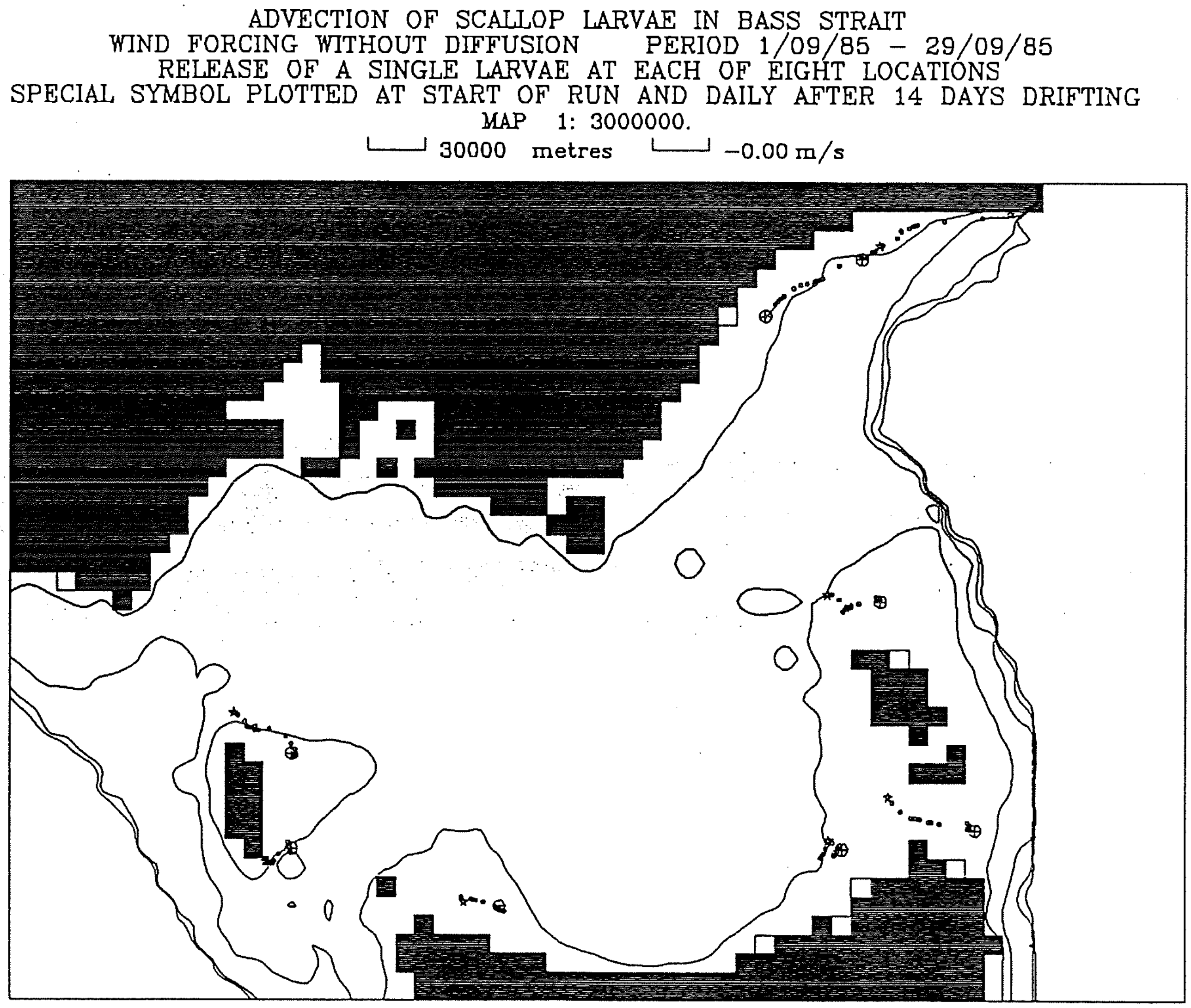

ADVECTION OF SCALLOP LARVAE IN BASS STRAIT
WIND FORCING WITHOUT DIFFUSION PERIOD 1/09/85 - 29/09/85
RELEASE OF A SINGLE LARVAE AT EACH OF EIGHT LOCATIONS
SPECIAL SYMBOL PLOTTED AT START OF RUN AND DAILY AFTER 14 DAYS DRIFTING
MAP 1: 3000000.

Fig. 4.1a Pelagic excursions from 8 modern beds over the 28 day period from September 1, 1985. The large crossed circle shows the release point and the straight line shows the excursion over the first non-viable 14 days. The small circles then show the positions at daily intervals in the 14-28 day interval, while the star shows the final position at the end of the 28 day pelagic period.

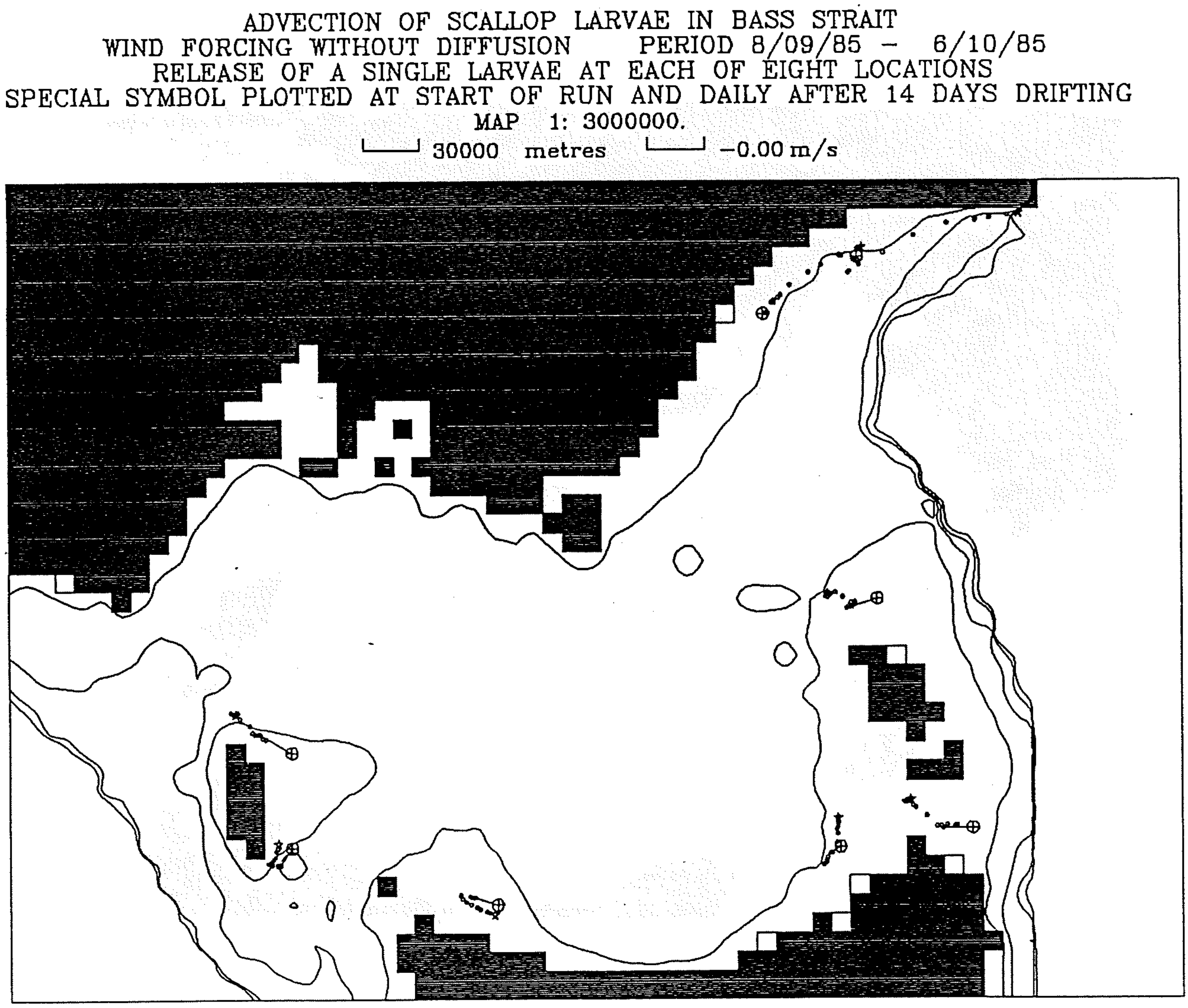

ADVECTION OF SCALLOP LARVAE IN BASS STRAIT
WIND FORCING WITHOUT DIFFUSION PERIOD 8/09/85 - 6/10/85
RELEASE OF A SINGLE LARVAE AT EACH OF EIGHT LOCATIONS
SPECIAL SYMBOL PLOTTED AT START OF RUN AND DAILY AFTER 14 DAYS DRIFTING
MAP 1: 3000000.

Fig. 4.1b Pelagic excursions from 8 modern beds over the 28 day period from September 8, 1985. The large crossed circle shows the release point and the straight line shows the excursion over the first non-viable 14 days. The small circles then show the positions at daily intervals in the 14-28 day interval, while the star shows the final position at the end of the 28 day pelagic period.

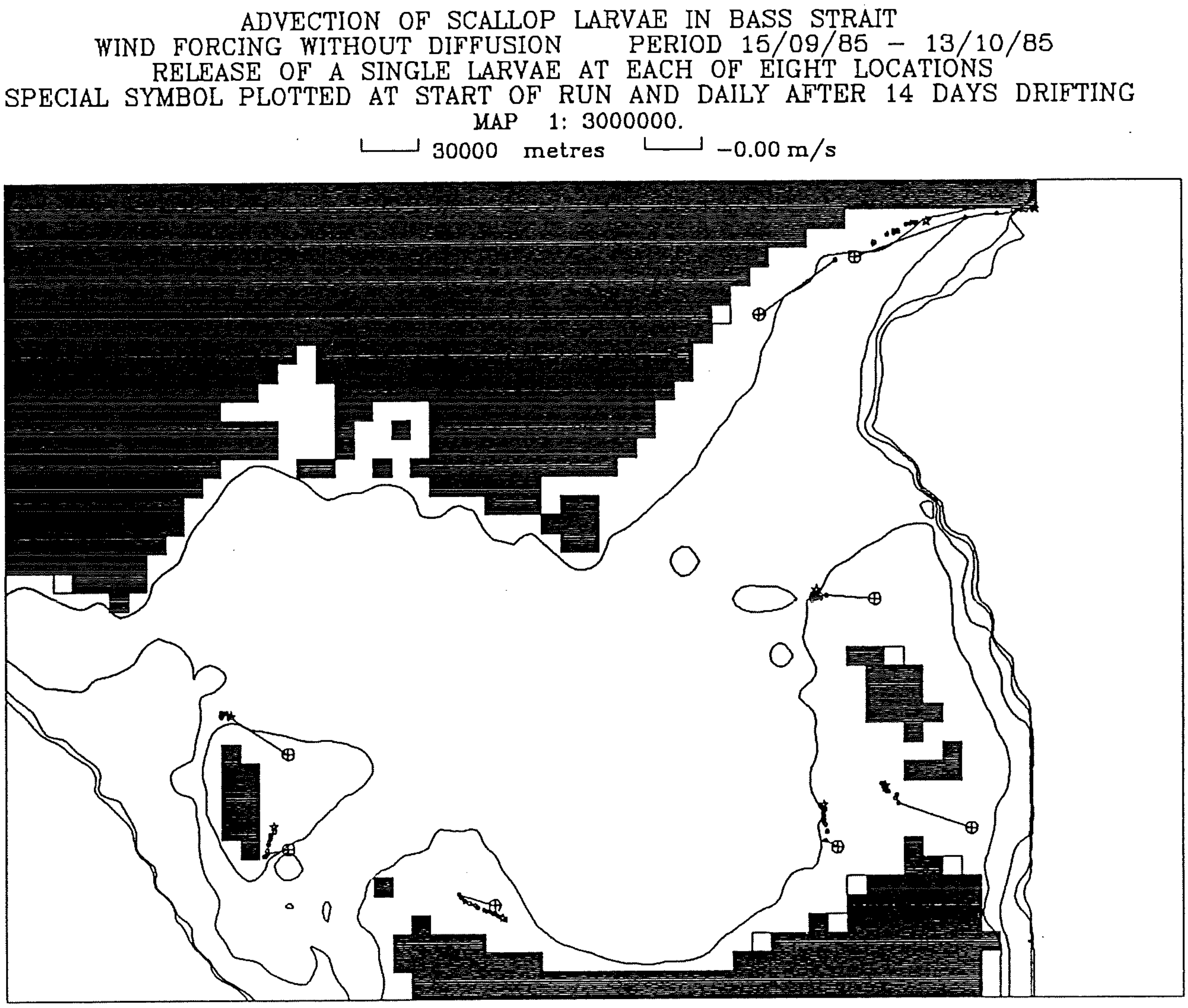

Fig. 4.1c Pelagic excursions from 8 modern beds over the 28 day period from September 15, 1985. The large crossed circle shows the release point and the straight line shows the excursion over the first non-viable 14 days. The small circles then show the positions at daily intervals in the 14-28 day interval, while the star shows the final position at the end of the 28 day pelagic period.

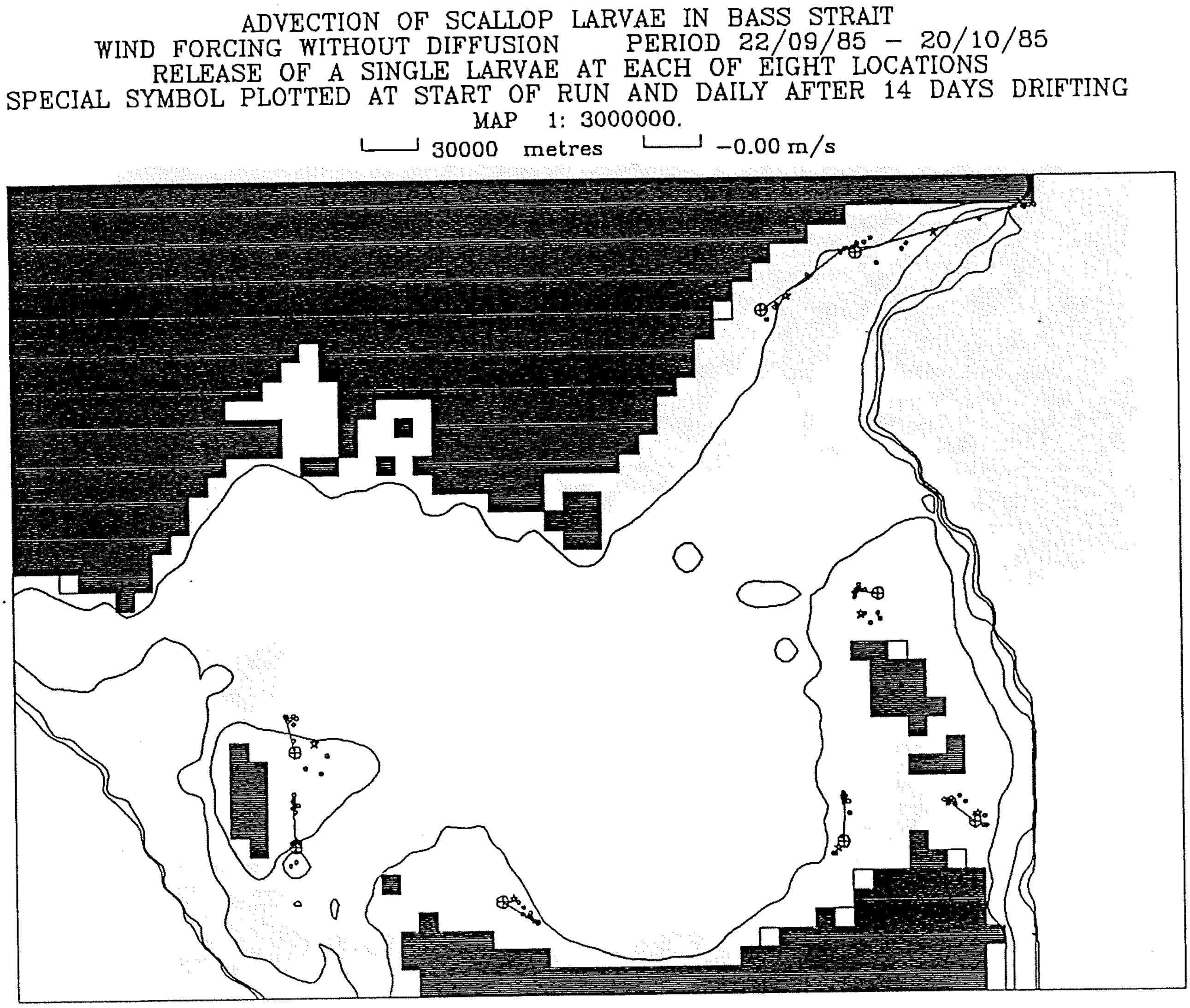

Fig. 4.1d Pelagic excursions from 8 modern beds over the 28 day period from September 22, 1985. The large crossed circle shows the release point and the straight line shows the excursion over the first non-viable 14 days. The small circles then show the positions at daily intervals in the 14-28 day interval, while the star shows the final position at the end of the 28 day pelagic period.

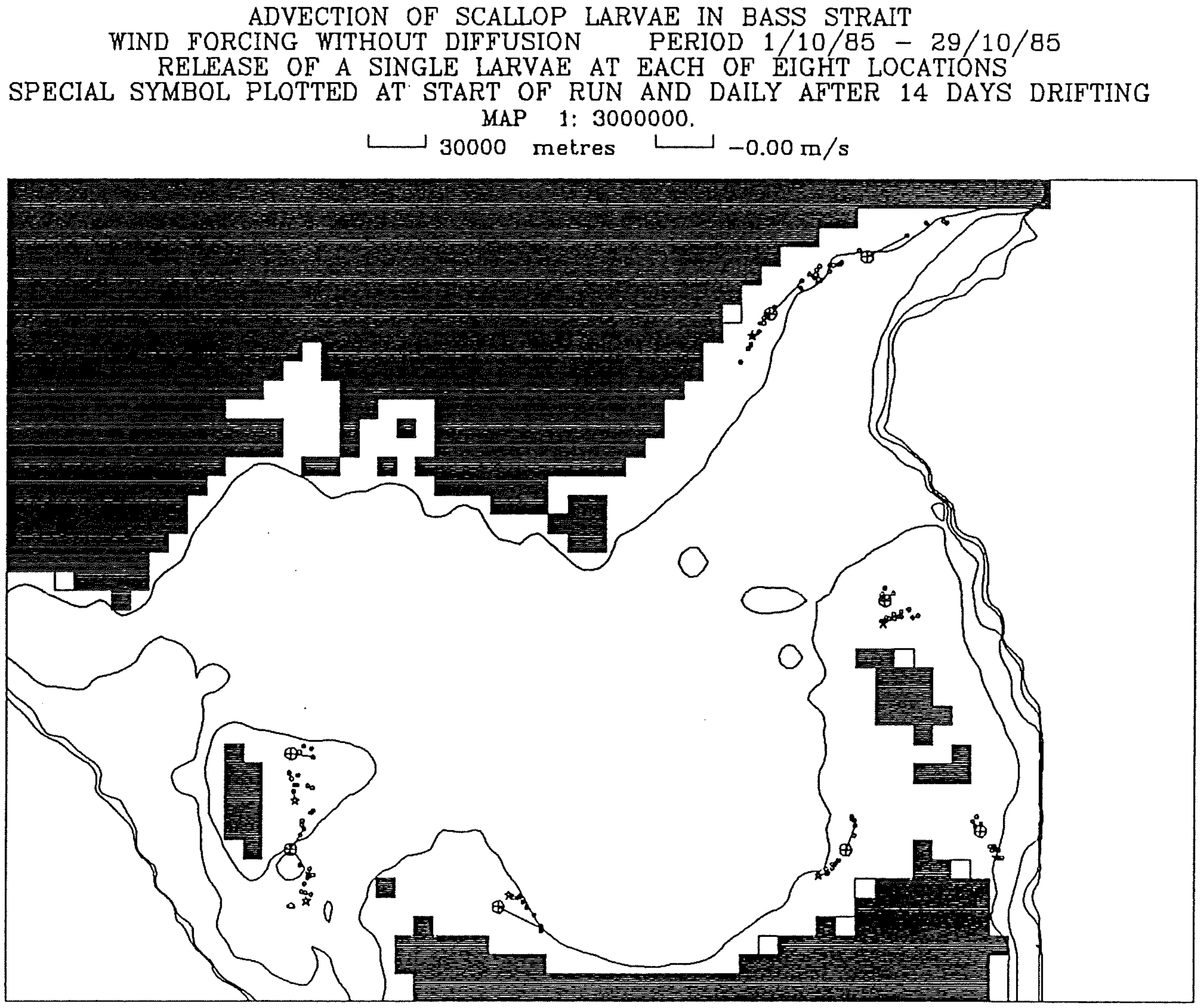
ADVECTION OF SCALLOP LARVAE IN BASS STRAIT
WIND FORCING WITHOUT DIFFUSION PERIOD 1/10/85 - 29/10/85
RELEASE OF A SINGLE LARVAE AT EACH OF EIGHT LOCATIONS
SPECIAL SYMBOL PLOTTED AT START OF RUN AND DAILY AFTER 14 DAYS DRIFTING
MAP 1: 3000000.

Fig. 4.1e Pelagic excursions from 8 modern beds over the 28 day period from October 1, 1985. The large crossed circle shows the release point and the straight line shows the excursion over the first non-viable 14 days. The small circles then show the positions at daily intervals in the 14-28 day interval, while the star shows the final position at the end of the 28 day pelagic period.

ADVECTION OF SCALLOP LARVAE IN BASS STRAIT
WIND FORCING WITHOUT DIFFUSION PERIOD 8/10/85 - 5/11/85
RELEASE OF A SINGLE LARVAE AT EACH OF EIGHT LOCATIONS
SPECIAL SYMBOL PLOTTED AT START OF RUN AND DAILY AFTER 14 DAYS DRIFTING
MAP 1: 3000000.
30000 metres −0.00 m/s

Fig. 4.1f Pelagic excursions from 8 modern beds over the 28 day period from October 8, 1985. The large crossed circle shows the release point and the straight line shows the excursion over the first non-viable 14 days. The small circles then show the positions at daily intervals in the 14-28 day interval, while the star shows the final position at the end of the 28 day pelagic period.

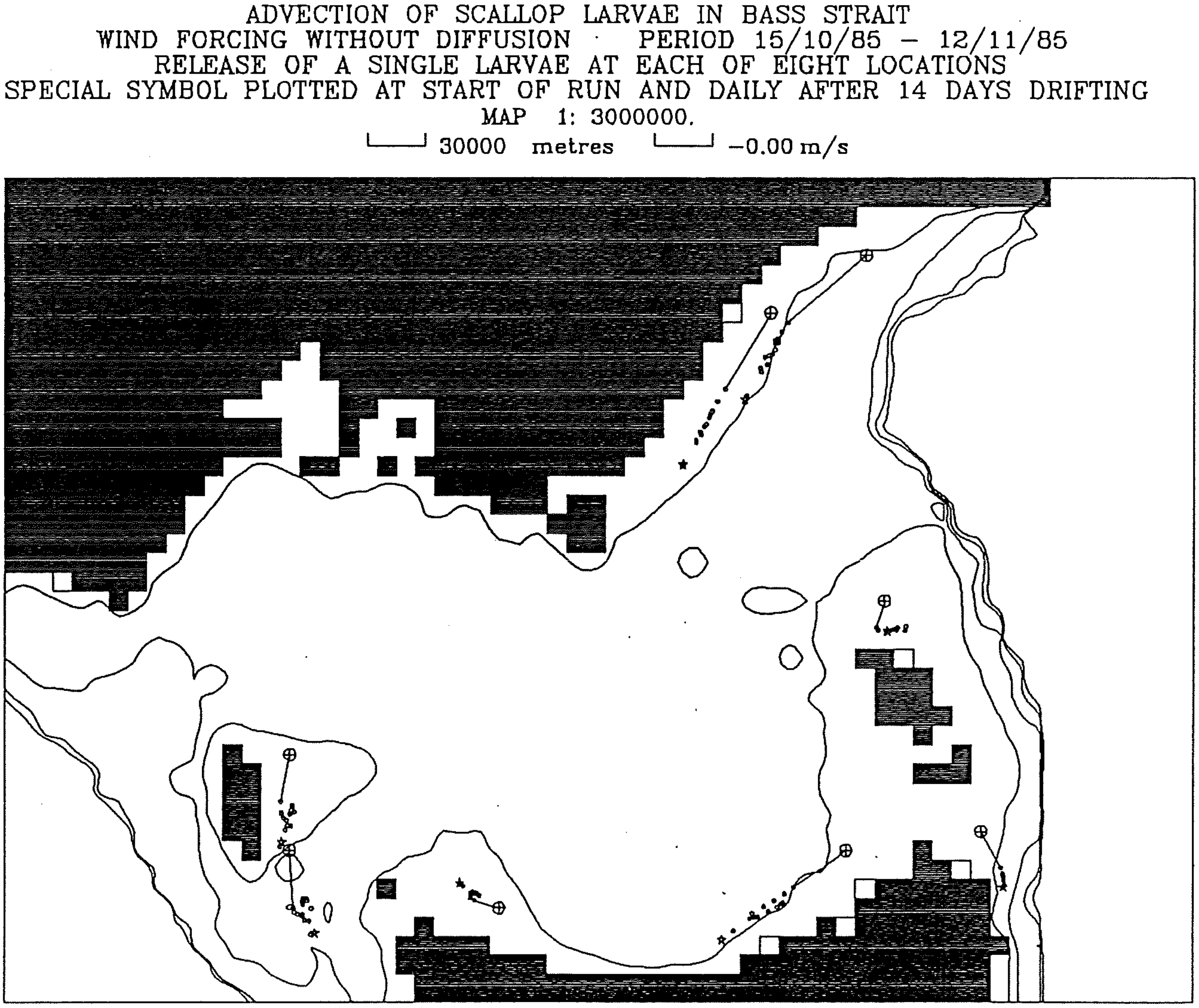

Fig. 4.1g Pelagic excursions from 8 modern beds over the 28 day period from October 15, 1985. The large crossed circle shows the release point and the straight line shows the excursion over the first non-viable 14 days. The small circles then show the positions at daily intervals in the 14-28 day interval, while the star shows the final position at the end of the 28 day pelagic period.

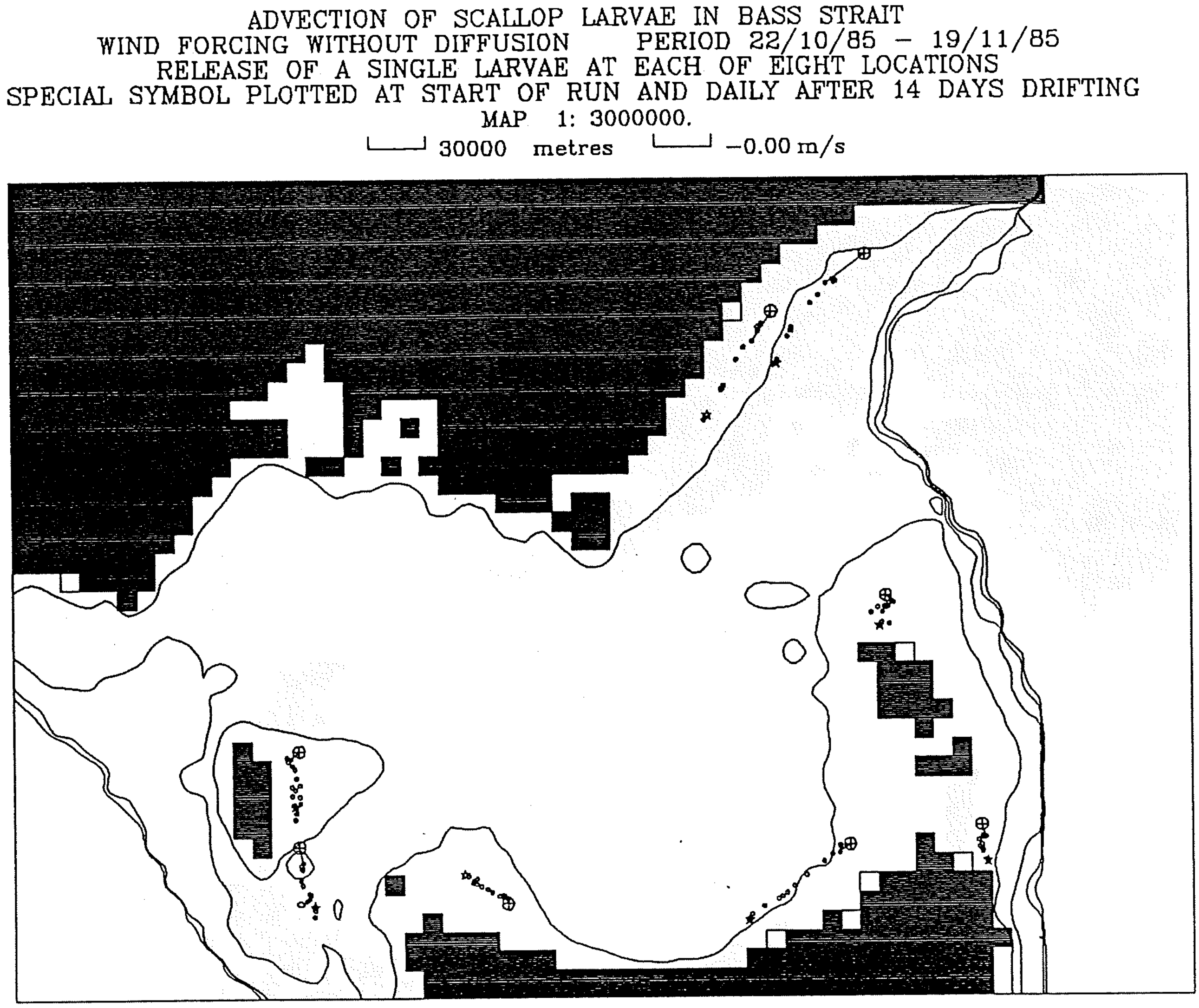

Fig. 4.1h Pelagic excursions from 8 modern beds over the 28 day period from October 22, 1985. The large crossed circle shows the release point and the straight line shows the excursion over the first non-viable 14 days. The small circles then show the positions at daily intervals in the 14-28 day interval, while the star shows the final position at the end of the 28 day pelagic period.

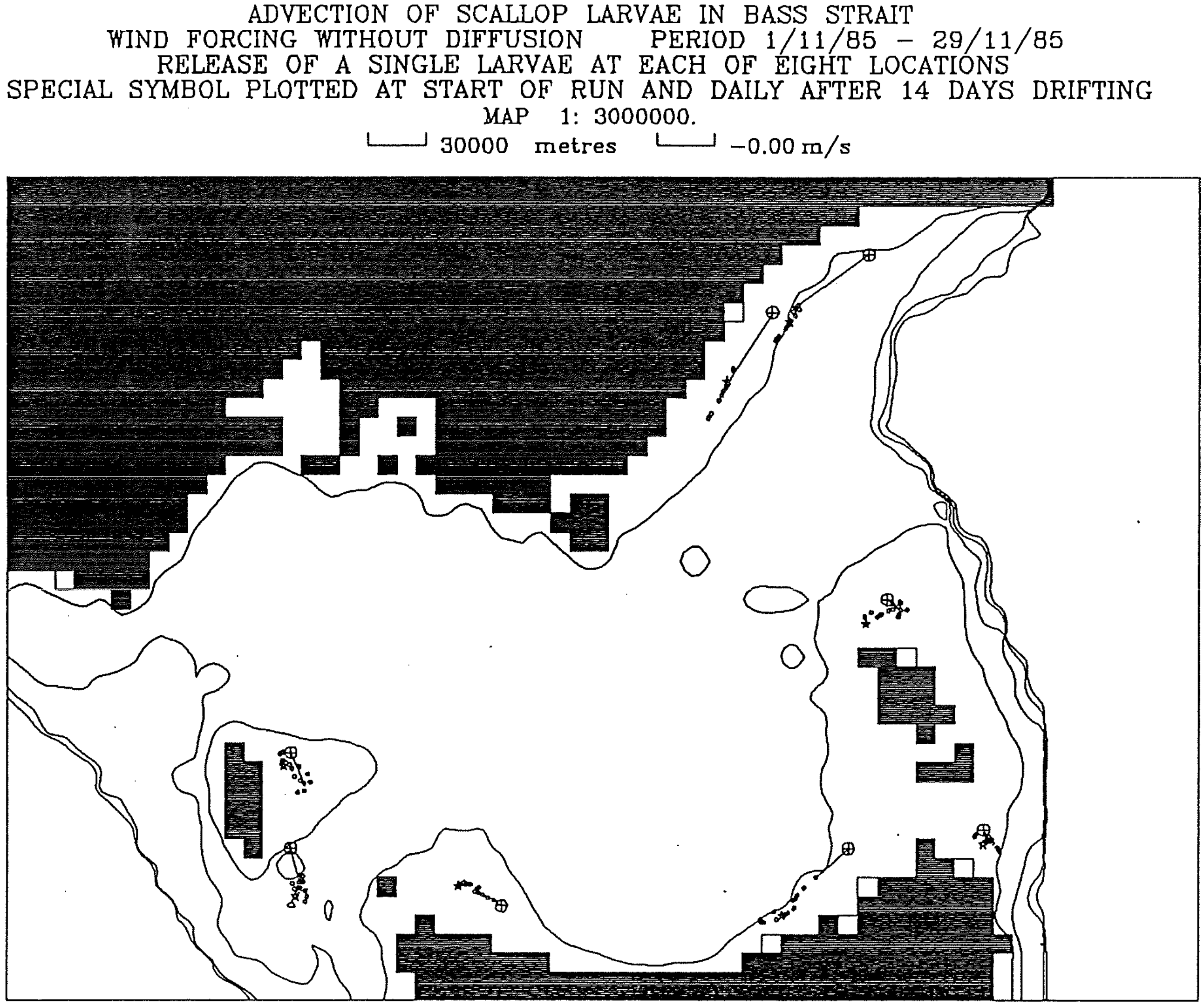

Fig. 4.1i Pelagic excursions from 8 modern beds over the 28 day period from November 1, 1985. The large crossed circle shows the release point and the straight line shows the excursion over the first non-viable 14 days. The small circles then show the positions at daily intervals in the 14-28 day interval, while the star shows the final position at the end of the 28 day pelagic period.

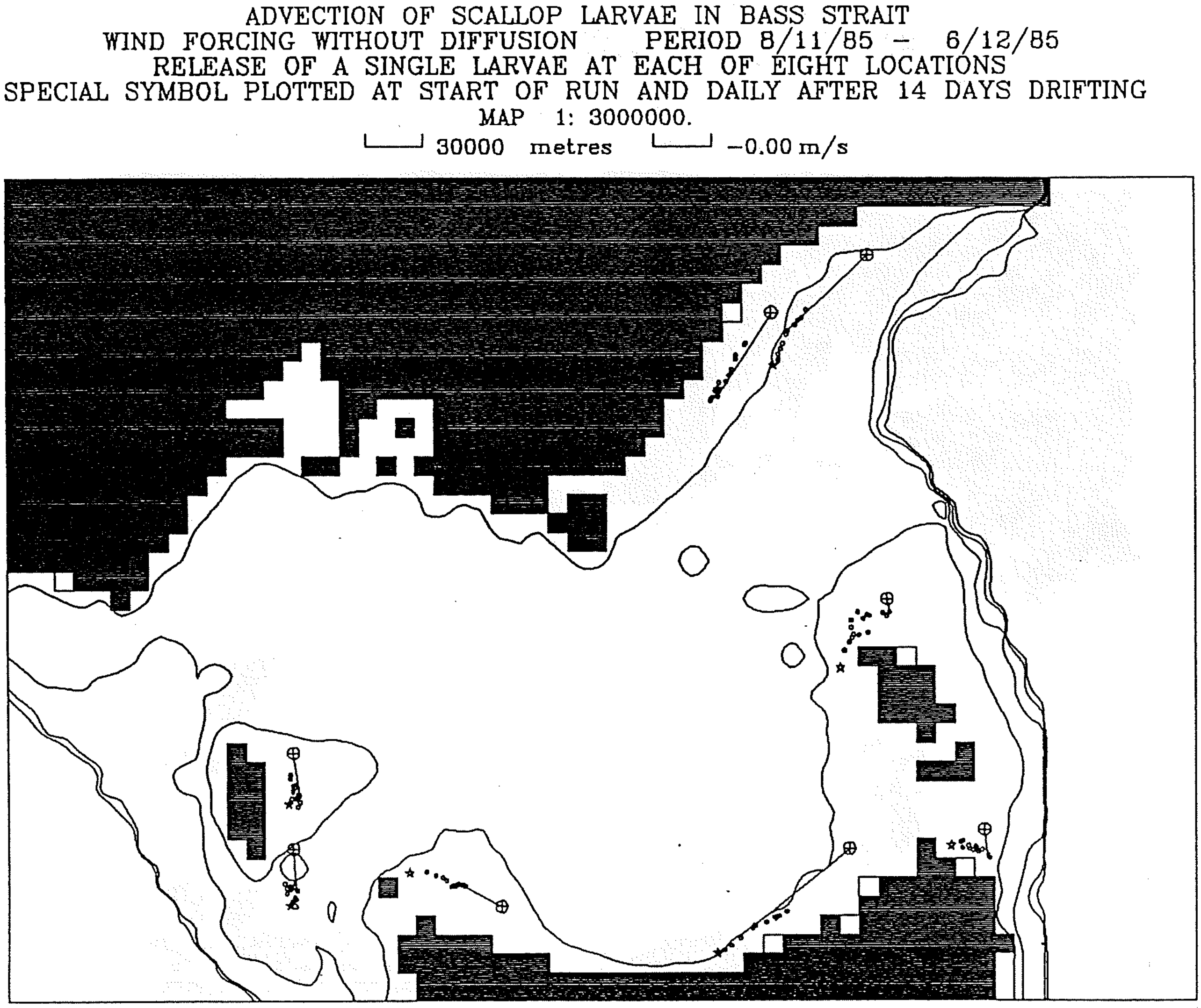

ADVECTION OF SCALLOP LARVAE IN BASS STRAIT
WIND FORCING WITHOUT DIFFUSION PERIOD 8/11/85 - 6/12/85
RELEASE OF A SINGLE LARVAE AT EACH OF EIGHT LOCATIONS
SPECIAL SYMBOL PLOTTED AT START OF RUN AND DAILY AFTER 14 DAYS DRIFTING
MAP 1: 3000000.

Fig. 4.1j Pelagic excursions from 8 modern beds over the 28 day period from November 8, 1985. The large crossed circle shows the release point and the straight line shows the excursion over the first non-viable 14 days. The small circles then show the positions at daily intervals in the 14-28 day interval, while the star shows the final position at the end of the 28 day pelagic period.

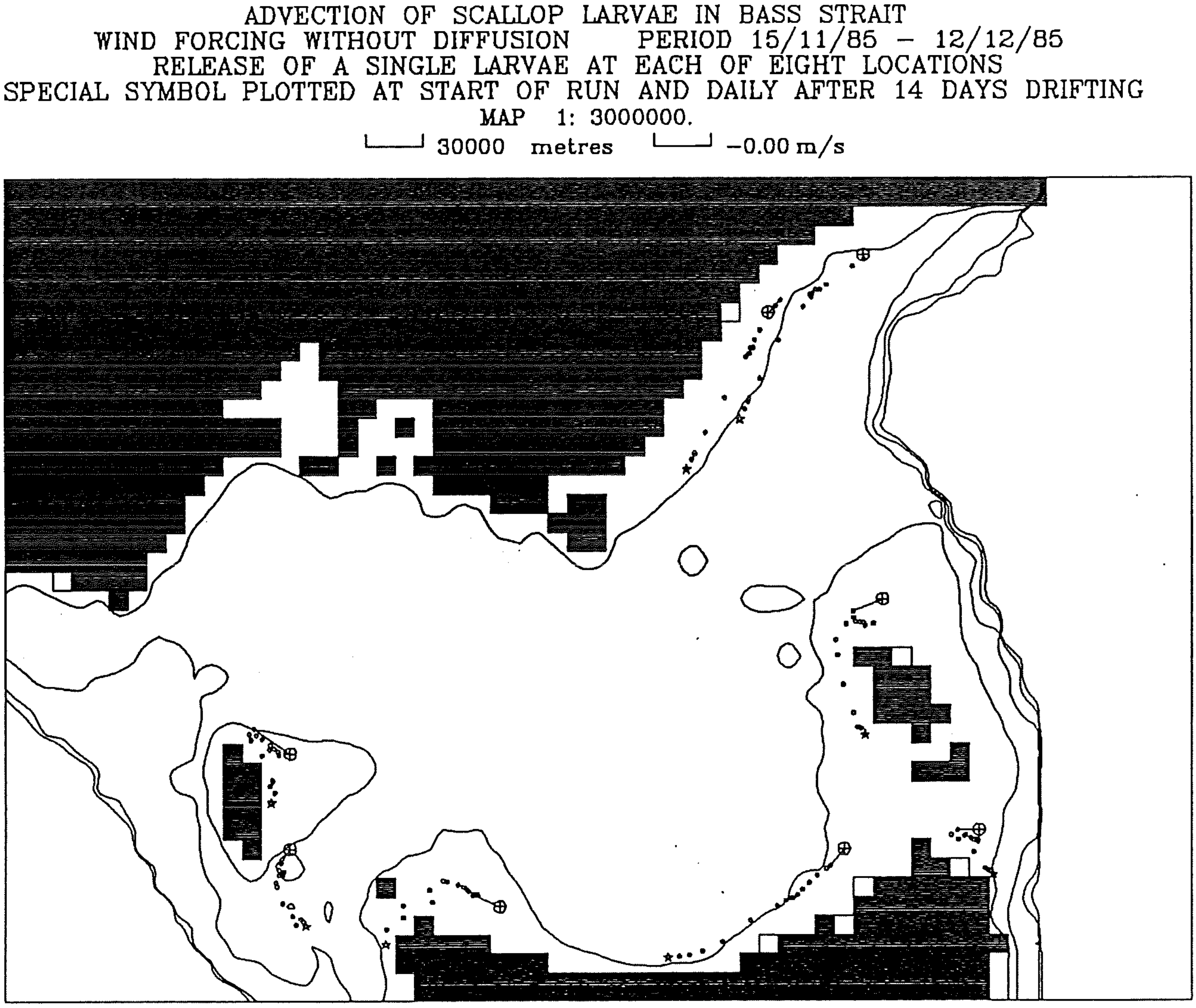

Fig. 4.1k Pelagic excursions from 8 modern beds over the 28 day period from November 15, 1985. The large crossed circle shows the release point and the straight line shows the excursion over the first non-viable 14 days. The small circles then show the positions at daily intervals in the 14-28 day interval, while the star shows the final position at the end of the 28 day pelagic period.

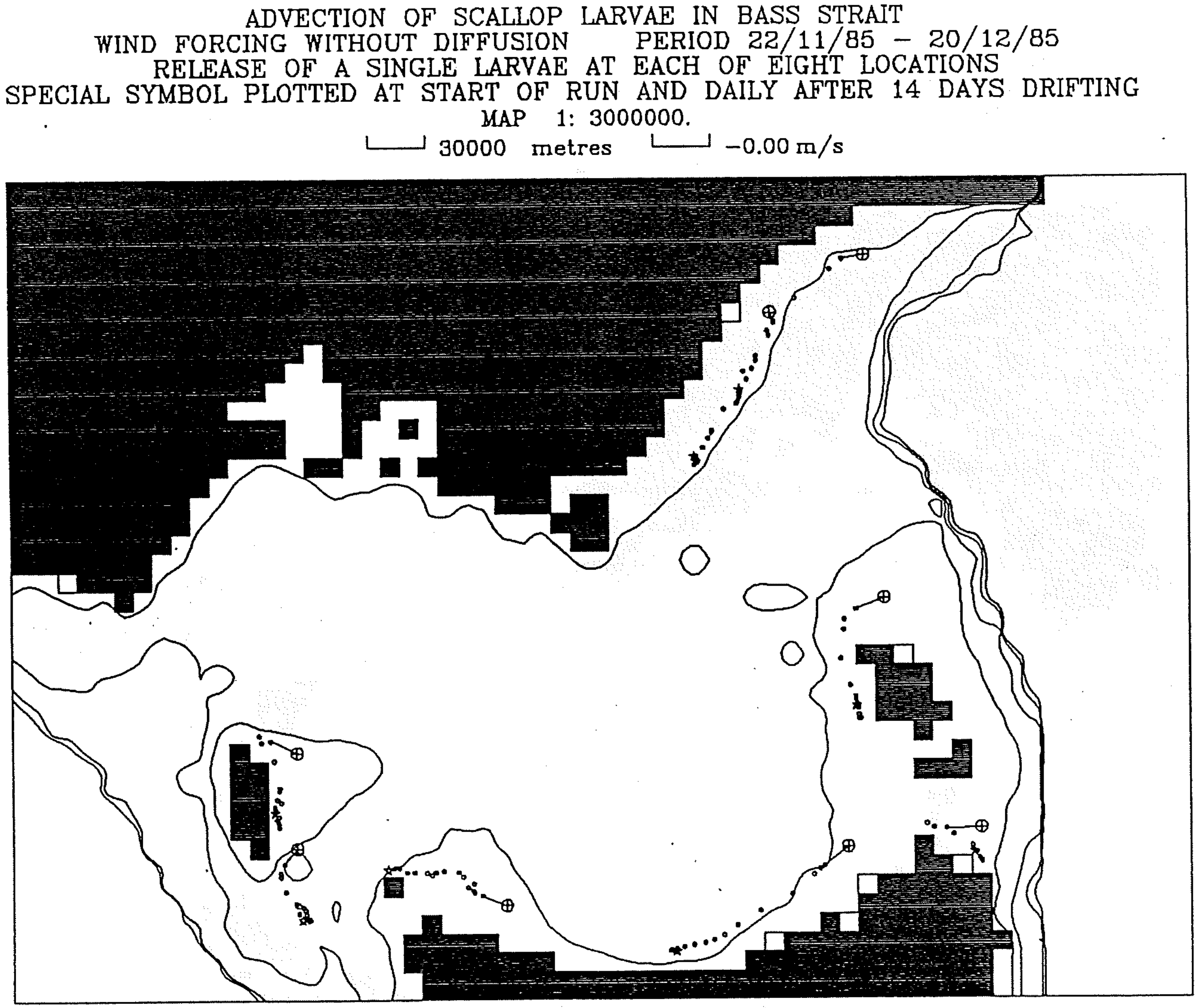

ADVECTION OF SCALLOP LARVAE IN BASS STRAIT
WIND FORCING WITHOUT DIFFUSION PERIOD 22/11/85 – 20/12/85
RELEASE OF A SINGLE LARVAE AT EACH OF EIGHT LOCATIONS
SPECIAL SYMBOL PLOTTED AT START OF RUN AND DAILY AFTER 14 DAYS DRIFTING
MAP 1: 3000000.

Fig. 4.11 Pelagic excursions from 8 modern beds over the 28 day period from November 22, 1985. The large crossed circle shows the release point and the straight line shows the excursion over the first non-viable 14 days. The small circles then show the positions at daily intervals in the 14-28 day interval, while the star shows the final position at the end of the 28 day pelagic period.

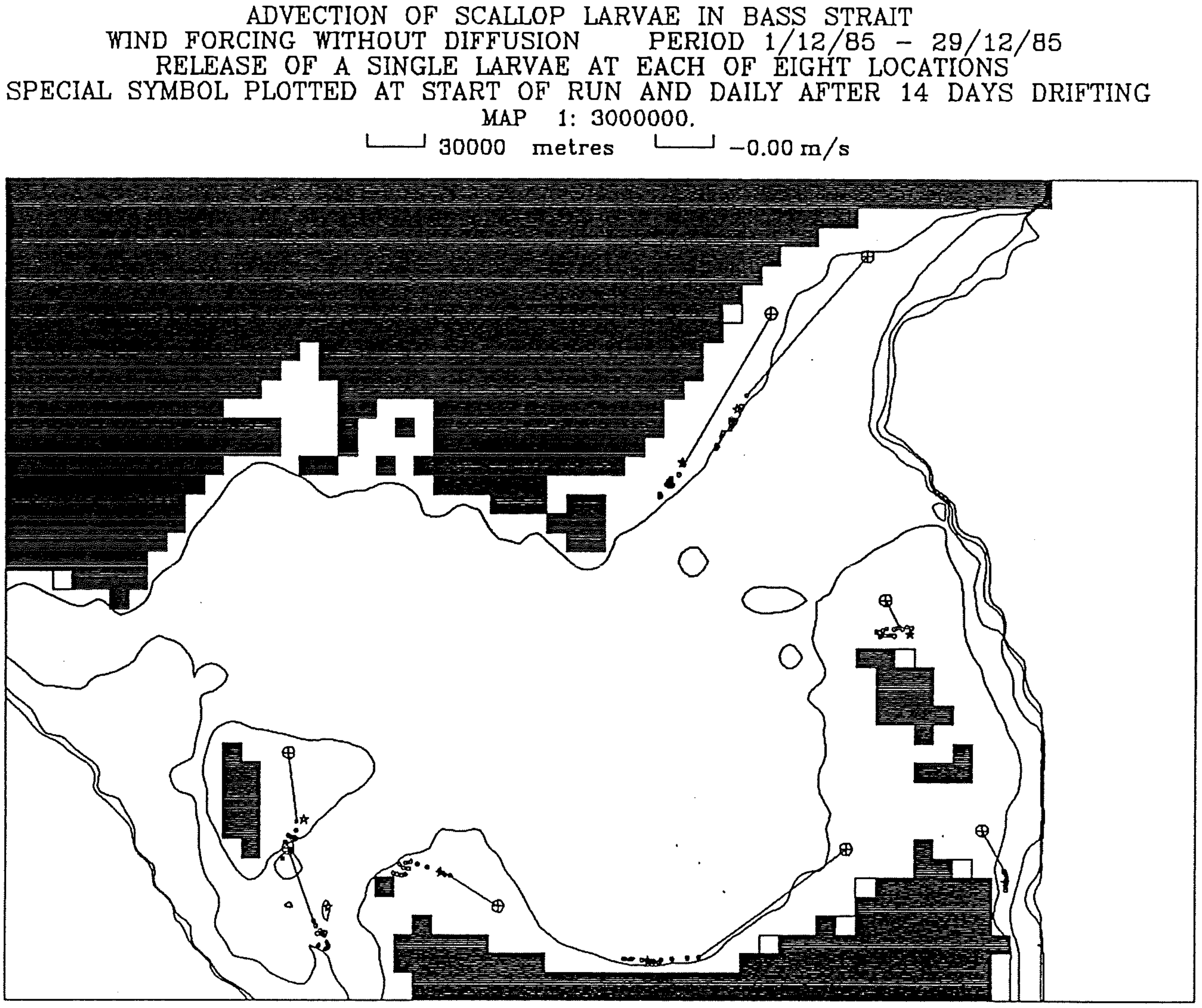

Fig. 4.1m Pelagic excursions from 8 modern beds over the 28 day period from December 1, 1985. The large crossed circle shows the release point and the straight line shows the excursion over the first non-viable 14 days. The small circles then show the positions at daily intervals in the 14-28 day interval, while the star shows the final position at the end of the 28 day pelagic period.

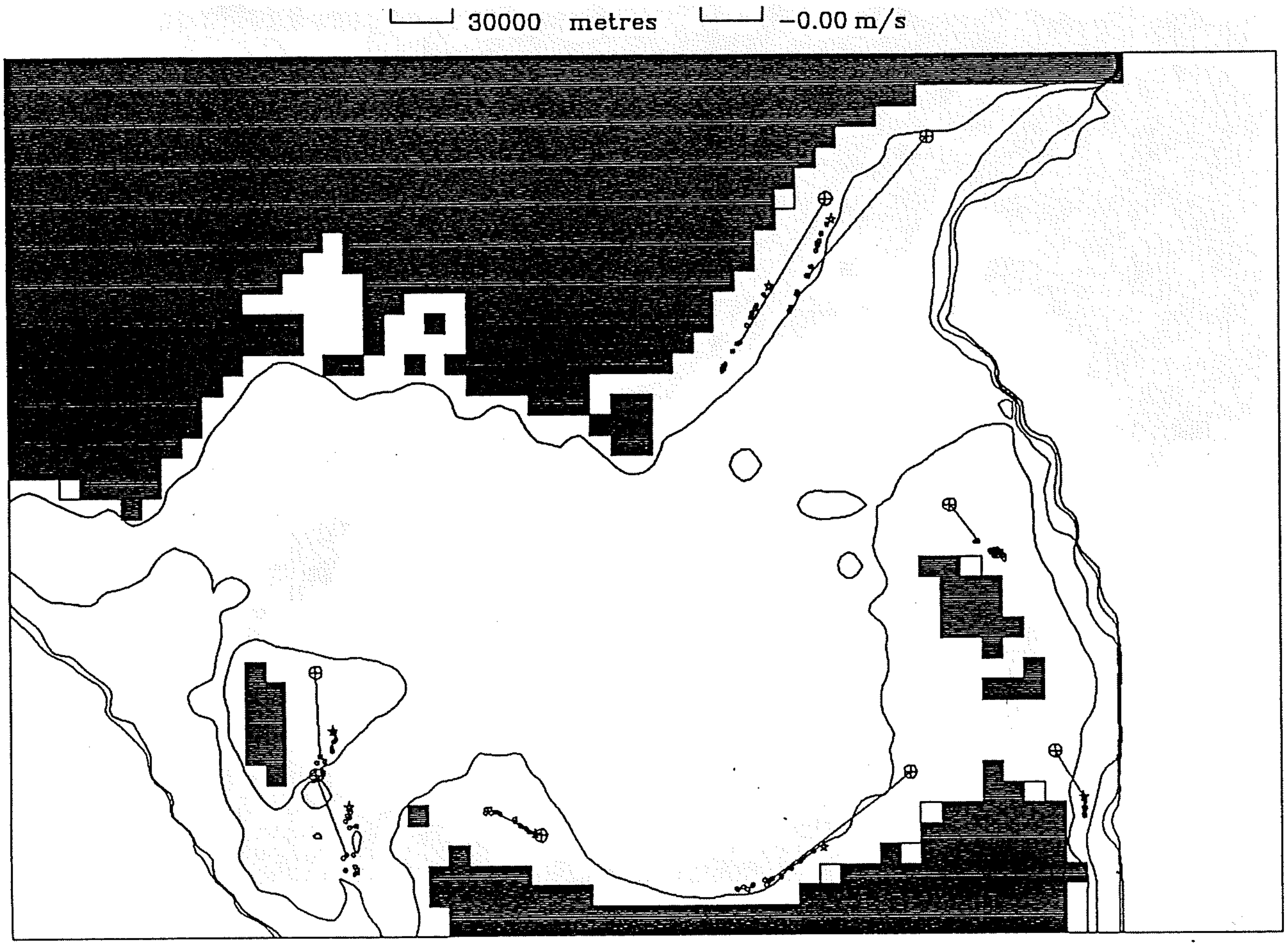

ADVECTION OF SCALLOP LARVAE IN BASS STRAIT
WIND FORCING WITHOUT DIFFUSION PERIOD 8/12/85 - 5/01/86
RELEASE OF A SINGLE LARVAE AT EACH OF EIGHT LOCATIONS
SPECIAL SYMBOL PLOTTED AT START OF RUN AND DAILY AFTER 14 DAYS DRIFTING
MAP 1: 3000000.

Fig. 4.1n Pelagic excursions from 8 modern beds over the 28 day period from December 8, 1985. The large crossed circle shows the release point and the straight line shows the excursion over the first non-viable 14 days. The small circles then show the positions at daily intervals in the 14-28 day interval, while the star shows the final position at the end of the 28 day pelagic period.

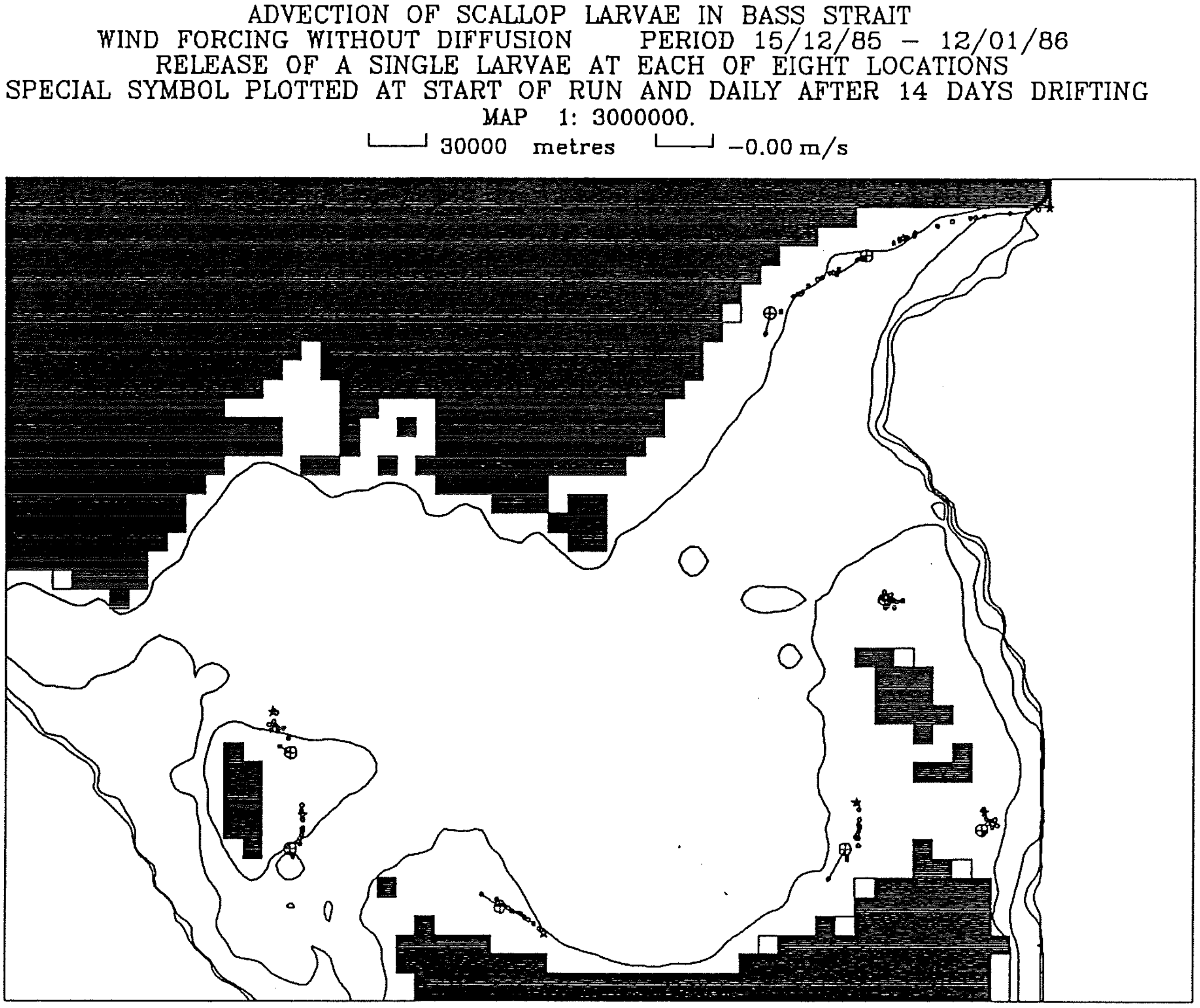

Fig. 4.1o Pelagic excursions from 8 modern beds over the 28 day period from December 15, 1985. The large crossed circle shows the release point and the straight line shows the excursion over the first non-viable 14 days. The small circles then show the positions at daily intervals in the 14-28 day interval, while the star shows the final position at the end of the 28 day pelagic period.

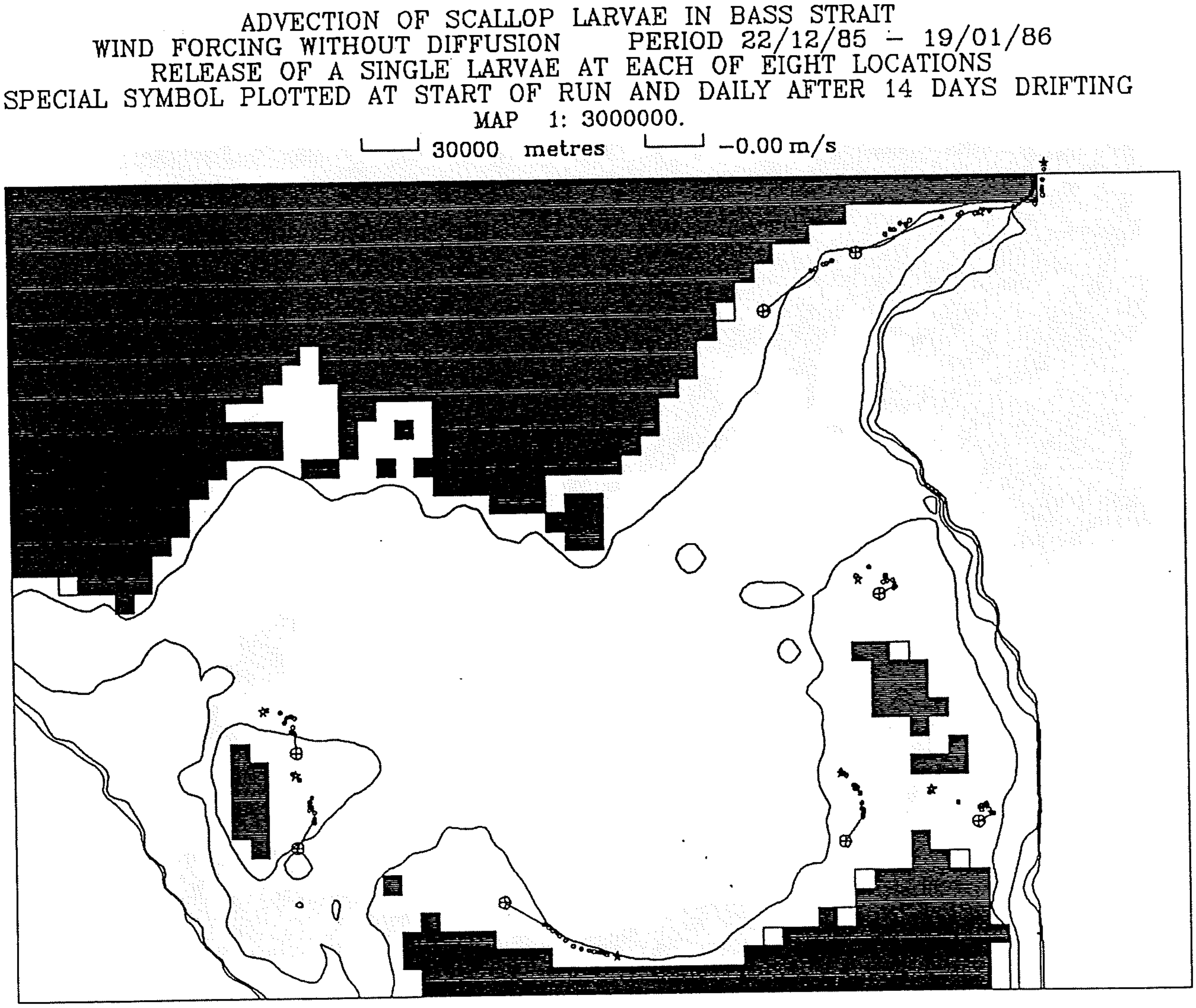

ADVECTION OF SCALLOP LARVAE IN BASS STRAIT
WIND FORCING WITHOUT DIFFUSION PERIOD 22/12/85 - 19/01/86
RELEASE OF A SINGLE LARVAE AT EACH OF EIGHT LOCATIONS
SPECIAL SYMBOL PLOTTED AT START OF RUN AND DAILY AFTER 14 DAYS DRIFTING
MAP 1: 3000000.

Fig. 4.1p Pelagic excursions from 8 modern beds over the 28 day period from December 22, 1985. The large crossed circle shows the release point and the straight line shows the excursion over the first non-viable 14 days. The small circles then show the positions at daily intervals in the 14-28 day interval, while the star shows the final position at the end of the 28 day pelagic period.

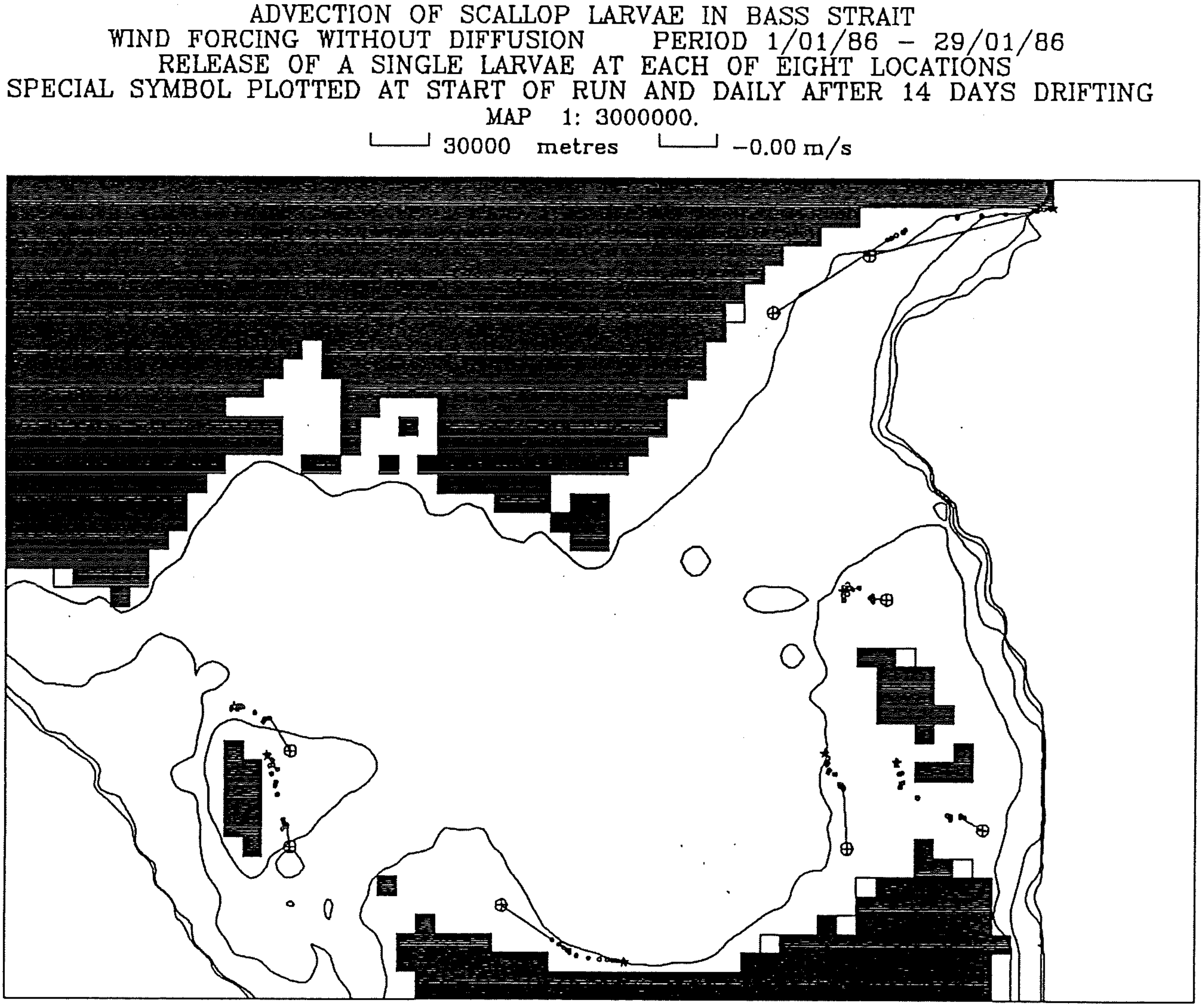

ADVECTION OF SCALLOP LARVAE IN BASS STRAIT
WIND FORCING WITHOUT DIFFUSION PERIOD 1/01/86 - 29/01/86
RELEASE OF A SINGLE LARVAE AT EACH OF EIGHT LOCATIONS
SPECIAL SYMBOL PLOTTED AT START OF RUN AND DAILY AFTER 14 DAYS DRIFTING
MAP 1: 3000000.

Fig. 4.1q Pelagic excursions from 8 modern beds over the 28 day period from January 1, 1986. The large crossed circle shows the release point and the straight line shows the excursion over the first non-viable 14 days. The small circles then show the positions at daily intervals in the 14-28 day interval, while the star shows the final position at the end of the 28 day pelagic period.

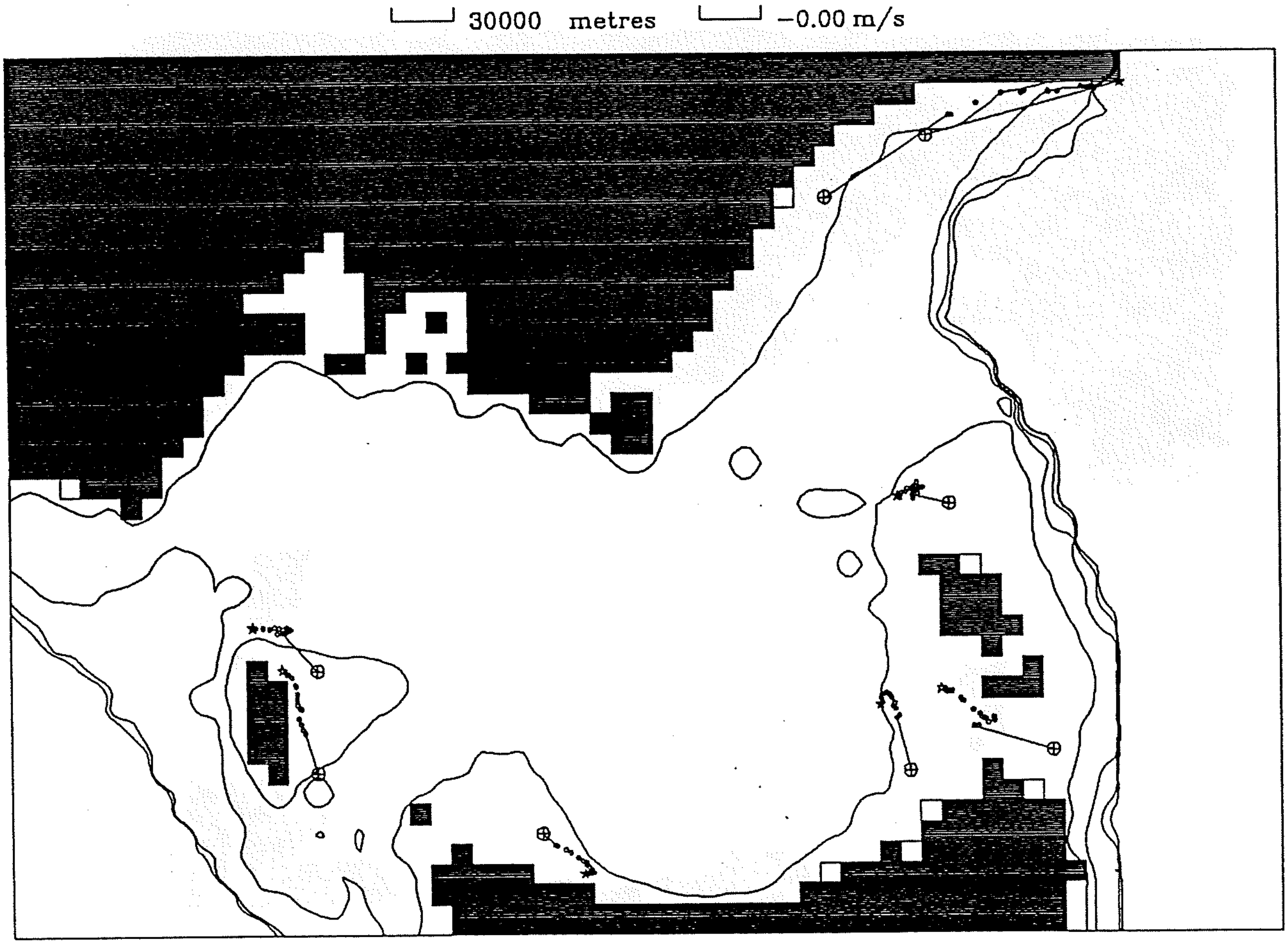

ADVECTION OF SCALLOP LARVAE IN BASS STRAIT
WIND FORCING WITHOUT DIFFUSION PERIOD 8/01/86 - 5/02/86
RELEASE OF A SINGLE LARVAE AT EACH OF EIGHT LOCATIONS
SPECIAL SYMBOL PLOTTED AT START OF RUN AND DAILY AFTER 14 DAYS DRIFTING
MAP 1: 3000000.

Fig. 4.1r Pelagic excursions from 8 modern beds over the 28 day period from January 8, 1986. The large crossed circle shows the release point and the straight line shows the excursion over the first non-viable 14 days. The small circles then show the positions at daily intervals in the 14-28 day interval, while the star shows the final position at the end of the 28 day pelagic period.

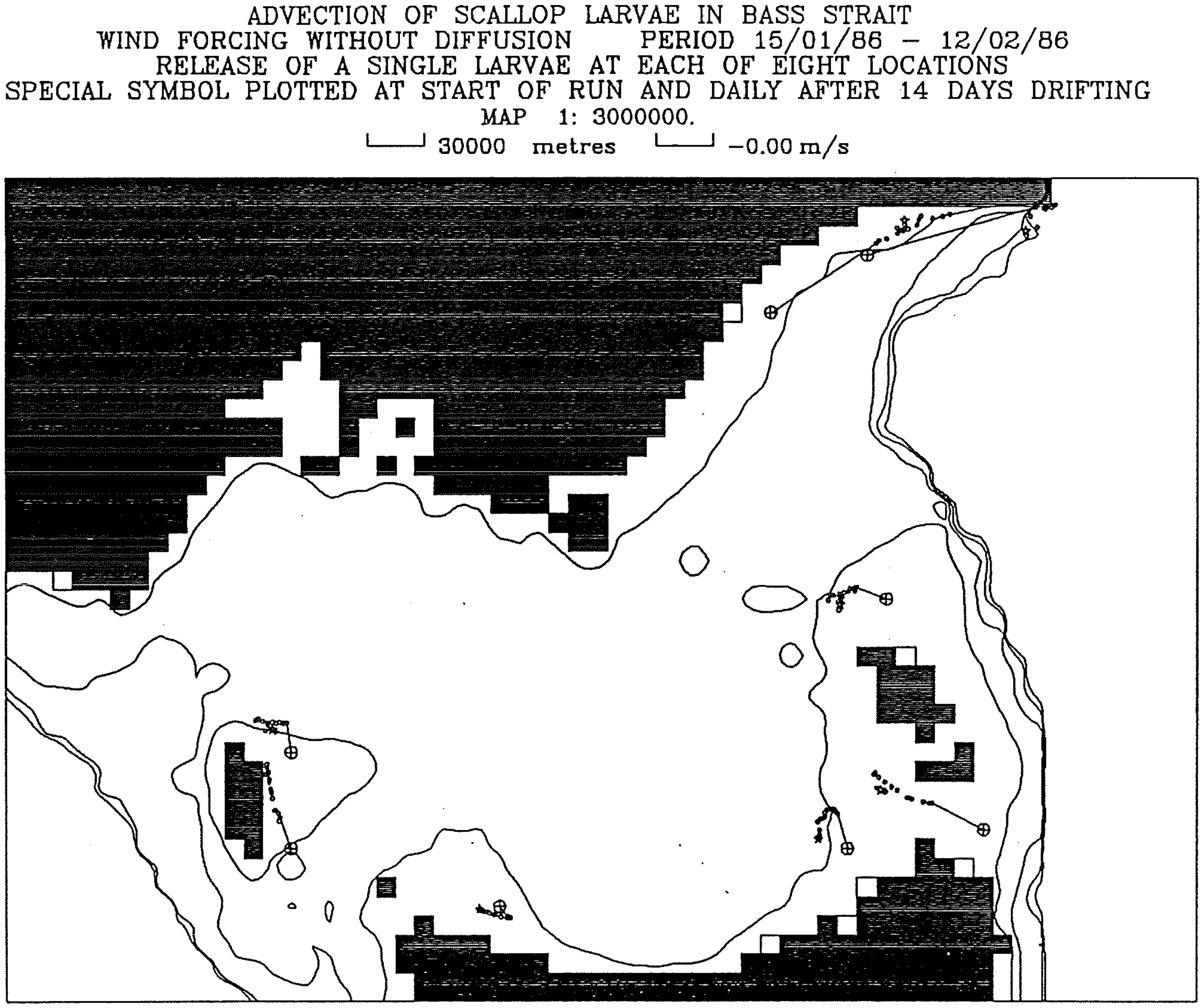

Fig. 4.1s Pelagic excursions from 8 modern beds over the 28 day period from January 15, 1986. The large crossed circle shows the release point and the straight line shows the excursion over the first non-viable 14 days. The small circles then show the positions at daily intervals in the 14-28 day interval, while the star shows the final position at the end of the 28 day pelagic period.

ADVECTION OF SCALLOP LARVAE IN BASS STRAIT
WIND FORCING WITHOUT DIFFUSION PERIOD 22/01/86 – 19/02/86
RELEASE OF A SINGLE LARVAE AT EACH OF EIGHT LOCATIONS
SPECIAL SYMBOL PLOTTED AT START OF RUN AND DAILY AFTER 14 DAYS DRIFTING
MAP 1: 3000000.
30000 metres –0.00 m/s

Fig. 4.1t Pelagic excursions from 8 modern beds over the 28 day period from January 22, 1986. The large crossed circle shows the release point and the straight line shows the excursion over the first non-viable 14 days. The small circles then show the positions at daily intervals in the 14-28 day interval, while the star shows the final position at the end of the 28 day pelagic period.

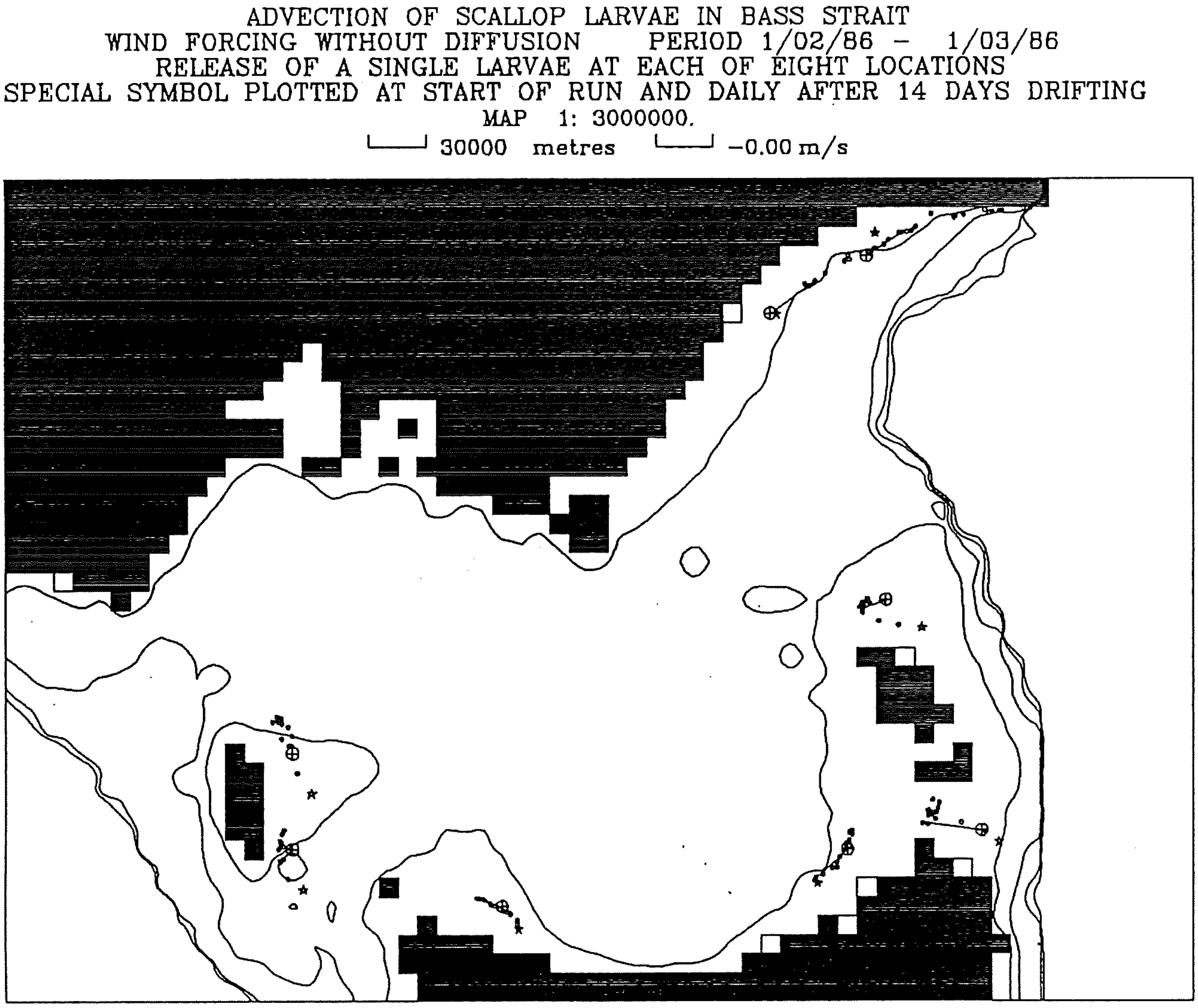

Fig. 4.1u Pelagic excursions from 8 modern beds over the 28 day period from February 1, 1986. The large crossed circle shows the release point and the straight line shows the excursion over the first non-viable 14 days. The small circles then show the positions at daily intervals in the 14-28 day interval, while the star shows the final position at the end of the 28 day pelagic period.

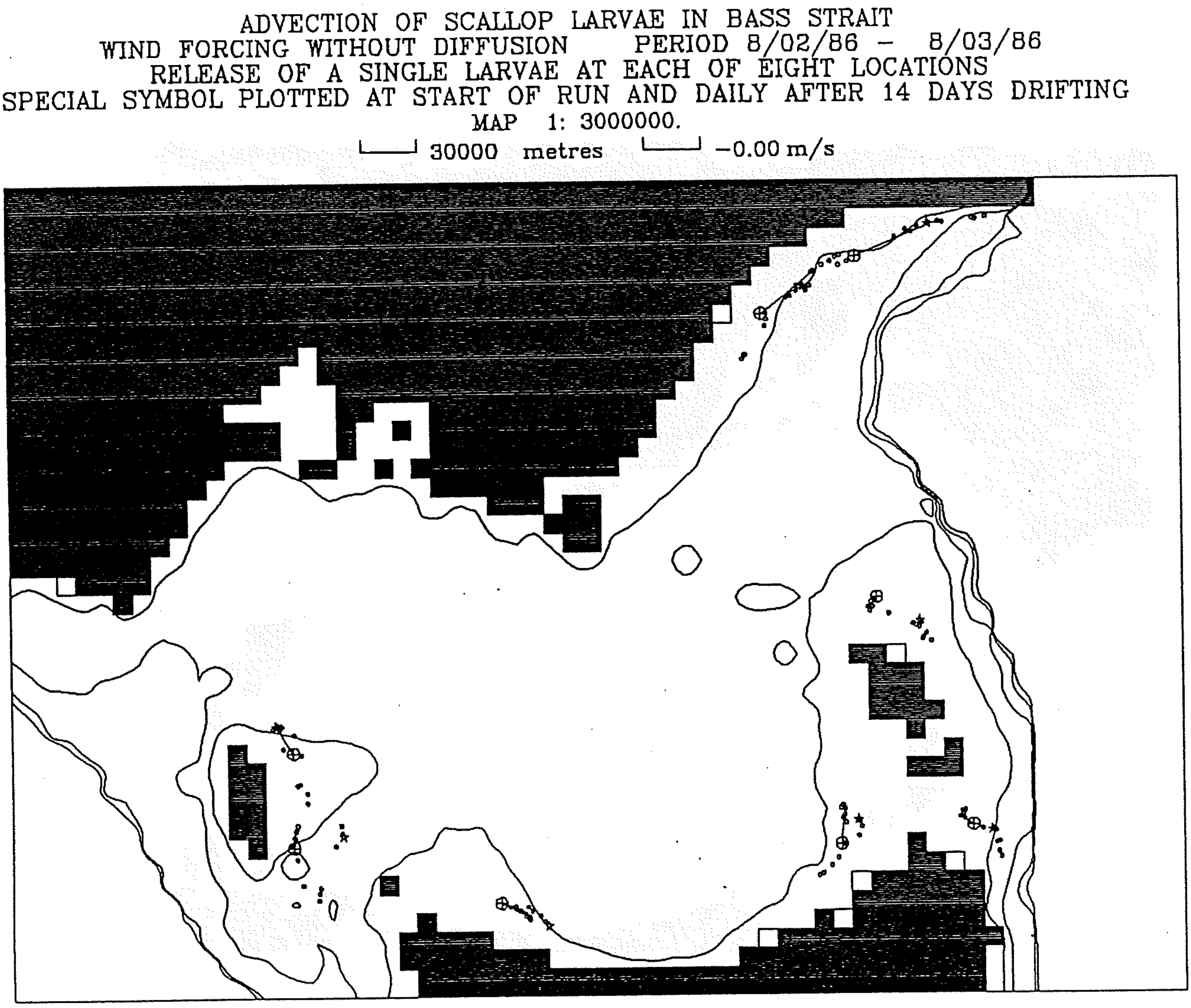

ADVECTION OF SCALLOP LARVAE IN BASS STRAIT
WIND FORCING WITHOUT DIFFUSION PERIOD 8/02/86 - 8/03/86
RELEASE OF A SINGLE LARVAE AT EACH OF EIGHT LOCATIONS
SPECIAL SYMBOL PLOTTED AT START OF RUN AND DAILY AFTER 14 DAYS DRIFTING
MAP 1: 3000000.

Fig. 4.1v Pelagic excursions from 8 modern beds over the 28 day period from February 8, 1986. The large crossed circle shows the release point and the straight line shows the excursion over the first non-viable 14 days. The small circles then show the positions at daily intervals in the 14-28 day interval, while the star shows the final position at the end of the 28 day pelagic period.

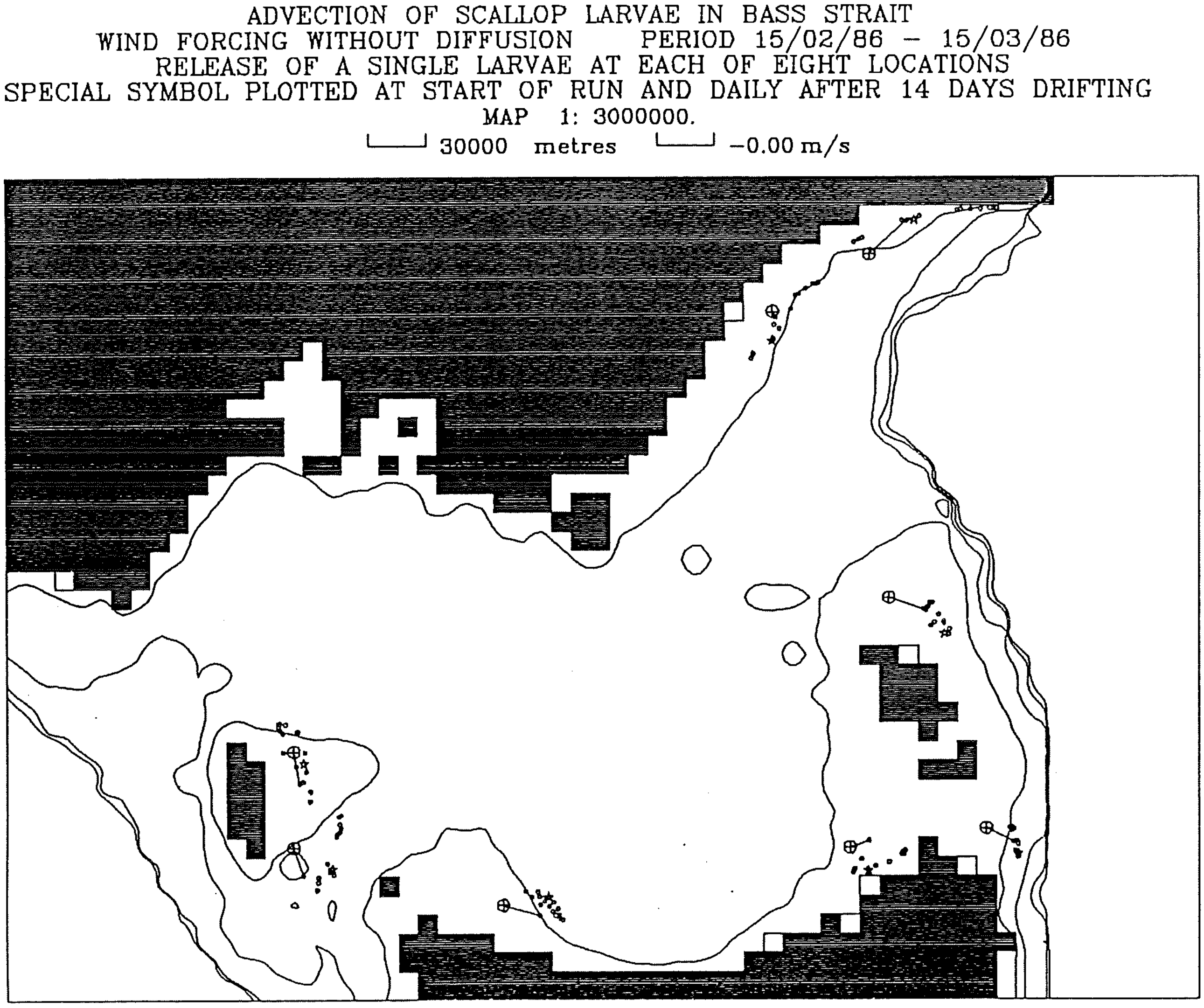

Fig. 4.1w Pelagic excursions from 8 modern beds over the 28 day period from February 15, 1986. The large crossed circle shows the release point and the straight line shows the excursion over the first non-viable 14 days. The small circles then show the positions at daily intervals in the 14-28 day interval, while the star shows the final position at the end of the 28 day pelagic period.

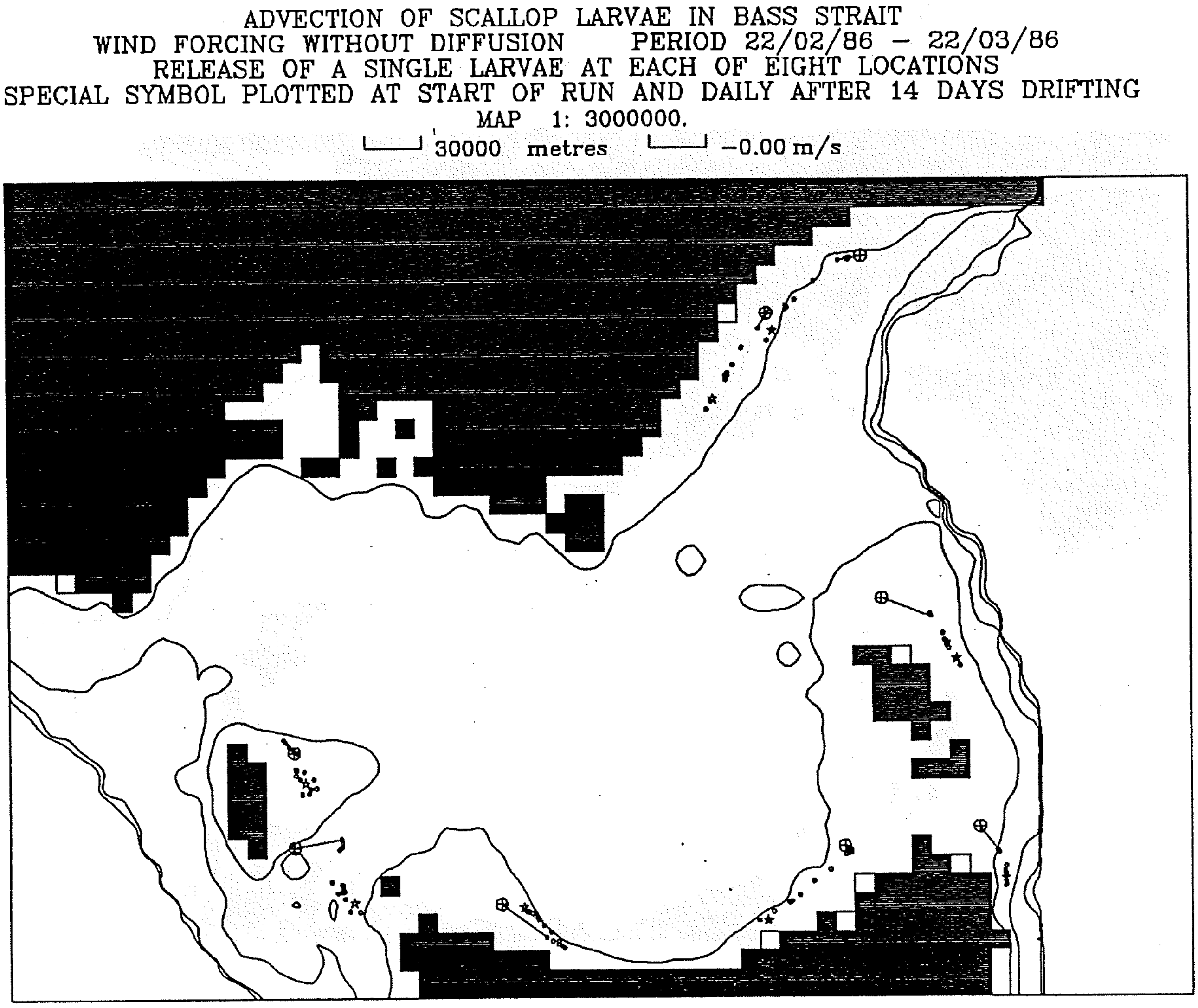

Fig. 4.1x Pelagic excursions from 8 modern beds over the 28 day period from February 22, 1986. The large crossed circle shows the release point and the straight line shows the excursion over the first non-viable 14 days. The small circles then show the positions at daily intervals in the 14-28 day interval, while the star shows the final position at the end of the 28 day pelagic period.

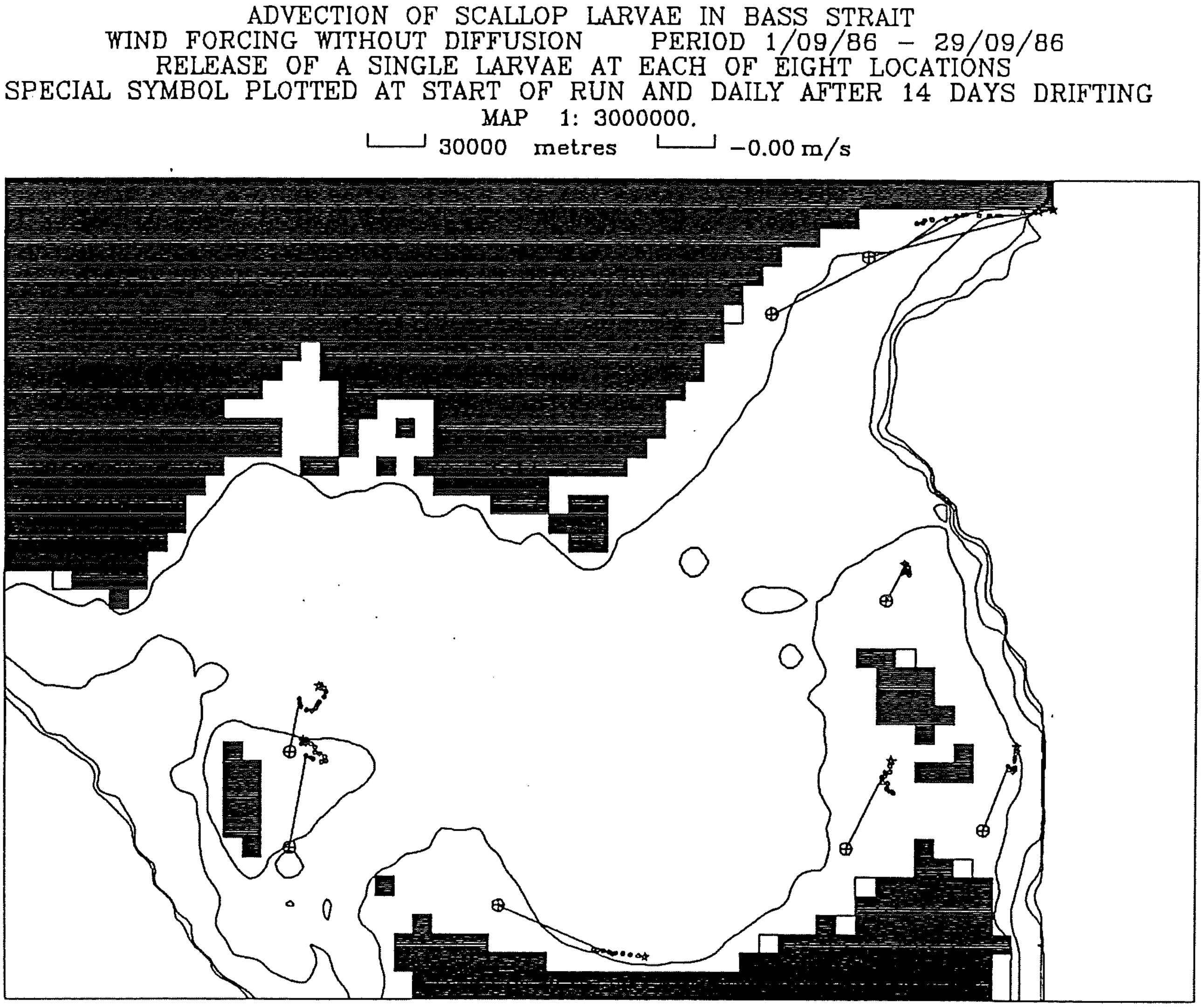

Fig. 4.2a Pelagic excursions from 8 modern beds over the 28 day period from September 1, 1986. The large crossed circle shows the release point and the straight line shows the excursion over the first non-viable 14 days. The small circles then show the positions at daily intervals in the 14-28 day interval, while the star shows the final position at the end of the 28 day pelagic period.

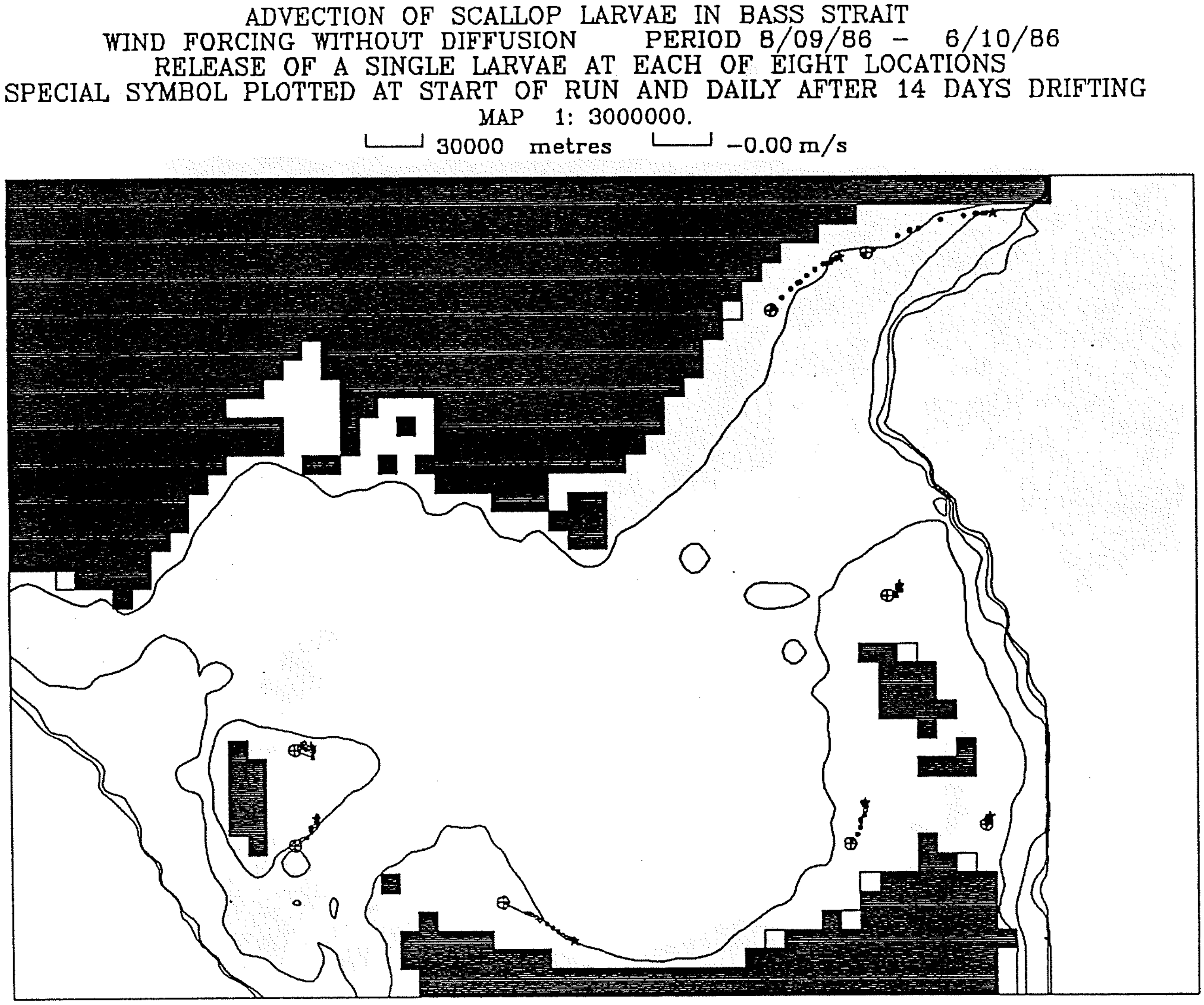

Fig. 4.2b Pelagic excursions from 8 modern beds over the 28 day period from September 8, 1986. The large crossed circle shows the release point and the straight line shows the excursion over the first non-viable 14 days. The small circles then show the positions at daily intervals in the 14-28 day interval, while the star shows the final position at the end of the 28 day pelagic period.

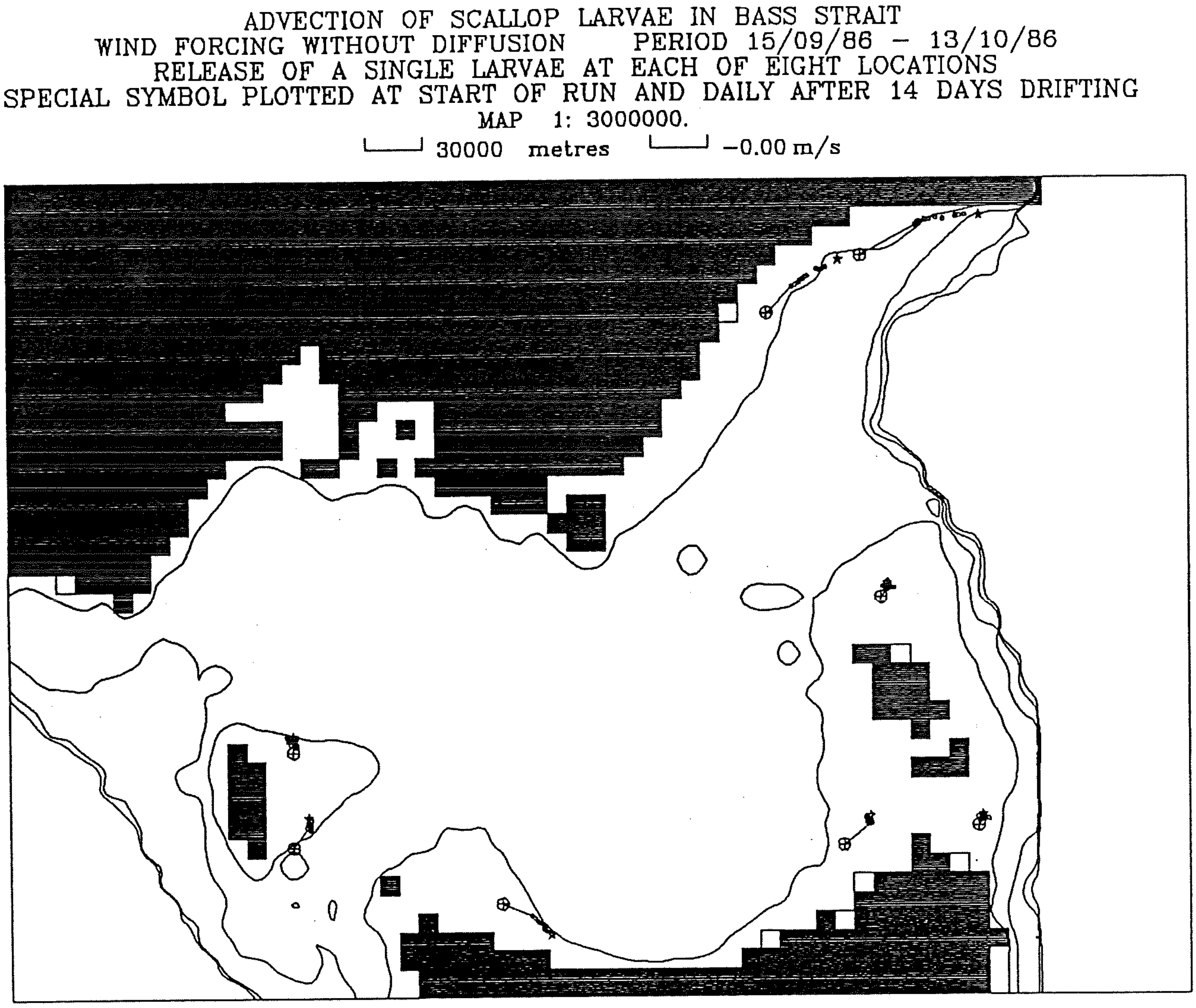

Fig. 4.2c Pelagic excursions from 8 modern beds over the 28 day period from September 15, 1986. The large crossed circle shows the release point and the straight line shows the excursion over the first non-viable 14 days. The small circles then show the positions at daily intervals in the 14-28 day interval, while the star shows the final position at the end of the 28 day pelagic period.

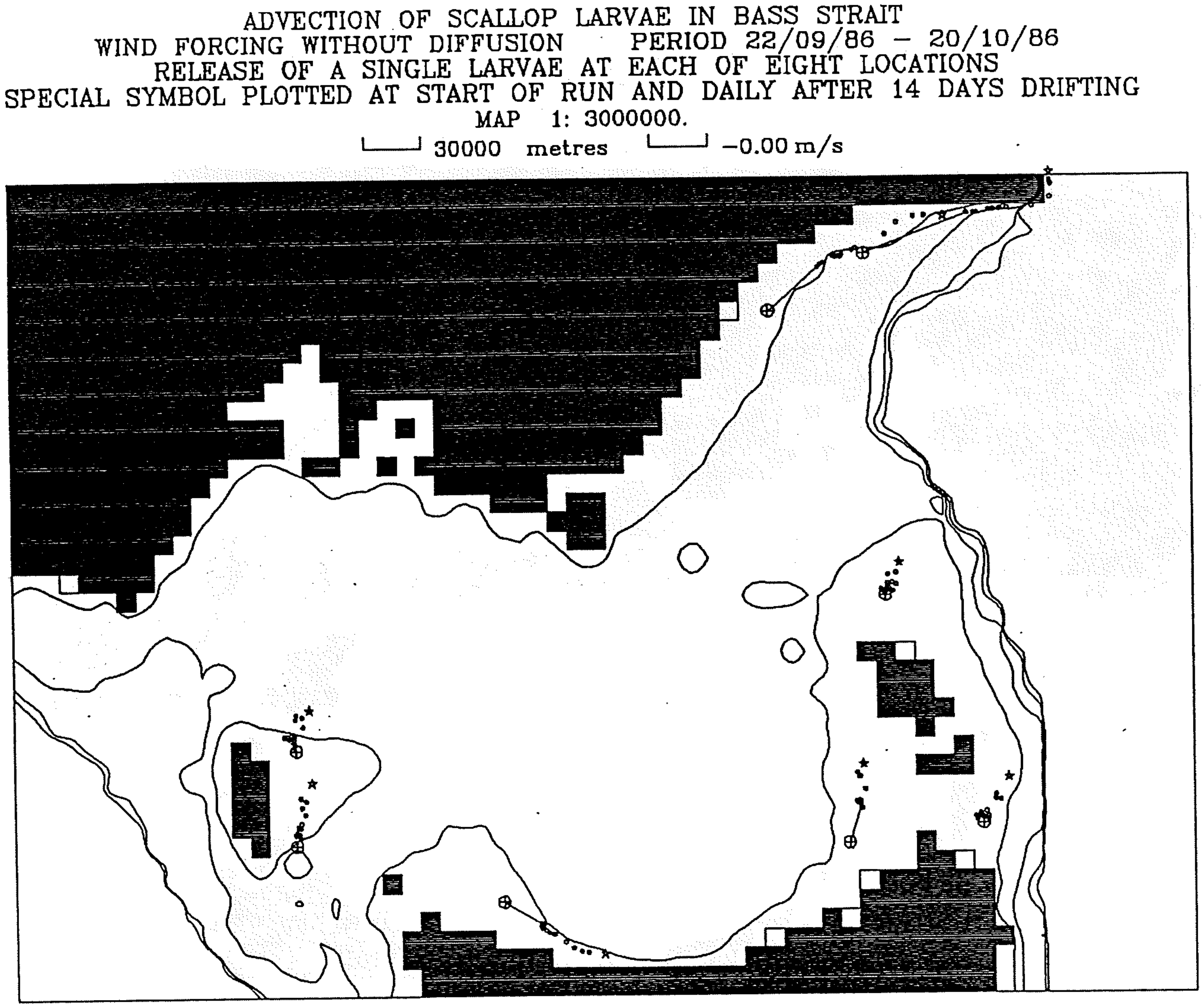

Fig. 4.2d Pelagic excursions from 8 modern beds over the 28 day period from September 22, 1986. The large crossed circle shows the release point and the straight line shows the excursion over the first non-viable 14 days. The small circles then show the positions at daily intervals in the 14-28 day interval, while the star shows the final position at the end of the 28 day pelagic period.

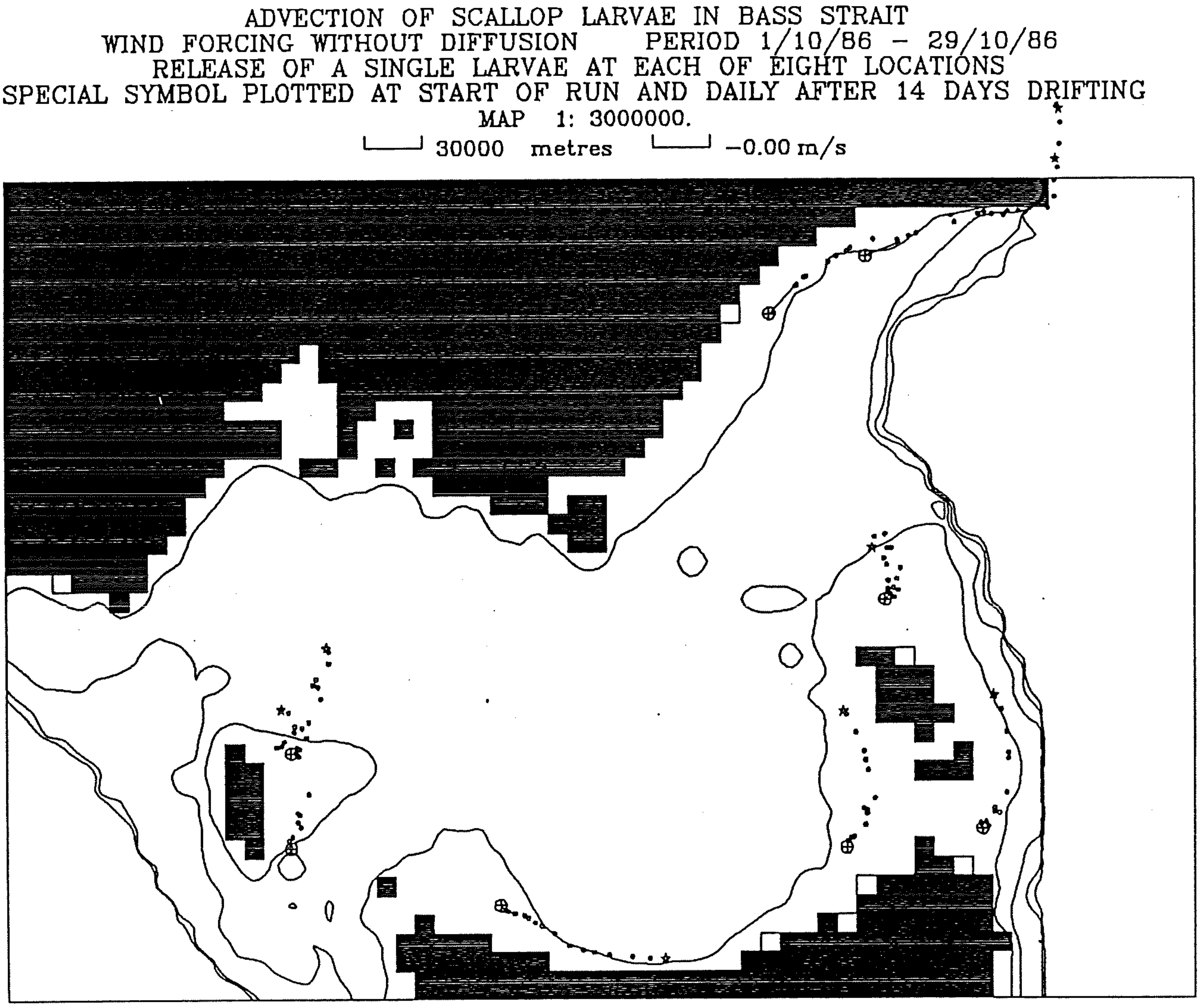

Fig. 4.2e Pelagic excursions from 8 modern beds over the 28 day period from October 1, 1986. The large crossed circle shows the release point and the straight line shows the excursion over the first non-viable 14 days. The small circles then show the positions at daily intervals in the 14-28 day interval, while the star shows the final position at the end of the 28 day pelagic period.

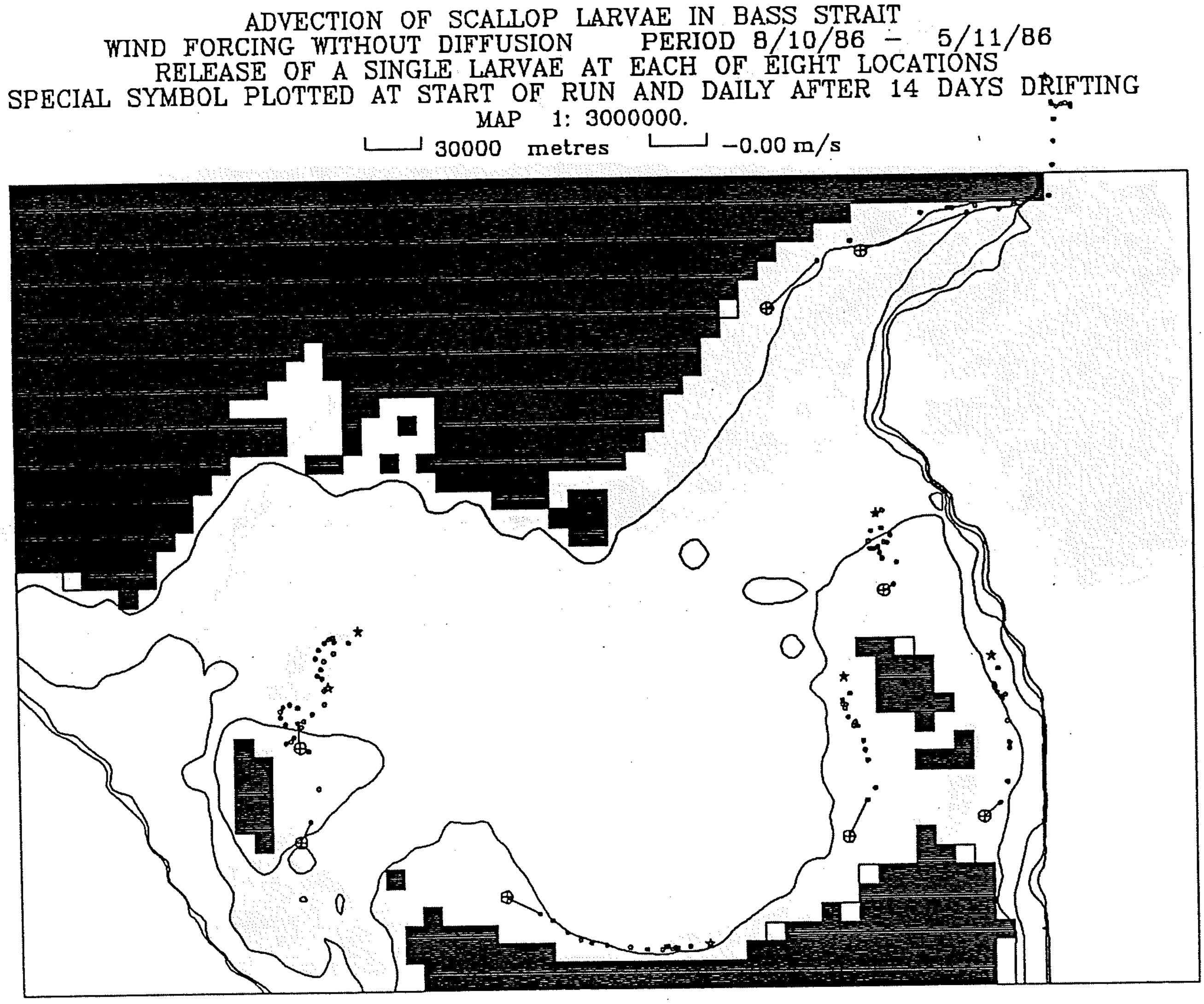

Fig. 4.2f Pelagic excursions from 8 modern beds over the 28 day period from October 8, 1986. The large crossed circle shows the release point and the straight line shows the excursion over the first non-viable 14 days. The small circles then show the positions at daily intervals in the 14-28 day interval, while the star shows the final position at the end of the 28 day pelagic period.

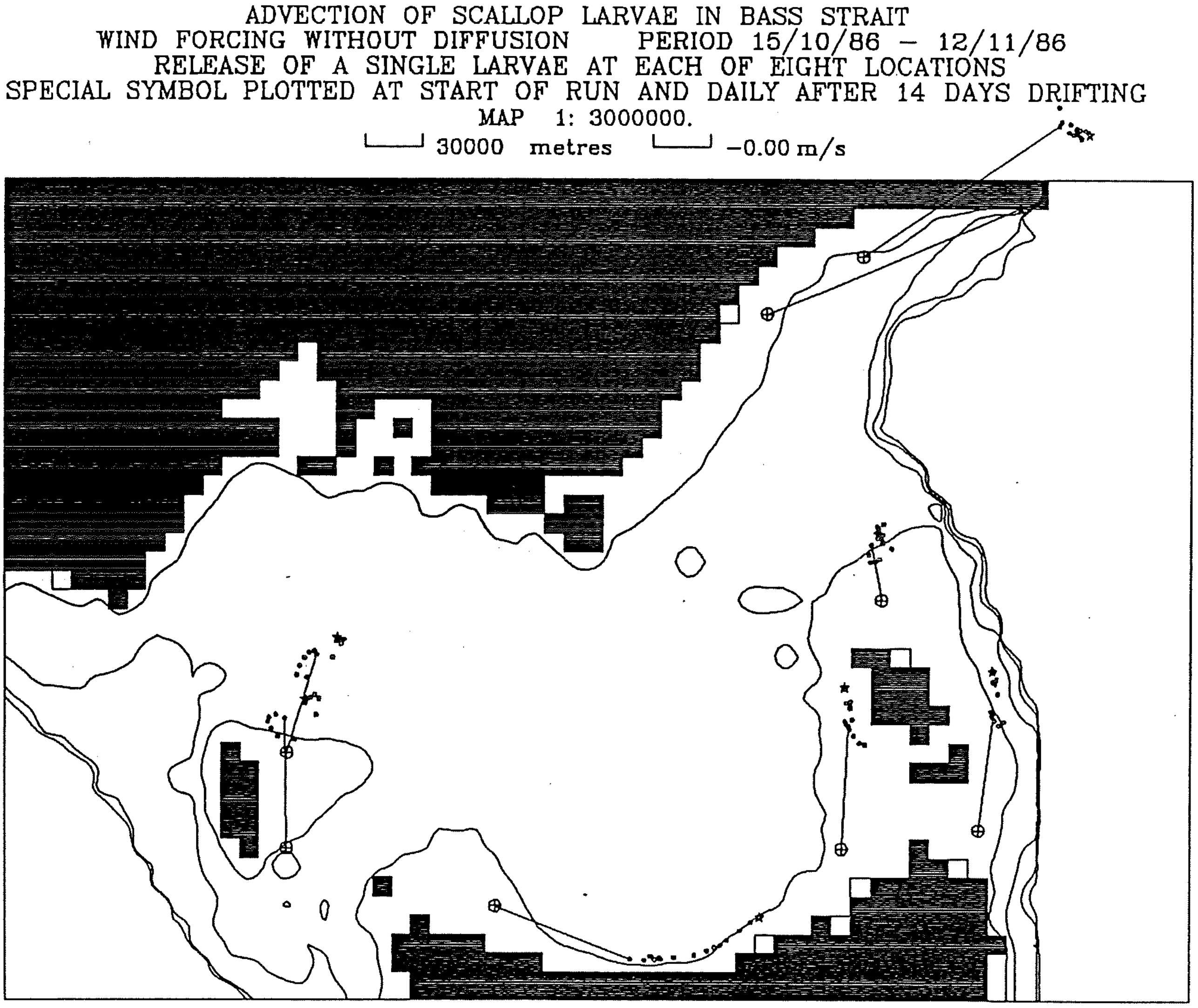

ADVECTION OF SCALLOP LARVAE IN BASS STRAIT
WIND FORCING WITHOUT DIFFUSION PERIOD 15/10/86 - 12/11/86
RELEASE OF A SINGLE LARVAE AT EACH OF EIGHT LOCATIONS
SPECIAL SYMBOL PLOTTED AT START OF RUN AND DAILY AFTER 14 DAYS DRIFTING
MAP 1: 3000000.

Fig. 4.2g Pelagic excursions from 8 modern beds over the 28 day period from October 15, 1986. The large crossed circle shows the release point and the straight line shows the excursion over the first non-viable 14 days. The small circles then show the positions at daily intervals in the 14-28 day interval, while the star shows the final position at the end of the 28 day pelagic period.

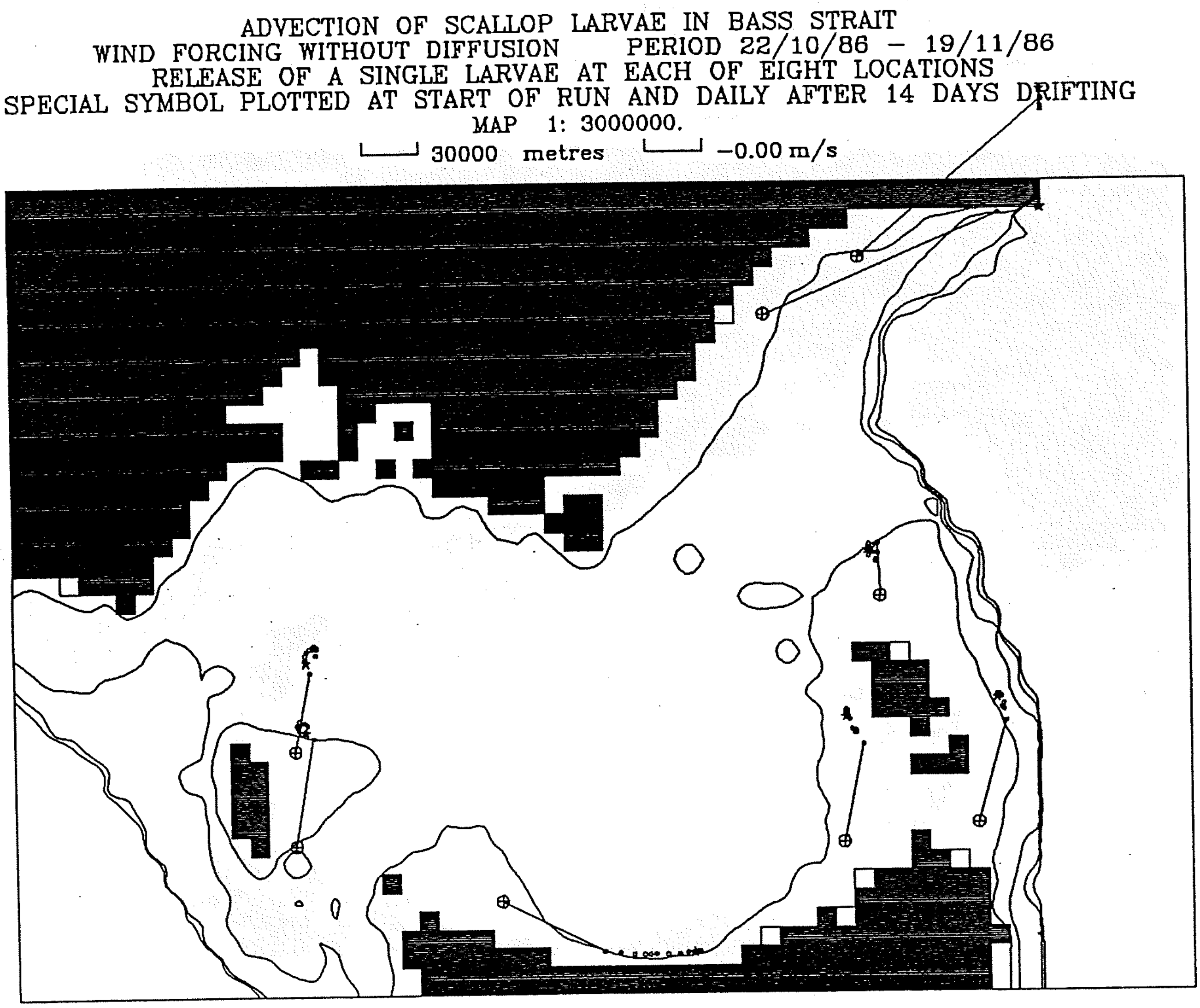

Fig. 4.2h Pelagic excursions from 8 modern beds over the 28 day period from October 22, 1986. The large crossed circle shows the release point and the straight line shows the excursion over the first non-viable 14 days. The small circles then show the positions at daily intervals in the 14-28 day interval, while the star shows the final position at the end of the 28 day pelagic period.

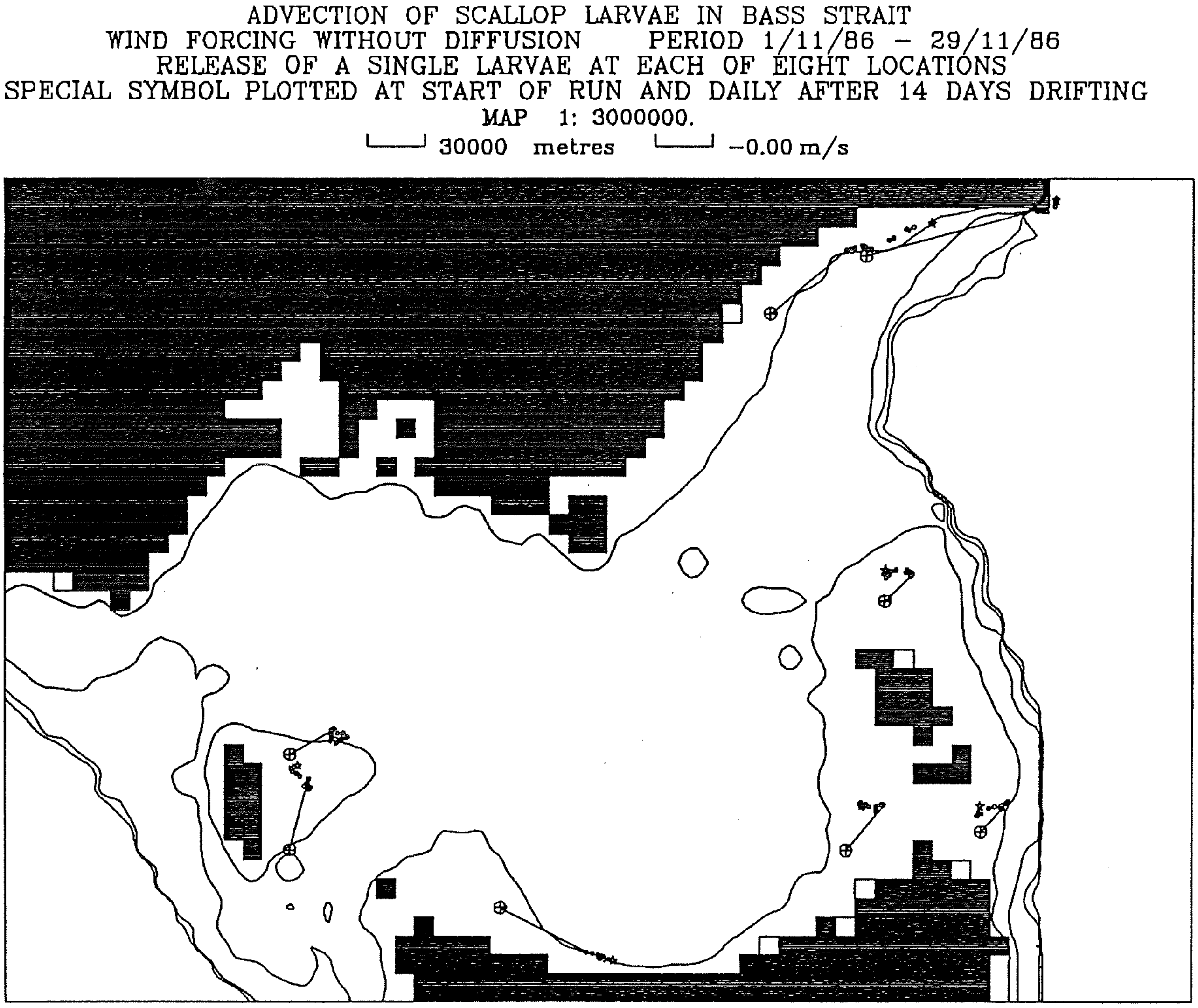

ADVECTION OF SCALLOP LARVAE IN BASS STRAIT
WIND FORCING WITHOUT DIFFUSION PERIOD 1/11/86 – 29/11/86
RELEASE OF A SINGLE LARVAE AT EACH OF EIGHT LOCATIONS
SPECIAL SYMBOL PLOTTED AT START OF RUN AND DAILY AFTER 14 DAYS DRIFTING
MAP 1: 3000000.

Fig. 4.2i Pelagic excursions from 8 modern beds over the 28 day period from November 1, 1986. The large crossed circle shows the release point and the straight line shows the excursion over the first non-viable 14 days. The small circles then show the positions at daily intervals in the 14-28 day interval, while the star shows the final position at the end of the 28 day pelagic period.

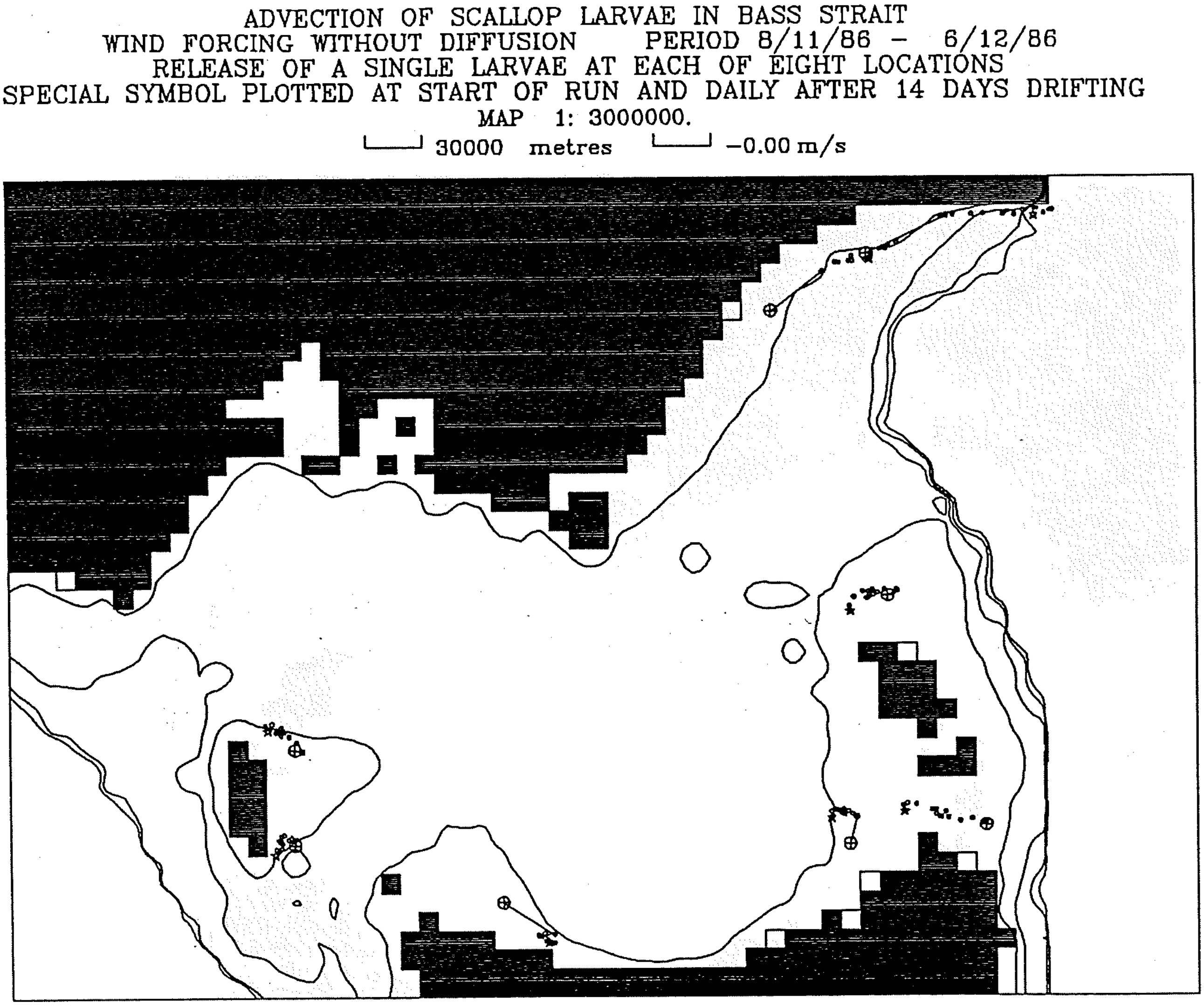

Fig. 4.2j Pelagic excursions from 8 modern beds over the 28 day period from November 8, 1986. The large crossed circle shows the release point and the straight line shows the excursion over the first non-viable 14 days. The small circles then show the positions at daily intervals in the 14-28 day interval, while the star shows the final position at the end of the 28 day pelagic period.

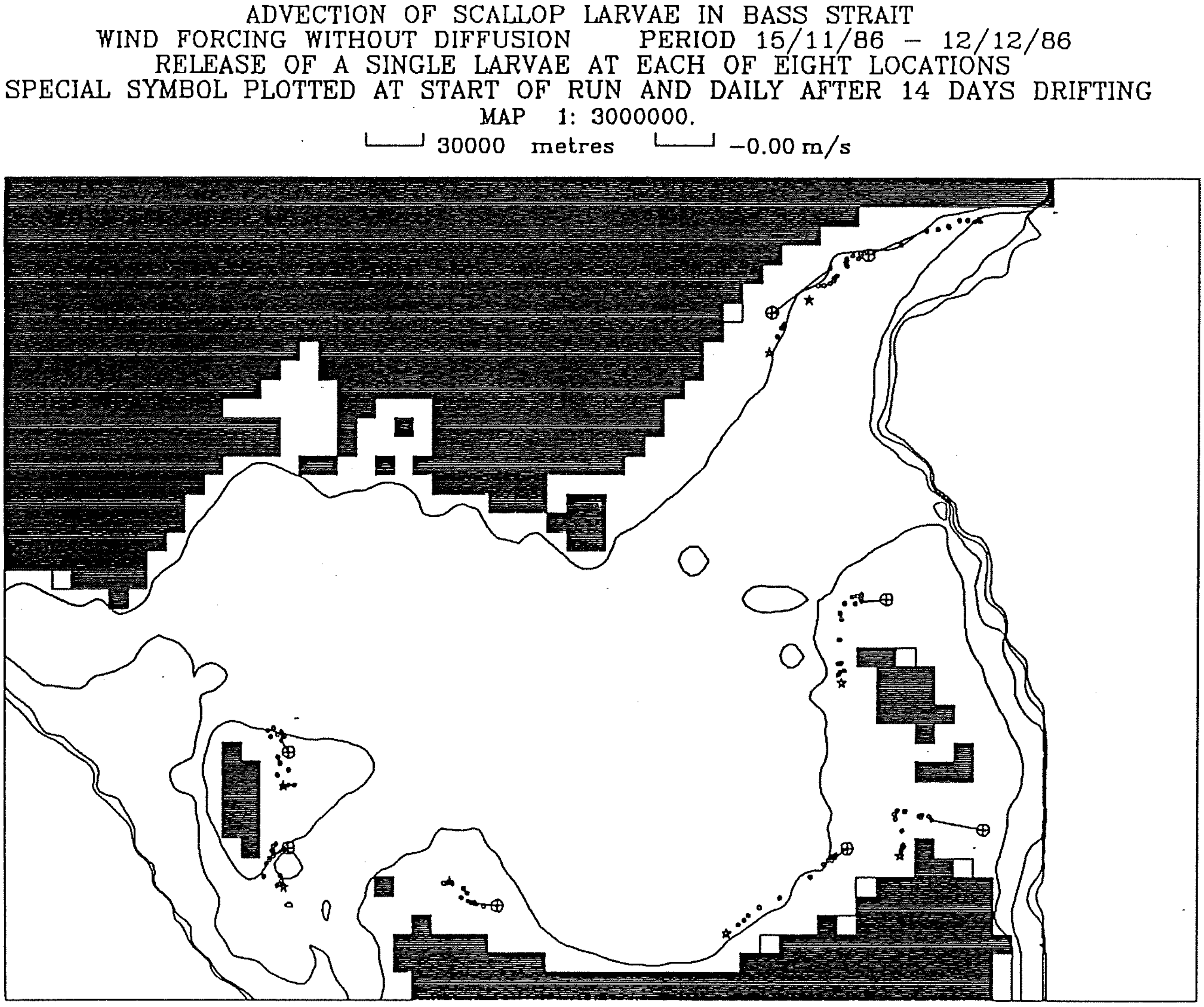

Fig. 4.2k Pelagic excursions from 8 modern beds over the 28 day period from November 15, 1986. The large crossed circle shows the release point and the straight line shows the excursion over the first non-viable 14 days. The small circles then show the positions at daily intervals in the 14-28 day interval, while the star shows the final position at the end of the 28 day pelagic period.

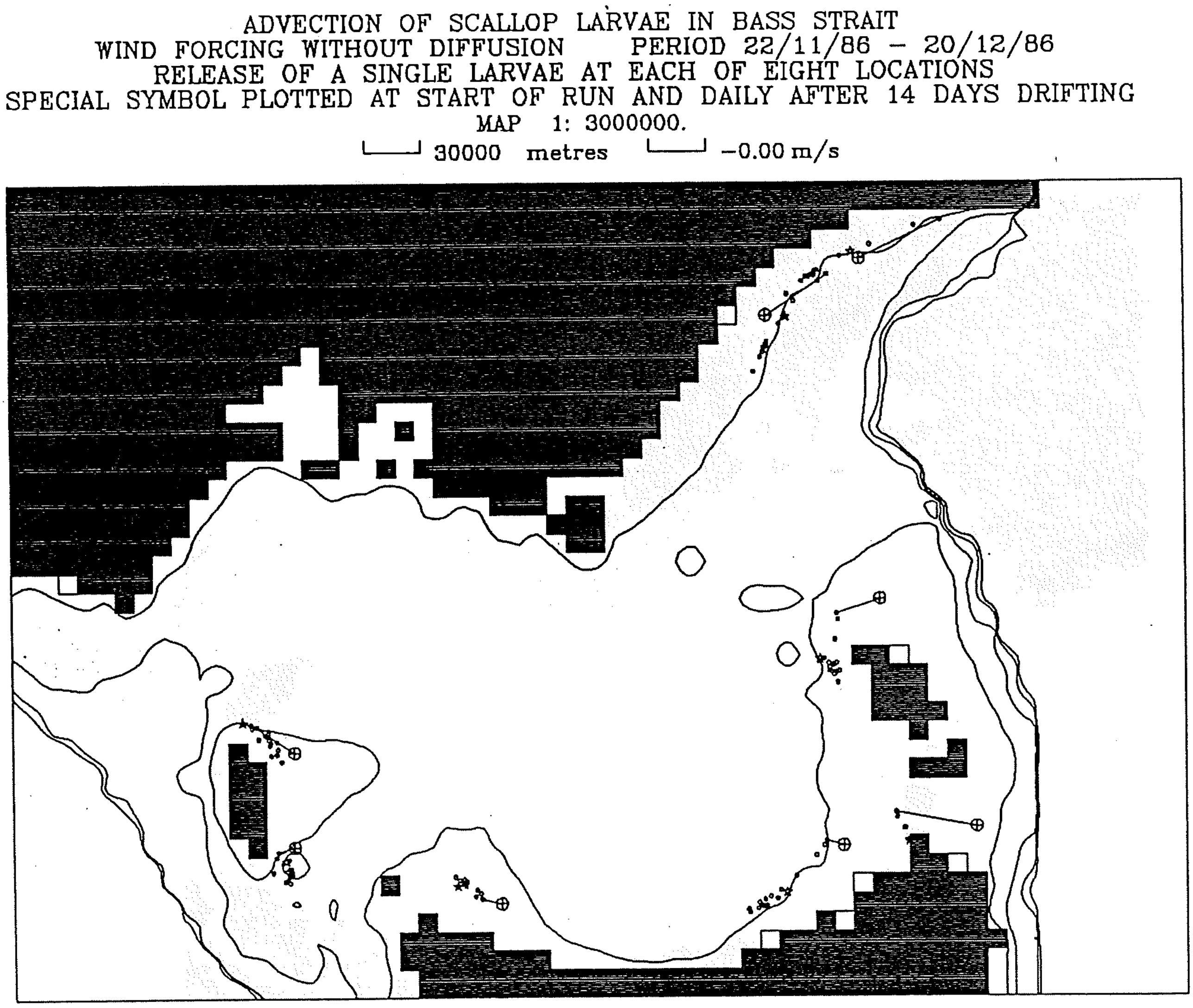

Fig. 4.21 Pelagic excursions from 8 modern beds over the 28 day period from November 22, 1986. The large crossed circle shows the release point and the straight line shows the excursion over the first non-viable 14 days. The small circles then show the positions at daily intervals in the 14-28 day interval, while the star shows the final position at the end of the 28 day pelagic period.

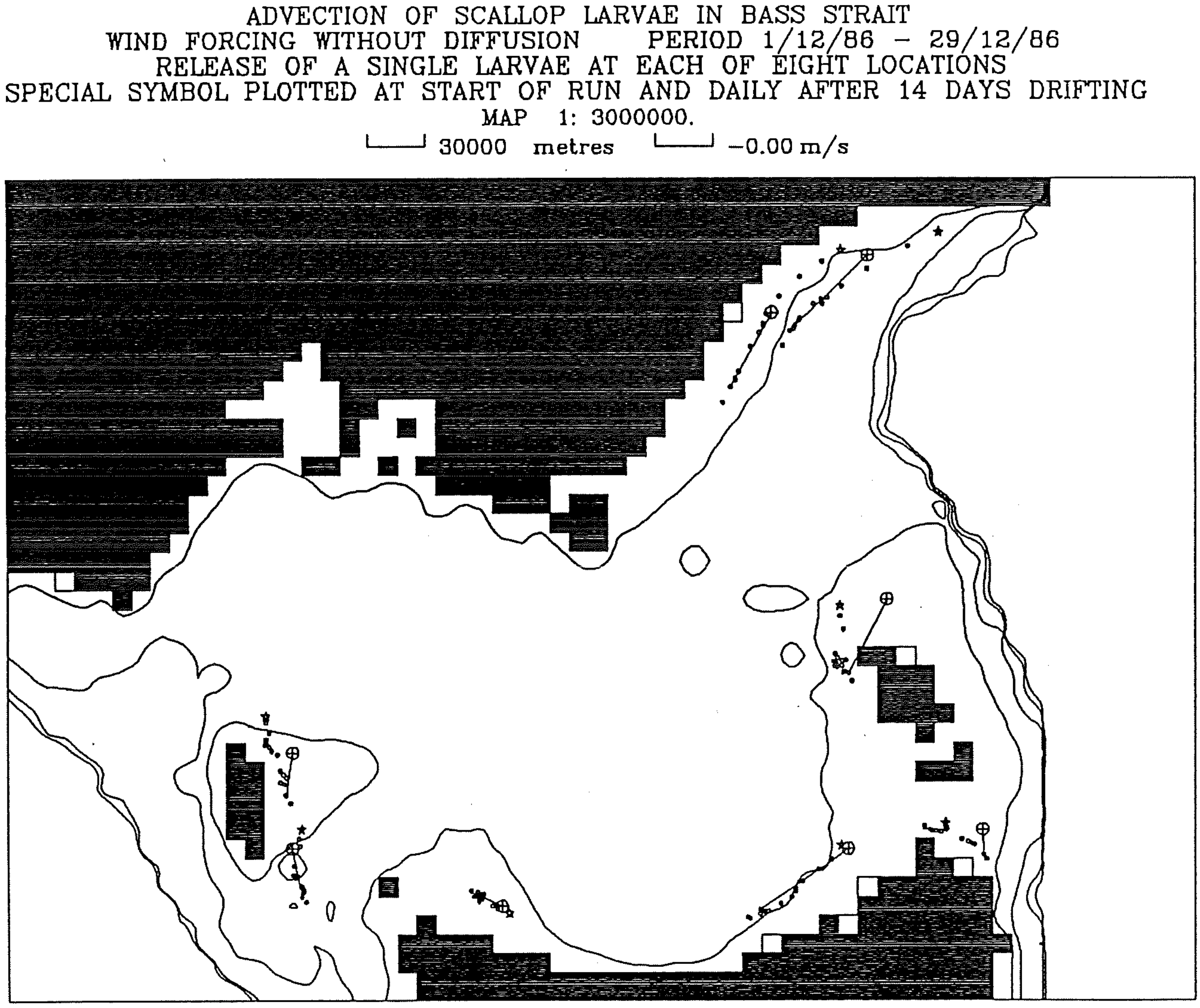

ADVECTION OF SCALLOP LARVAE IN BASS STRAIT
WIND FORCING WITHOUT DIFFUSION PERIOD 1/12/86 - 29/12/86
RELEASE OF A SINGLE LARVAE AT EACH OF EIGHT LOCATIONS
SPECIAL SYMBOL PLOTTED AT START OF RUN AND DAILY AFTER 14 DAYS DRIFTING
MAP 1: 3000000.

Fig. 4.2m Pelagic excursions from 8 modern beds over the 28 day period from December 1, 1986. The large crossed circle shows the release point and the straight line shows the excursion over the first non-viable 14 days. The small circles then show the positions at daily intervals in the 14-28 day interval, while the star shows the final position at the end of the 28 day pelagic period.

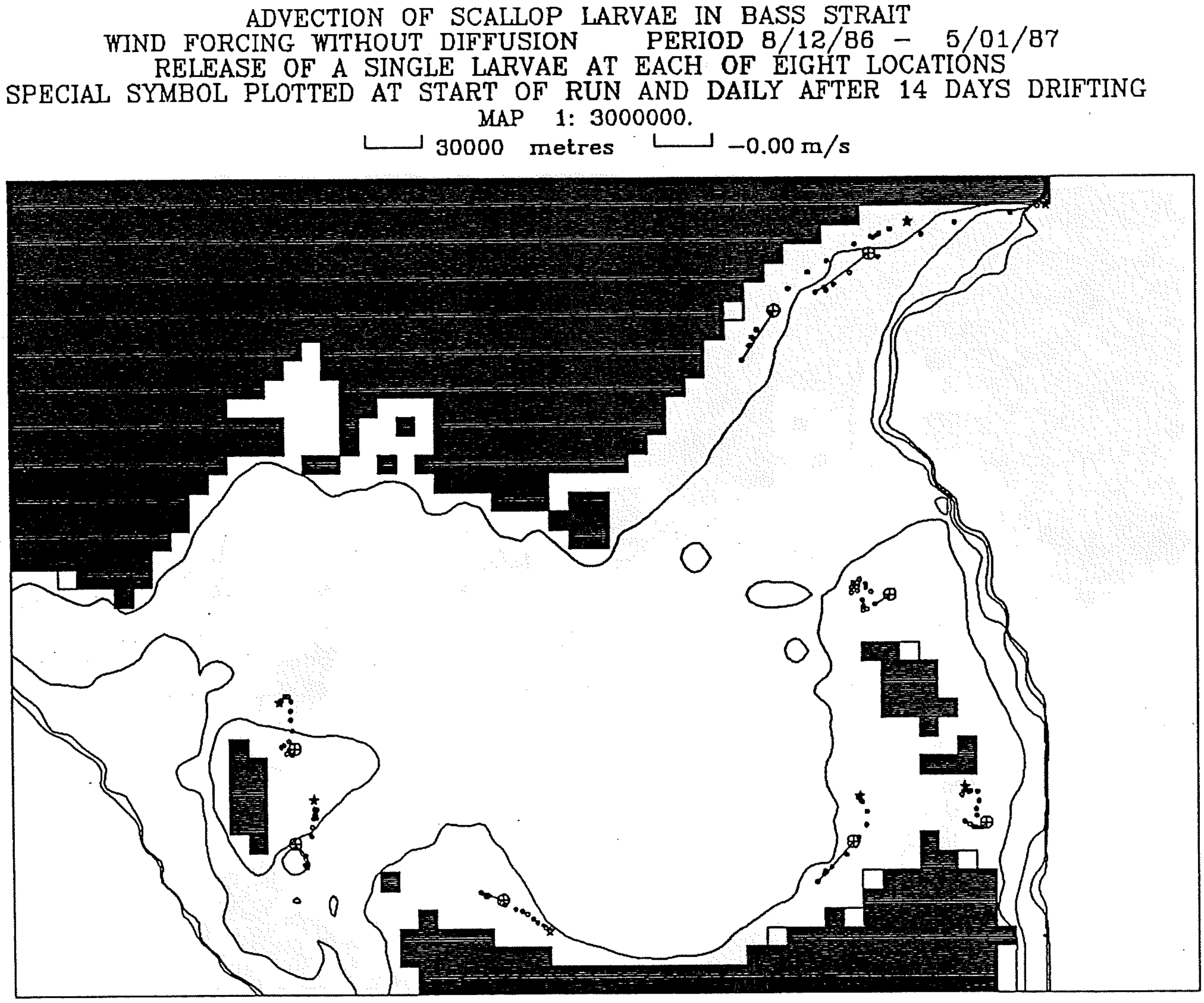

ADVECTION OF SCALLOP LARVAE IN BASS STRAIT
WIND FORCING WITHOUT DIFFUSION   PERIOD 8/12/86 - 5/01/87
RELEASE OF A SINGLE LARVAE AT EACH OF EIGHT LOCATIONS
SPECIAL SYMBOL PLOTTED AT START OF RUN AND DAILY AFTER 14 DAYS DRIFTING
MAP 1: 3000000.

Fig. 4.2n Pelagic excursions from 8 modern beds over the 28 day period from December 8, 1986. The large crossed circle shows the release point and the straight line shows the excursion over the first non-viable 14 days. The small circles then show the positions at daily intervals in the 14-28 day interval, while the star shows the final position at the end of the 28 day pelagic period.

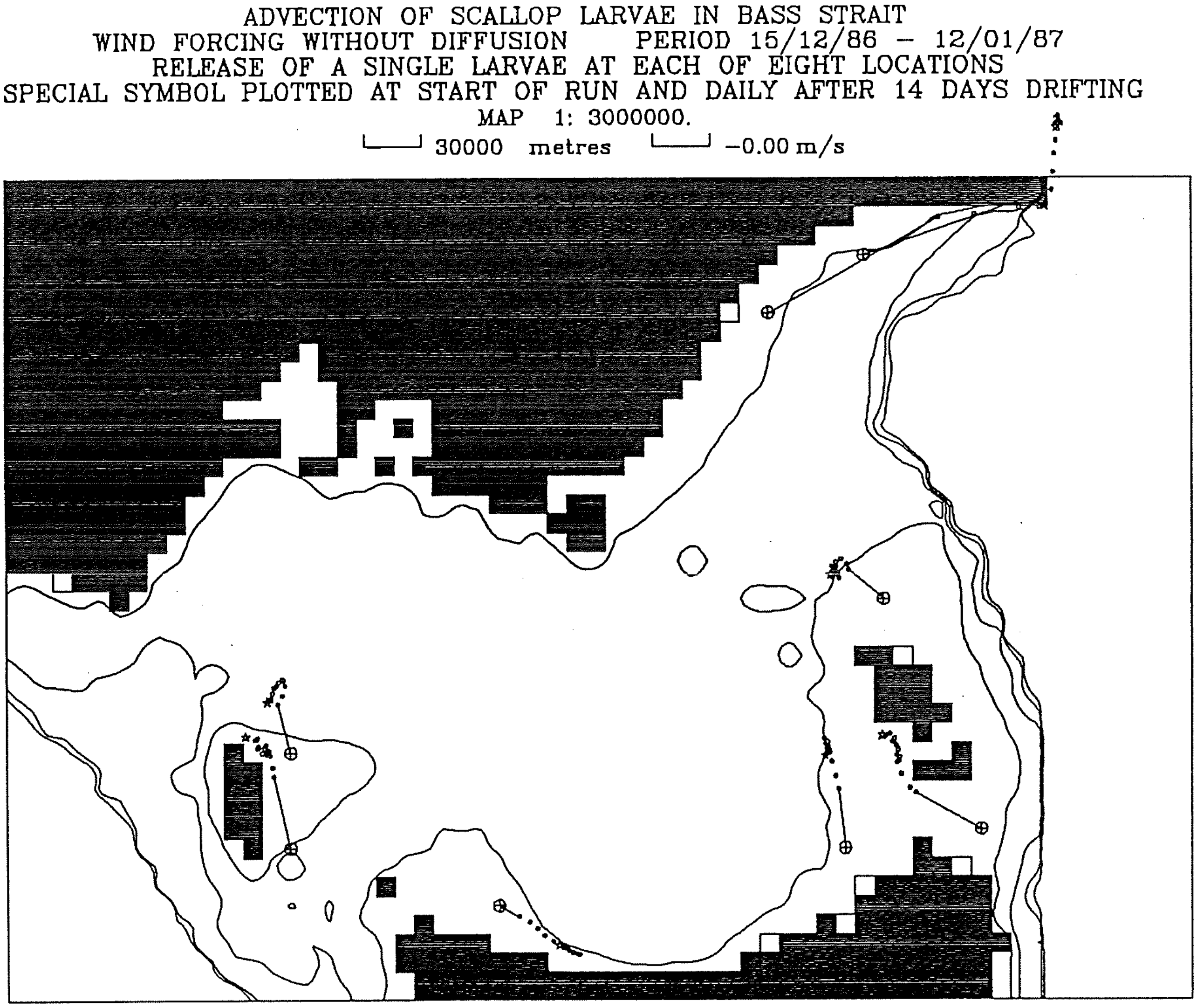

ADVECTION OF SCALLOP LARVAE IN BASS STRAIT
WIND FORCING WITHOUT DIFFUSION PERIOD 15/12/86 - 12/01/87
RELEASE OF A SINGLE LARVAE AT EACH OF EIGHT LOCATIONS
SPECIAL SYMBOL PLOTTED AT START OF RUN AND DAILY AFTER 14 DAYS DRIFTING

Fig. 4.2o Pelagic excursions from 8 modern beds over the 28 day period from December 15, 1986. The large crossed circle shows the release point and the straight line shows the excursion over the first non-viable 14 days. The small circles then show the positions at daily intervals in the 14-28 day interval, while the star shows the final position at the end of the 28 day pelagic period.

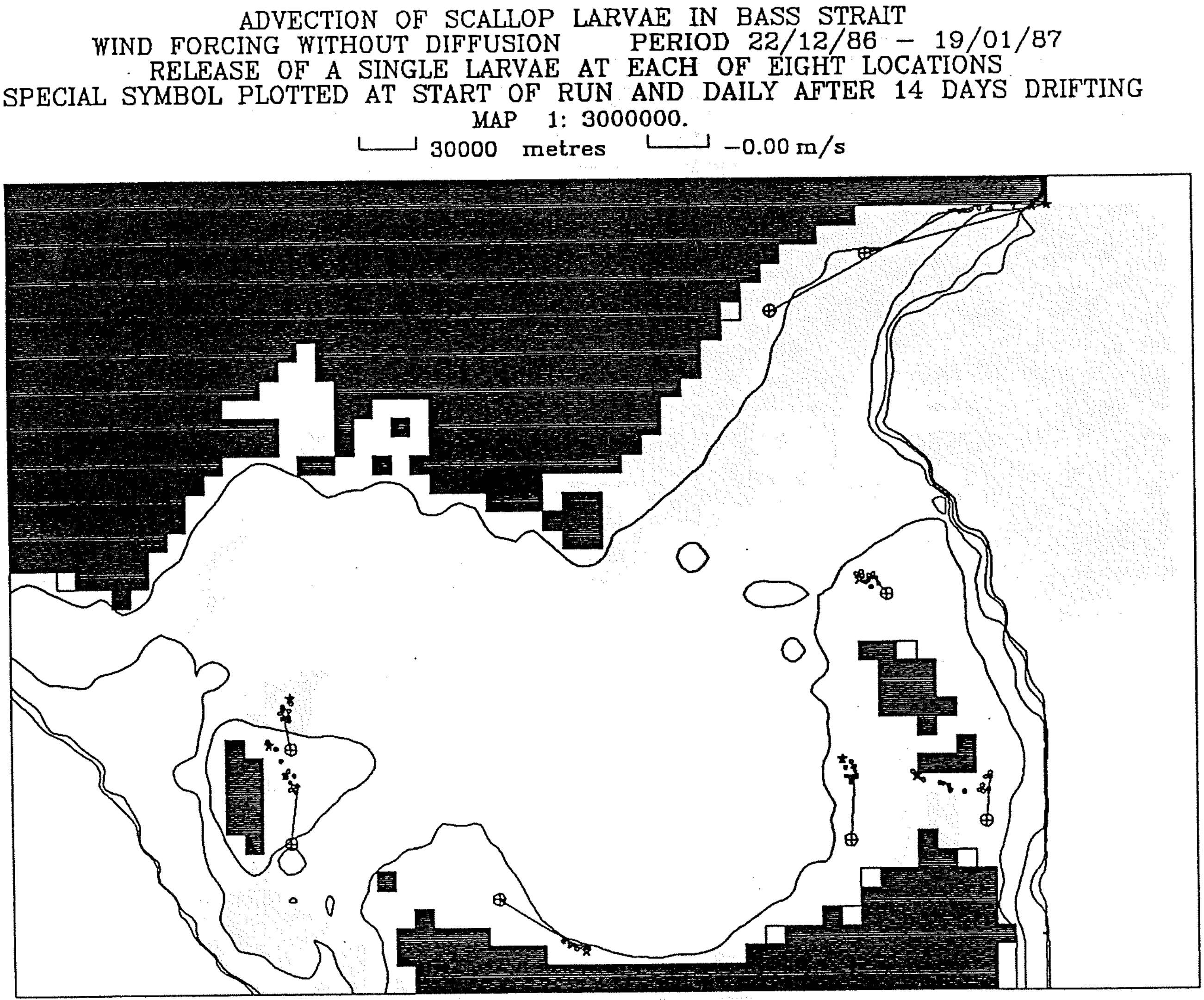

ADVECTION OF SCALLOP LARVAE IN BASS STRAIT
WIND FORCING WITHOUT DIFFUSION PERIOD 22/12/86 – 19/01/87
RELEASE OF A SINGLE LARVAE AT EACH OF EIGHT LOCATIONS
SPECIAL SYMBOL PLOTTED AT START OF RUN AND DAILY AFTER 14 DAYS DRIFTING
MAP 1: 3000000.

Fig. 4.2p Pelagic excursions from 8 modern beds over the 28 day period from December 22, 1986. The large crossed circle shows the release point and the straight line shows the excursion over the first non-viable 14 days. The small circles then show the positions at daily intervals in the 14-28 day interval, while the star shows the final position at the end of the 28 day pelagic period.

ADVECTION OF SCALLOP LARVAE IN BASS STRAIT
WIND FORCING WITHOUT DIFFUSION PERIOD 1/01/87 - 29/01/87
RELEASE OF A SINGLE LARVAE AT EACH OF EIGHT LOCATIONS
SPECIAL SYMBOL PLOTTED AT START OF RUN AND DAILY AFTER 14 DAYS DRIFTING
MAP 1: 3000000.
30000 metres -0.00 m/s

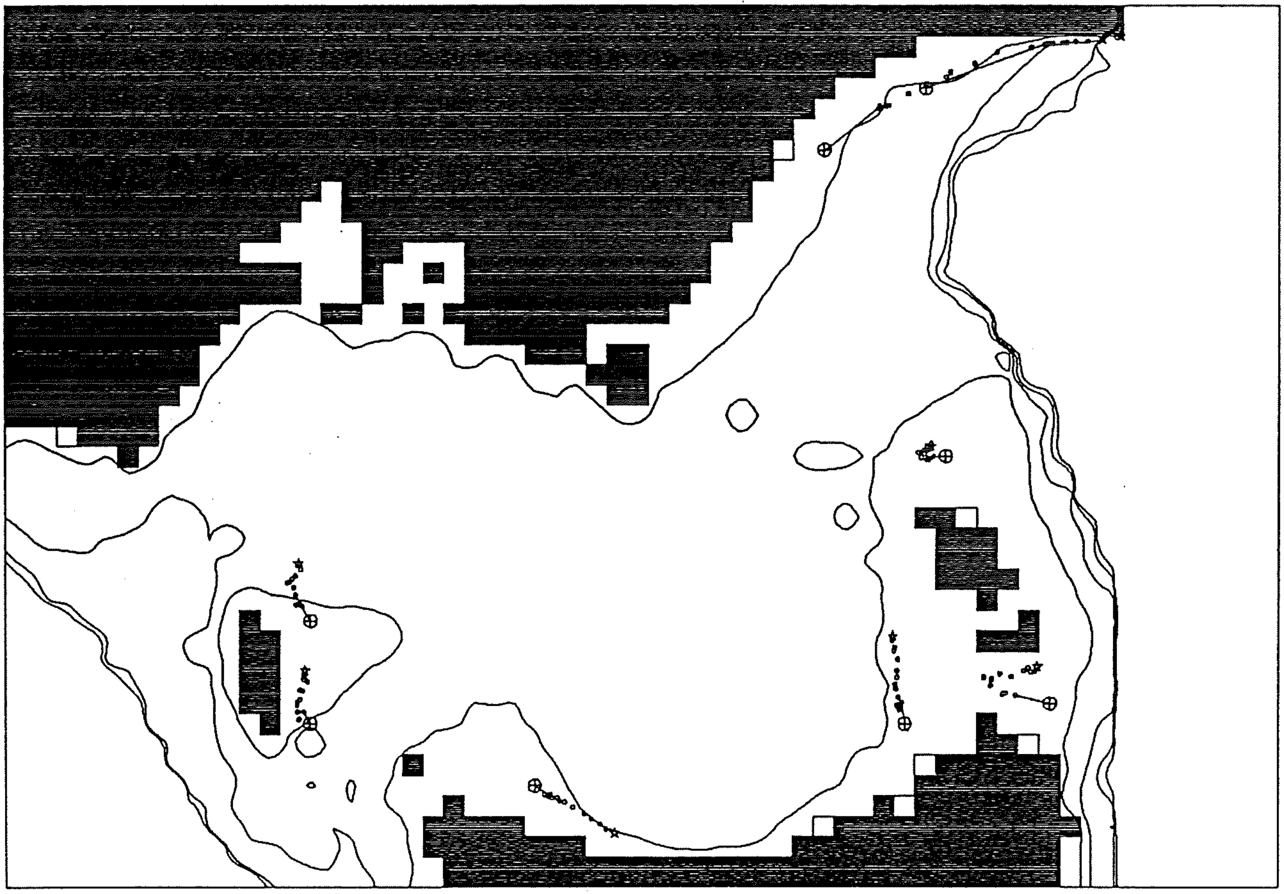

Fig. 4.2q Pelagic excursions from 8 modern beds over the 28 day period from January 1, 1987. The large crossed circle shows the release point and the straight line shows the excursion over the first non-viable 14 days. The small circles then show the positions at daily intervals in the 14-28 day interval, while the star shows the final position at the end of the 28 day pelagic period.

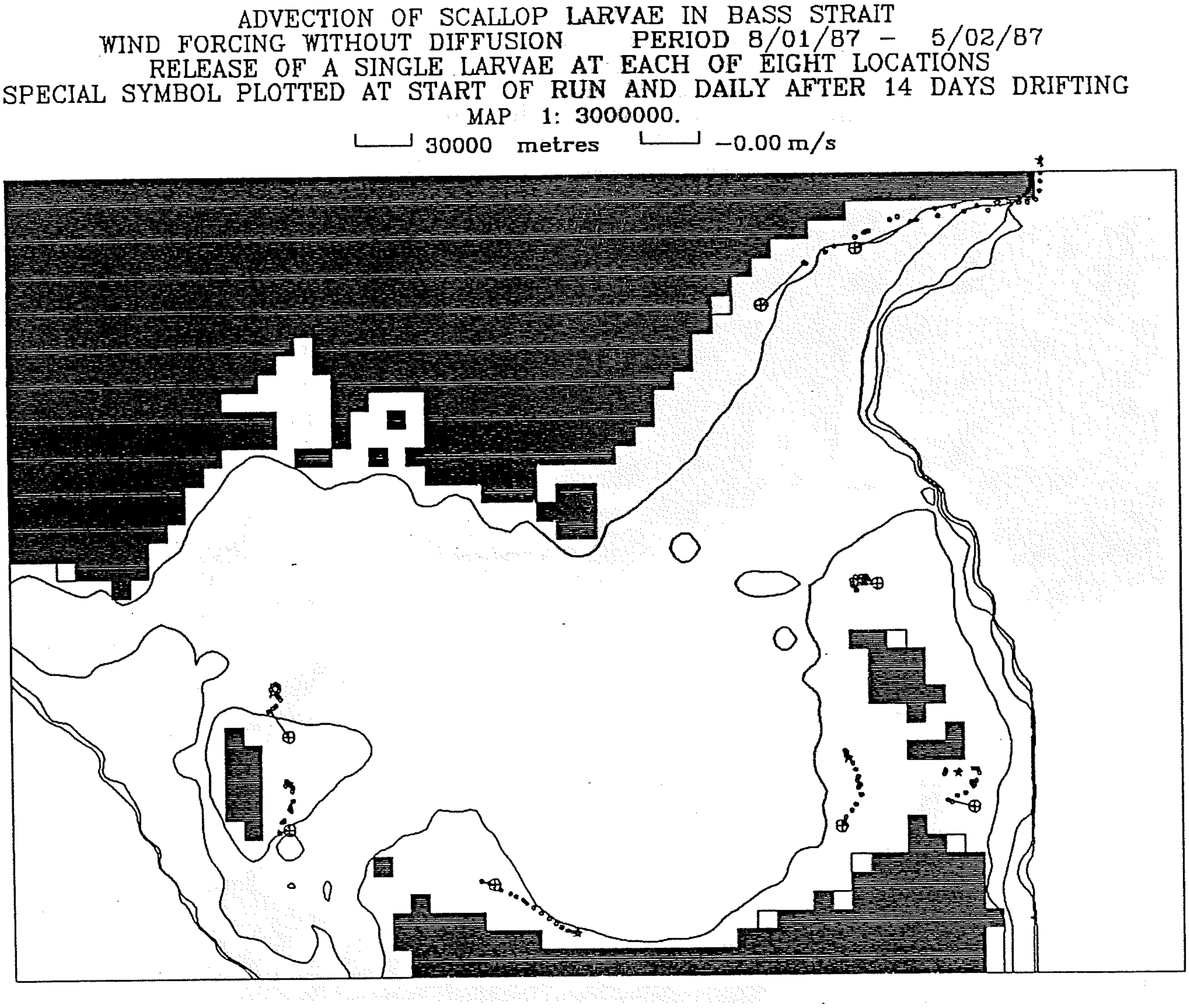

Fig. 4.2r Pelagic excursions from 8 modern beds over the 28 day period from January 8, 1987. The large crossed circle shows the release point and the straight line shows the excursion over the first non-viable 14 days. The small circles then show the positions at daily intervals in the 14-28 day interval, while the star shows the final position at the end of the 28 day pelagic period.

ADVECTION OF SCALLOP LARVAE IN BASS STRAIT
WIND FORCING WITHOUT DIFFUSION PERIOD 15/01/87 - 12/02/87
RELEASE OF A SINGLE LARVAE AT EACH OF EIGHT LOCATIONS
SPECIAL SYMBOL PLOTTED AT START OF RUN AND DAILY AFTER 14 DAYS DRIFTING
MAP 1: 3000000.

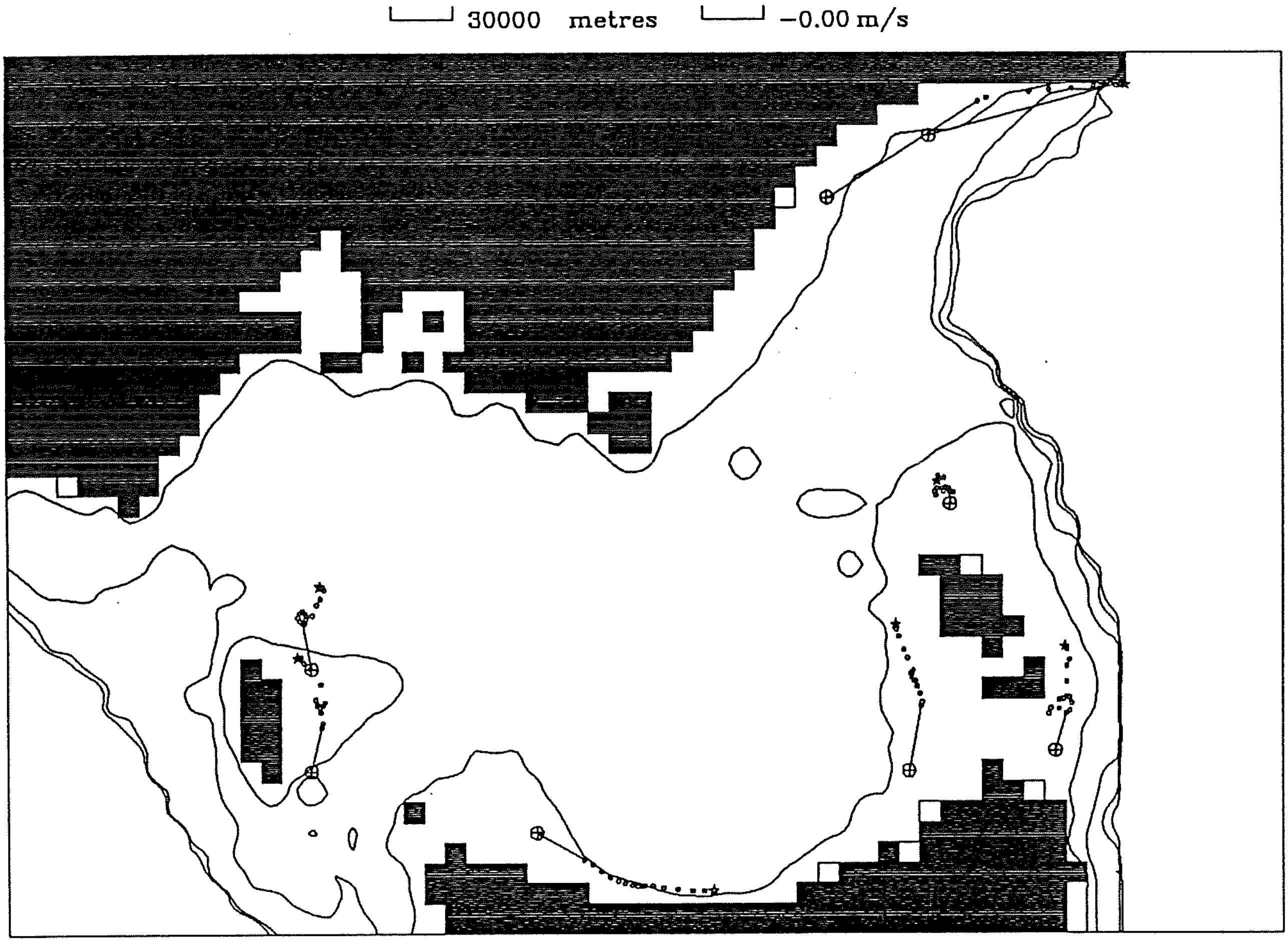

Fig. 4.2s Pelagic excursions from 8 modern beds over the 28 day period from January 15, 1987. The large crossed circle shows the release point and the straight line shows the excursion over the first non-viable 14 days. The small circles then show the positions at daily intervals in the 14-28 day interval, while the star shows the final position at the end of the 28 day pelagic period.

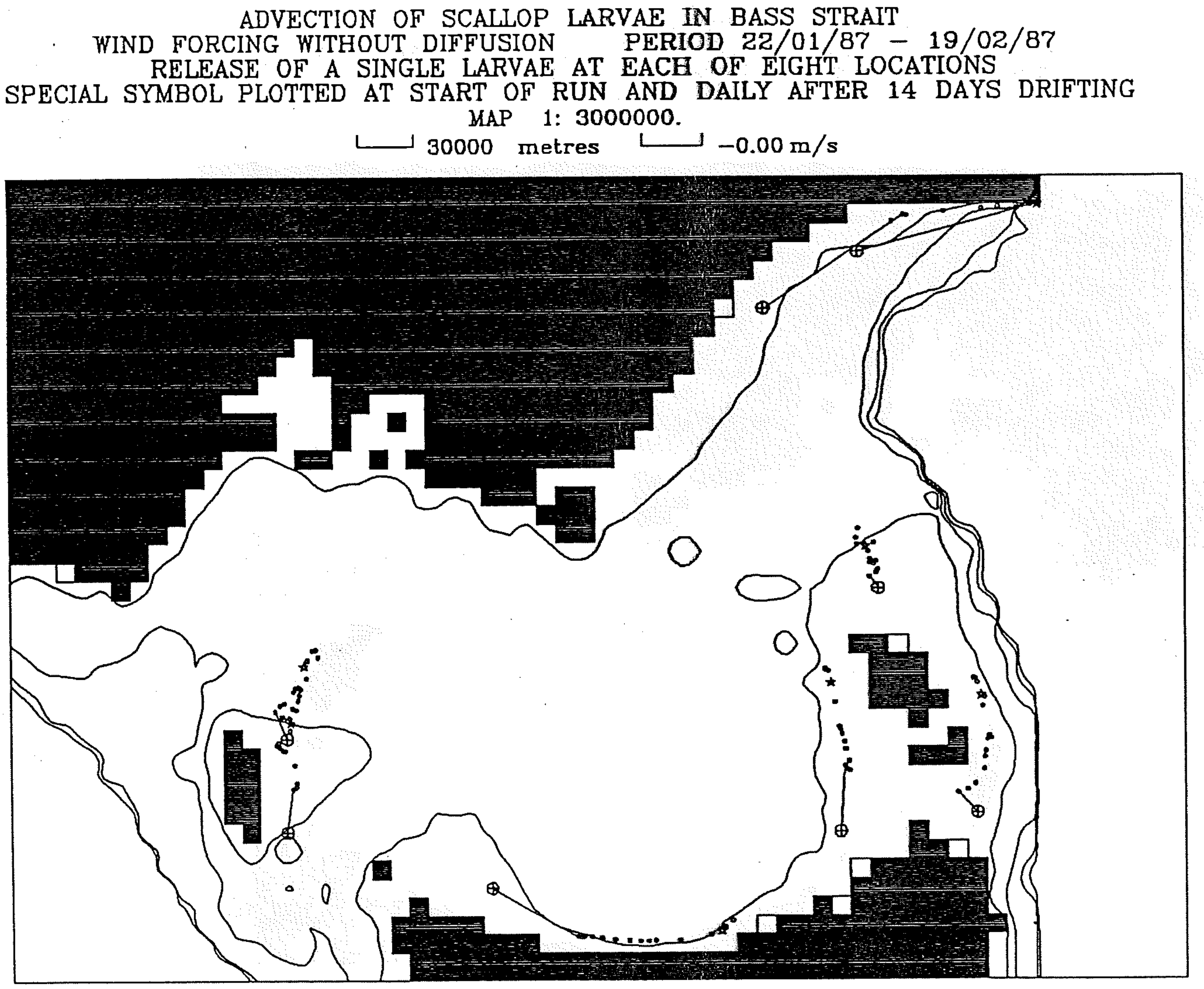

Fig. 4.2t Pelagic excursions from 8 modern beds over the 28 day period from January 22, 1987. The large crossed circle shows the release point and the straight line shows the excursion over the first non-viable 14 days. The small circles then show the positions at daily intervals in the 14-28 day interval, while the star shows the final position at the end of the 28 day pelagic period.

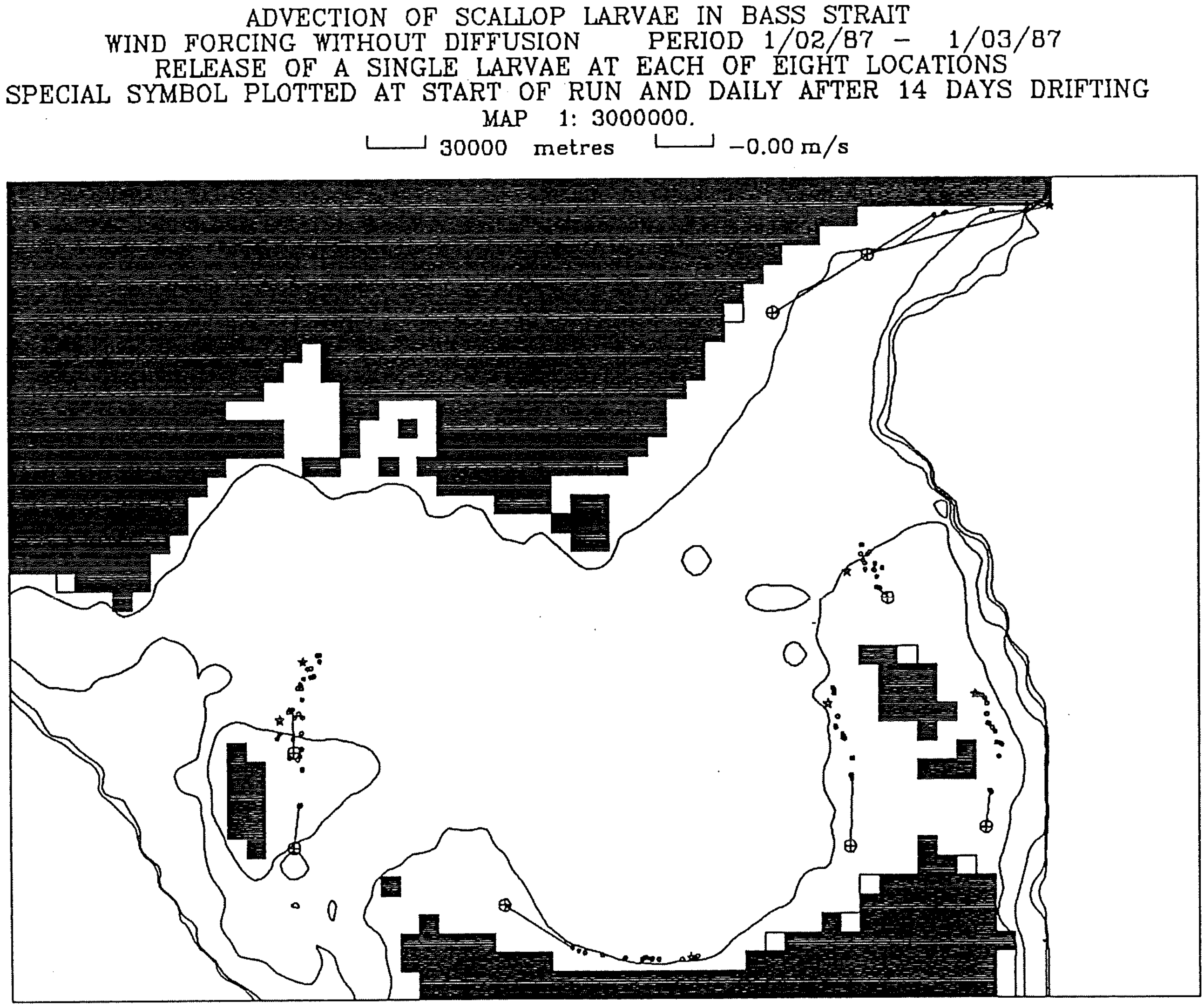

Fig. 4.2u Pelagic excursions from 8 modern beds over the 28 day period from February 1, 1987. The large crossed circle shows the release point and the straight line shows the excursion over the first non-viable 14 days. The small circles then show the positions at daily intervals in the 14-28 day interval, while the star shows the final position at the end of the 28 day pelagic period.

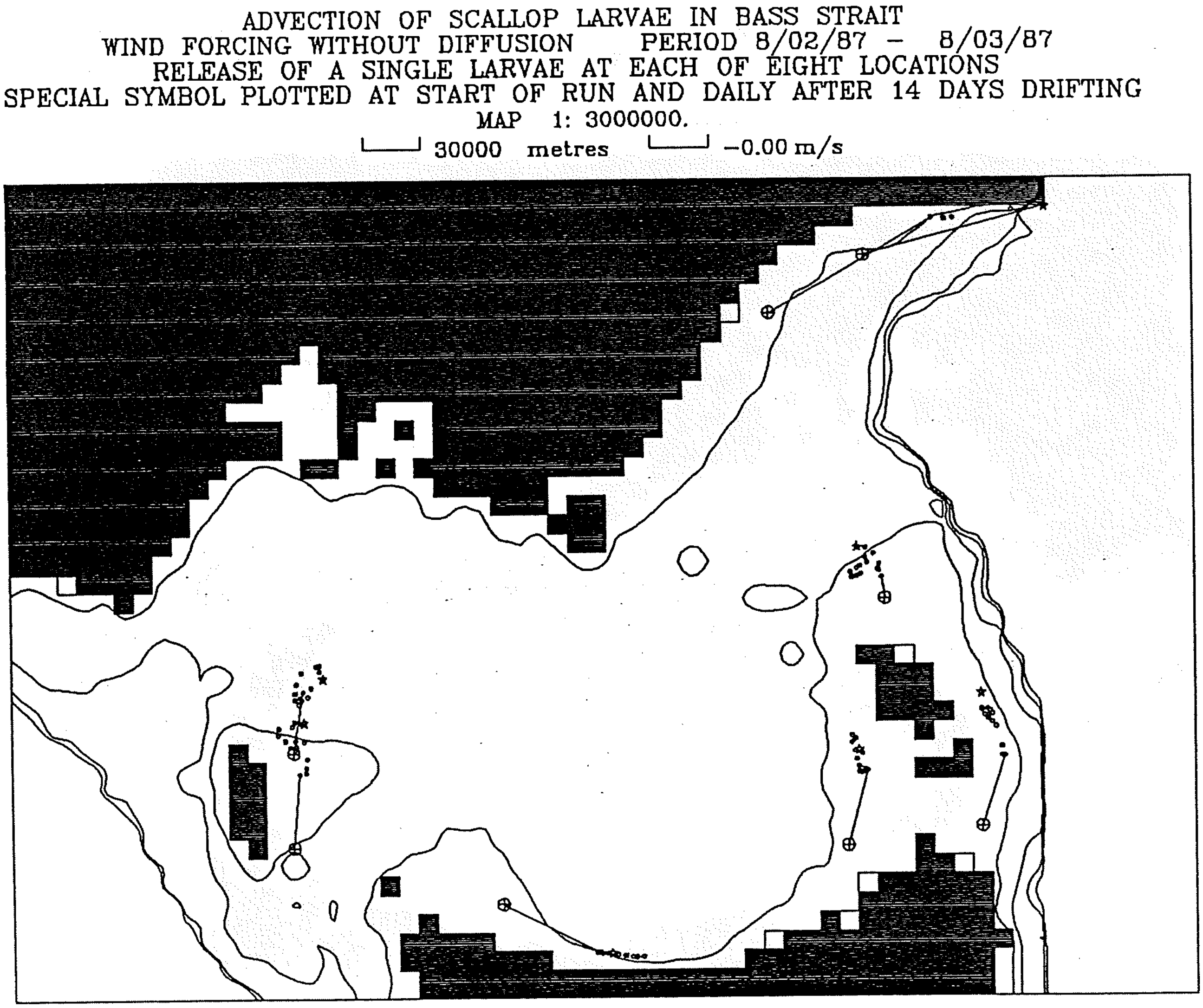

Fig. 4.2v Pelagic excursions from 8 modern beds over the 28 day period from February 8, 1987. The large crossed circle shows the release point and the straight line shows the excursion over the first non-viable 14 days. The small circles then show the positions at daily intervals in the 14-28 day interval, while the star shows the final position at the end of the 28 day pelagic period.

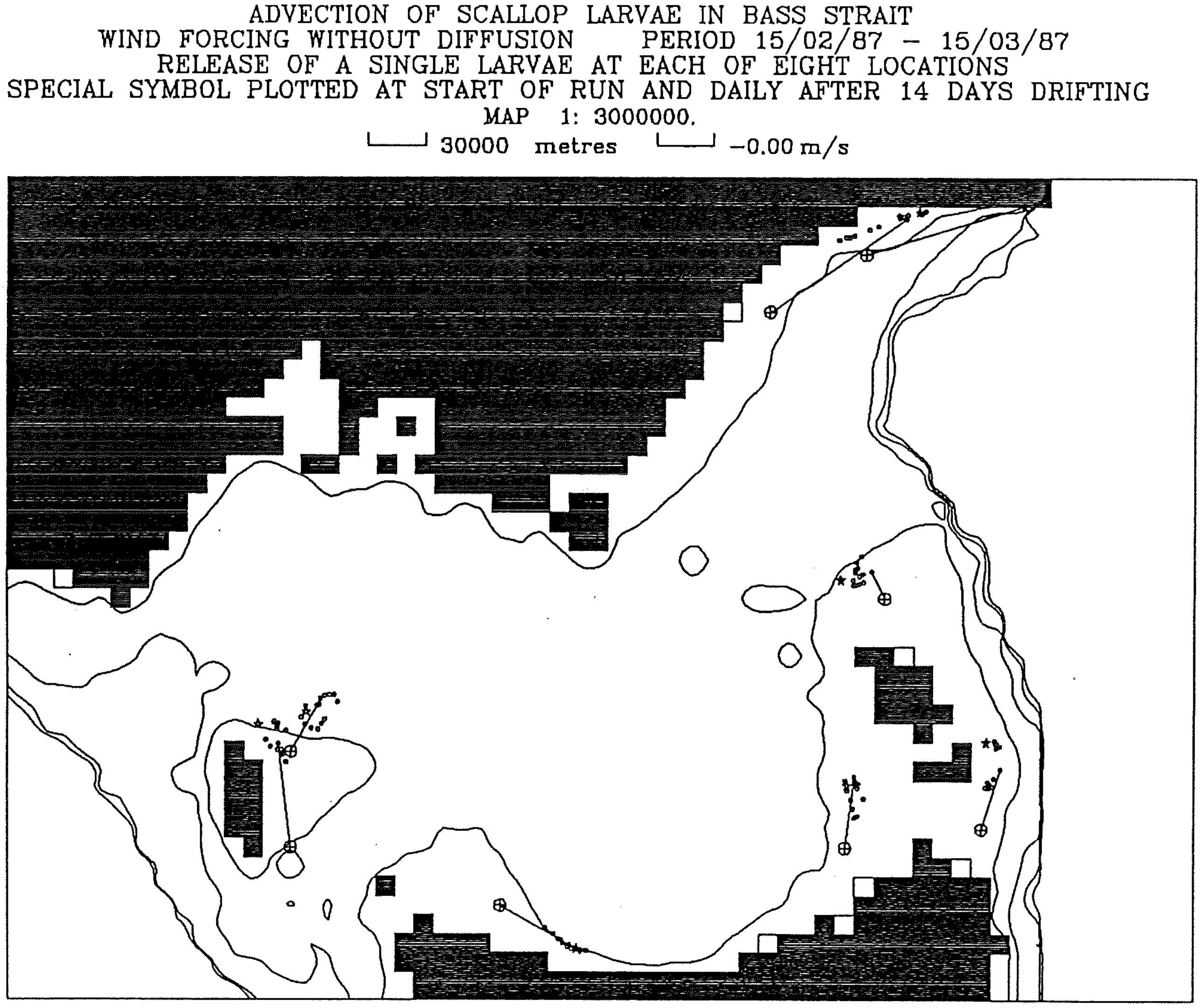

Fig. 4.2w Pelagic excursions from 8 modern beds over the 28 day period from February 15, 1987. The large crossed circle shows the release point and the straight line shows the excursion over the first non-viable 14 days. The small circles then show the positions at daily intervals in the 14-28 day interval, while the star shows the final position at the end of the 28 day pelagic period.

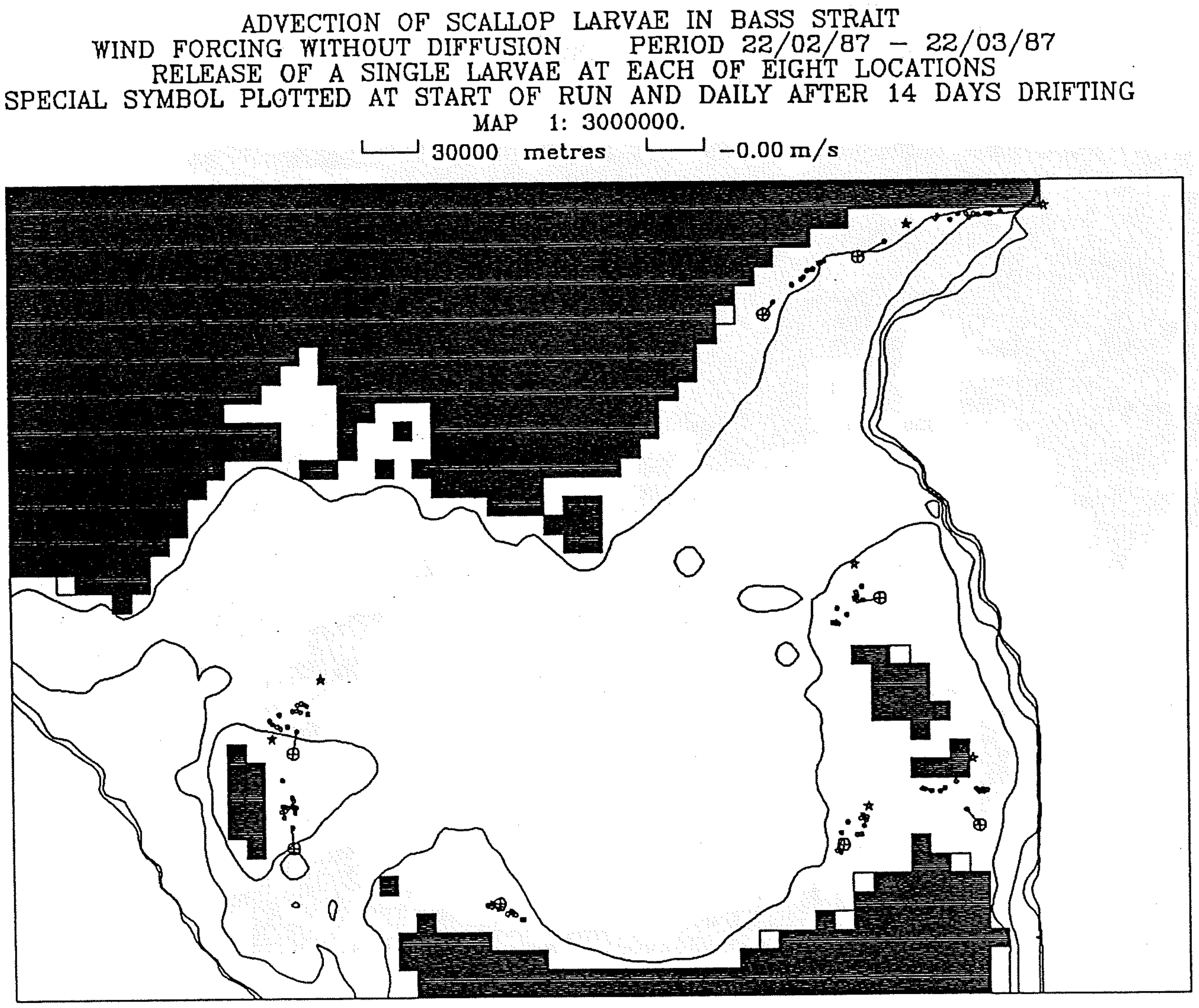

Fig. 4.2x Pelagic excursions from 8 modern beds over the 28 day period from February 22, 1987. The large crossed circle shows the release point and the straight line shows the excursion over the first non-viable 14 days. The small circles then show the positions at daily intervals in the 14-28 day interval, while the star shows the final position at the end of the 28 day pelagic period.

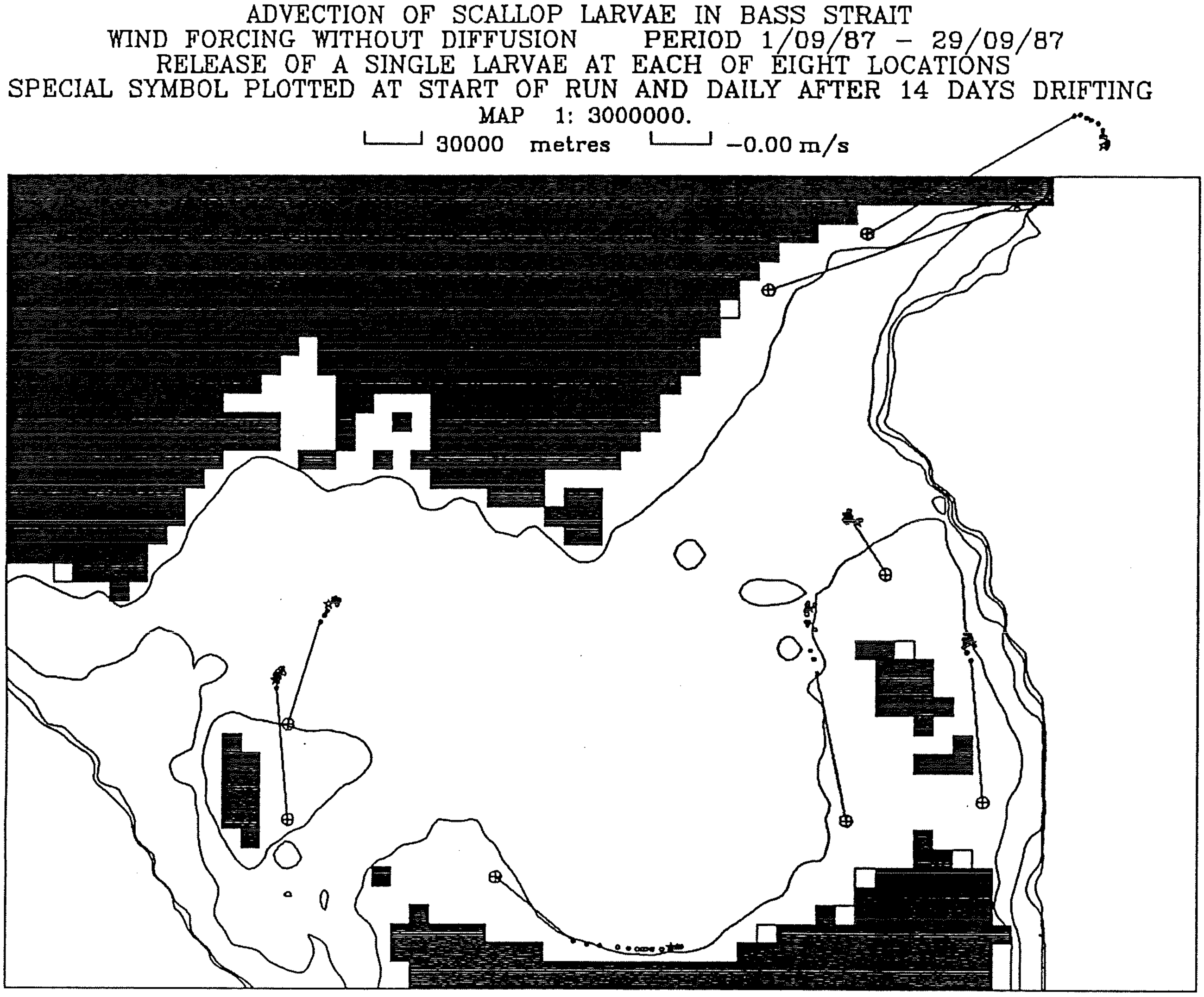

Fig. 4.3a Pelagic excursions from 8 modern beds over the 28 day period from September 1, 1987. The large crossed circle shows the release point and the straight line shows the excursion over the first non-viable 14 days. The small circles then show the positions at daily intervals in the 14-28 day interval, while the star shows the final position at the end of the 28 day pelagic period.

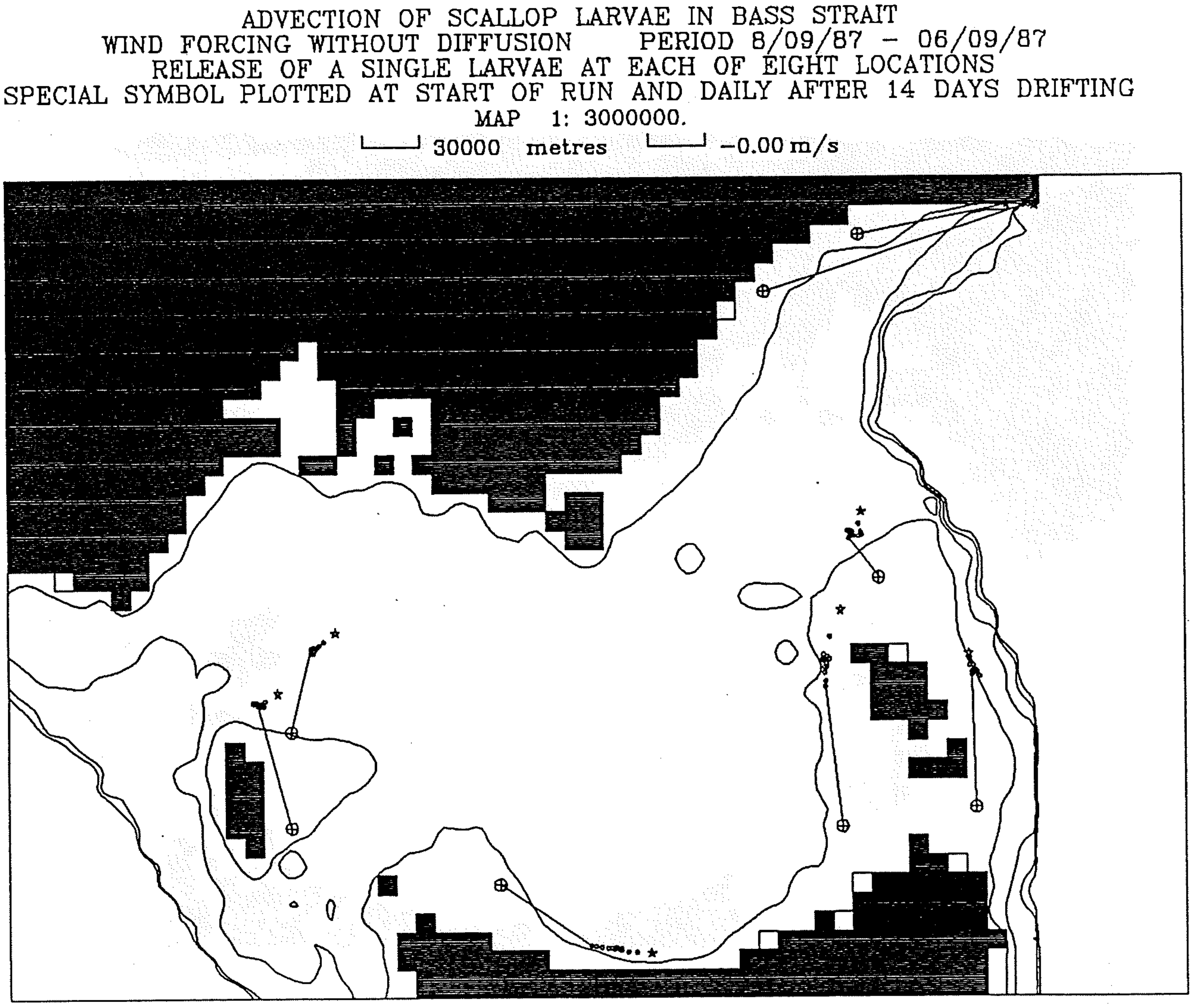

Fig. 4.3b Pelagic excursions from 8 modern beds over the 28 day period from September 8, 1987. The large crossed circle shows the release point and the straight line shows the excursion over the first non-viable 14 days. The small circles then show the positions at daily intervals in the 14-28 day interval, while the star shows the final position at the end of the 28 day pelagic period.

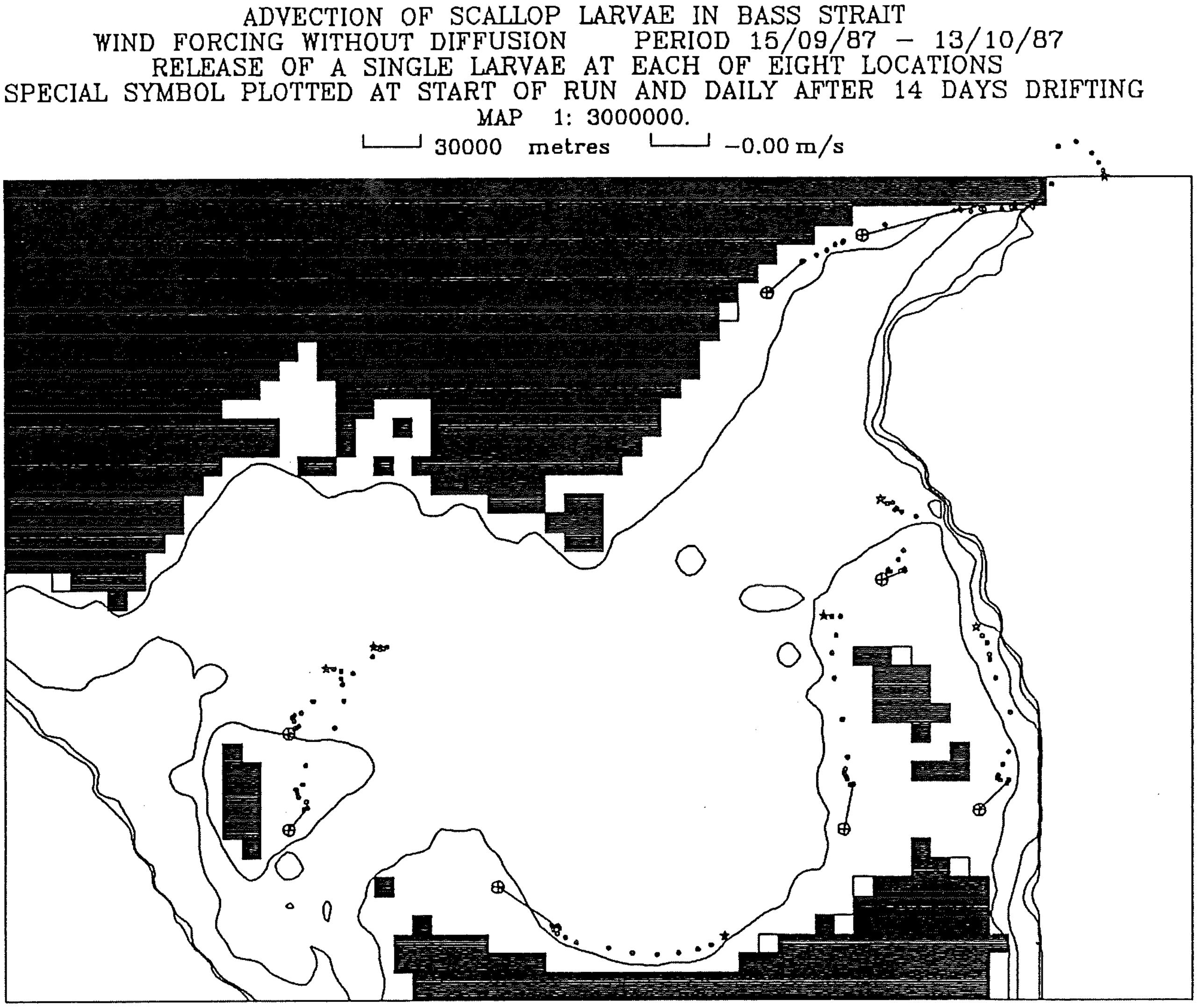

Fig. 4.3c Pelagic excursions from 8 modern beds over the 28 day period from September 15, 1987. The large crossed circle shows the release point and the straight line shows the excursion over the first non-viable 14 days. The small circles then show the positions at daily intervals in the 14-28 day interval, while the star shows the final position at the end of the 28 day pelagic period.

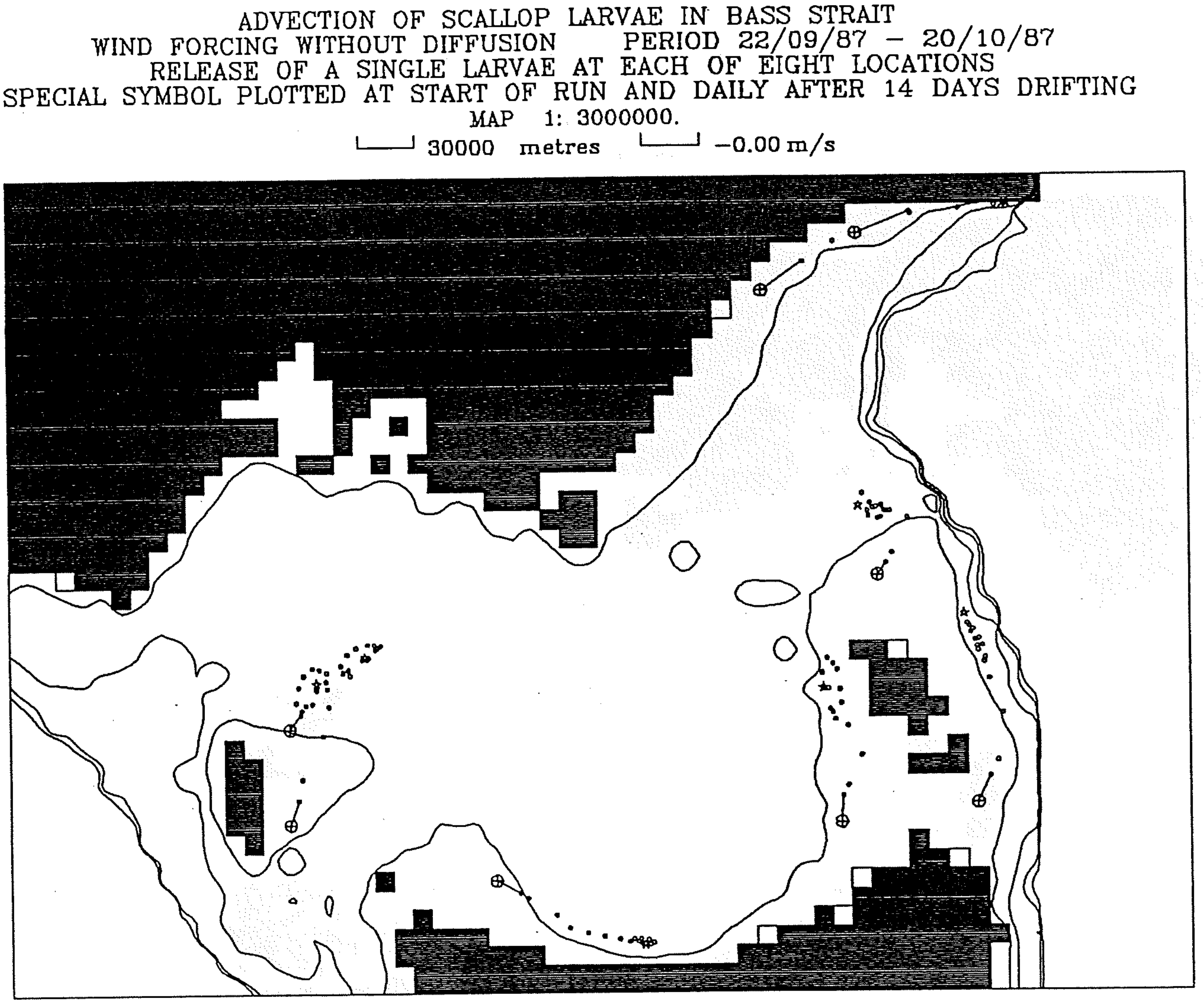

Fig. 4.3d Pelagic excursions from 8 modern beds over the 28 day period from September 22, 1987. The large crossed circle shows the release point and the straight line shows the excursion over the first non-viable 14 days. The small circles then show the positions at daily intervals in the 14-28 day interval, while the star shows the final position at the end of the 28 day pelagic period.

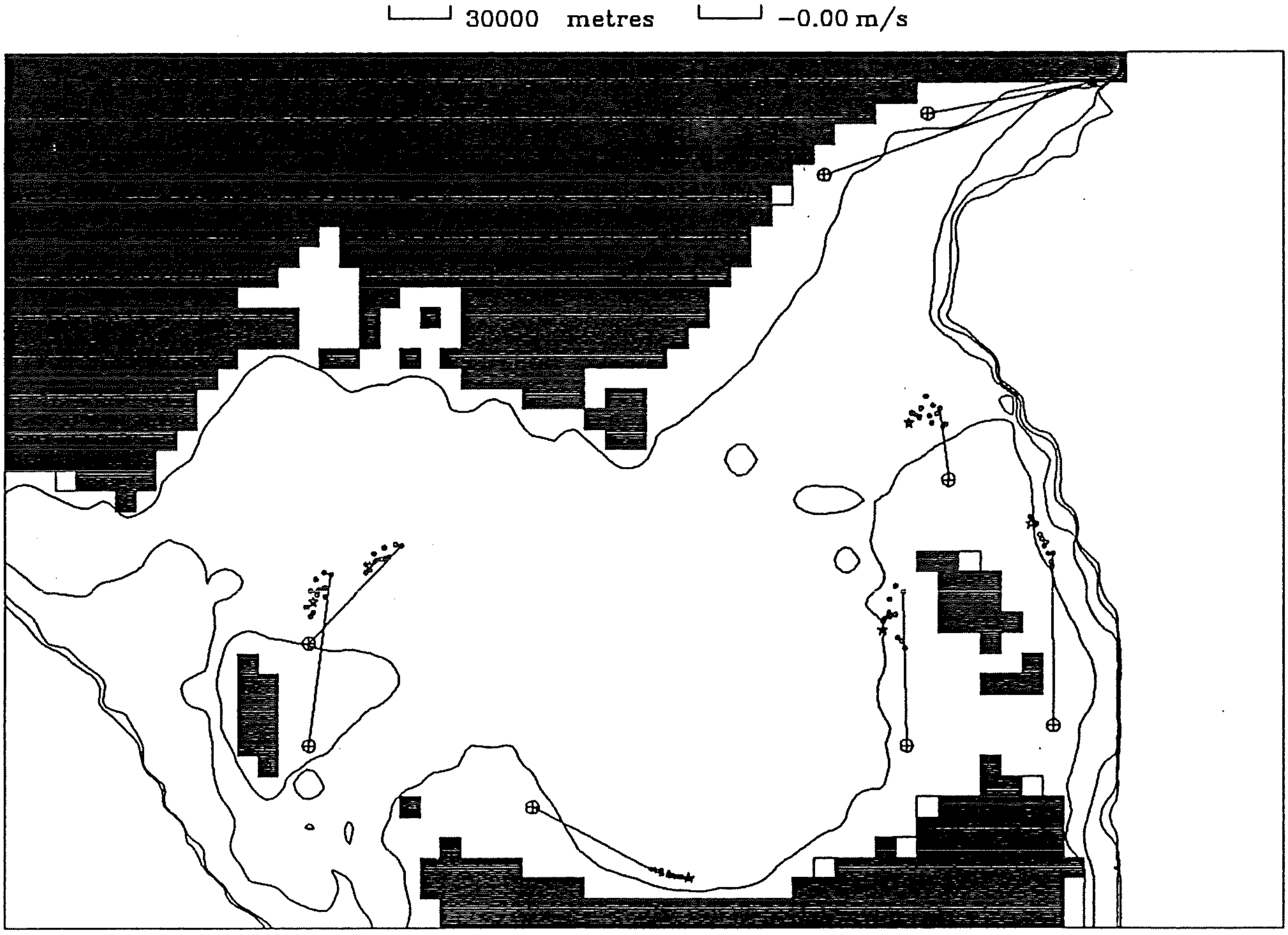

ADVECTION OF SCALLOP LARVAE IN BASS STRAIT
WIND FORCING WITHOUT DIFFUSION PERIOD 1/10/87 - 29/10/87
RELEASE OF A SINGLE LARVAE AT EACH OF EIGHT LOCATIONS
SPECIAL SYMBOL PLOTTED AT START OF RUN AND DAILY AFTER 14 DAYS DRIFTING
MAP 1: 3000000.

Fig. 4.3e Pelagic excursions from 8 modern beds over the 28 day period from October 1, 1987. The large crossed circle shows the release point and the straight line shows the excursion over the first non-viable 14 days. The small circles then show the positions at daily intervals in the 14-28 day interval, while the star shows the final position at the end of the 28 day pelagic period.

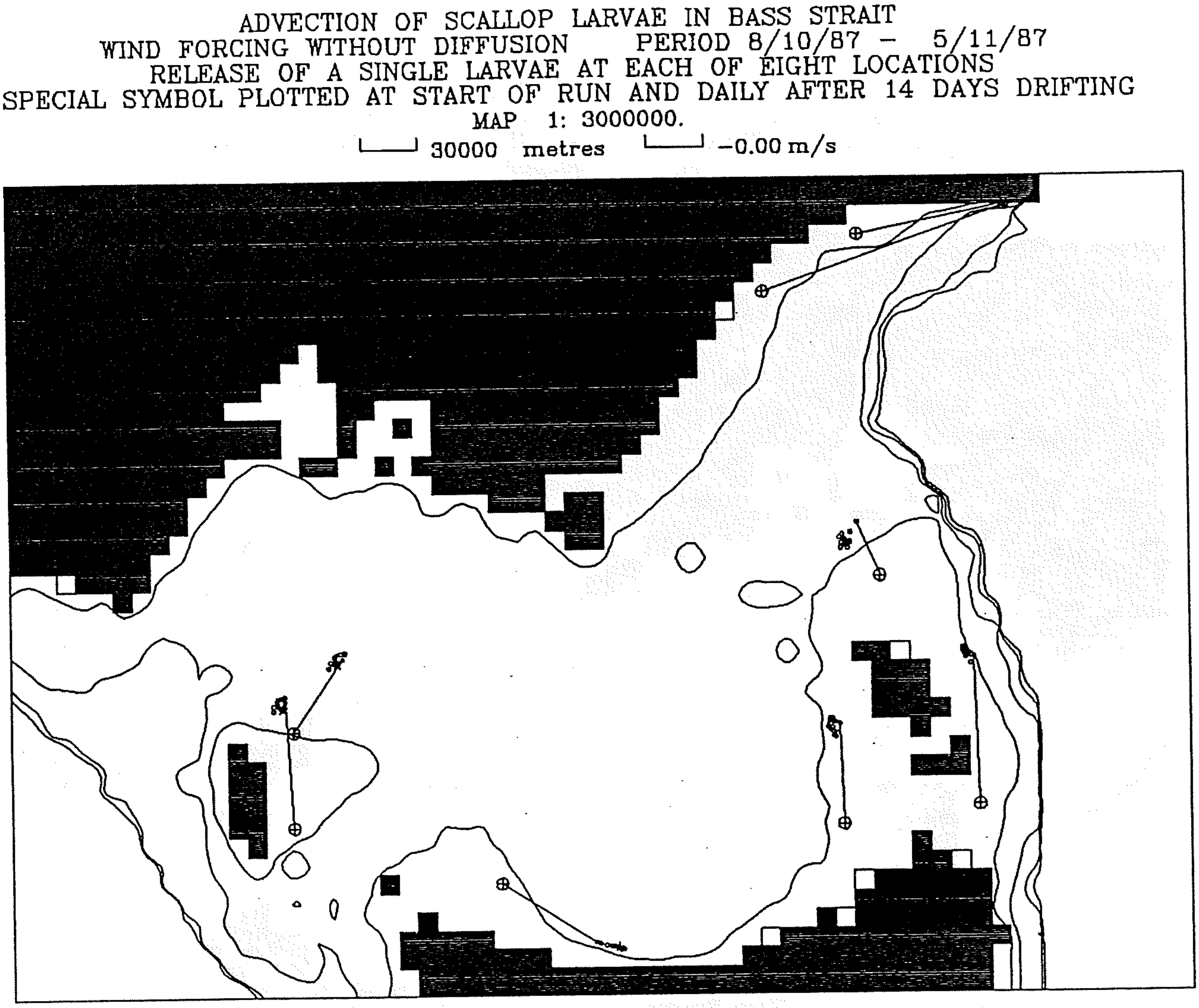

Fig. 4.3f Pelagic excursions from 8 modern beds over the 28 day period from October 8, 1987. The large crossed circle shows the release point and the straight line shows the excursion over the first non-viable 14 days. The small circles then show the positions at daily intervals in the 14-28 day interval, while the star shows the final position at the end of the 28 day pelagic period.

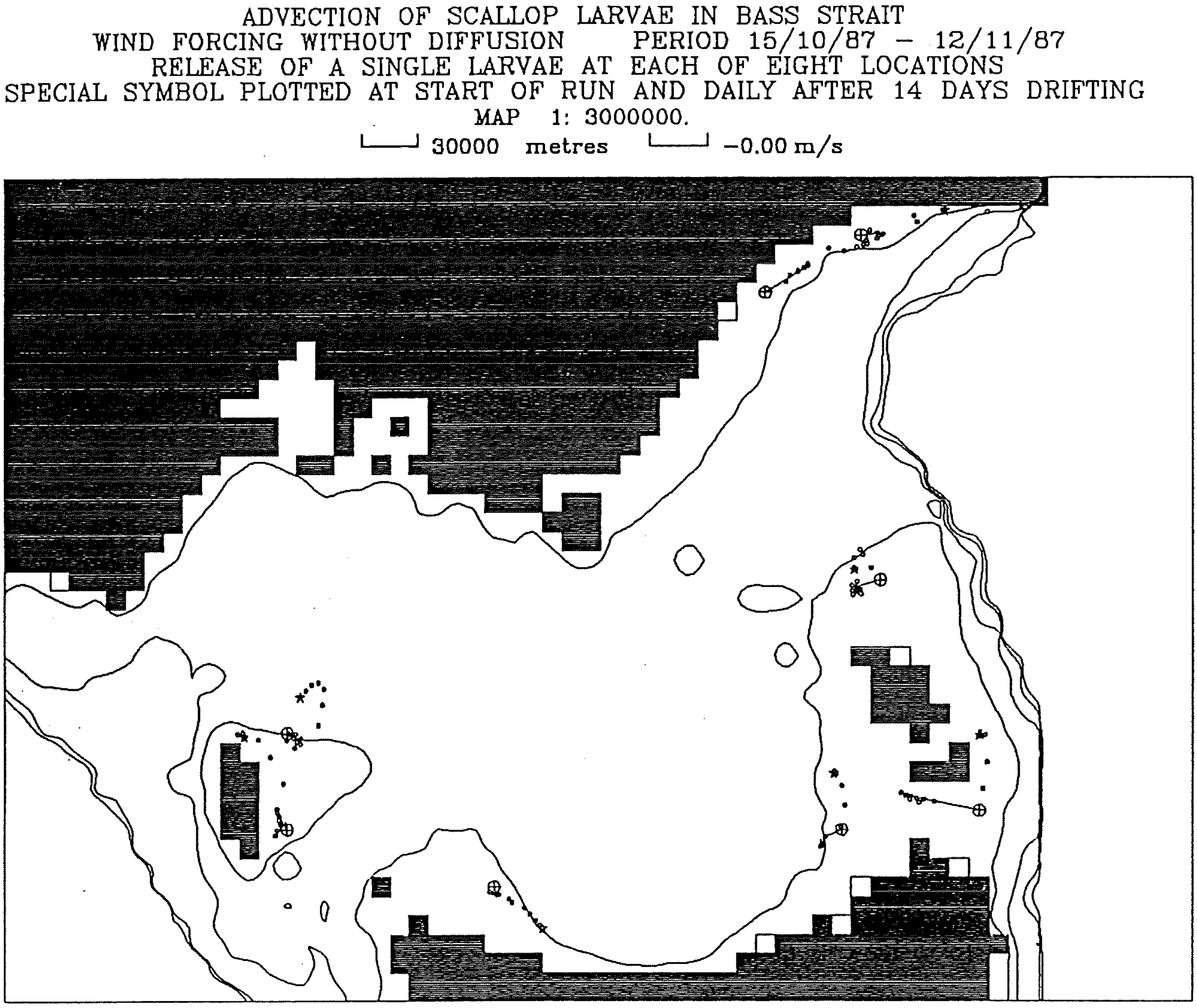

Fig. 4.3g Pelagic excursions from 8 modern beds over the 28 day period from October 15, 1987. The large crossed circle shows the release point and the straight line shows the excursion over the first non-viable 14 days. The small circles then show the positions at daily intervals in the 14-28 day interval, while the star shows the final position at the end of the 28 day pelagic period.

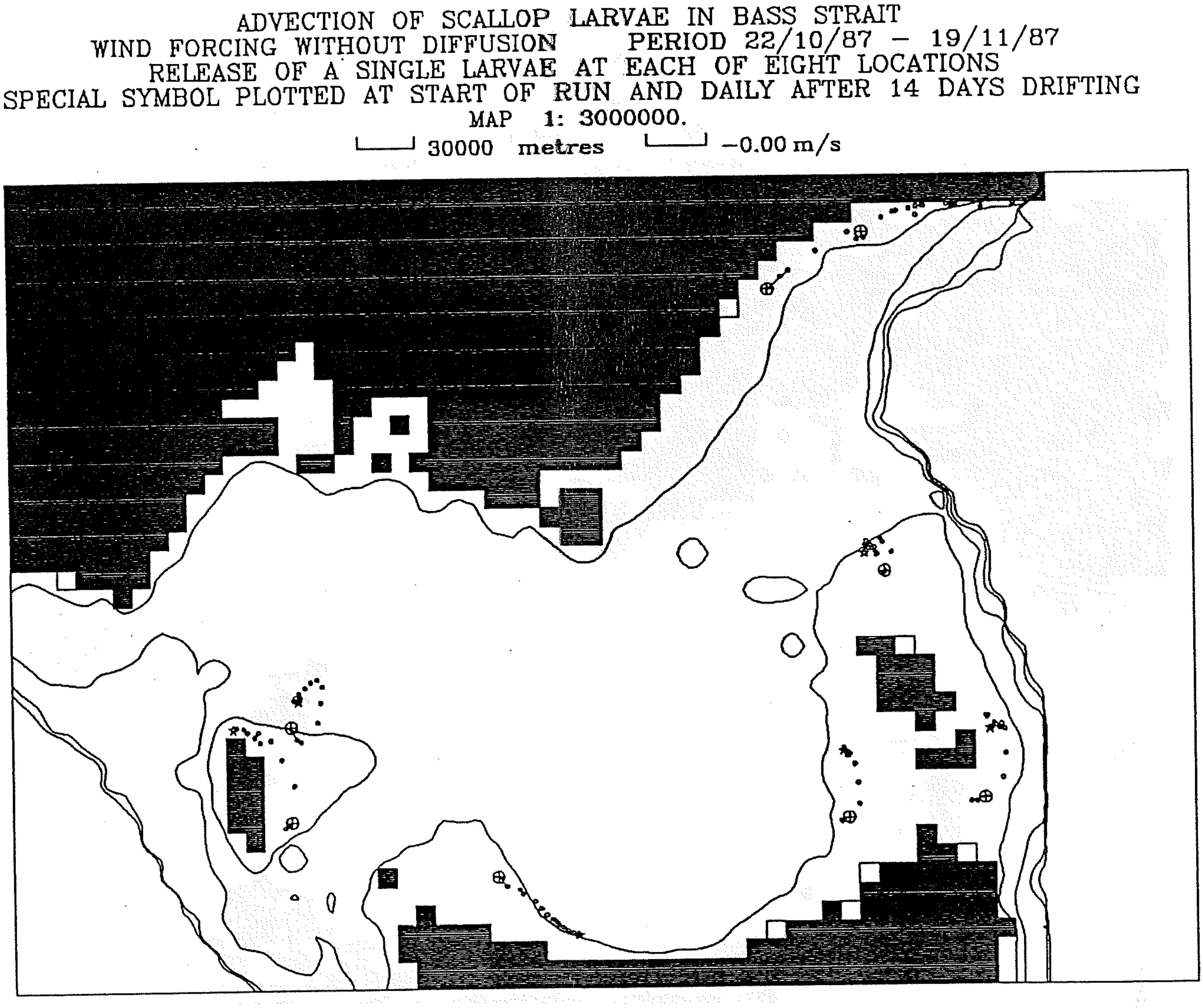

ADVECTION OF SCALLOP LARVAE IN BASS STRAIT
WIND FORCING WITHOUT DIFFUSION PERIOD 22/10/87 – 19/11/87
RELEASE OF A SINGLE LARVAE AT EACH OF EIGHT LOCATIONS
SPECIAL SYMBOL PLOTTED AT START OF RUN AND DAILY AFTER 14 DAYS DRIFTING
MAP 1: 3000000.

Fig. 4.3h Pelagic excursions from 8 modern beds over the 28 day period from October 22, 1987. The large crossed circle shows the release point and the straight line shows the excursion over the first non-viable 14 days. The small circles then show the positions at daily intervals in the 14-28 day interval, while the star shows the final position at the end of the 28 day pelagic period.

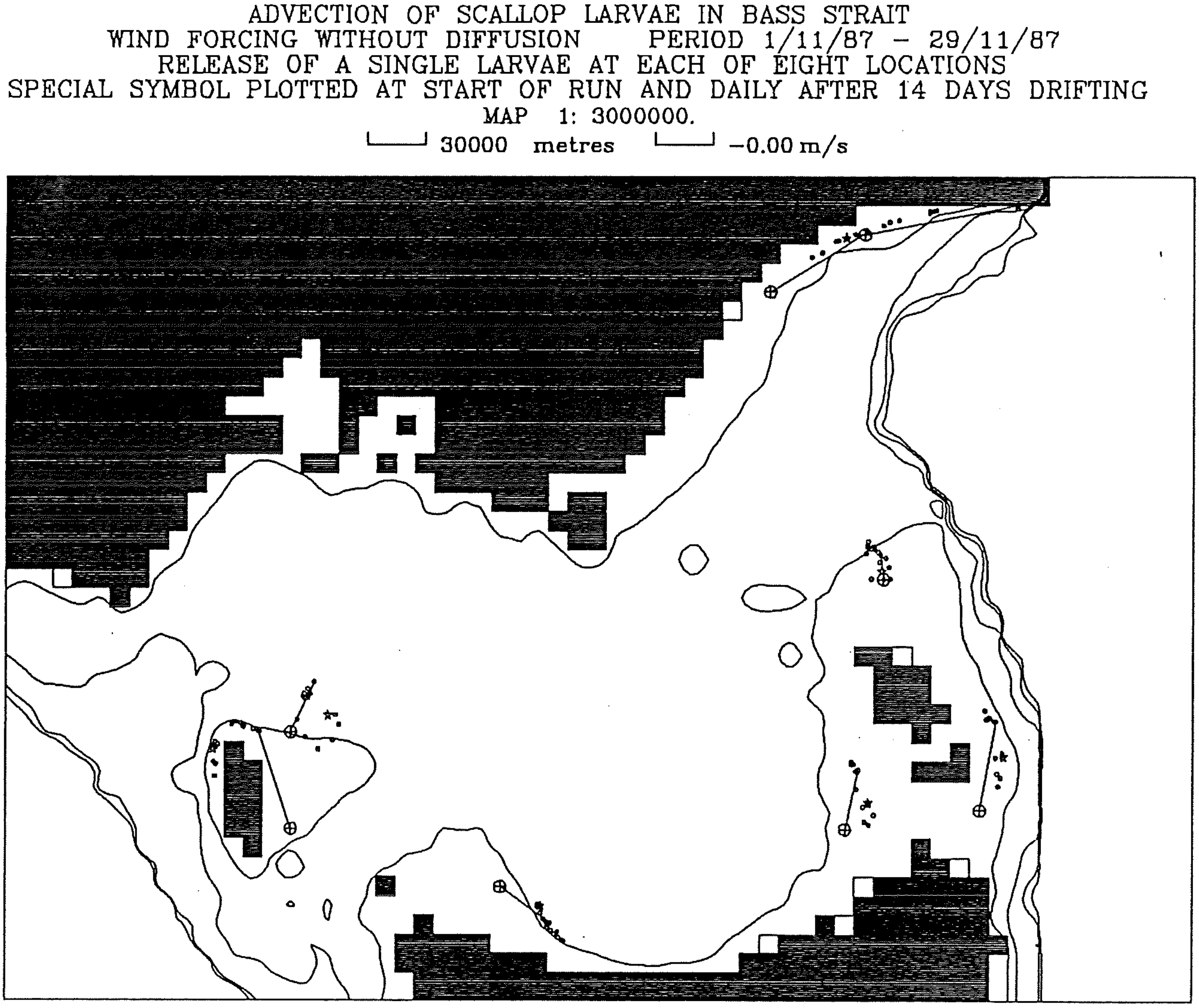

ADVECTION OF SCALLOP LARVAE IN BASS STRAIT
WIND FORCING WITHOUT DIFFUSION PERIOD 1/11/87 - 29/11/87
RELEASE OF A SINGLE LARVAE AT EACH OF EIGHT LOCATIONS
SPECIAL SYMBOL PLOTTED AT START OF RUN AND DAILY AFTER 14 DAYS DRIFTING
MAP 1: 3000000.

Fig. 4.3i Pelagic excursions from 8 modern beds over the 28 day period from November 1, 1987. The large crossed circle shows the release point and the straight line shows the excursion over the first non-viable 14 days. The small circles then show the positions at daily intervals in the 14-28 day interval, while the star shows the final position at the end of the 28 day pelagic period.

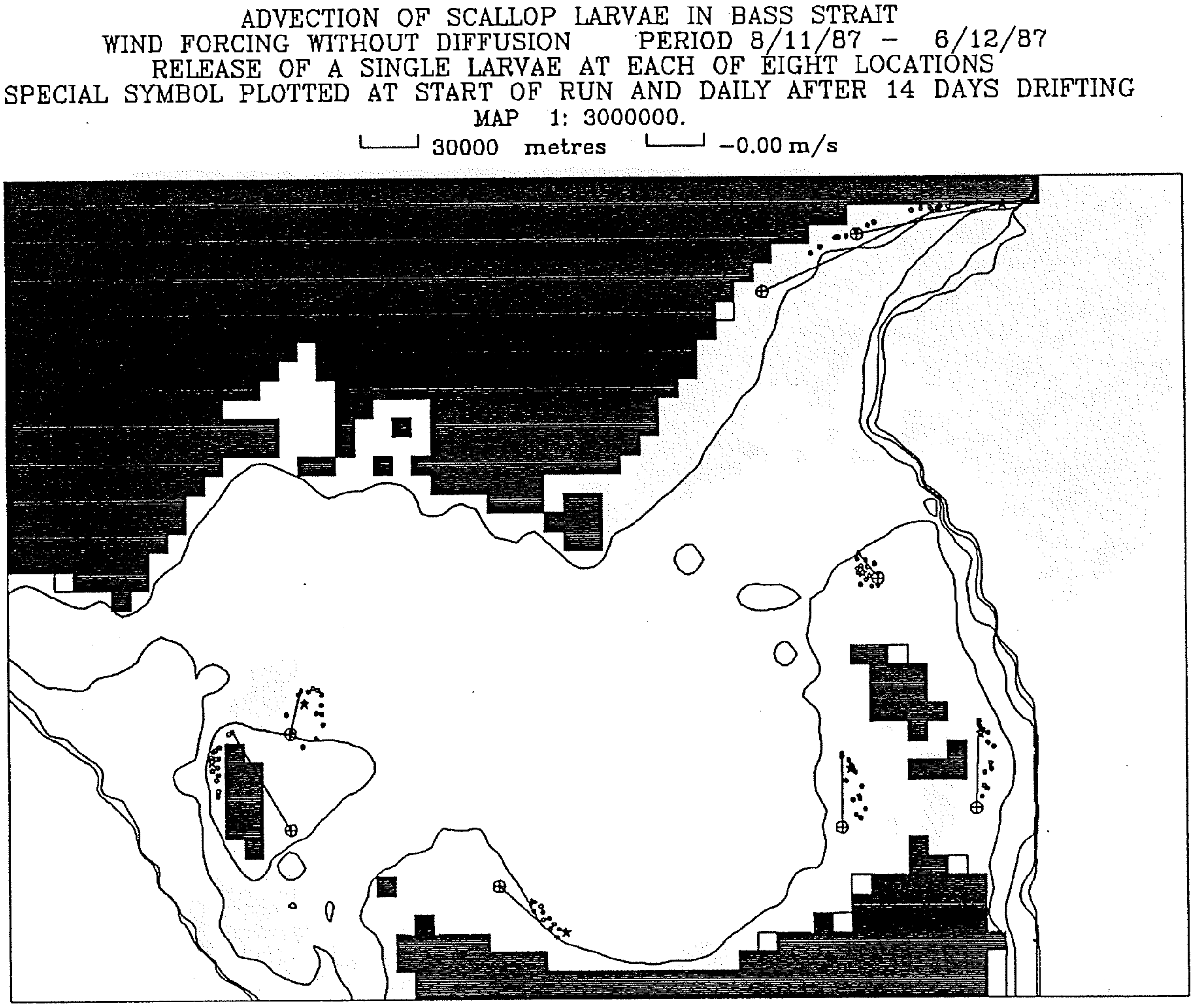

Fig. 4.3j Pelagic excursions from 8 modern beds over the 28 day period from November 8, 1987. The large crossed circle shows the release point and the straight line shows the excursion over the first non-viable 14 days. The small circles then show the positions at daily intervals in the 14-28 day interval, while the star shows the final position at the end of the 28 day pelagic period.

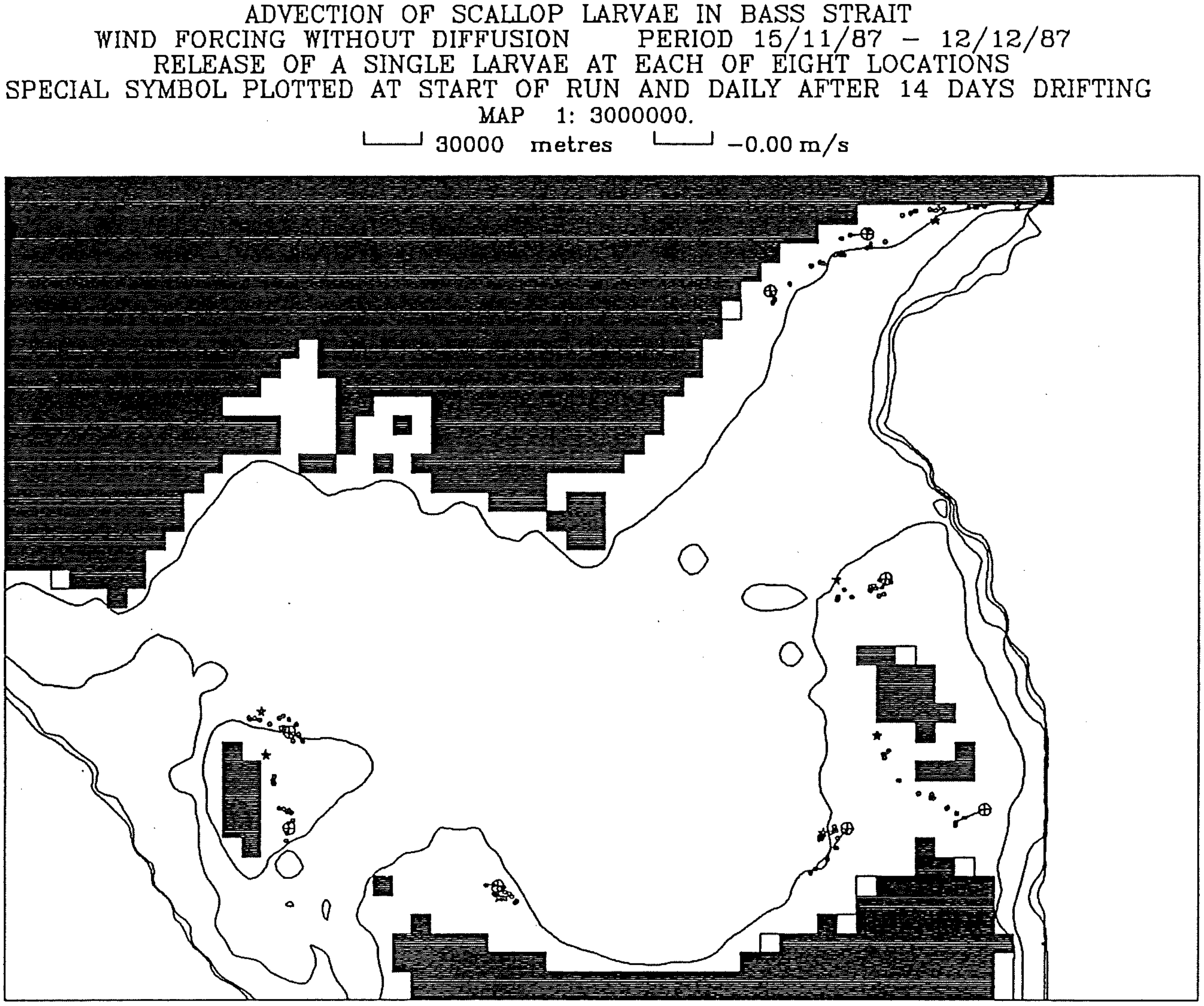

Fig. 4.3k Pelagic excursions from 8 modern beds over the 28 day period from November 15, 1987. The large crossed circle shows the release point and the straight line shows the excursion over the first non-viable 14 days. The small circles then show the positions at daily intervals in the 14-28 day interval, while the star shows the final position at the end of the 28 day pelagic period.

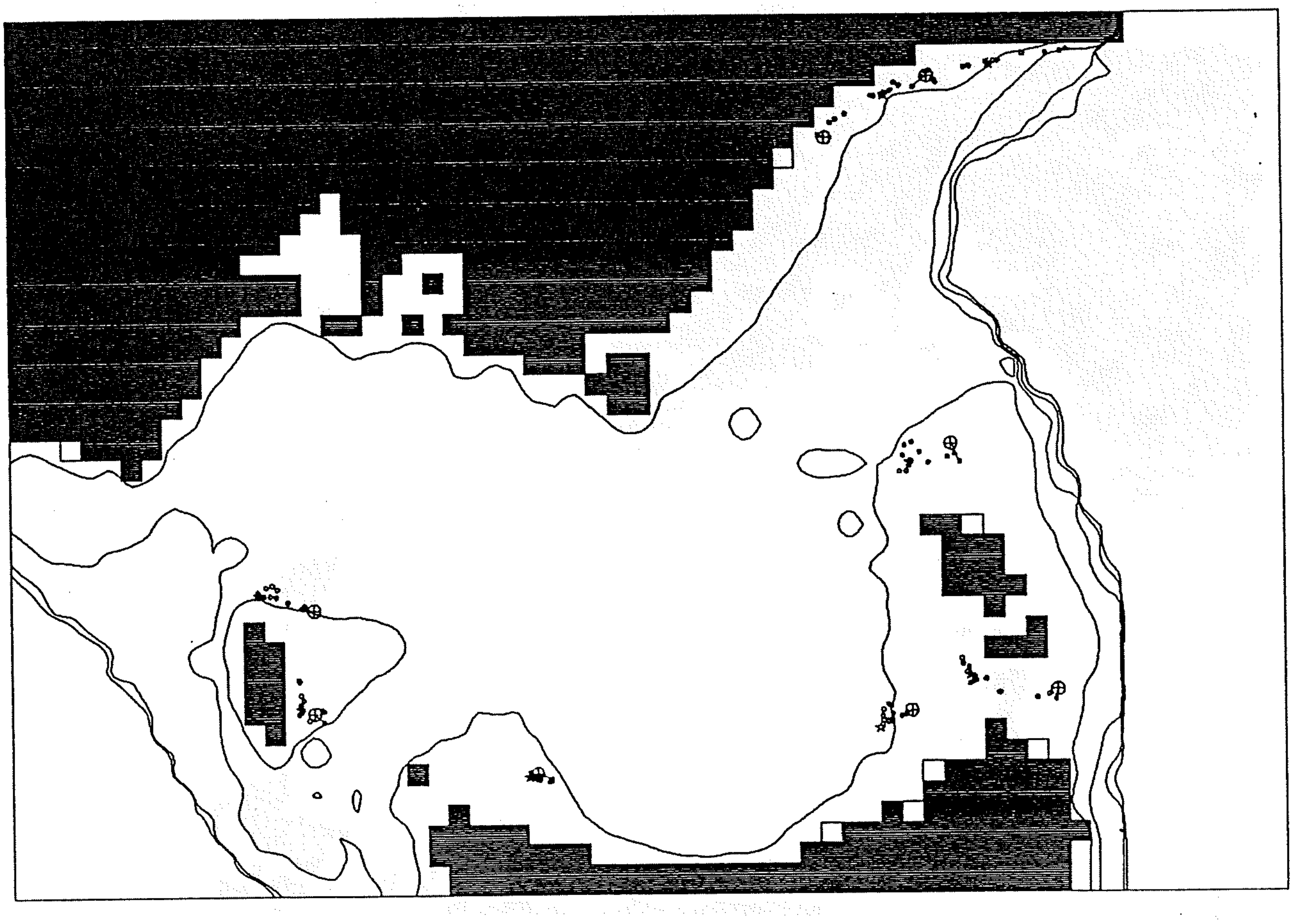

ADVECTION OF SCALLOP LARVAE IN BASS STRAIT
WIND FORCING WITHOUT DIFFUSION PERIOD 22/11/87 - 20/12/87
RELEASE OF A SINGLE LARVAE AT EACH OF EIGHT LOCATIONS
SPECIAL SYMBOL PLOTTED AT START OF RUN AND DAILY AFTER 14 DAYS DRIFTING
MAP 1: 3000000.
30000 metres -0.00 m/s

Fig. 4.31 Pelagic excursions from 8 modern beds over the 28 day period from November 22, 1987. The large crossed circle shows the release point and the straight line shows the excursion over the first non-viable 14 days. The small circles then show the positions at daily intervals in the 14-28 day interval, while the star shows the final position at the end of the 28 day pelagic period.

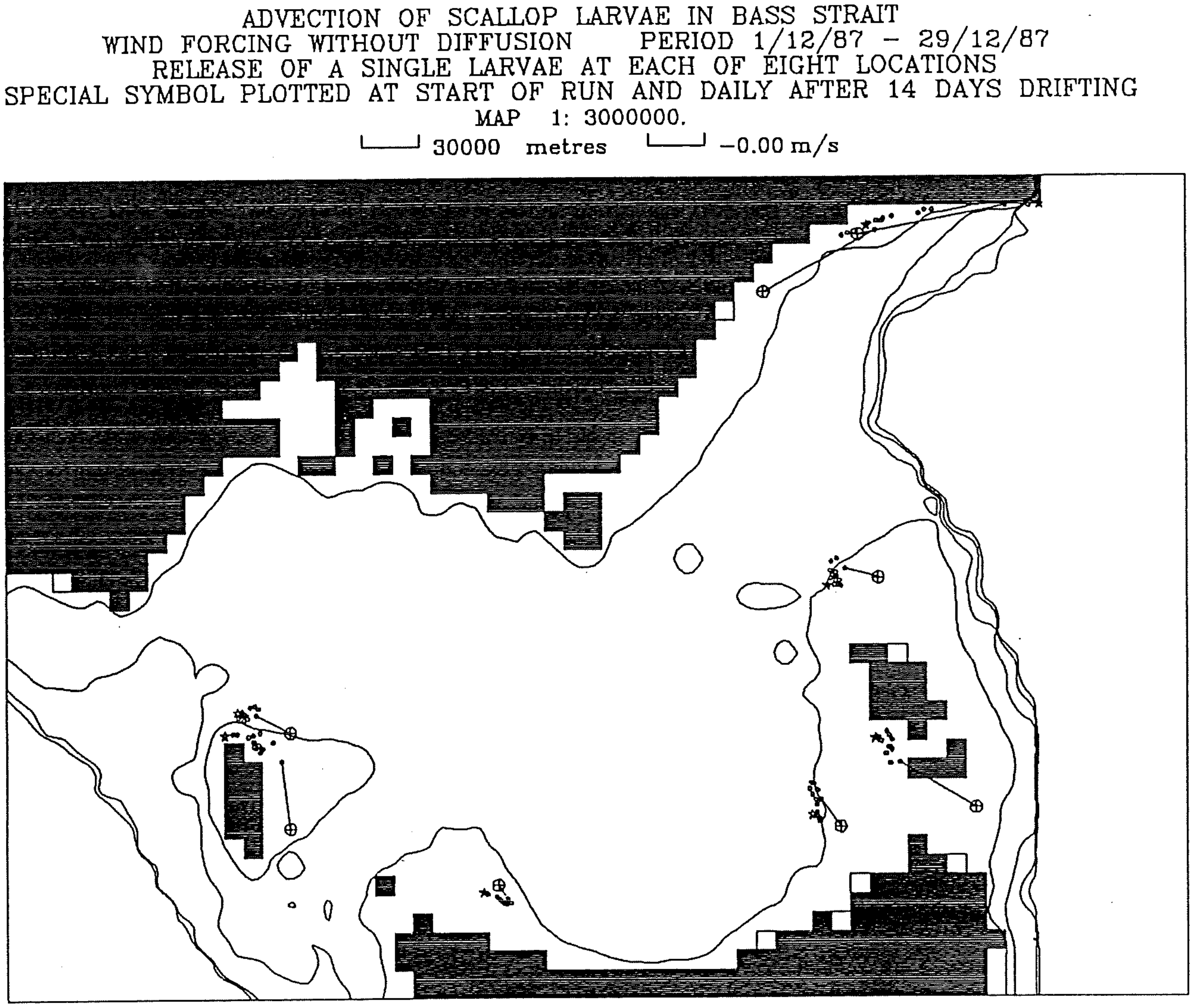

Fig. 4.3m Pelagic excursions from 8 modern beds over the 28 day period from December 1, 1987. The large crossed circle shows the release point and the straight line shows the excursion over the first non-viable 14 days. The small circles then show the positions at daily intervals in the 14-28 day interval, while the star shows the final position at the end of the 28 day pelagic period.

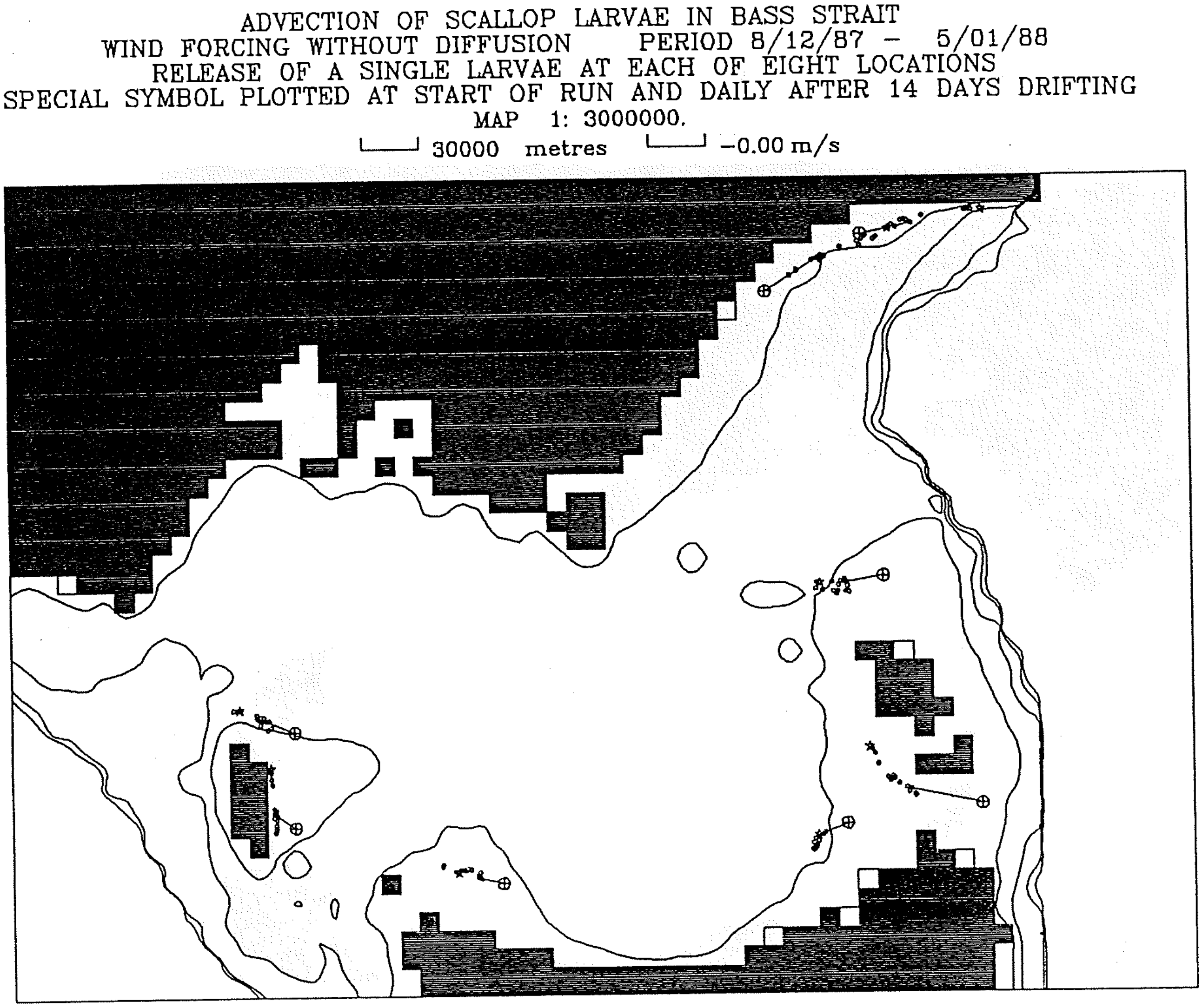

Fig. 4.3n Pelagic excursions from 8 modern beds over the 28 day period from December 8, 1987. The large crossed circle shows the release point and the straight line shows the excursion over the first non-viable 14 days. The small circles then show the positions at daily intervals in the 14-28 day interval, while the star shows the final position at the end of the 28 day pelagic period.

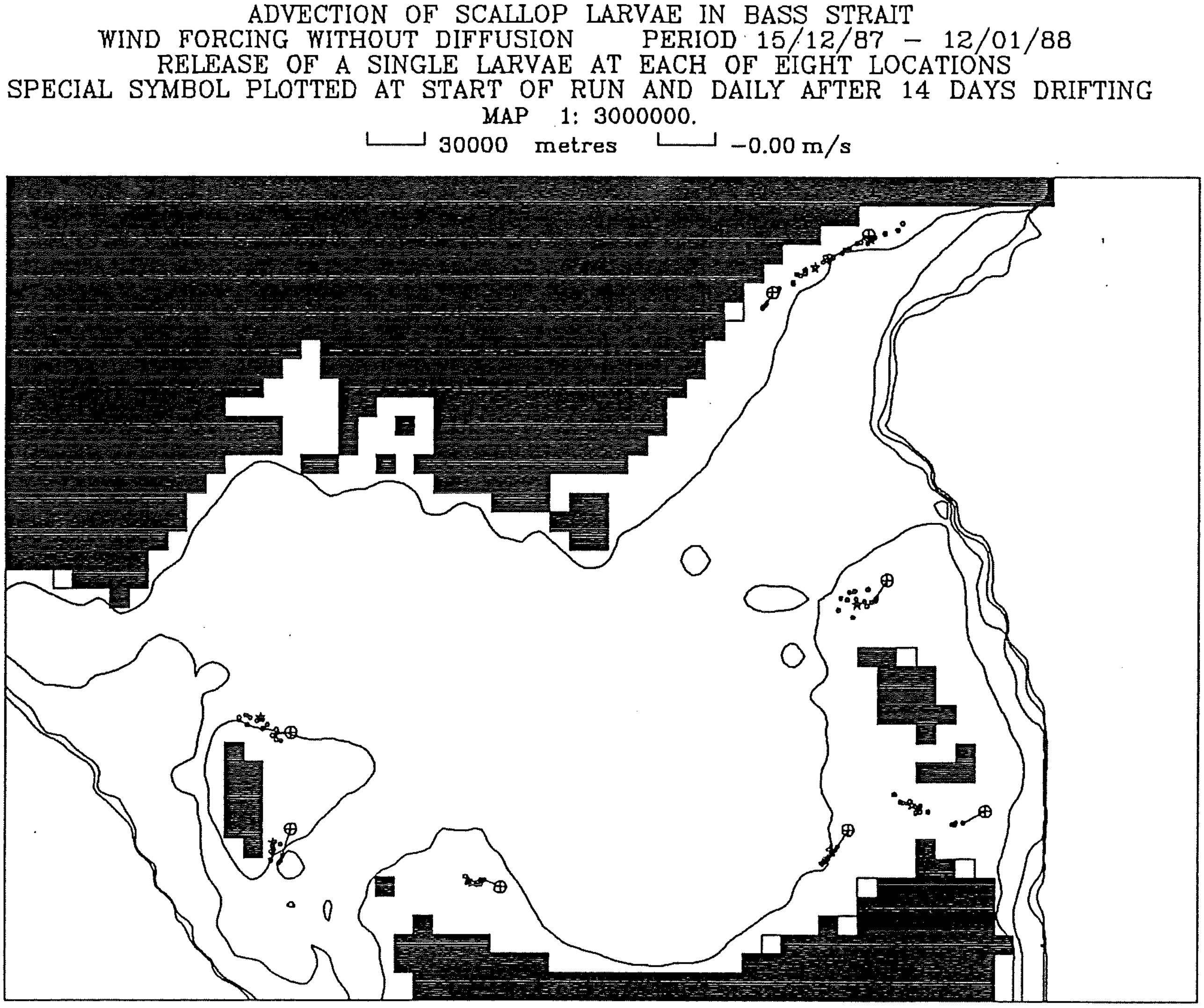

Fig. 4.3o Pelagic excursions from 8 modern beds over the 28 day period from December 15, 1987. The large crossed circle shows the release point and the straight line shows the excursion over the first non-viable 14 days. The small circles then show the positions at daily intervals in the 14-28 day interval, while the star shows the final position at the end of the 28 day pelagic period.

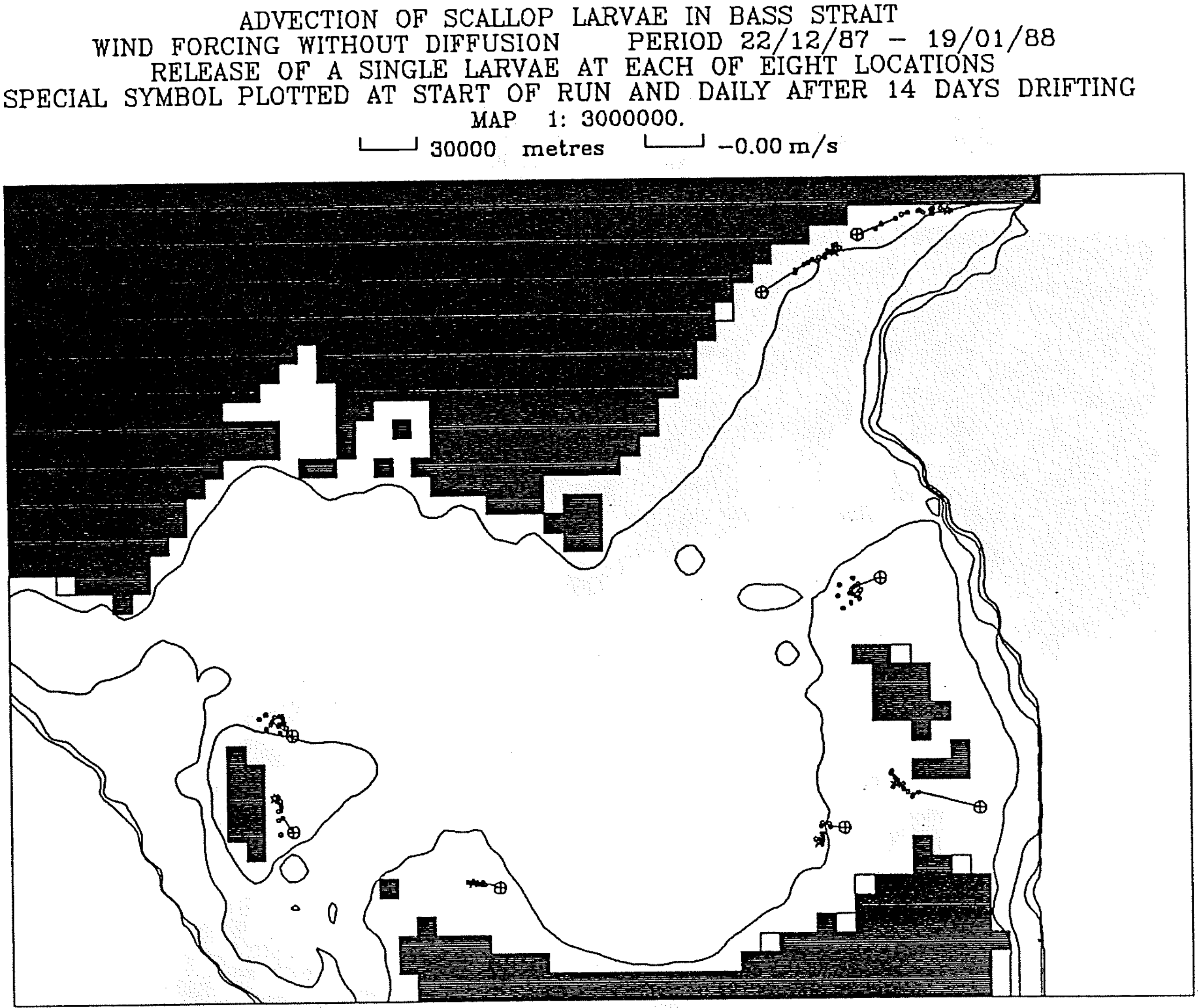

ADVECTION OF SCALLOP LARVAE IN BASS STRAIT
WIND FORCING WITHOUT DIFFUSION PERIOD 22/12/87 - 19/01/88
RELEASE OF A SINGLE LARVAE AT EACH OF EIGHT LOCATIONS
SPECIAL SYMBOL PLOTTED AT START OF RUN AND DAILY AFTER 14 DAYS DRIFTING
MAP 1: 3000000.

Fig. 4.3p Pelagic excursions from 8 modern beds over the 28 day period from December 22, 1987. The large crossed circle shows the release point and the straight line shows the excursion over the first non-viable 14 days. The small circles then show the positions at daily intervals in the 14-28 day interval, while the star shows the final position at the end of the 28 day pelagic period.

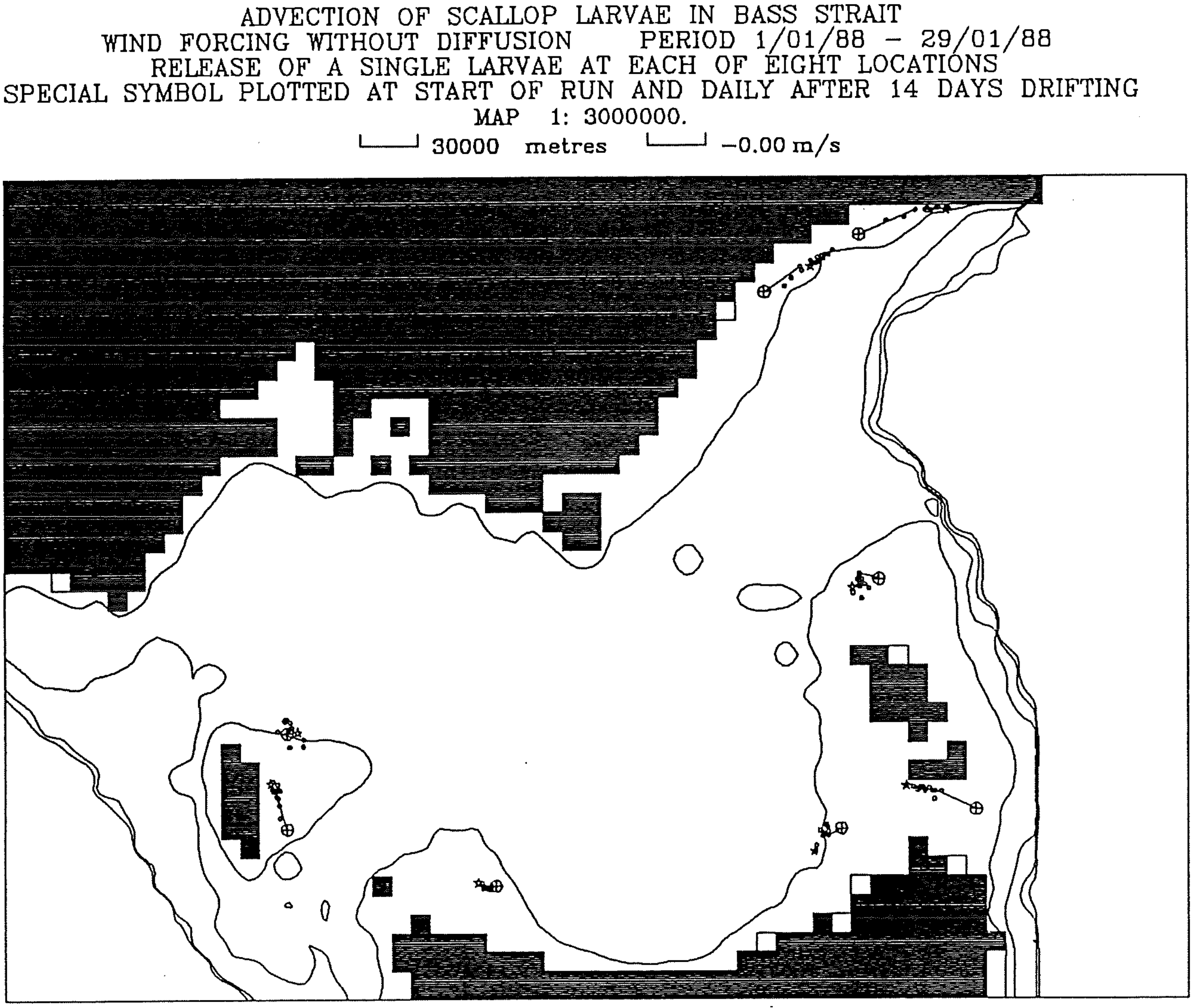

Fig. 4.3q Pelagic excursions from 8 modern beds over the 28 day period from January 1, 1988. The large crossed circle shows the release point and the straight line shows the excursion over the first non-viable 14 days. The small circles then show the positions at daily intervals in the 14-28 day interval, while the star shows the final position at the end of the 28 day pelagic period.

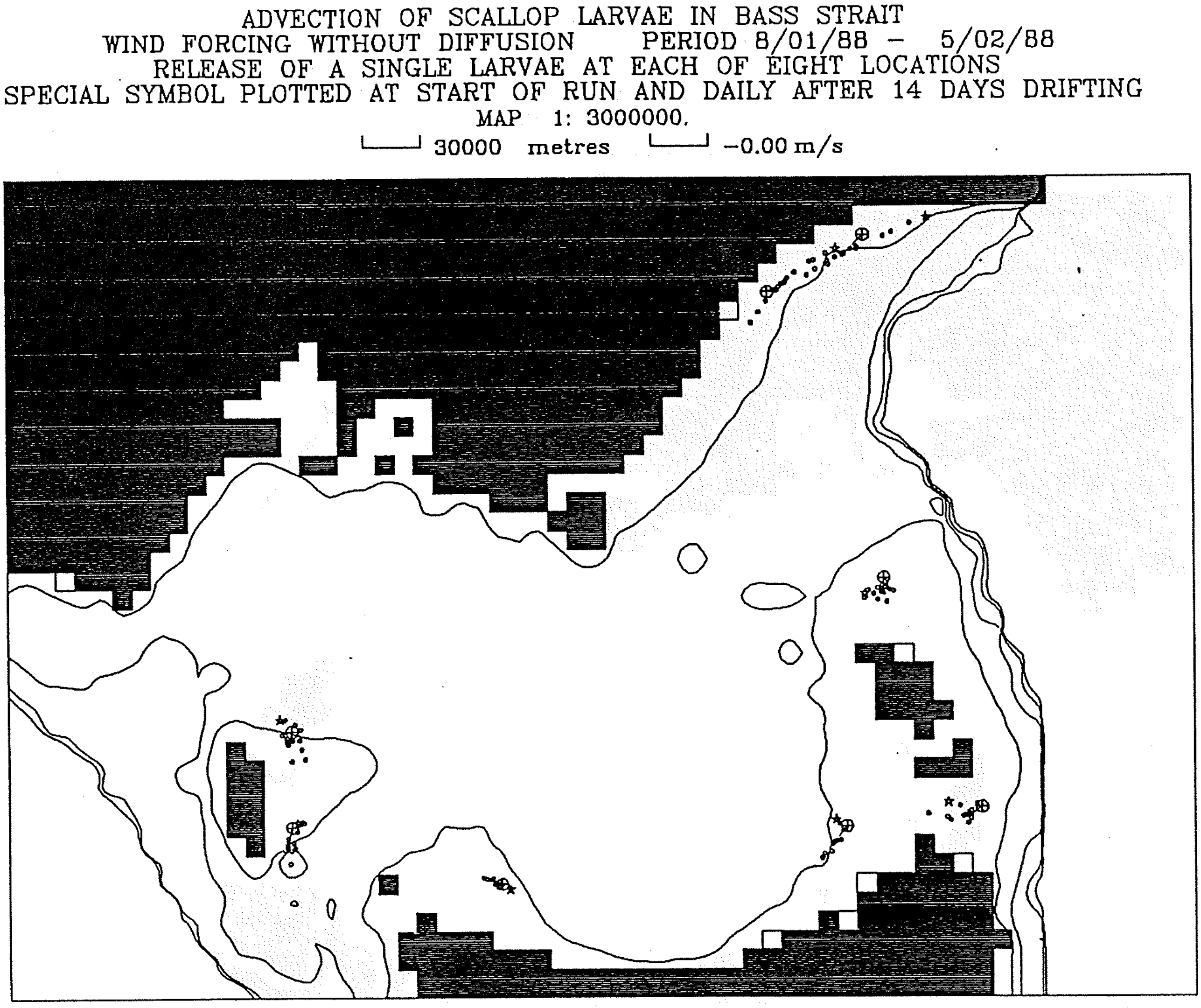

ADVECTION OF SCALLOP LARVAE IN BASS STRAIT
WIND FORCING WITHOUT DIFFUSION PERIOD 8/01/88 - 5/02/88
RELEASE OF A SINGLE LARVAE AT EACH OF EIGHT LOCATIONS
SPECIAL SYMBOL PLOTTED AT START OF RUN AND DAILY AFTER 14 DAYS DRIFTING
MAP 1: 3000000.

Fig. 4.3r Pelagic excursions from 8 modern beds over the 28 day period from January 8, 1988. The large crossed circle shows the release point and the straight line shows the excursion over the first non-viable 14 days. The small circles then show the positions at daily intervals in the 14-28 day interval, while the star shows the final position at the end of the 28 day pelagic period.

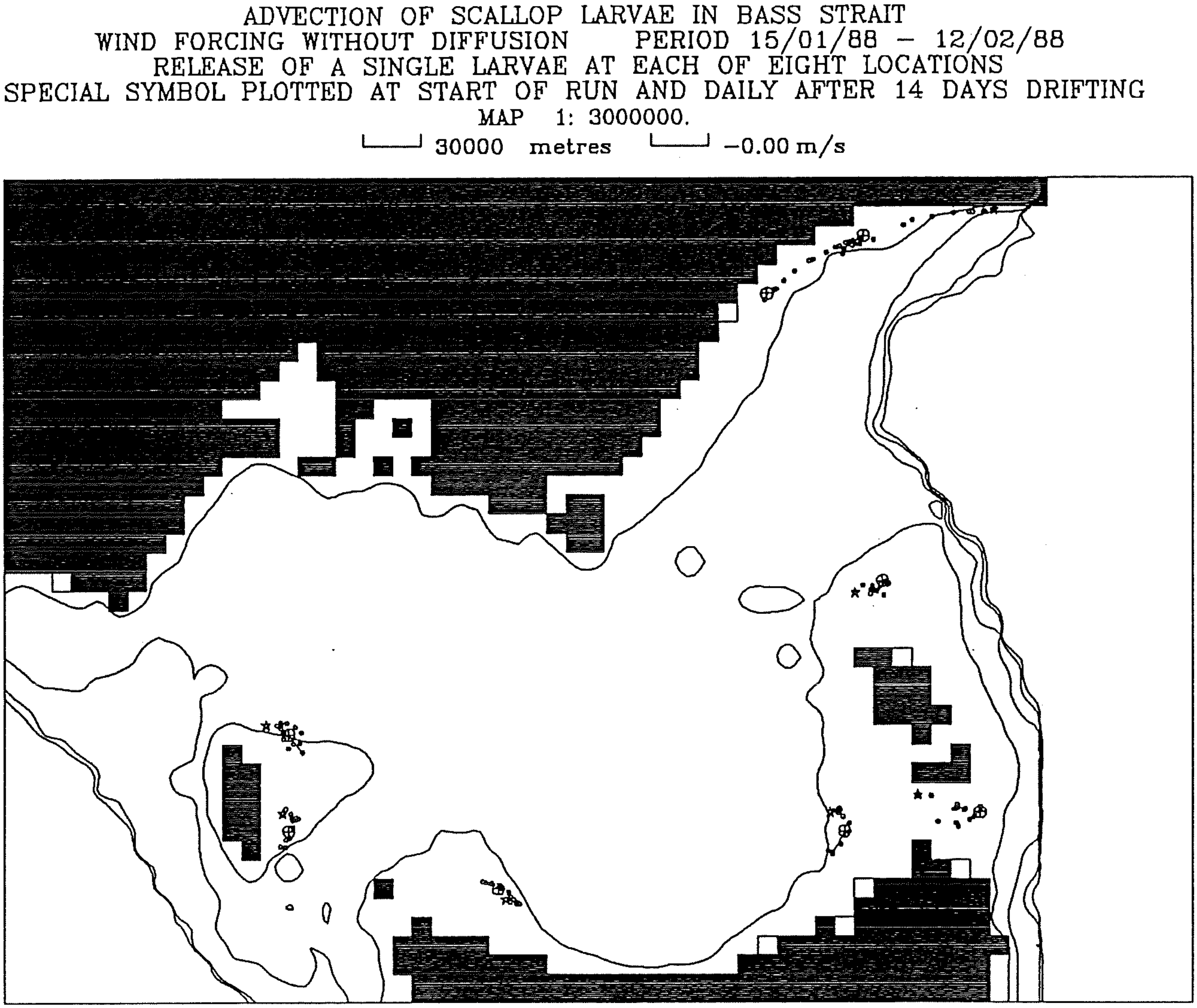

Fig. 4.3s Pelagic excursions from 8 modern beds over the 28 day period from January 15, 1988. The large crossed circle shows the release point and the straight line shows the excursion over the first non-viable 14 days. The small circles then show the positions at daily intervals in the 14-28 day interval, while the star shows the final position at the end of the 28 day pelagic period.

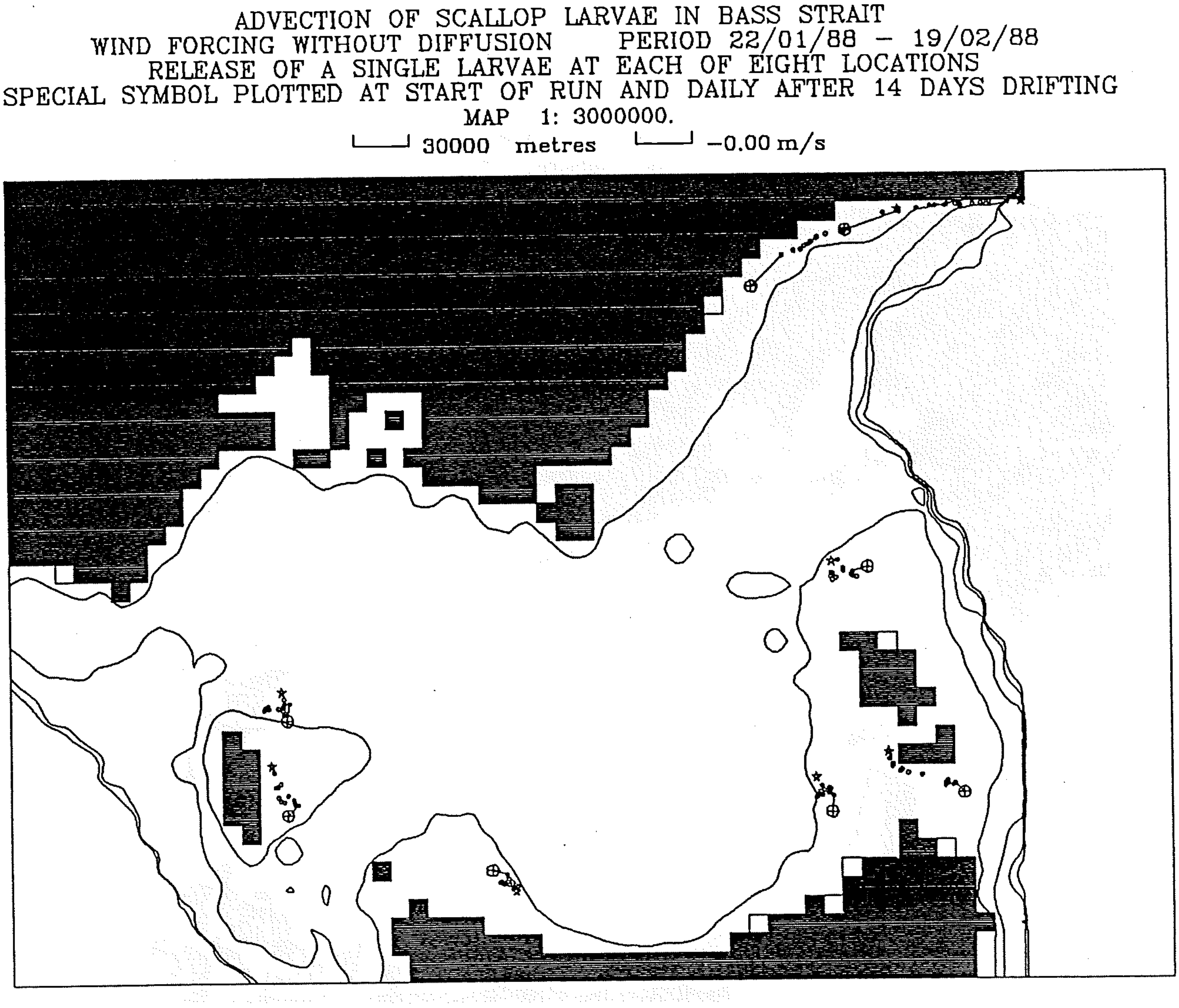

ADVECTION OF SCALLOP LARVAE IN BASS STRAIT
WIND FORCING WITHOUT DIFFUSION PERIOD 22/01/88 - 19/02/88
RELEASE OF A SINGLE LARVAE AT EACH OF EIGHT LOCATIONS
SPECIAL SYMBOL PLOTTED AT START OF RUN AND DAILY AFTER 14 DAYS DRIFTING
MAP 1: 3000000.

Fig. 4.3t Pelagic excursions from 8 modern beds over the 28 day period from January 22, 1988. The large crossed circle shows the release point and the straight line shows the excursion over the first non-viable 14 days. The small circles then show the positions at daily intervals in the 14-28 day interval, while the star shows the final position at the end of the 28 day pelagic period.

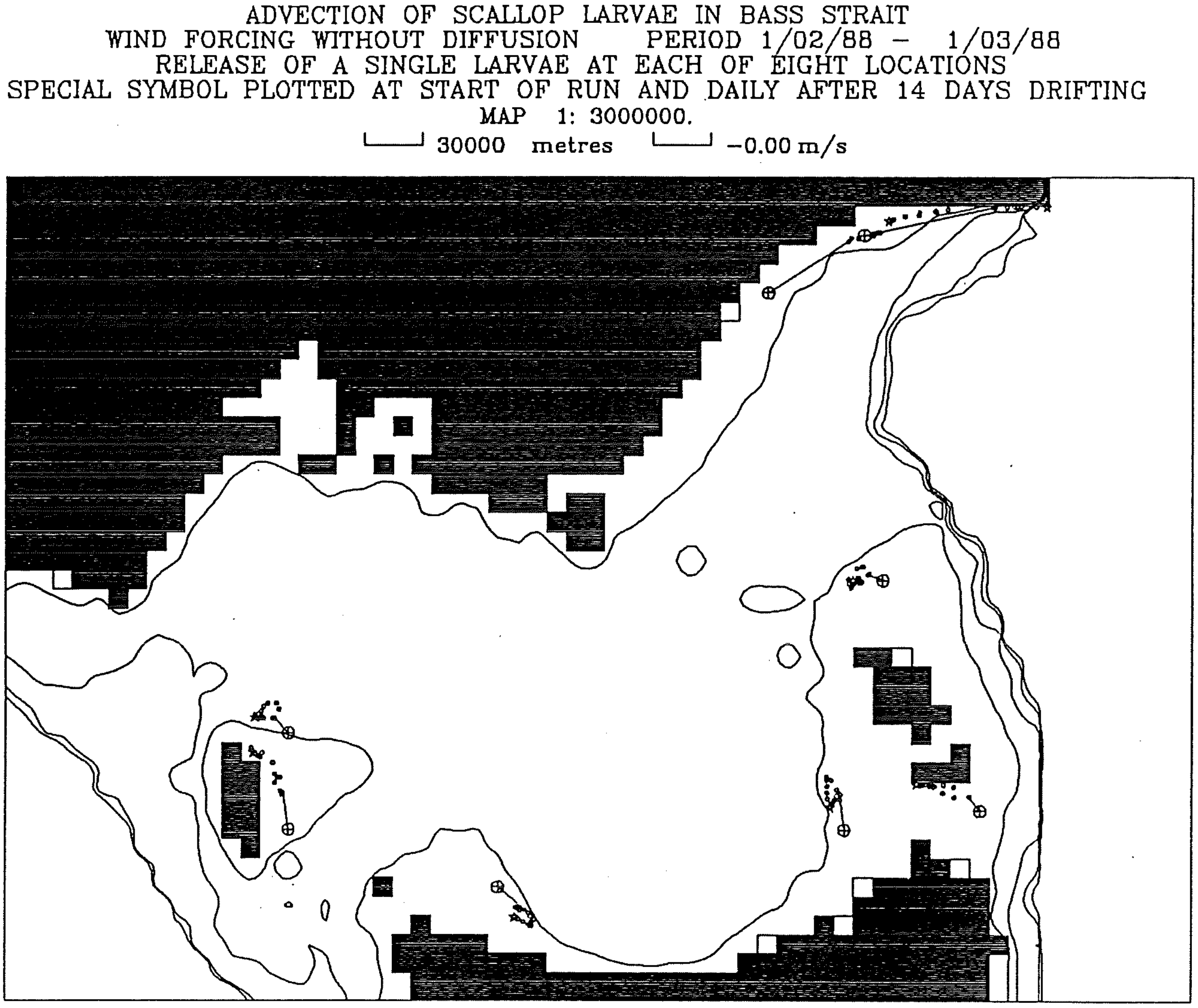

ADVECTION OF SCALLOP LARVAE IN BASS STRAIT
WIND FORCING WITHOUT DIFFUSION PERIOD 1/02/88 - 1/03/88
RELEASE OF A SINGLE LARVAE AT EACH OF EIGHT LOCATIONS
SPECIAL SYMBOL PLOTTED AT START OF RUN AND DAILY AFTER 14 DAYS DRIFTING
MAP 1: 3000000.

Fig. 4.3u Pelagic excursions from 8 modern beds over the 28 day period from February 1, 1988. The large crossed circle shows the release point and the straight line shows the excursion over the first non-viable 14 days. The small circles then show the positions at daily intervals in the 14-28 day interval, while the star shows the final position at the end of the 28 day pelagic period.

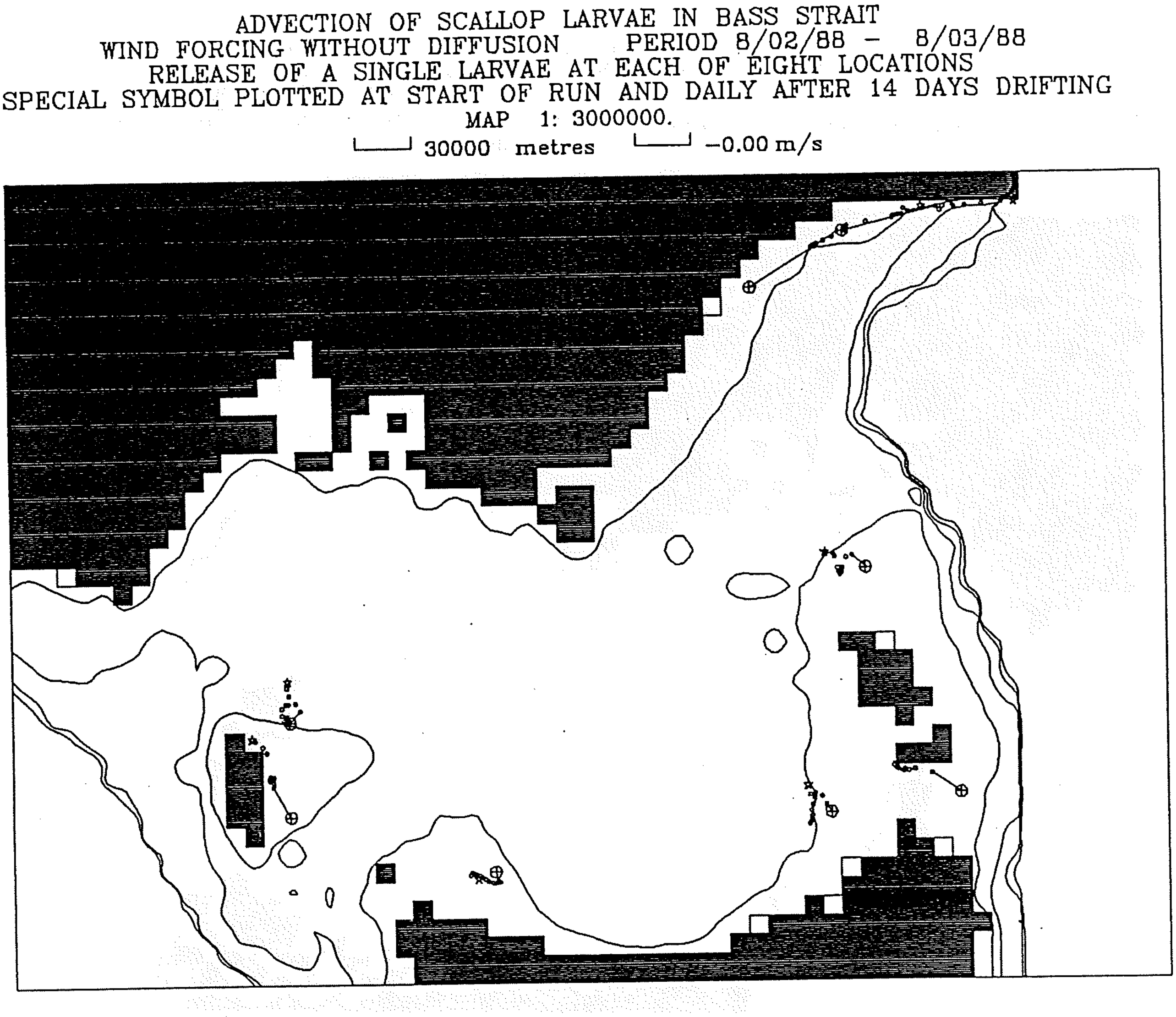

Fig. 4.3v Pelagic excursions from 8 modern beds over the 28 day period from February 8, 1988. The large crossed circle shows the release point and the straight line shows the excursion over the first non-viable 14 days. The small circles then show the positions at daily intervals in the 14-28 day interval, while the star shows the final position at the end of the 28 day pelagic period.

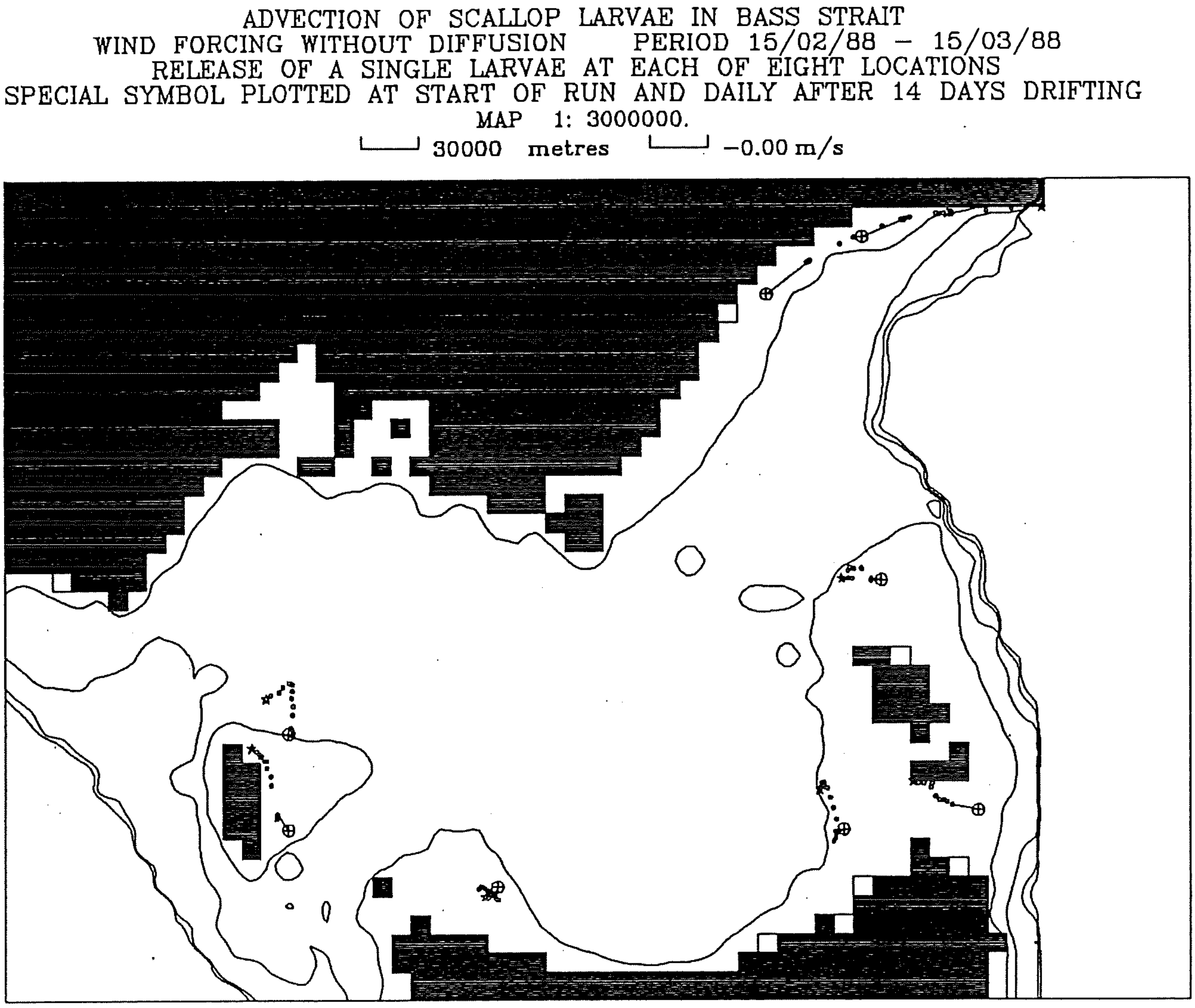

ADVECTION OF SCALLOP LARVAE IN BASS STRAIT
WIND FORCING WITHOUT DIFFUSION PERIOD 15/02/88 - 15/03/88
RELEASE OF A SINGLE LARVAE AT EACH OF EIGHT LOCATIONS
SPECIAL SYMBOL PLOTTED AT START OF RUN AND DAILY AFTER 14 DAYS DRIFTING
MAP 1: 3000000.

Fig. 4.3w Pelagic excursions from 8 modern beds over the 28 day period from February 15, 1988. The large crossed circle shows the release point and the straight line shows the excursion over the first non-viable 14 days. The small circles then show the positions at daily intervals in the 14-28 day interval, while the star shows the final position at the end of the 28 day pelagic period.

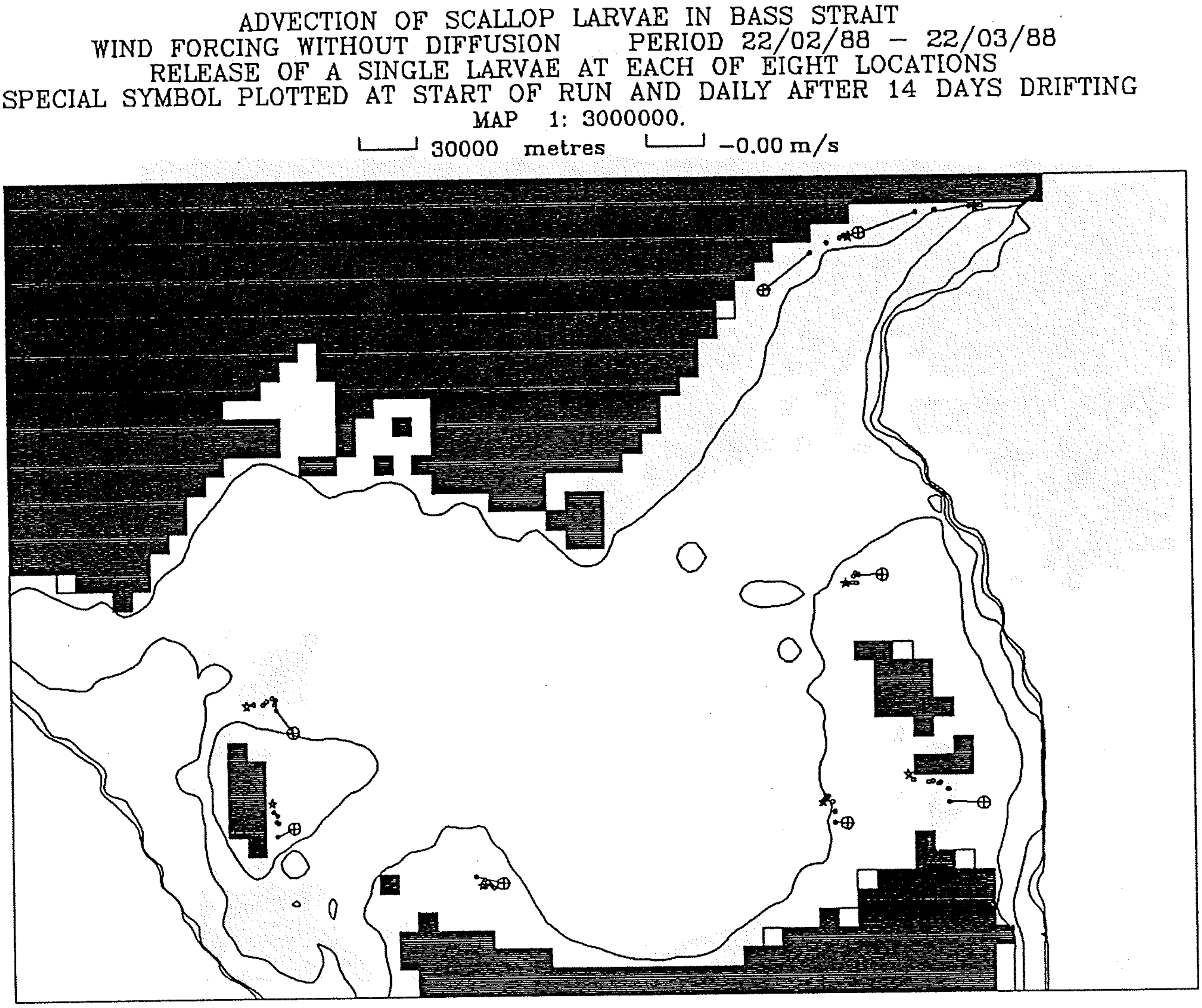

Fig. 4.3x Pelagic excursions from 8 modern beds over the 28 day period from February 22, 1988. The large crossed circle shows the release point and the straight line shows the excursion over the first non-viable 14 days. The small circles then show the positions at daily intervals in the 14-28 day interval, while the star shows the final position at the end of the 28 day pelagic period.

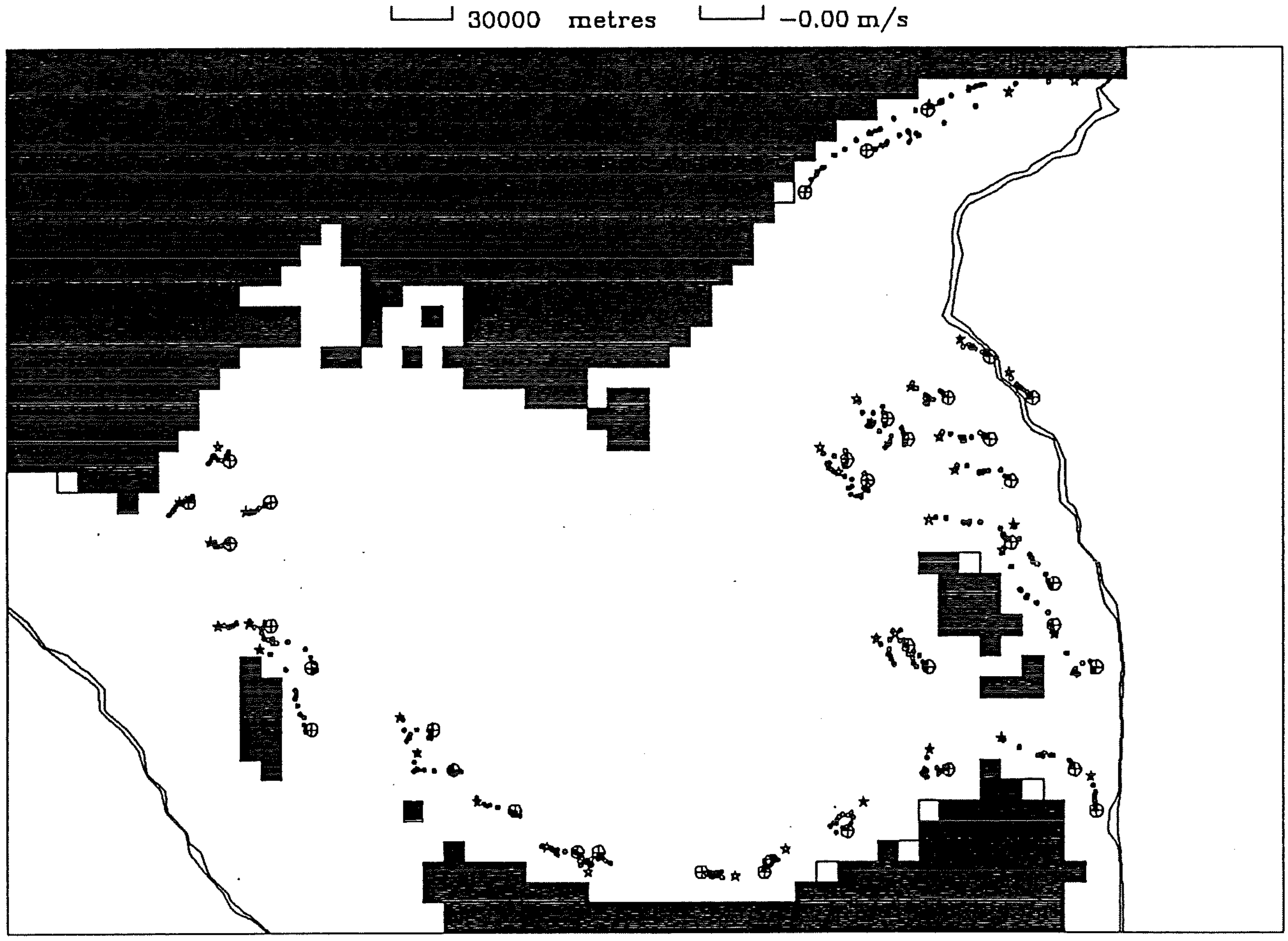

ADVECTION OF SCALLOP LARVAE IN BASS STRAIT
WIND FORCING WITHOUT DIFFUSION PERIOD 1/09/86 - 29/09/86
RELEASE OF A SINGLE LARVAE AT ALL DOCUMENTED PAST AND PRESENT SCALLOP BED SITES
SPECIAL SYMBOL PLOTTED AT START OF RUN AND DAILY AFTER 14 DAYS DRIFTING
MAP 1: 3000000.

Fig. 4.4a Pelagic excursions from modern and historical scallop beds over the 28 day period from September 1, 1986. The large crossed circle shows the release point and the straight line shows the excursion over the first non-viable 14 days. The small circles then show the positions at daily intervals in the 14-28 day interval, while the star shows the final position at the end of the 28 day pelagic period.

ADVECTION OF SCALLOP LARVAE IN BASS STRAIT
WIND FORCING WITHOUT DIFFUSION PERIOD 8/09/86 – 8/10/86
RELEASE OF A SINGLE LARVAE AT ALL DOCUMENTED PAST AND PRESENT SCALLOP BED SITES
SPECIAL SYMBOL PLOTTED AT START OF RUN AND DAILY AFTER 14 DAYS DRIFTING
MAP 1: 3000000.

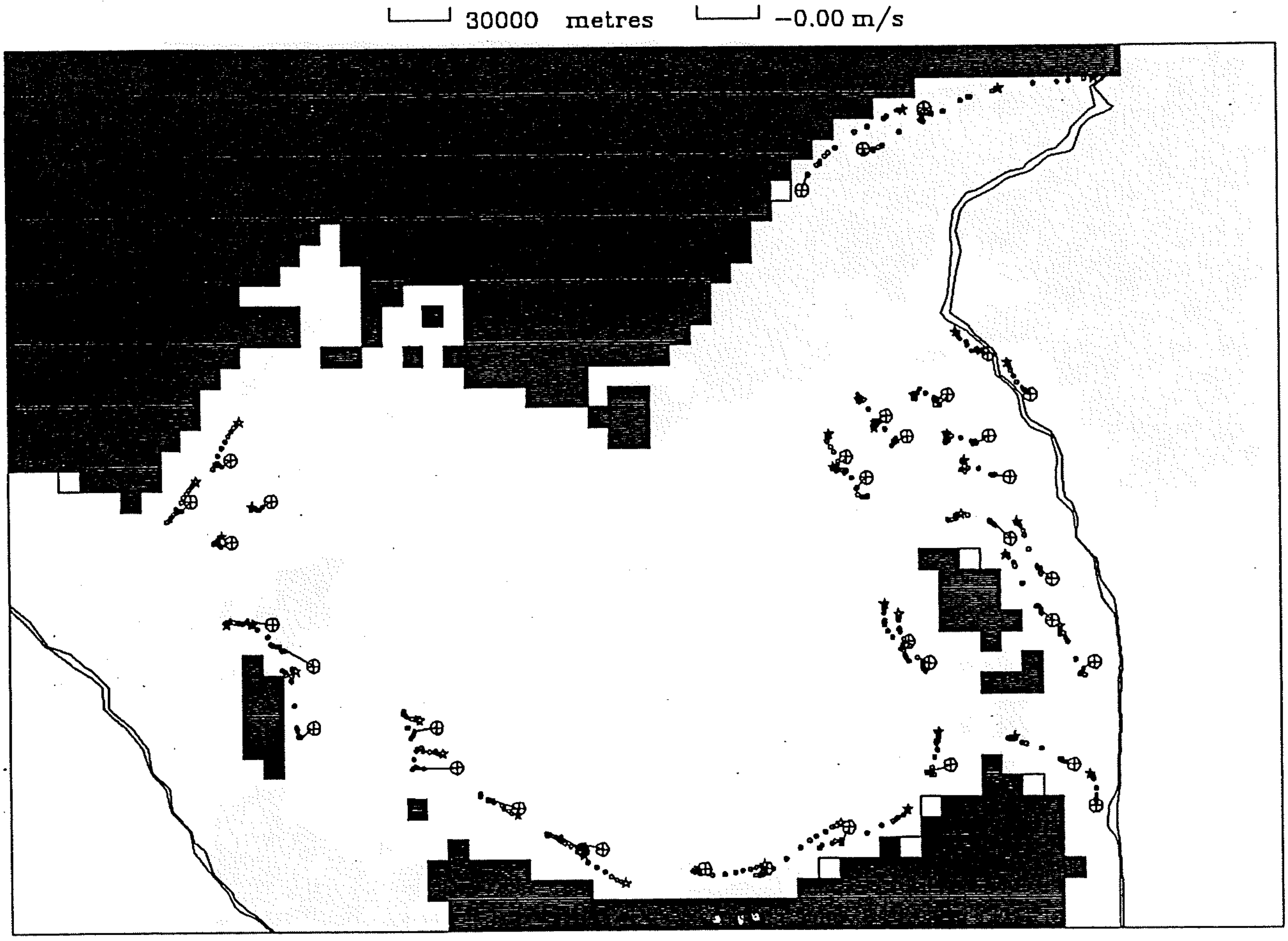

Fig. 4.4b Pelagic excursions from modern and historical scallop beds over the 28 day period from September 8, 1986. The large crossed circle shows the release point and the straight line shows the excursion over the first non-viable 14 days. The small circles then show the positions at daily intervals in the 14-28 day interval, while the star shows the final position at the end of the 28 day pelagic period.

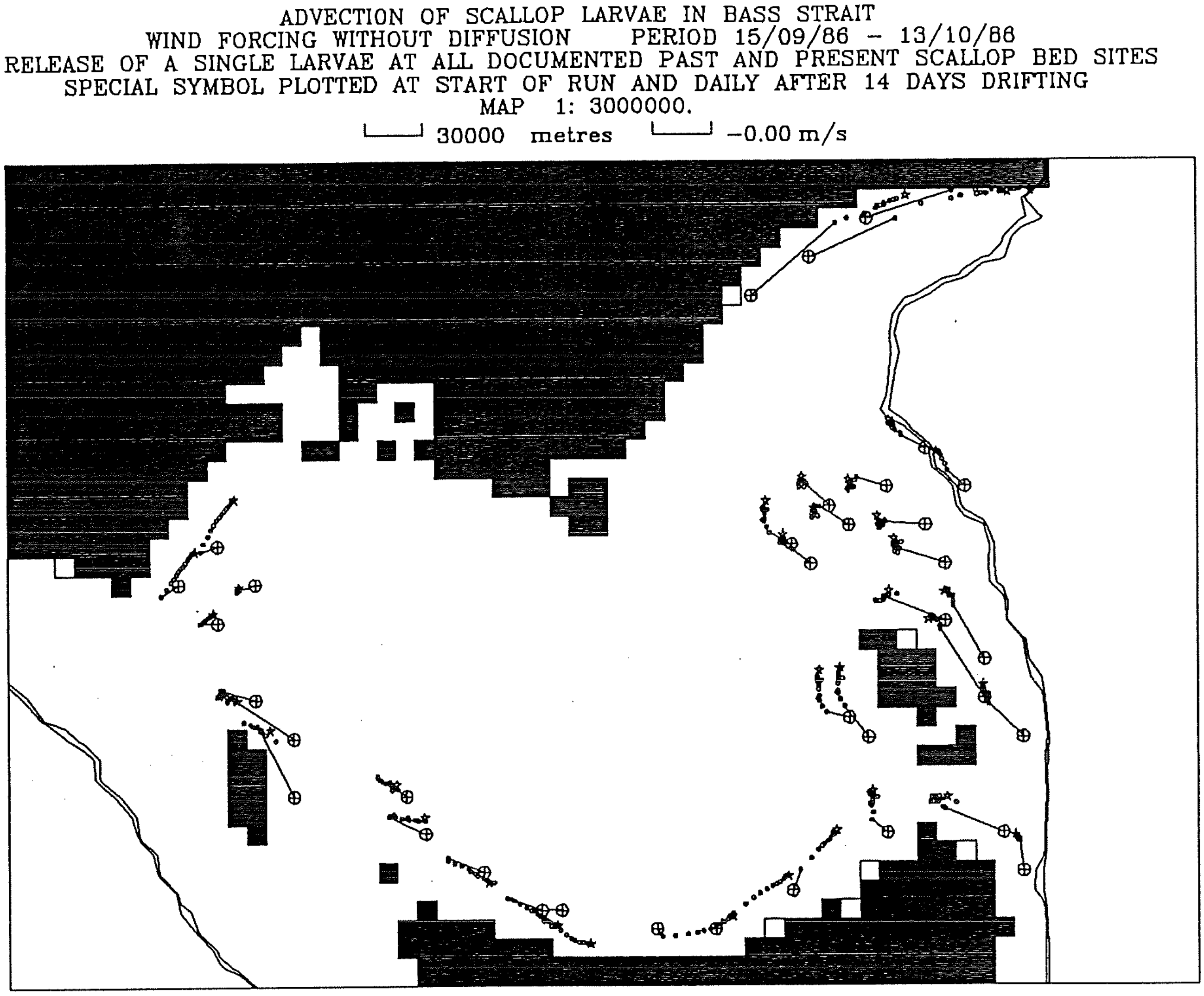

Fig. 4.4c Pelagic excursions from modern and historical scallop beds over the 28 day period from September 15, 1986. The large crossed circle shows the release point and the straight line shows the excursion over the first non-viable 14 days. The small circles then show the positions at daily intervals in the 14-28 day interval, while the star shows the final position at the end of the 28 day pelagic period.

ADVECTION OF SCALLOP LARVAE IN BASS STRAIT
WIND FORCING WITHOUT DIFFUSION PERIOD 22/09/86 - 20/10/86
RELEASE OF A SINGLE LARVAE AT ALL DOCUMENTED PAST AND PRESENT SCALLOP BED SITES
SPECIAL SYMBOL PLOTTED AT START OF RUN AND DAILY AFTER 14 DAYS DRIFTING
MAP 1: 3000000.

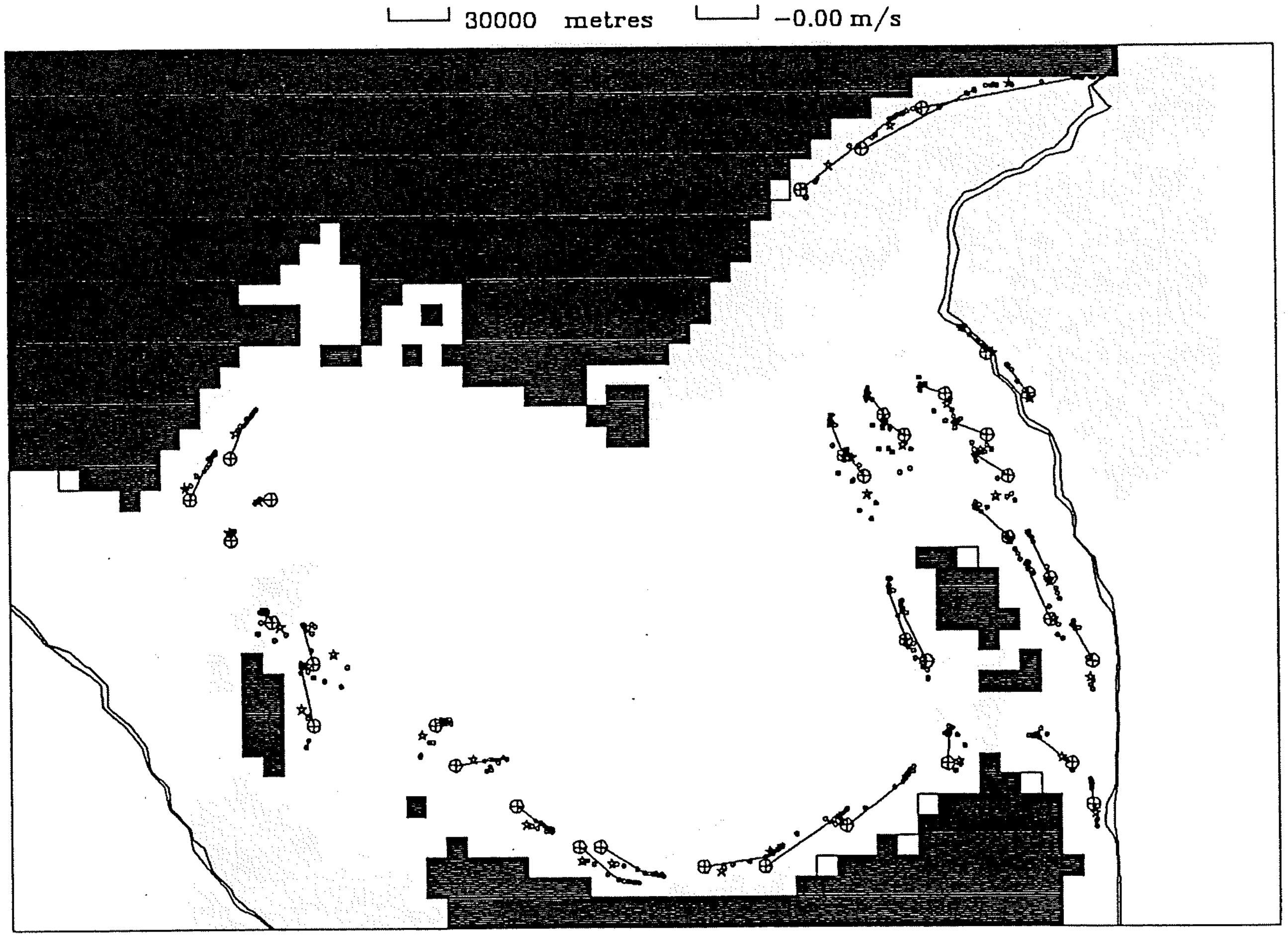

Fig. 4.4d Pelagic excursions from modern and historical scallop beds over the 28 day period from September 22, 1986. The large crossed circle shows the release point and the straight line shows the excursion over the first non-viable 14 days. The small circles then show the positions at daily intervals in the 14-28 day interval, while the star shows the final position at the end of the 28 day pelagic period.

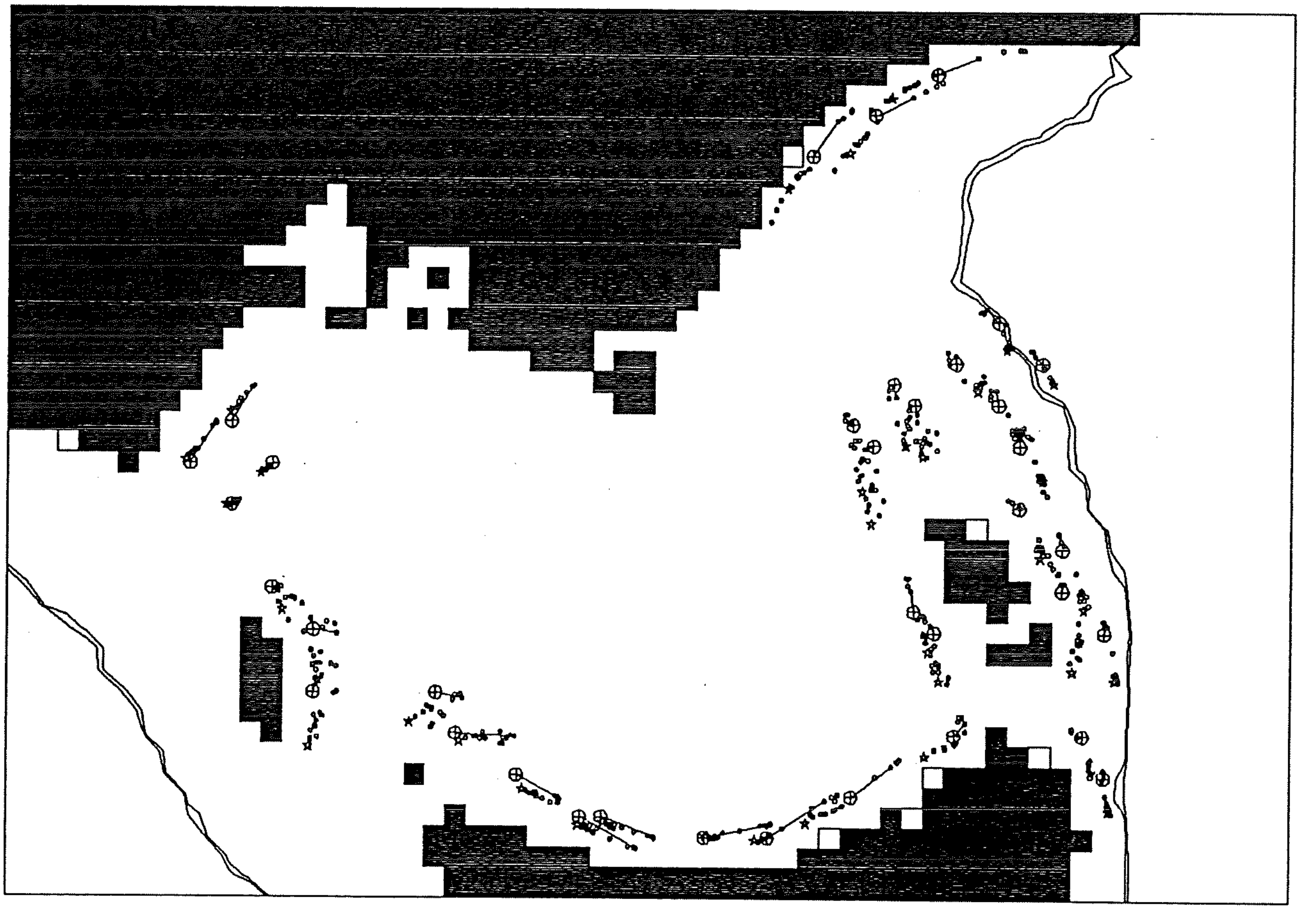

ADVECTION OF SCALLOP LARVAE IN BASS STRAIT
WIND FORCING WITHOUT DIFFUSION PERIOD 1/10/86 - 29/10/86
RELEASE OF A SINGLE LARVAE AT ALL DOCUMENTED PAST AND PRESENT SCALLOP BED SITES
SPECIAL SYMBOL PLOTTED AT START OF RUN AND DAILY AFTER 14 DAYS DRIFTING
MAP 1: 3000000.

Fig. 4.4e Pelagic excursions from modern and historical scallop beds over the 28 day period from October 1, 1986. The large crossed circle shows the release point and the straight line shows the excursion over the first non-viable 14 days. The small circles then show the positions at daily intervals in the 14-28 day interval, while the star shows the final position at the end of the 28 day pelagic period.

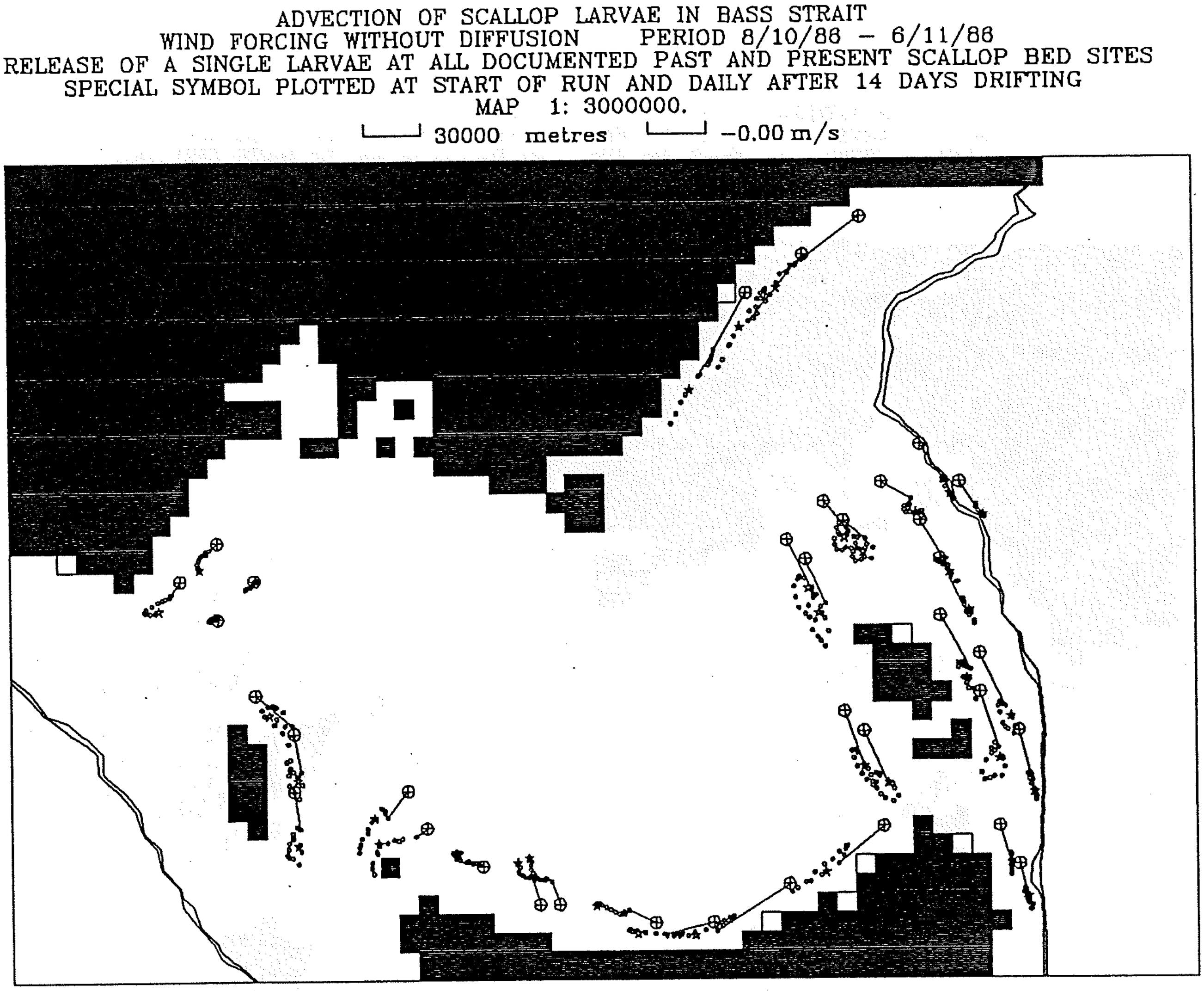

ADVECTION OF SCALLOP LARVAE IN BASS STRAIT
WIND FORCING WITHOUT DIFFUSION PERIOD 8/10/86 – 6/11/86
RELEASE OF A SINGLE LARVAE AT ALL DOCUMENTED PAST AND PRESENT SCALLOP BED SITES
SPECIAL SYMBOL PLOTTED AT START OF RUN AND DAILY AFTER 14 DAYS DRIFTING
MAP 1: 3000000.

Fig. 4.4f Pelagic excursions from modern and historical scallop beds over the 28 day period from October 8, 1986. The large crossed circle shows the release point and the straight line shows the excursion over the first non-viable 14 days. The small circles then show the positions at daily intervals in the 14-28 day interval, while the star shows the final position at the end of the 28 day pelagic period.

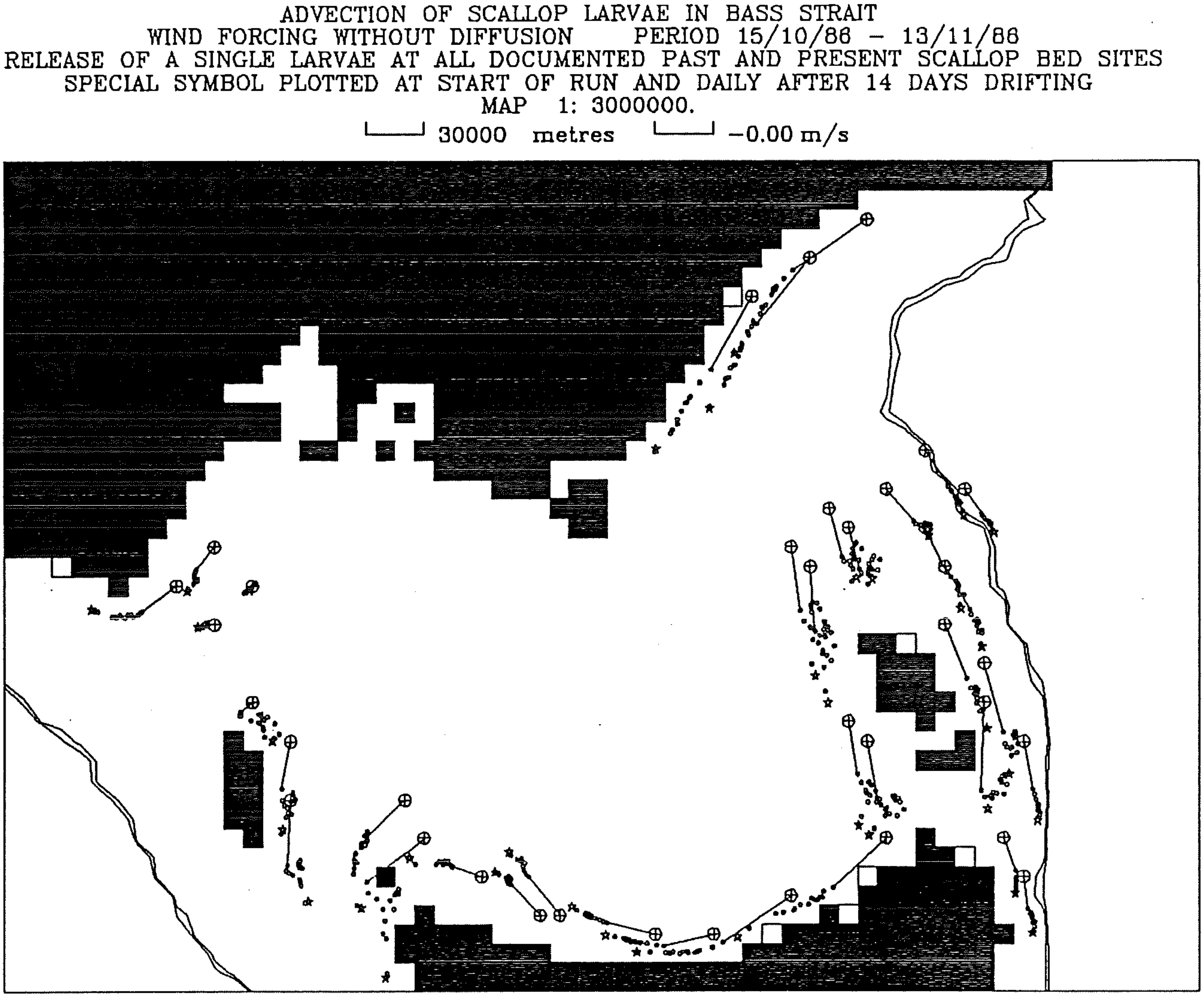

Fig. 4.4g Pelagic excursions from modern and historical scallop beds over the 28 day period from October 15, 1986. The large crossed circle shows the release point and the straight line shows the excursion over the first non-viable 14 days. The small circles then show the positions at daily intervals in the 14-28 day interval, while the star shows the final position at the end of the 28 day pelagic period.

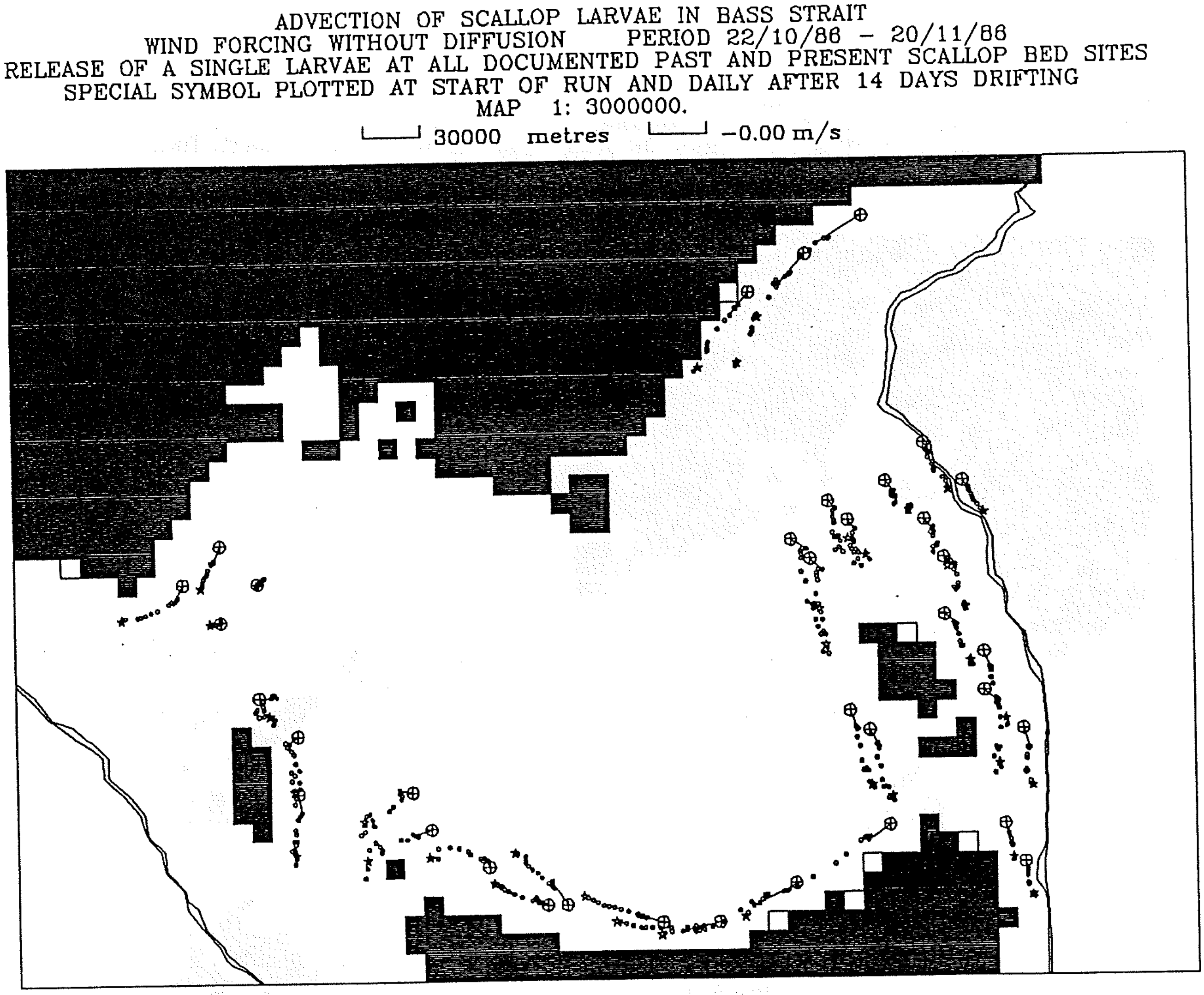

Fig. 4.4h Pelagic excursions from modern and historical scallop beds over the 28 day period from October 22, 1986. The large crossed circle shows the release point and the straight line shows the excursion over the first non-viable 14 days. The small circles then show the positions at daily intervals in the 14-28 day interval, while the star shows the final position at the end of the 28 day pelagic period.

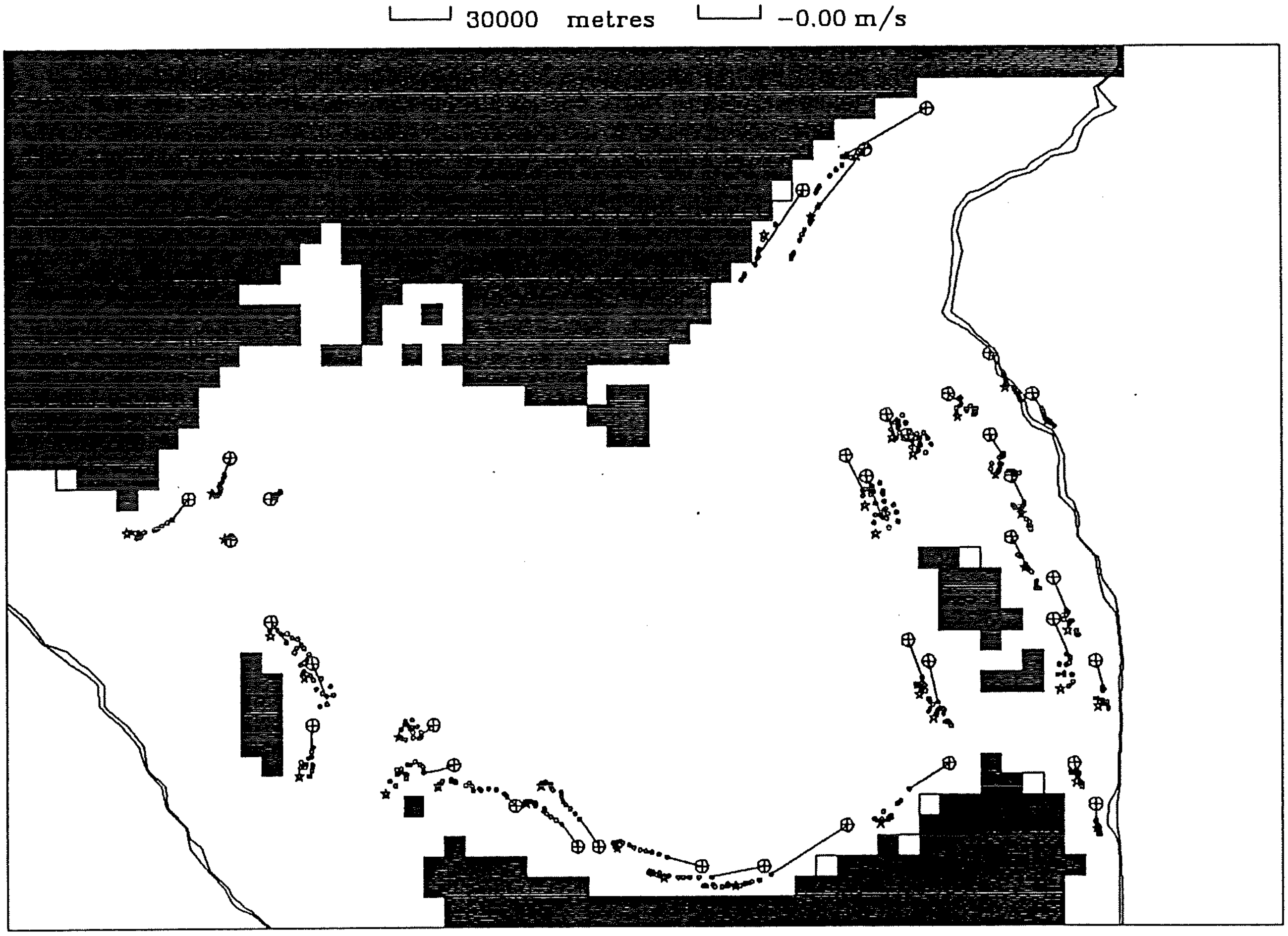

ADVECTION OF SCALLOP LARVAE IN BASS STRAIT
WIND FORCING WITHOUT DIFFUSION PERIOD 1/11/86 - 29/11/86
RELEASE OF A SINGLE LARVAE AT ALL DOCUMENTED PAST AND PRESENT SCALLOP BED SITES
SPECIAL SYMBOL PLOTTED AT START OF RUN AND DAILY AFTER 14 DAYS DRIFTING
MAP 1: 3000000.

Fig. 4.4i Pelagic excursions from modern and historical scallop beds over the 28 day period from November 1, 1986. The large crossed circle shows the release point and the straight line shows the excursion over the first non-viable 14 days. The small circles then show the positions at daily intervals in the 14-28 day interval, while the star shows the final position at the end of the 28 day pelagic period.

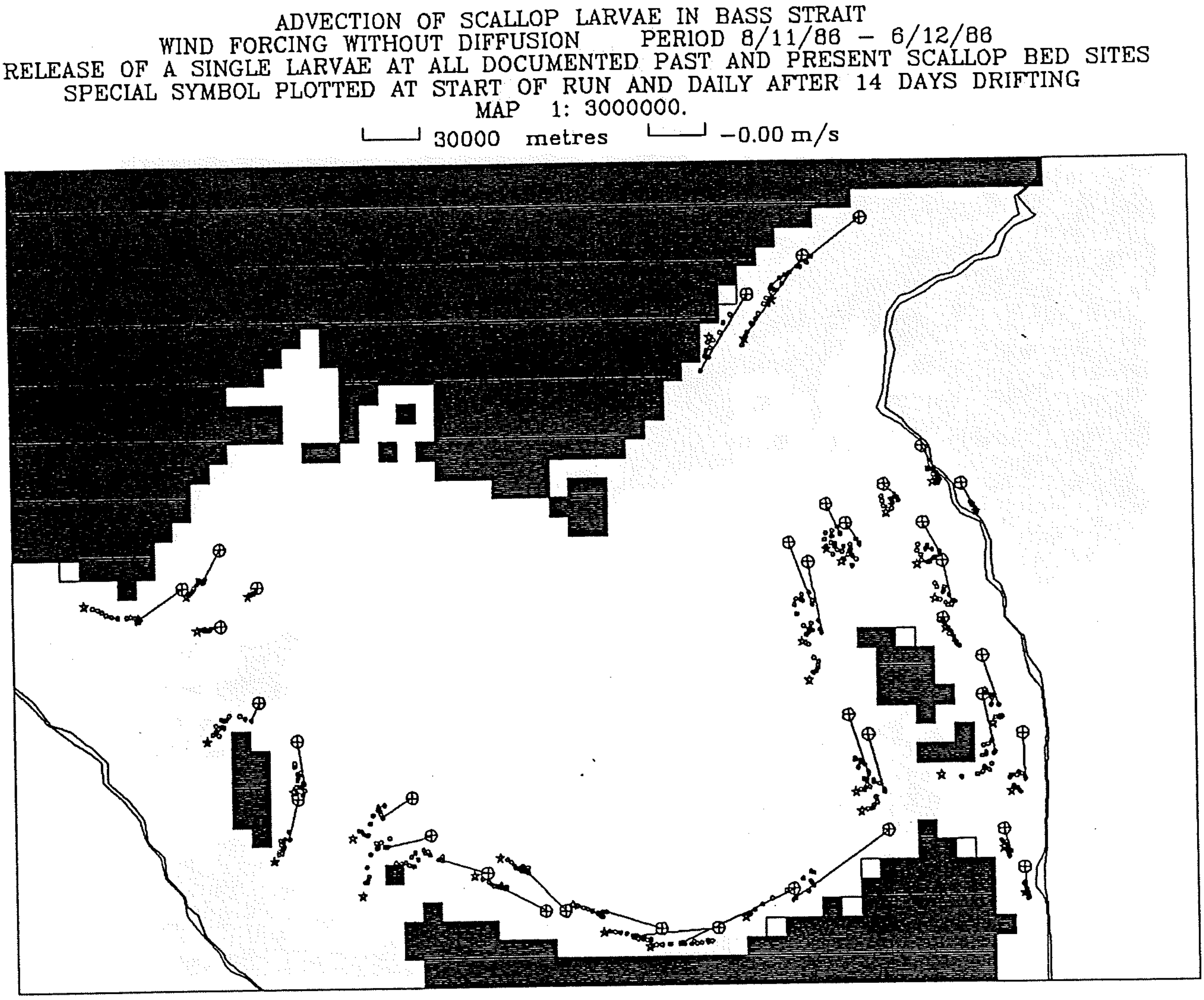

Fig. 4.4j Pelagic excursions from modern and historical scallop beds over the 28 day period from November 8, 1986. The large crossed circle shows the release point and the straight line shows the excursion over the first non-viable 14 days. The small circles then show the positions at daily intervals in the 14-28 day interval, while the star shows the final position at the end of the 28 day pelagic period.

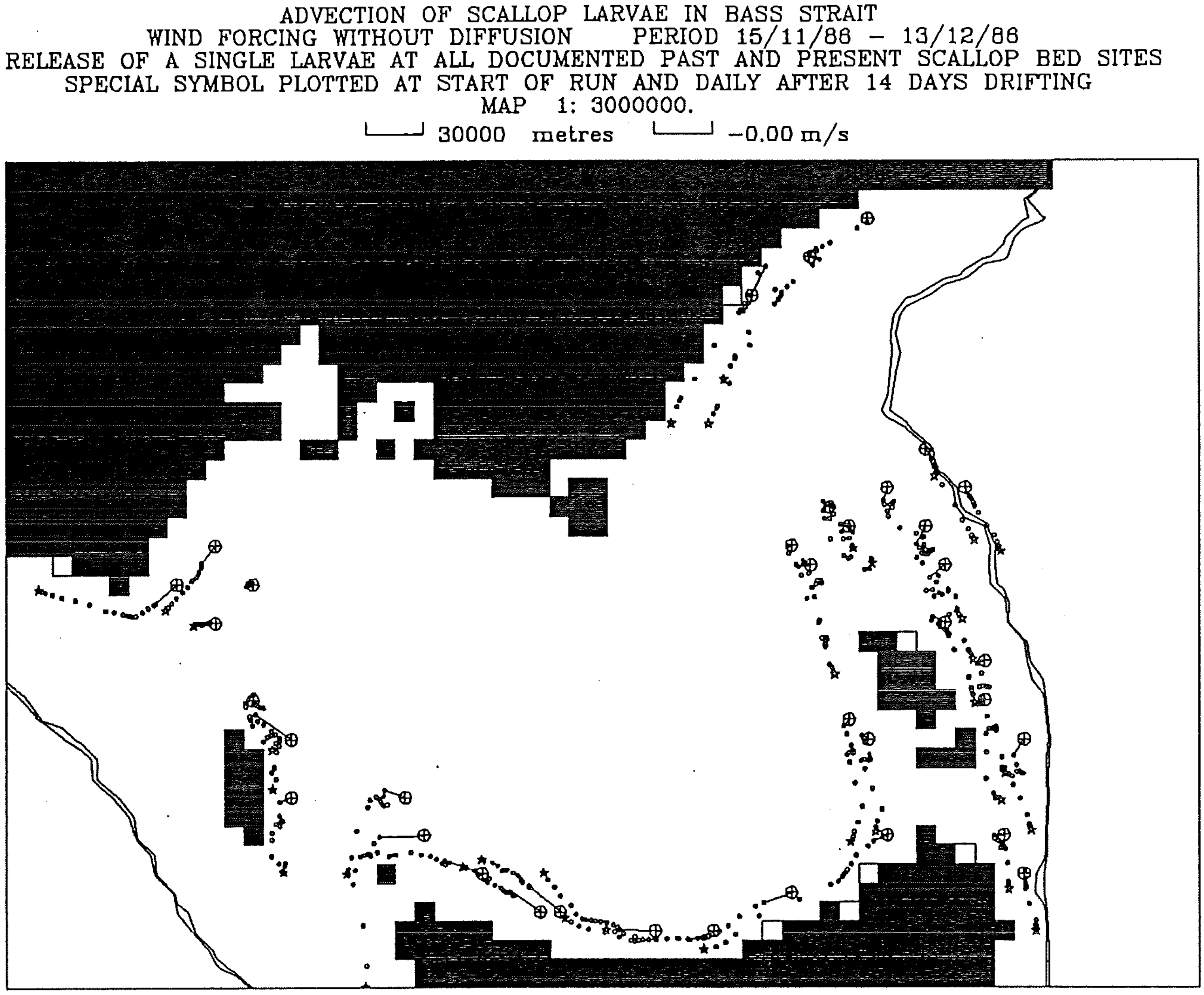

Fig. 4.4k Pelagic excursions from modern and historical scallop beds over the 28 day period from November 15, 1986. The large crossed circle shows the release point and the straight line shows the excursion over the first non-viable 14 days. The small circles then show the positions at daily intervals in the 14-28 day interval, while the star shows the final position at the end of the 28 day pelagic period.

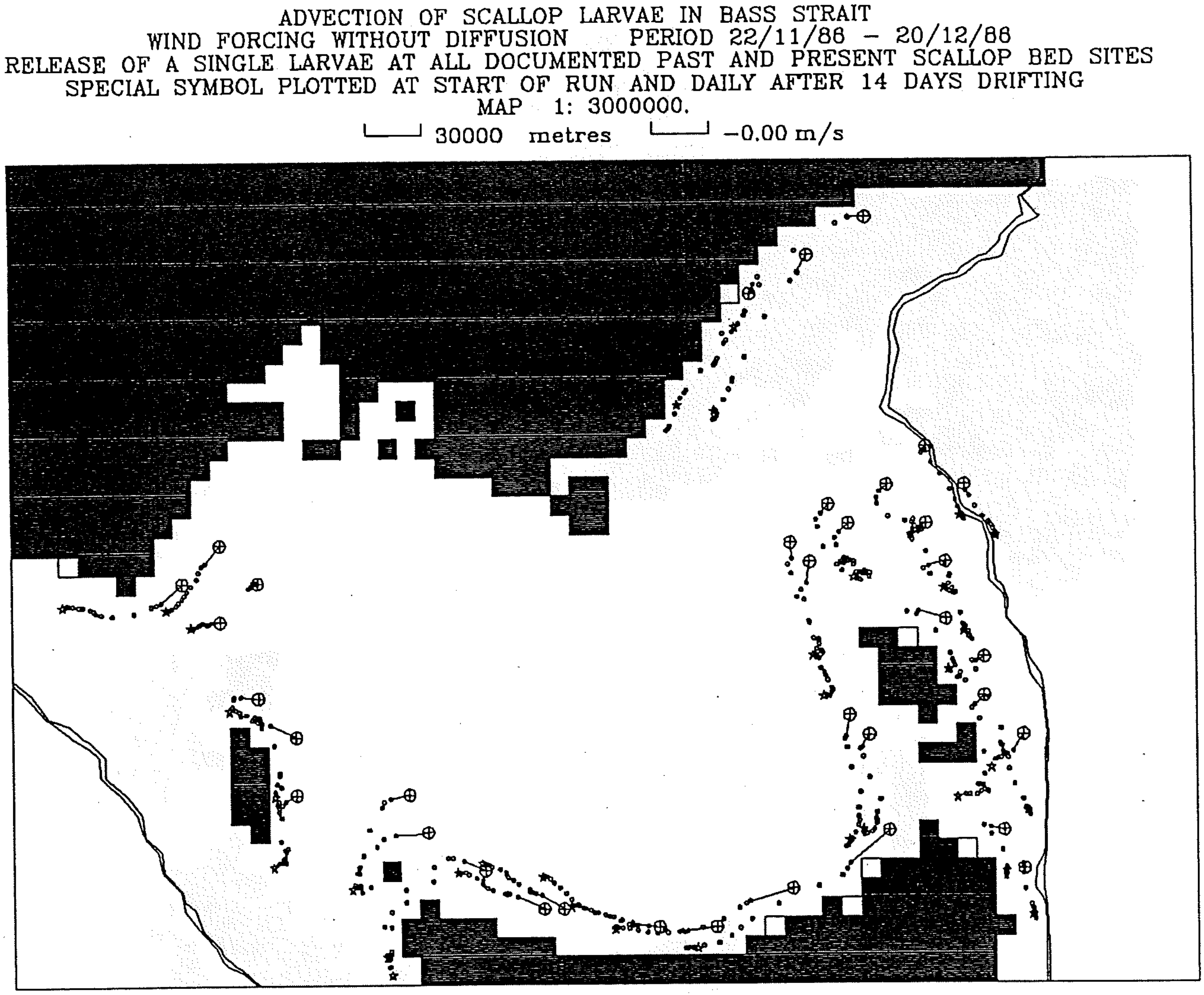

Fig. 4.41 Pelagic excursions from modern and historical scallop beds over the 28 day period from November 22, 1986. The large crossed circle shows the release point and the straight line shows the excursion over the first non-viable 14 days. The small circles then show the positions at daily intervals in the 14-28 day interval, while the star shows the final position at the end of the 28 day pelagic period.

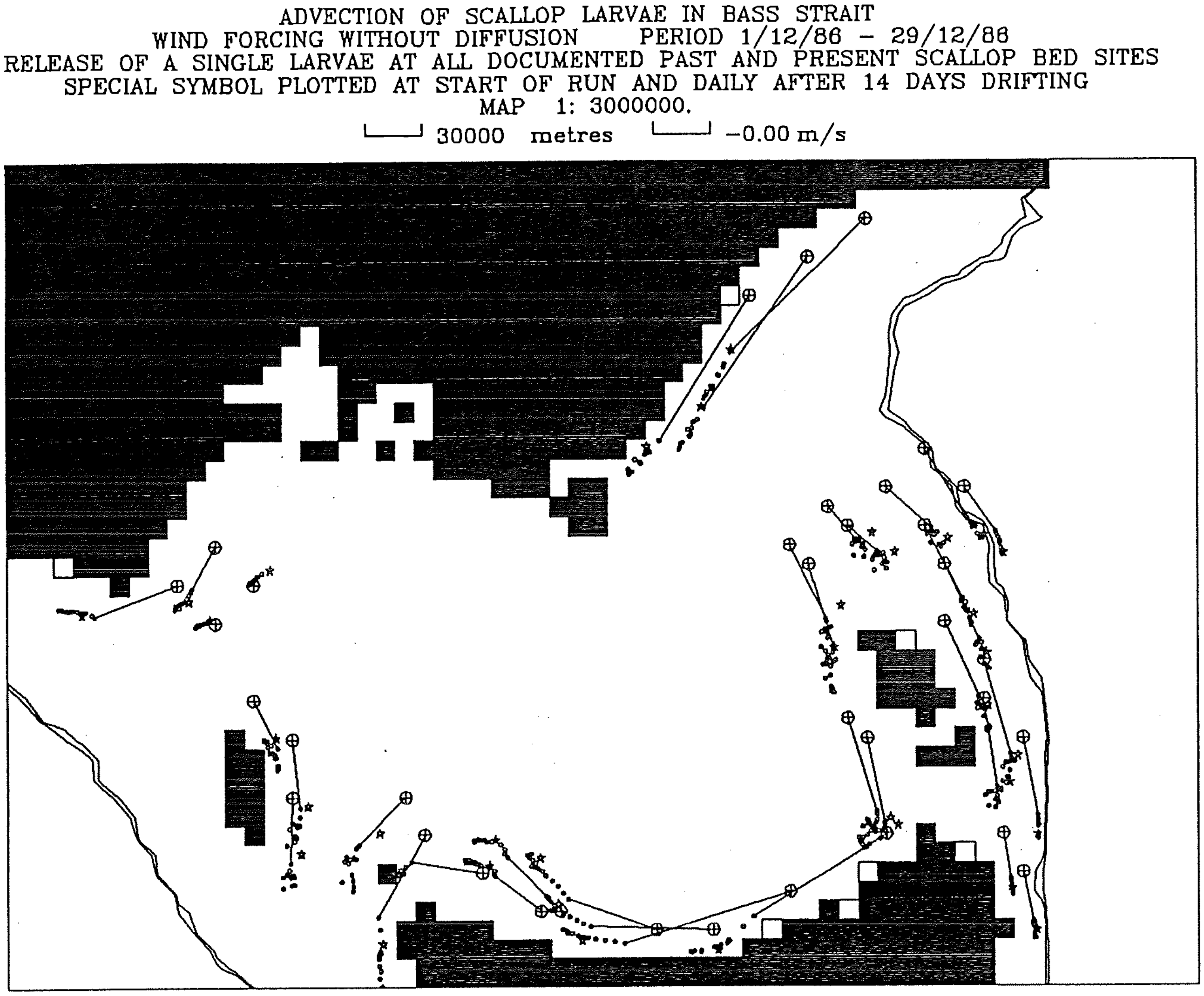

ADVECTION OF SCALLOP LARVAE IN BASS STRAIT
WIND FORCING WITHOUT DIFFUSION PERIOD 1/12/86 - 29/12/86
RELEASE OF A SINGLE LARVAE AT ALL DOCUMENTED PAST AND PRESENT SCALLOP BED SITES
SPECIAL SYMBOL PLOTTED AT START OF RUN AND DAILY AFTER 14 DAYS DRIFTING
MAP 1: 3000000.

Fig. 4.4m Pelagic excursions from modern and historical scallop beds over the 28 day period from December 1, 1986. The large crossed circle shows the release point and the straight line shows the excursion over the first non-viable 14 days. The small circles then show the positions at daily intervals in the 14-28 day interval, while the star shows the final position at the end of the 28 day pelagic period.

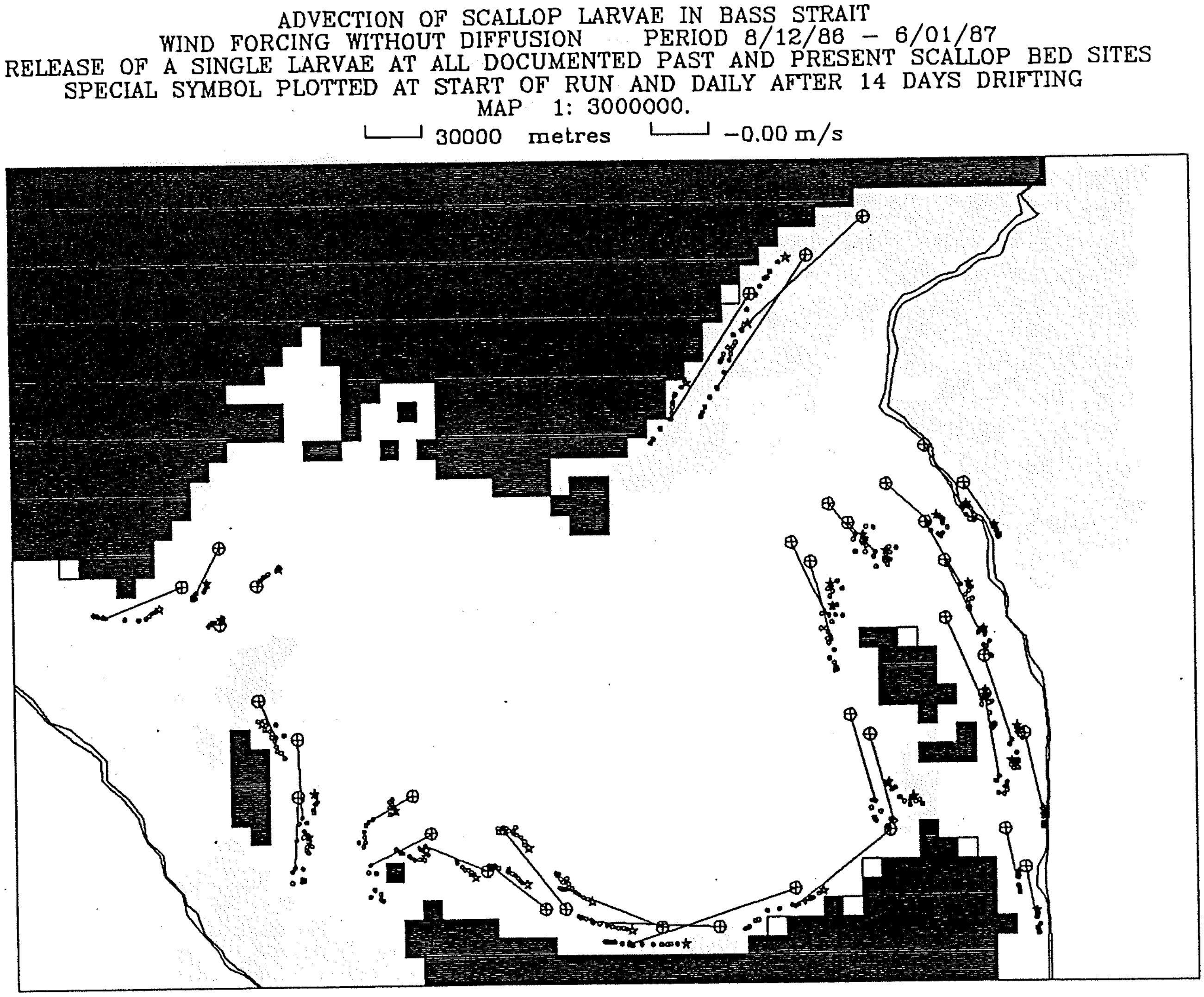

Fig. 4.4n Pelagic excursions from modern and historical scallop beds over the 28 day period from December 8, 1986. The large crossed circle shows the release point and the straight line shows the excursion over the first non-viable 14 days. The small circles then show the positions at daily intervals in the 14-28 day interval, while the star shows the final position at the end of the 28 day pelagic period.

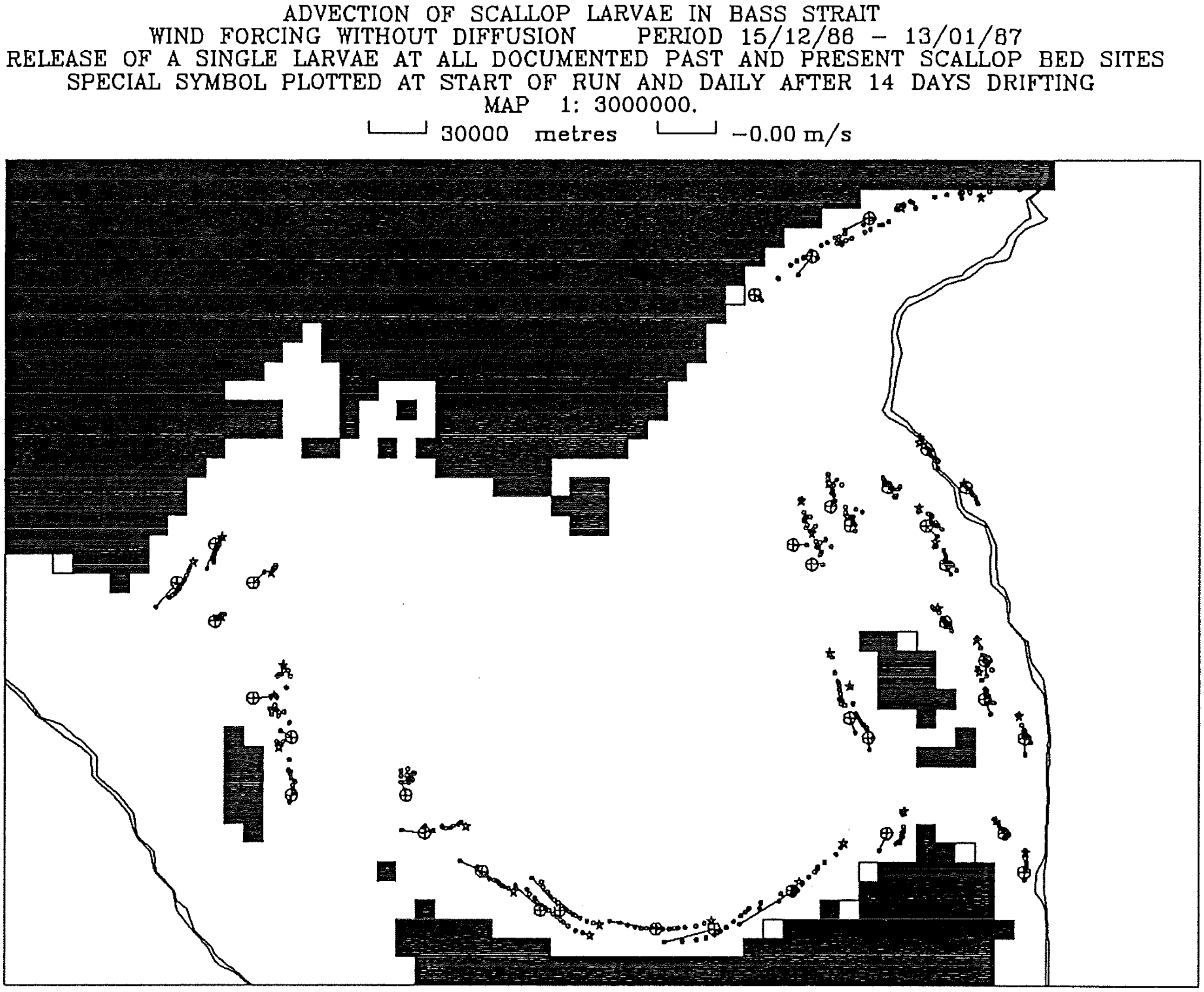
ADVECTION OF SCALLOP LARVAE IN BASS STRAIT
WIND FORCING WITHOUT DIFFUSION PERIOD 15/12/86 - 13/01/87
RELEASE OF A SINGLE LARVAE AT ALL DOCUMENTED PAST AND PRESENT SCALLOP BED SITES
SPECIAL SYMBOL PLOTTED AT START OF RUN AND DAILY AFTER 14 DAYS DRIFTING
MAP 1: 3000000.

Fig. 4.4o Pelagic excursions from modern and historical scallop beds over the 28 day period from December 15, 1986. The large crossed circle shows the release point and the straight line shows the excursion over the first non-viable 14 days. The small circles then show the positions at daily intervals in the 14-28 day interval, while the star shows the final position at the end of the 28 day pelagic period.

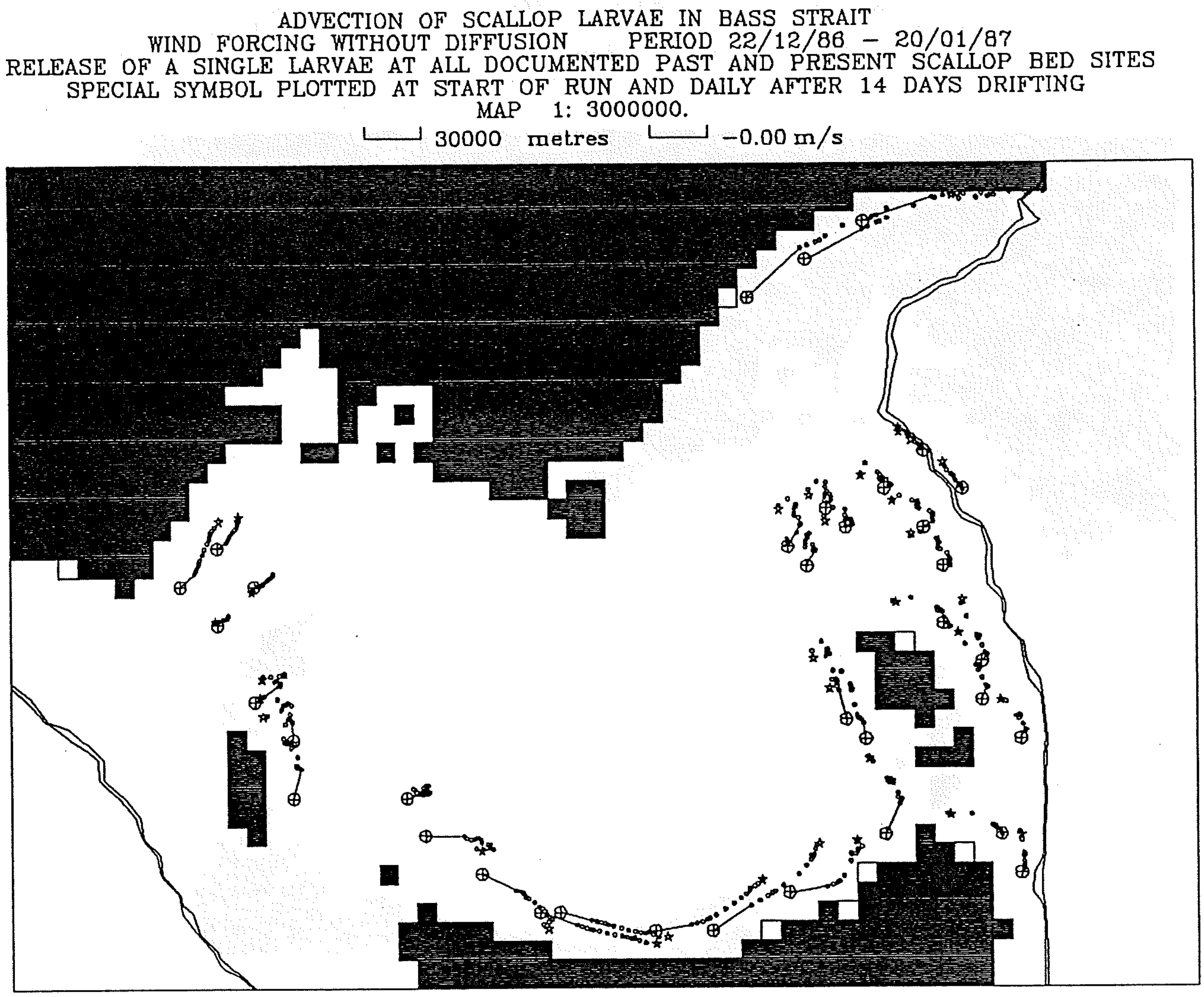

Fig. 4.4p Pelagic excursions from modern and historical scallop beds over the 28 day period from December 22, 1986. The large crossed circle shows the release point and the straight line shows the excursion over the first non-viable 14 days. The small circles then show the positions at daily intervals in the 14-28 day interval, while the star shows the final position at the end of the 28 day pelagic period.

ADVECTION OF SCALLOP LARVAE IN BASS STRAIT
WIND FORCING WITHOUT DIFFUSION PERIOD 1/01/87 - 29/01/87
RELEASE OF A SINGLE LARVAE AT ALL DOCUMENTED PAST AND PRESENT SCALLOP BED SITES
SPECIAL SYMBOL PLOTTED AT START OF RUN AND DAILY AFTER 14 DAYS DRIFTING
MAP 1: 3000000.
30000 metres −0.00 m/s

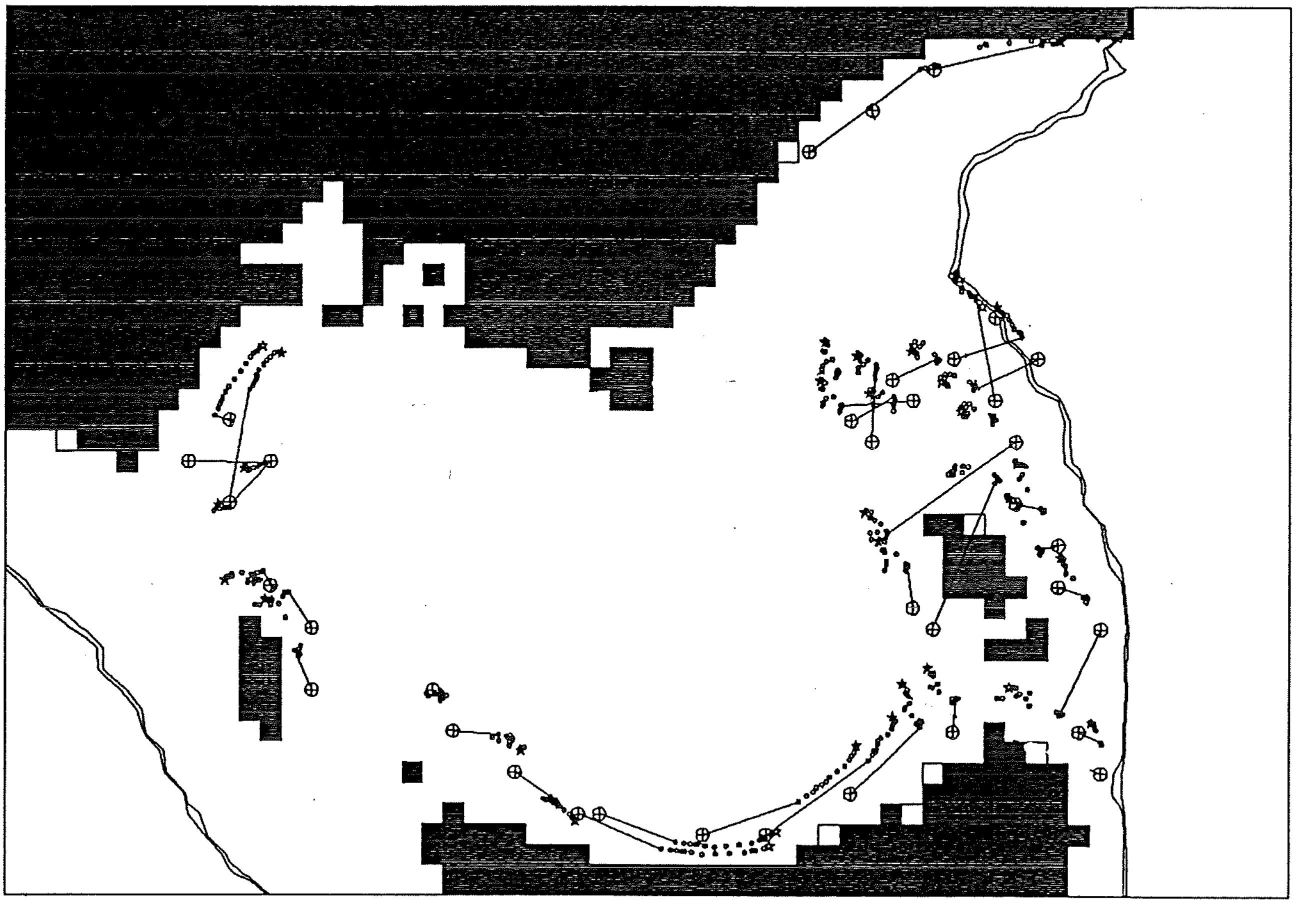

Fig. 4.4q Pelagic excursions from modern and historical scallop beds over the 28 day period from January 1, 1987. The large crossed circle shows the release point and the straight line shows the excursion over the first non-viable 14 days. The small circles then show the positions at daily intervals in the 14-28 day interval, while the star shows the final position at the end of the 28 day pelagic period.

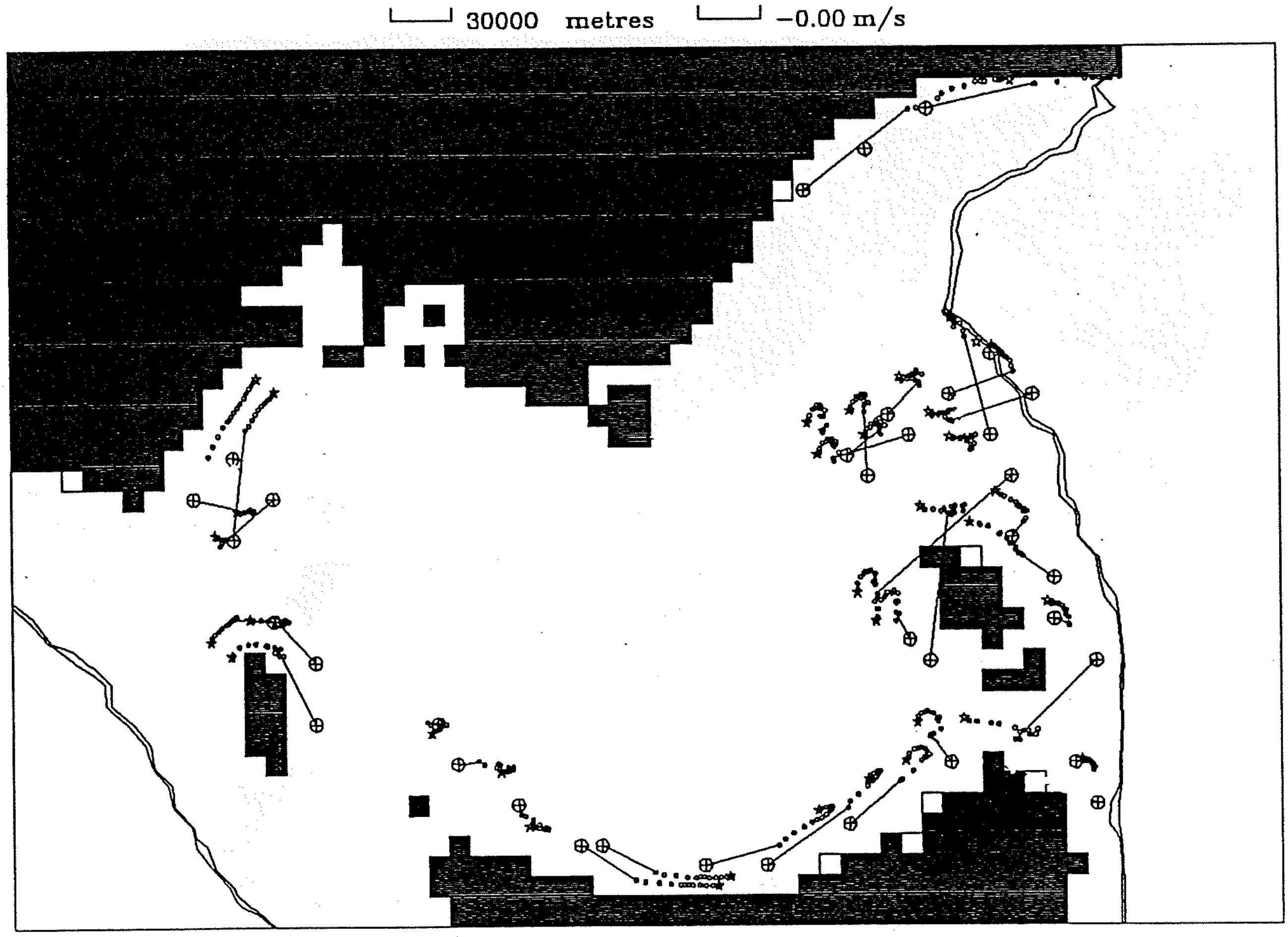

ADVECTION OF SCALLOP LARVAE IN BASS STRAIT
WIND FORCING WITHOUT DIFFUSION PERIOD 8/01/87 – 6/02/87
RELEASE OF A SINGLE LARVAE AT ALL DOCUMENTED PAST AND PRESENT SCALLOP BED SITES
SPECIAL SYMBOL PLOTTED AT START OF RUN AND DAILY AFTER 14 DAYS DRIFTING
MAP 1: 3000000.

Fig. 4.4r Pelagic excursions from modern and historical scallop beds over the 28 day period from January 8, 1987. The large crossed circle shows the release point and the straight line shows the excursion over the first non-viable 14 days. The small circles then show the positions at daily intervals in the 14-28 day interval, while the star shows the final position at the end of the 28 day pelagic period.

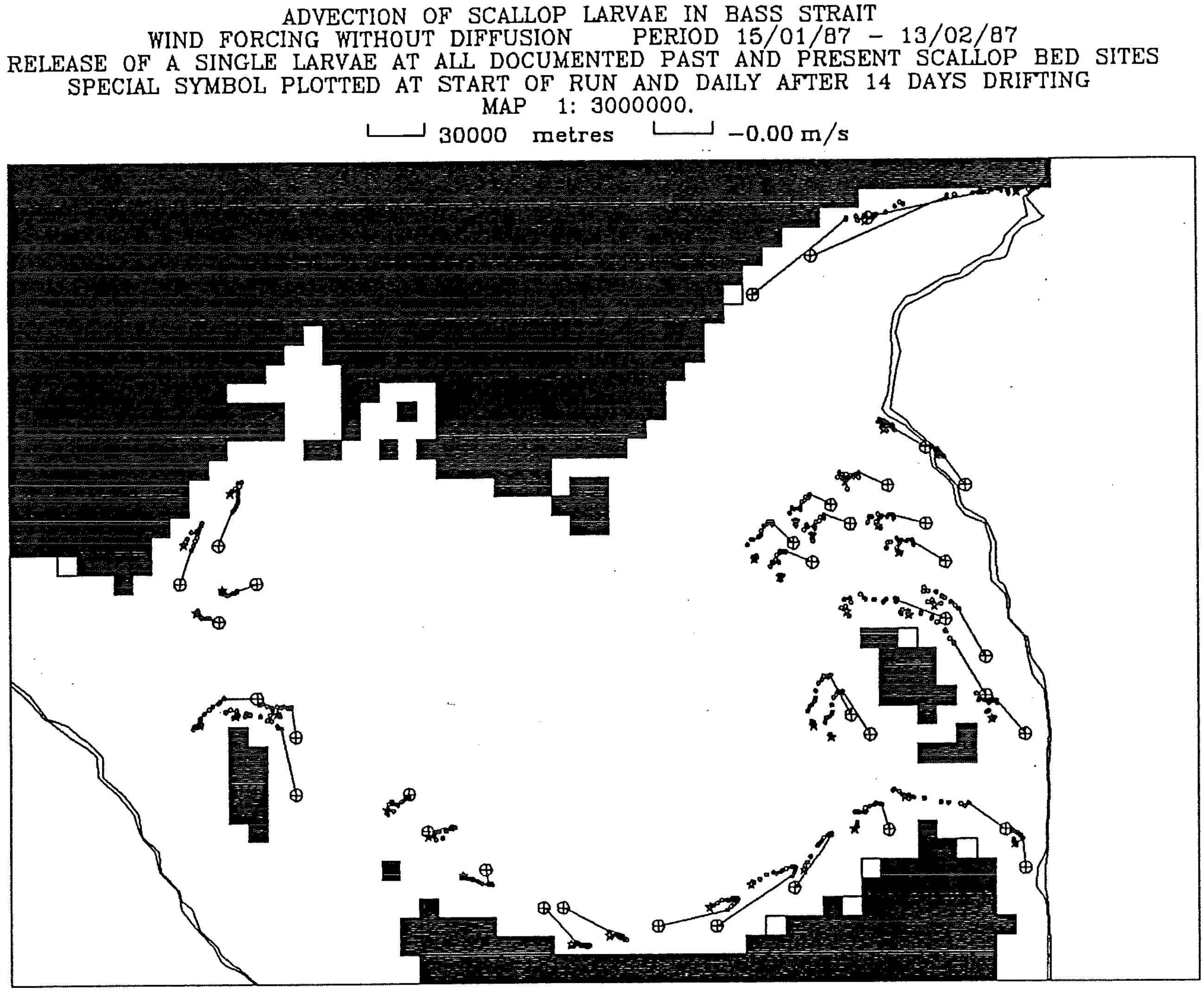

Fig. 4.4s Pelagic excursions from modern and historical scallop beds over the 28 day period from January 15, 1987. The large crossed circle shows the release point and the straight line shows the excursion over the first non-viable 14 days. The small circles then show the positions at daily intervals in the 14-28 day interval, while the star shows the final position at the end of the 28 day pelagic period.

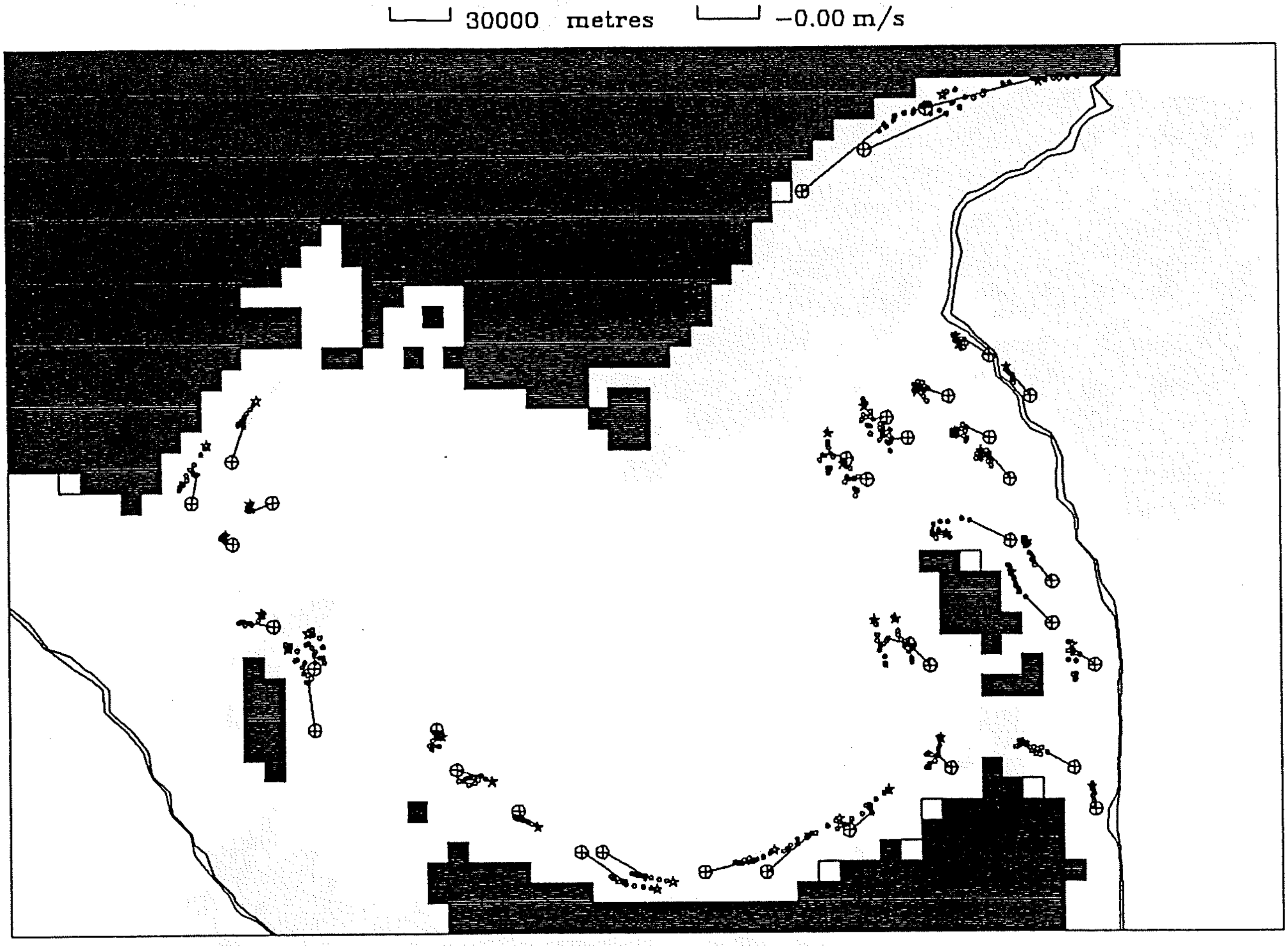

ADVECTION OF SCALLOP LARVAE IN BASS STRAIT
WIND FORCING WITHOUT DIFFUSION PERIOD 22/01/87 – 20/02/87
RELEASE OF A SINGLE LARVAE AT ALL DOCUMENTED PAST AND PRESENT SCALLOP BED SITES
SPECIAL SYMBOL PLOTTED AT START OF RUN AND DAILY AFTER 14 DAYS DRIFTING
MAP 1: 3000000.

Fig. 4.4t Pelagic excursions from modern and historical scallop beds over the 28 day period from January 22, 1987. The large crossed circle shows the release point and the straight line shows the excursion over the first non-viable 14 days. The small circles then show the positions at daily intervals in the 14-28 day interval, while the star shows the final position at the end of the 28 day pelagic period.

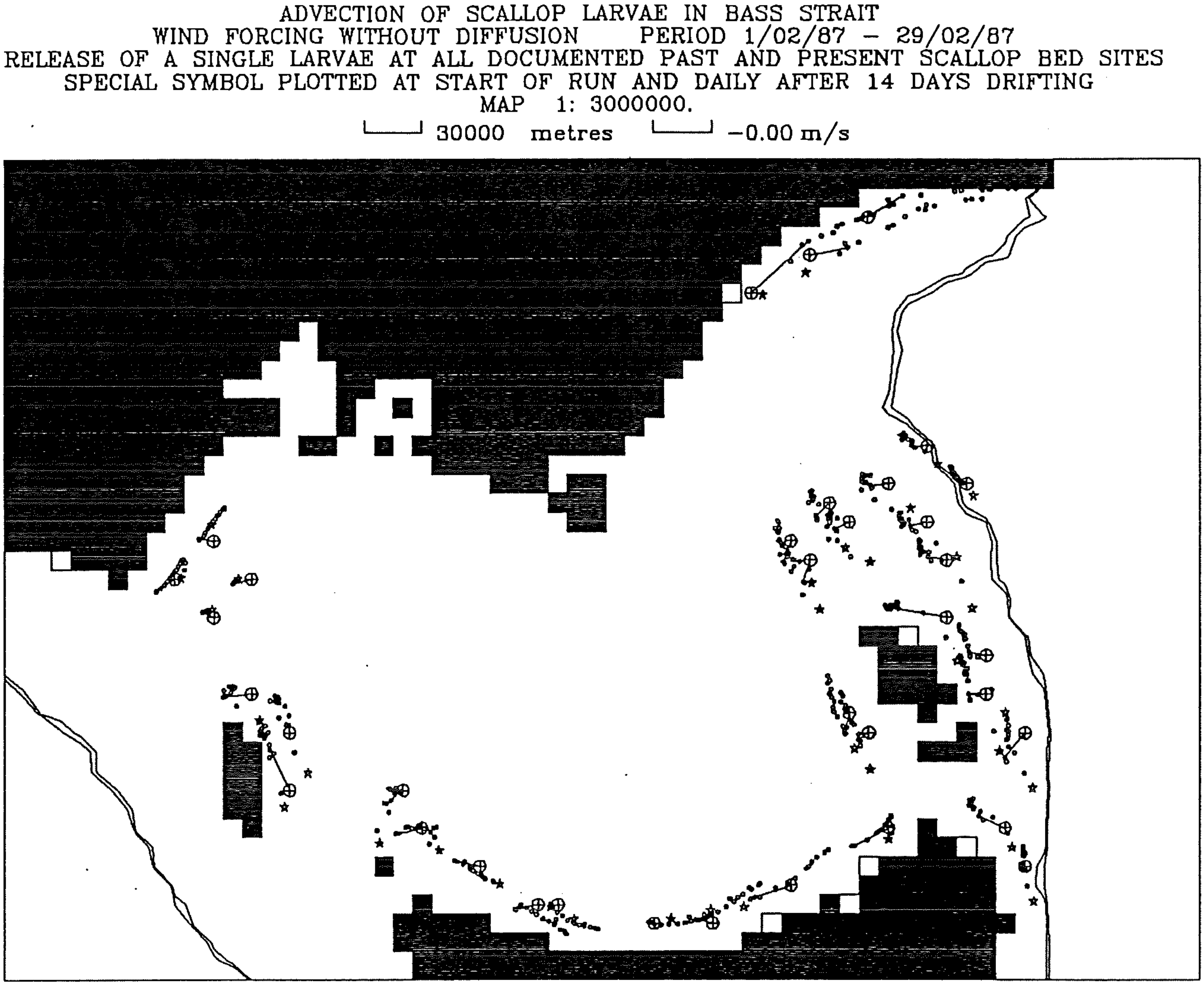

Fig. 4.4u Pelagic excursions from modern and historical scallop beds over the 28 day period from February 1, 1987. The large crossed circle shows the release point and the straight line shows the excursion over the first non-viable 14 days. The small circles then show the positions at daily intervals in the 14-28 day interval, while the star shows the final position at the end of the 28 day pelagic period.

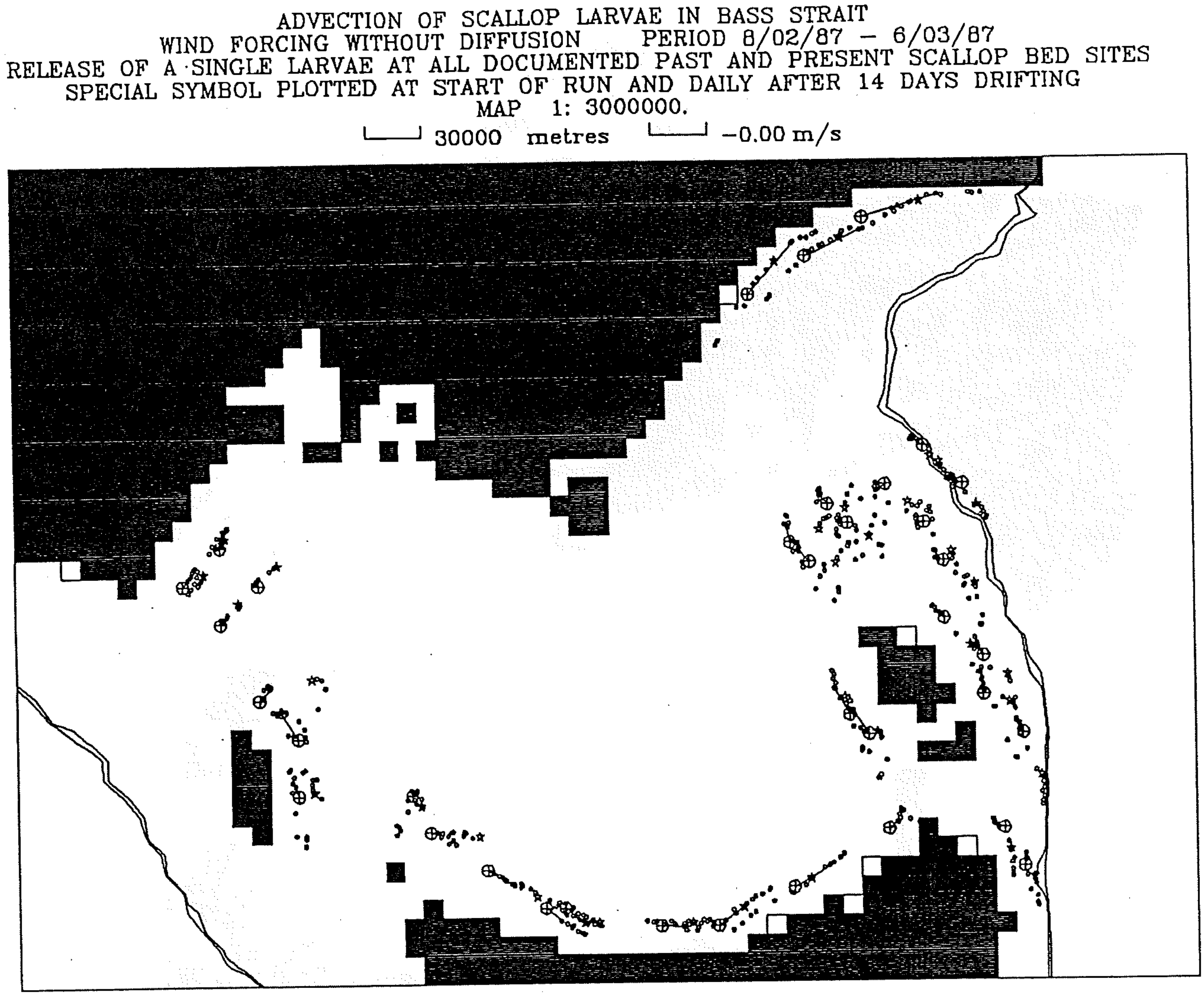

Fig. 4.4v Pelagic excursions from modern and historical scallop beds over the 28 day period from February 8, 1987. The large crossed circle shows the release point and the straight line shows the excursion over the first non-viable 14 days. The small circles then show the positions at daily intervals in the 14-28 day interval, while the star shows the final position at the end of the 28 day pelagic period.

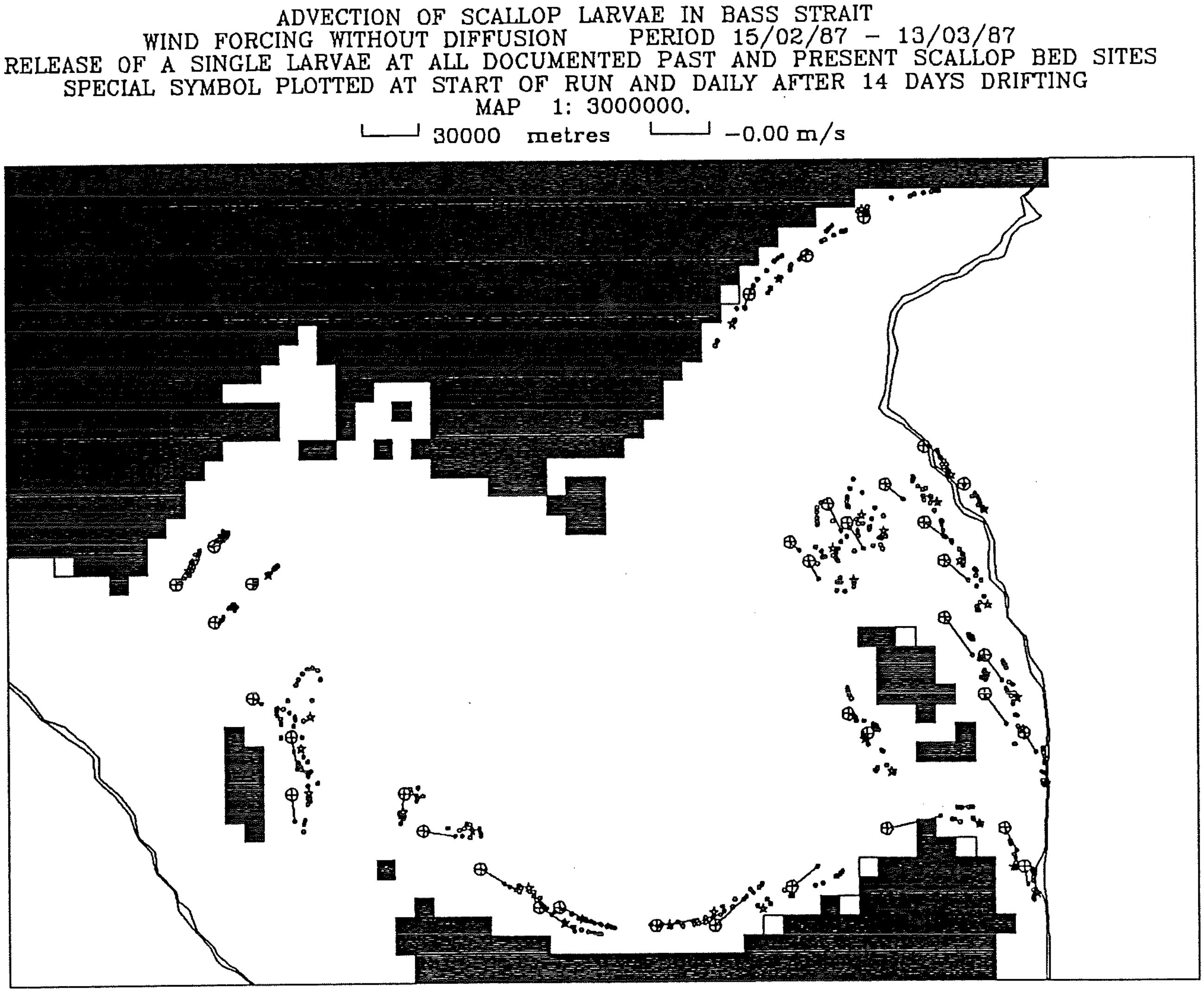

Fig. 4.4w Pelagic excursions from modern and historical scallop beds over the 28 day period from February 15, 1987. The large crossed circle shows the release point and the straight line shows the excursion over the first non-viable 14 days. The small circles then show the positions at daily intervals in the 14-28 day interval, while the star shows the final position at the end of the 28 day pelagic period.

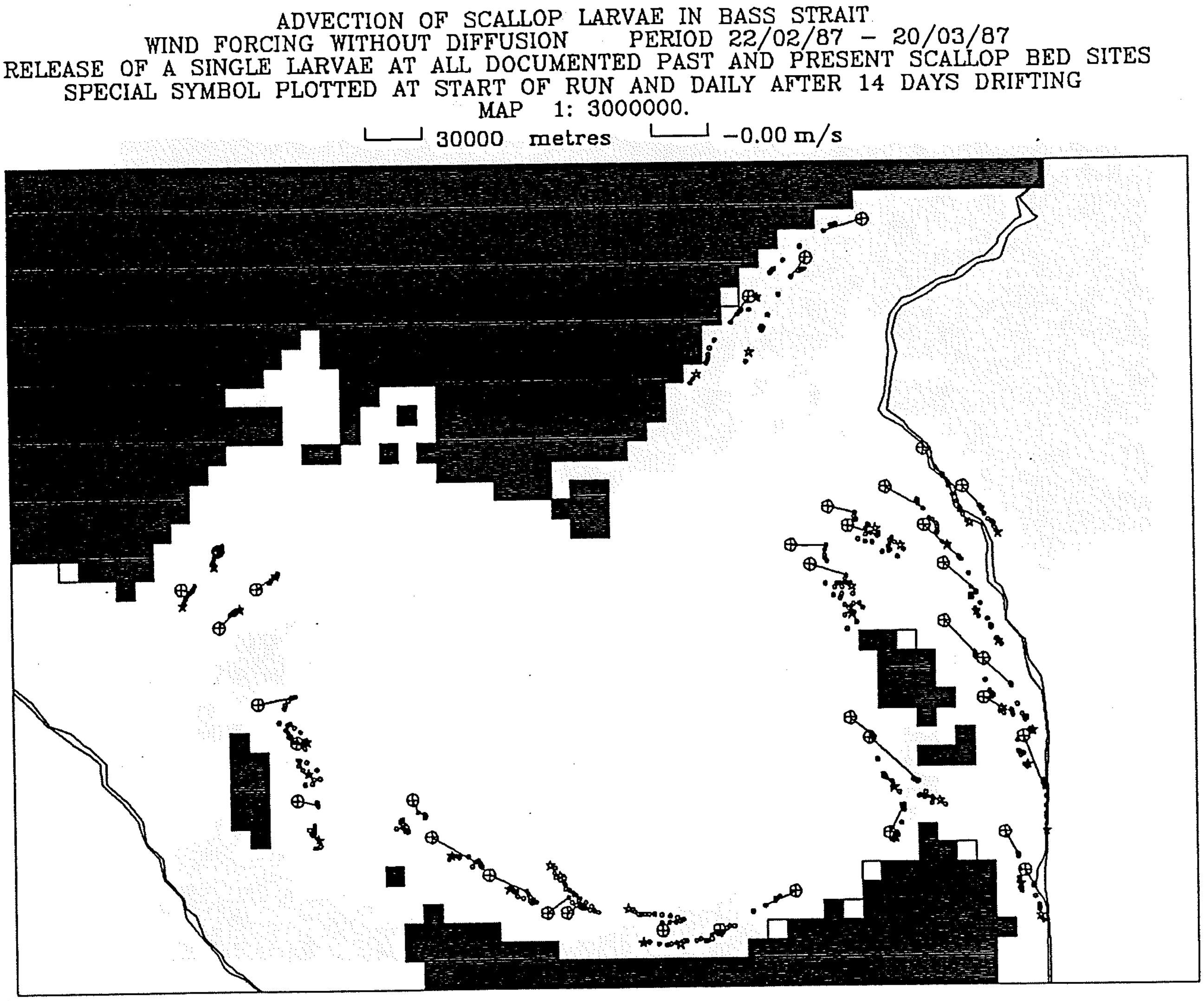

Fig. 4.4x Pelagic excursions from modern and historical scallop beds over the 28 day period from February 22, 1987. The large crossed circle shows the release point and the straight line shows the excursion over the first non-viable 14 days. The small circles then show the positions at daily intervals in the 14-28 day interval, while the star shows the final position at the end of the 28 day pelagic period.

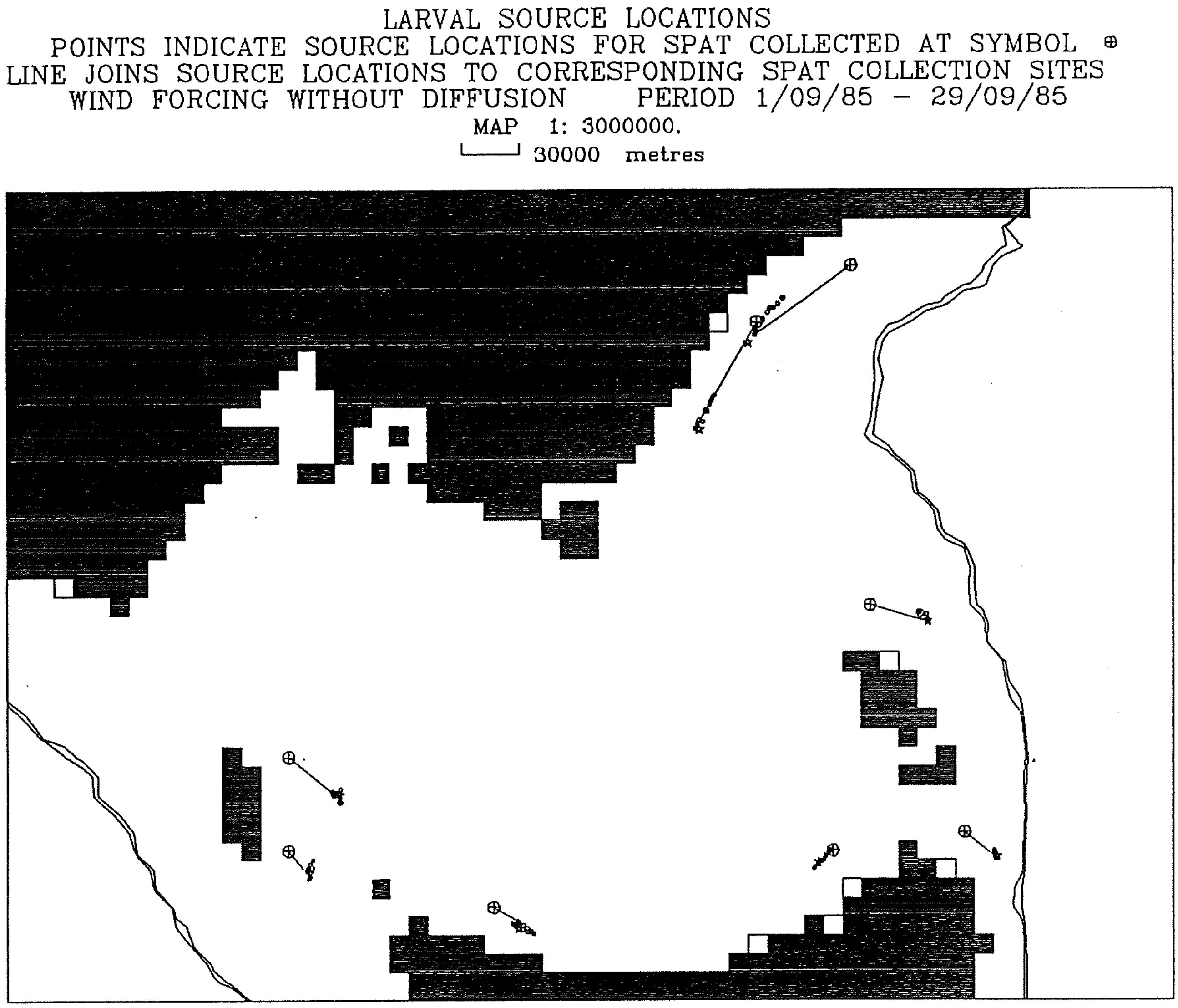
LARVAL SOURCE LOCATIONS
POINTS INDICATE SOURCE LOCATIONS FOR SPAT COLLECTED AT SYMBOL ⊕
LINE JOINS SOURCE LOCATIONS TO CORRESPONDING SPAT COLLECTION SITES
WIND FORCING WITHOUT DIFFUSION PERIOD 1/09/85 - 29/09/85
MAP 1: 3000000.
30000 metres

Fig. 4.5a Reverse model tracking showing the possible source locations (small circles) for a spat collection site within the modern scallop beds (marked by the crossed circle) over the 28 day period from September 1, 1985.

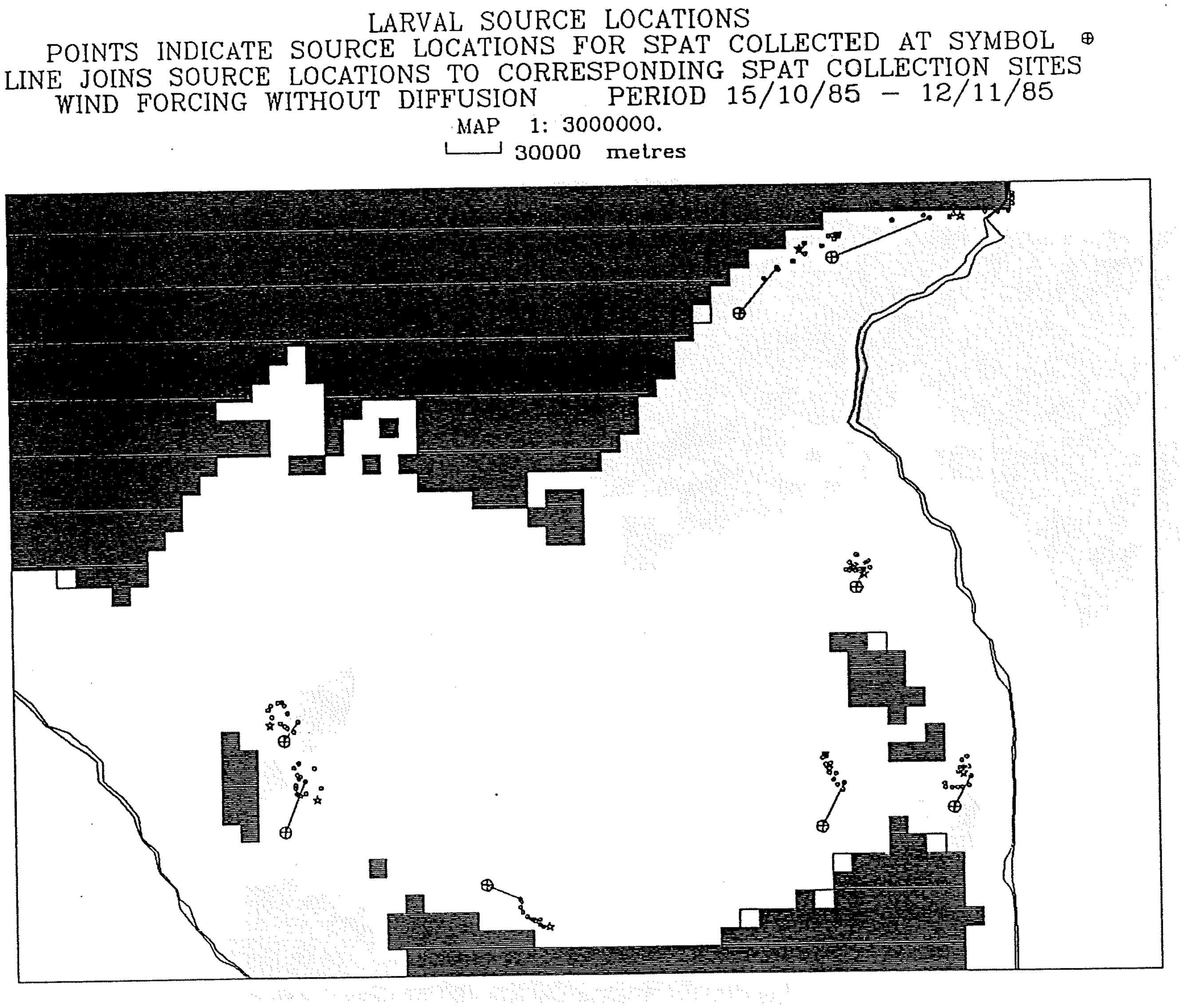

Fig. 4.5b Reverse model tracking showing the possible source locations (small circles) for a spat collection site within the modern scallop beds (marked by the crossed circle) over the 28 day period from October 15, 1985.

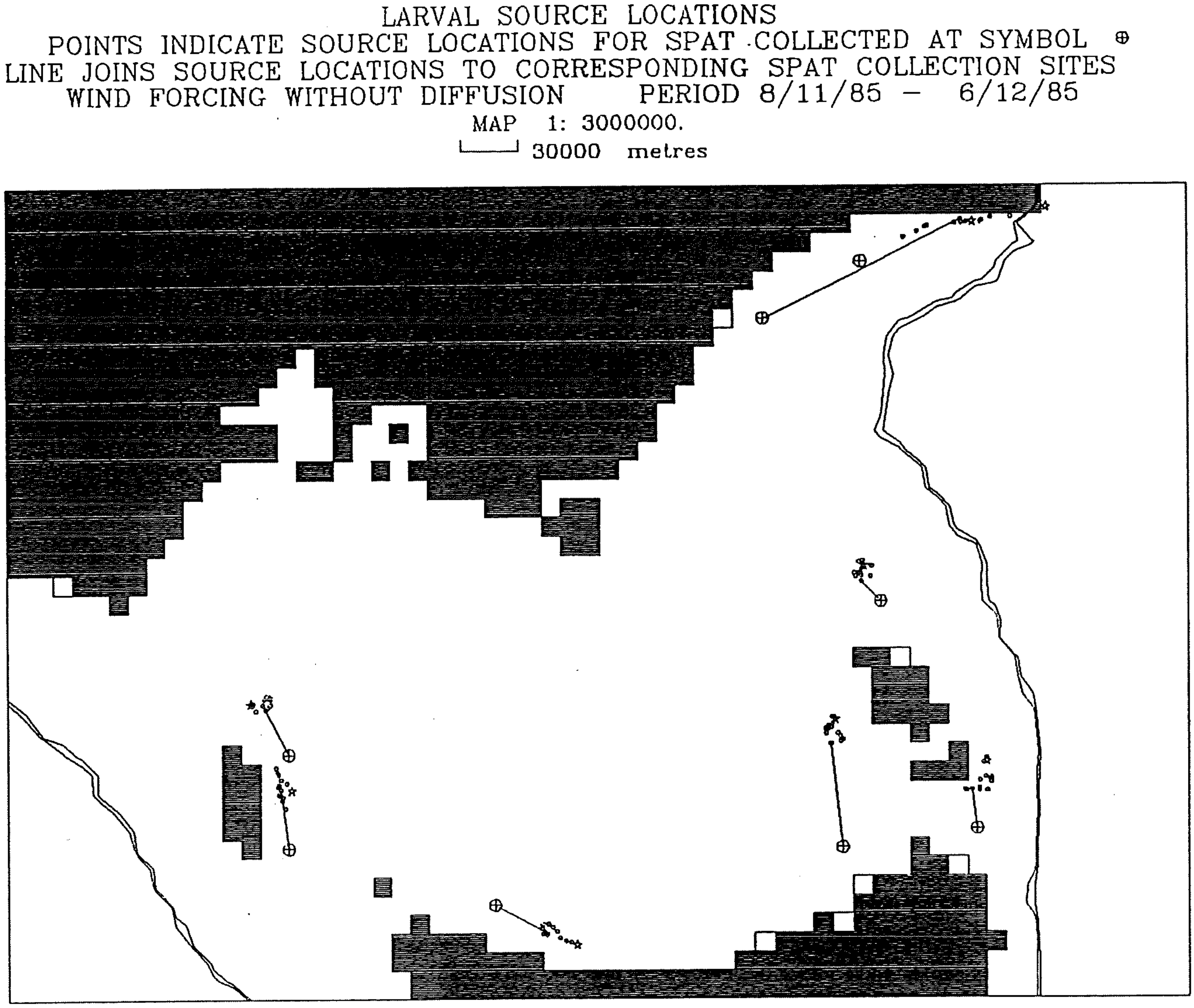

Fig. 4.5c Reverse model tracking showing the possible source locations (small circles) for a spat collection site within the modern scallop beds (marked by the crossed circle) over the 28 day period from November 8, 1985.

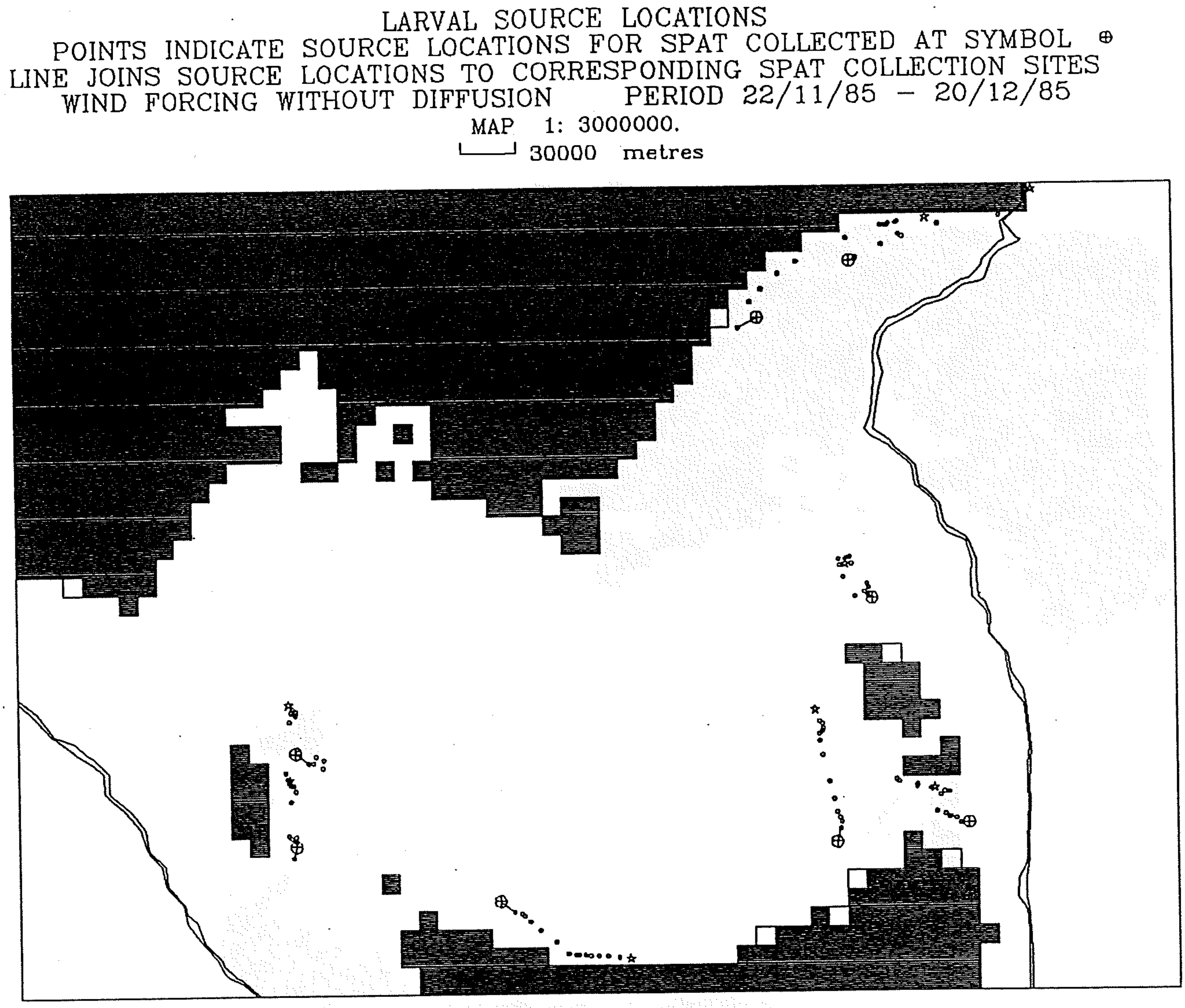

Fig. 4.5d Reverse model tracking showing the possible source locations (small circles) for a spat collection site within the modern scallop beds (marked by the crossed circle) over the 28 day period from November 22, 1985.

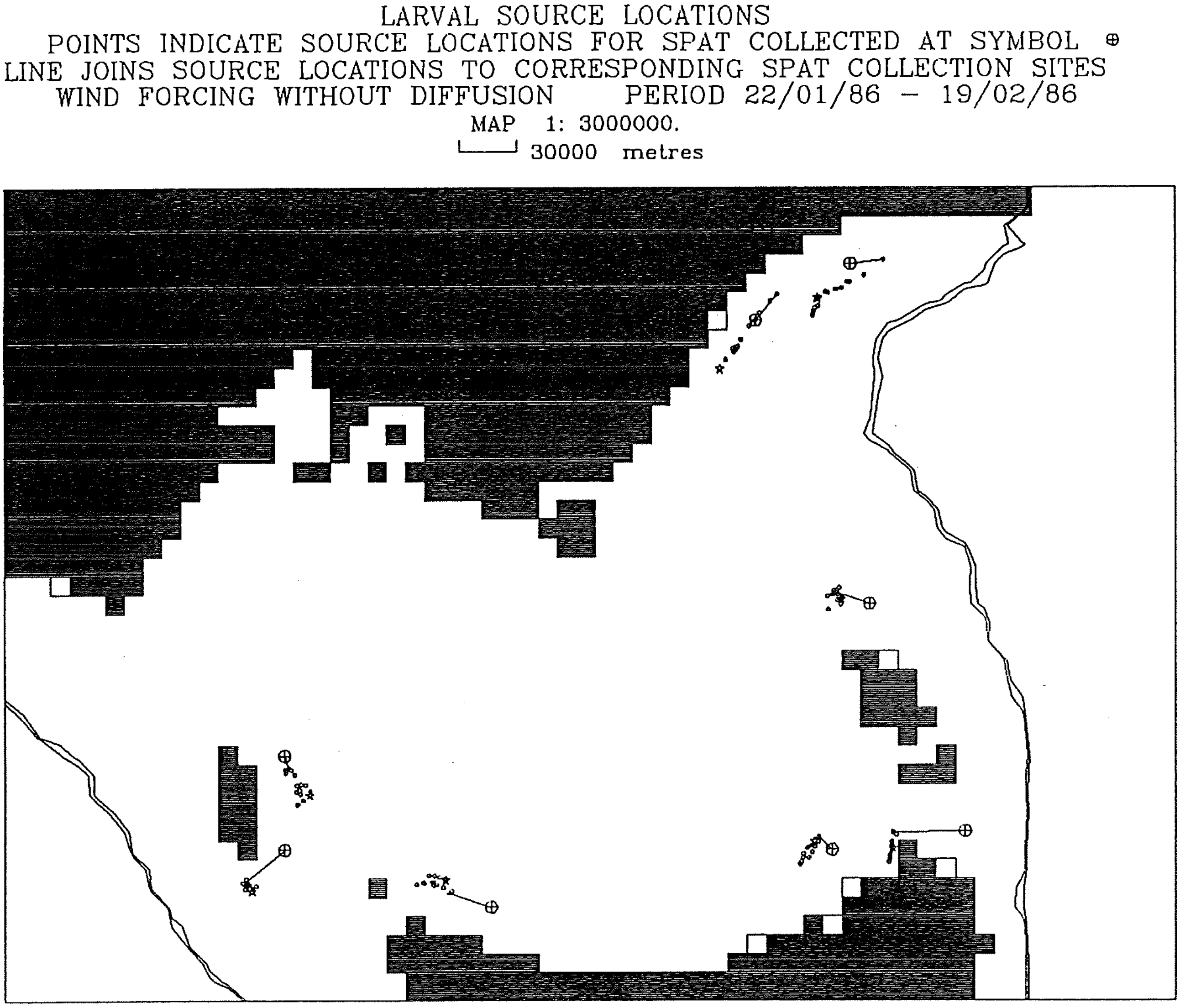

LARVAL SOURCE LOCATIONS
POINTS INDICATE SOURCE LOCATIONS FOR SPAT COLLECTED AT SYMBOL ⊕
LINE JOINS SOURCE LOCATIONS TO CORRESPONDING SPAT COLLECTION SITES
WIND FORCING WITHOUT DIFFUSION PERIOD 22/01/86 - 19/02/86
MAP 1: 3000000.

Fig. 4.5e Reverse model tracking showing the possible source locations (small circles) for a spat collection site within the modern scallop beds (marked by the crossed circle) over the 28 day period from January 22, 1986.

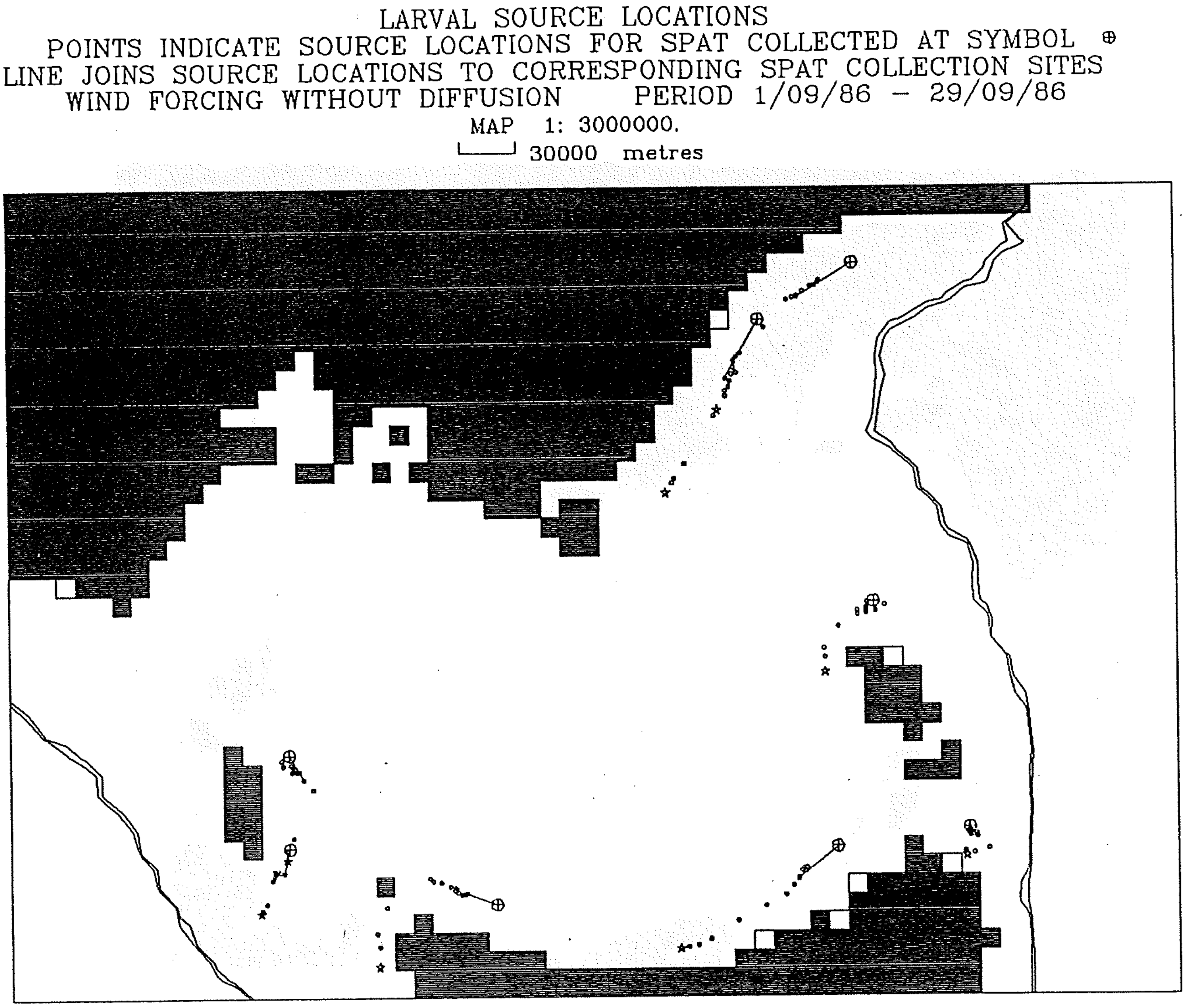

LARVAL SOURCE LOCATIONS
POINTS INDICATE SOURCE LOCATIONS FOR SPAT COLLECTED AT SYMBOL ⊕
LINE JOINS SOURCE LOCATIONS TO CORRESPONDING SPAT COLLECTION SITES
WIND FORCING WITHOUT DIFFUSION PERIOD 1/09/86 - 29/09/86
MAP 1: 3000000.
30000 metres

Fig. 4.5f Reverse model tracking showing the possible source locations (small circles) for a spat collection site within the modern scallop beds (marked by the crossed circle) over the 28 day period from September 1, 1986.

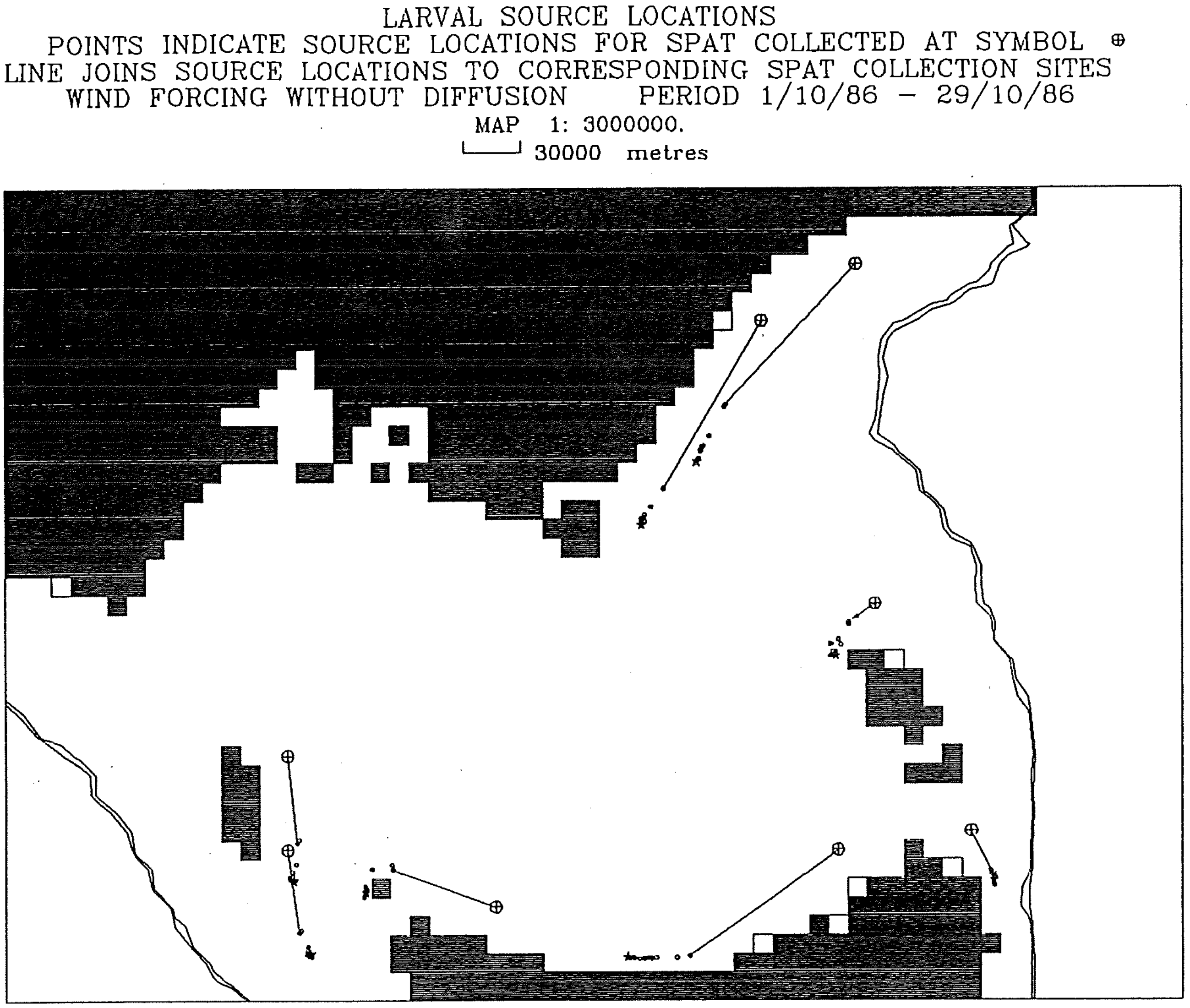

LARVAL SOURCE LOCATIONS
POINTS INDICATE SOURCE LOCATIONS FOR SPAT COLLECTED AT SYMBOL ⊕
LINE JOINS SOURCE LOCATIONS TO CORRESPONDING SPAT COLLECTION SITES
WIND FORCING WITHOUT DIFFUSION PERIOD 1/10/86 - 29/10/86
MAP 1: 3000000.

Fig. 4.5g Reverse model tracking showing the possible source locations (small circles) for a spat collection site within the modern scallop beds (marked by the crossed circle) over the 28 day period from October 1, 1986.

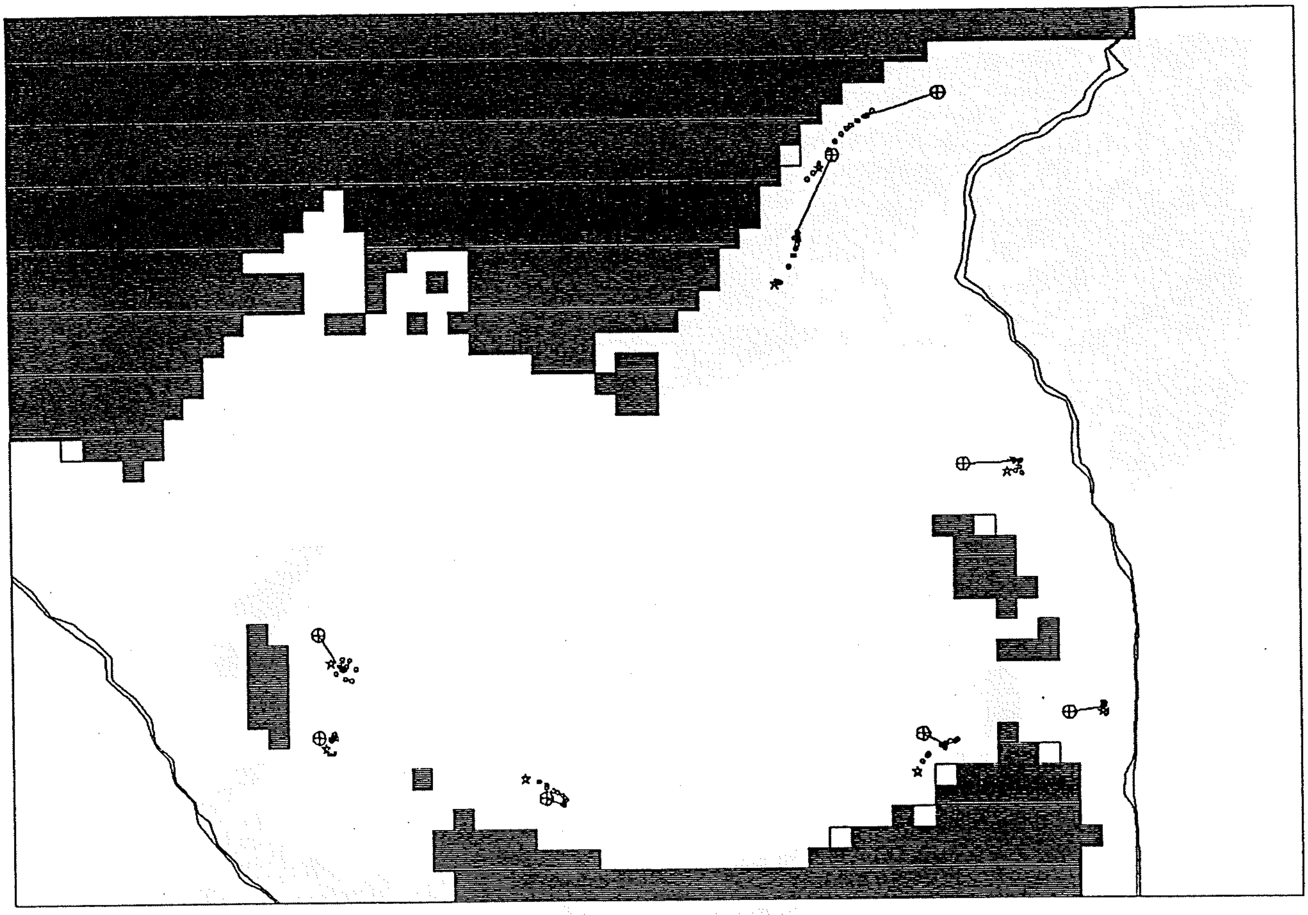

LARVAL SOURCE LOCATIONS
POINTS INDICATE SOURCE LOCATIONS FOR SPAT COLLECTED AT SYMBOL ⊕
LINE JOINS SOURCE LOCATIONS TO CORRESPONDING SPAT COLLECTION SITES
WIND FORCING WITHOUT DIFFUSION PERIOD 1/11/86 - 29/10/86
MAP 1: 3000000.
30000 metres

Fig. 4.5h Reverse model tracking showing the possible source locations (small circles) for a spat collection site within the modern scallop beds (marked by the crossed circle) over the 28 day period from November 1, 1986.

LARVAL SOURCE LOCATIONS
POINTS INDICATE SOURCE LOCATIONS FOR SPAT COLLECTED AT SYMBOL
LINE JOINS SOURCE LOCATIONS TO CORRESPONDING SPAT COLLECTION SITES
WIND FORCING WITHOUT DIFFUSION PERIOD 22/01/87 - 19/02/87
MAP 1: 3000000.
30000 metres

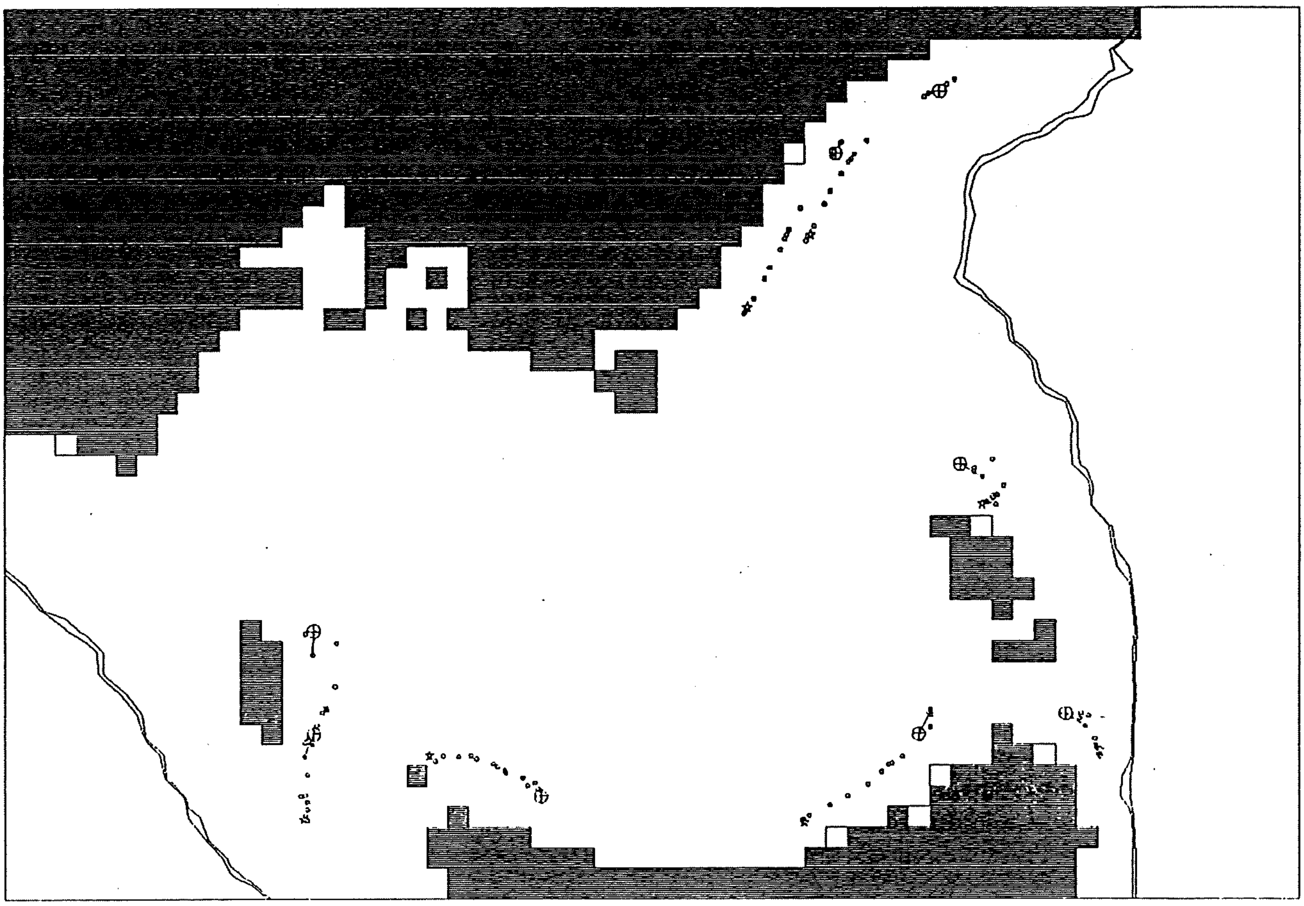

Fig. 4.5i Reverse model tracking showing the possible source locations (small circles) for a spat collection site within the modern scallop beds (marked by the crossed circle) over the 28 day period from January 22, 1987.

LARVAL SOURCE LOCATIONS
POINTS INDICATE SOURCE LOCATIONS FOR SPAT COLLECTED AT SYMBOL ⊕
LINE JOINS SOURCE LOCATIONS TO CORRESPONDING SPAT COLLECTION SITES
WIND FORCING WITHOUT DIFFUSION PERIOD 15/09/87 - 13/10/87
MAP 1: 3000000.
30000 metres

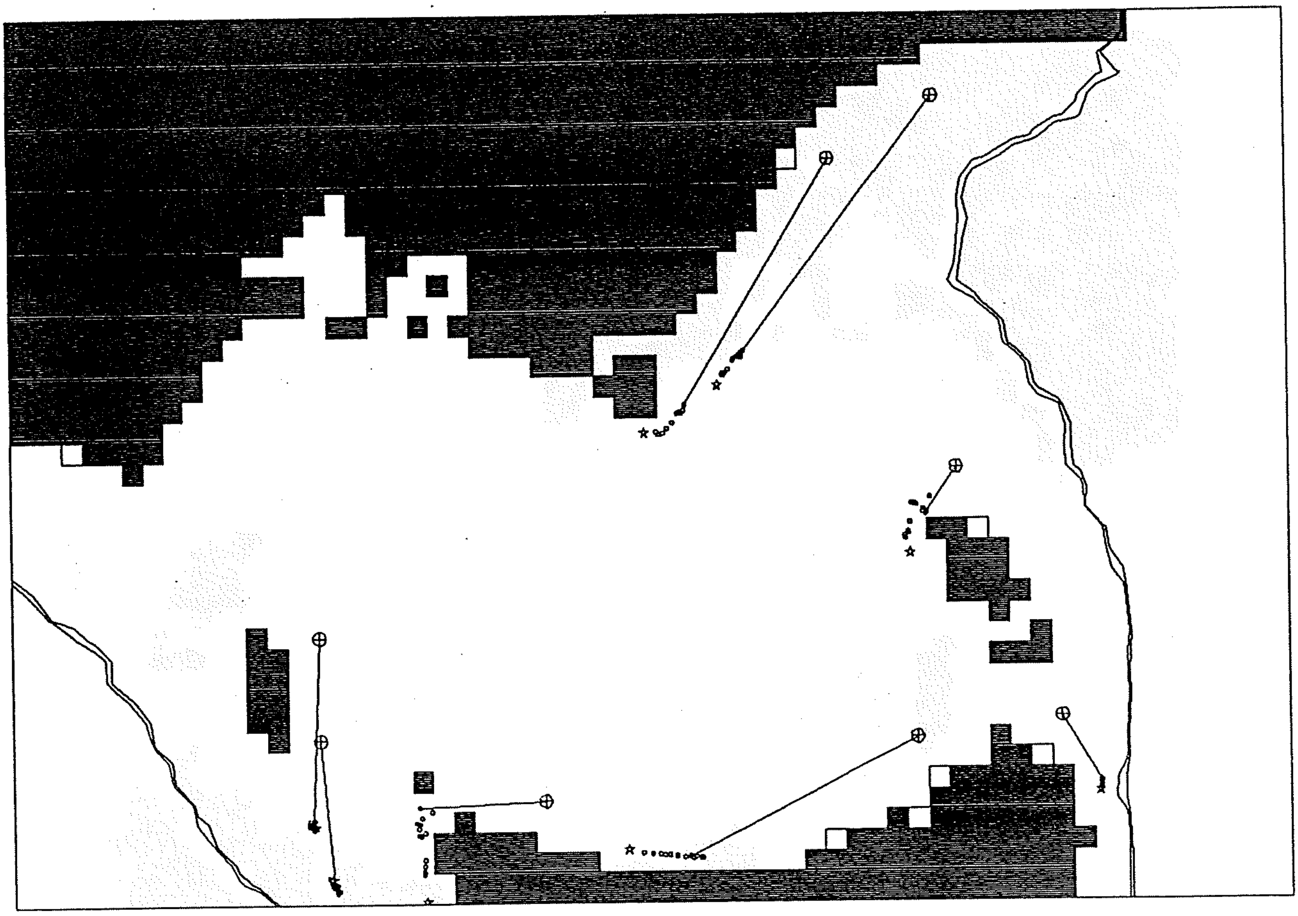

Fig. 4.5j Reverse model tracking showing the possible source locations (small circles) for a spat collection site within the modern scallop beds (marked by the crossed circle) over the 28 day period from September 15, 1987.

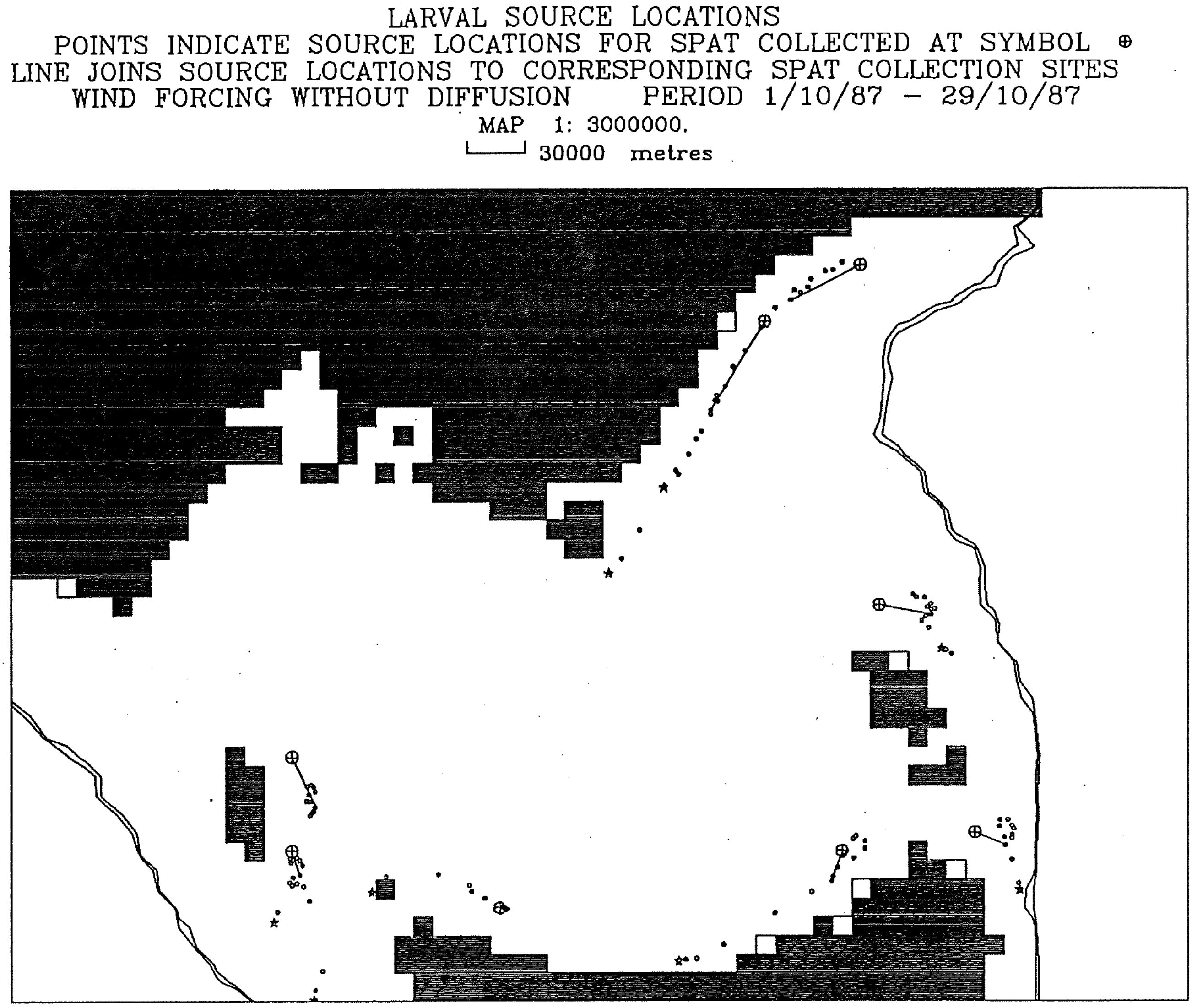

Fig. 4.5k Reverse model tracking showing the possible source locations (small circles) for a spat collection site within the modern scallop beds (marked by the crossed circle) over the 28 day period from October 1, 1987.

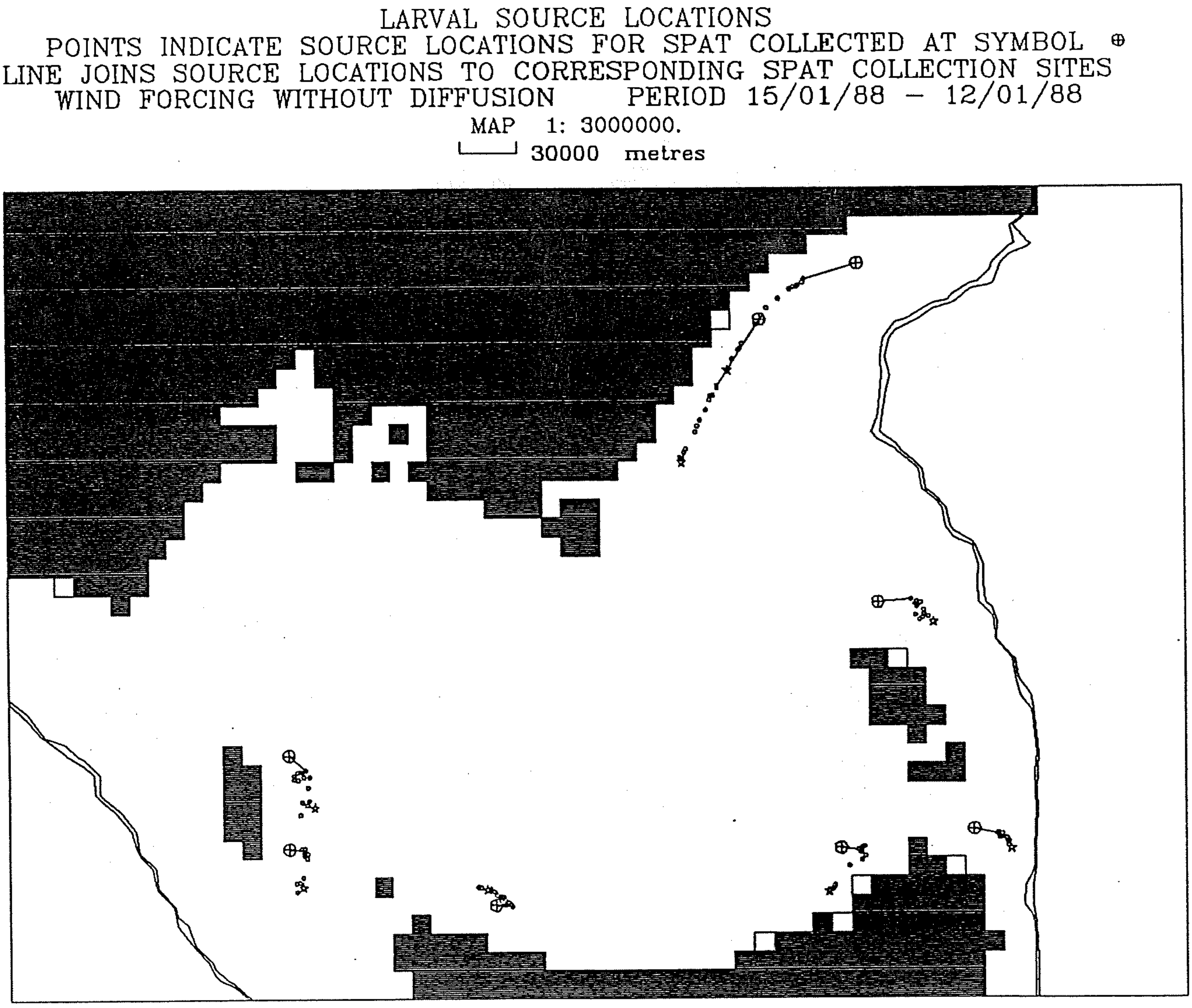

LARVAL SOURCE LOCATIONS
POINTS INDICATE SOURCE LOCATIONS FOR SPAT COLLECTED AT SYMBOL ⊕
LINE JOINS SOURCE LOCATIONS TO CORRESPONDING SPAT COLLECTION SITES
WIND FORCING WITHOUT DIFFUSION PERIOD 15/01/88 – 12/01/88
MAP 1: 3000000.
30000 metres

Fig. 4.51 Reverse model tracking showing the possible source locations (small circles) for a spat collection site within the modern scallop beds (marked by the crossed circle) over the 28 day period from January 1, 1988.

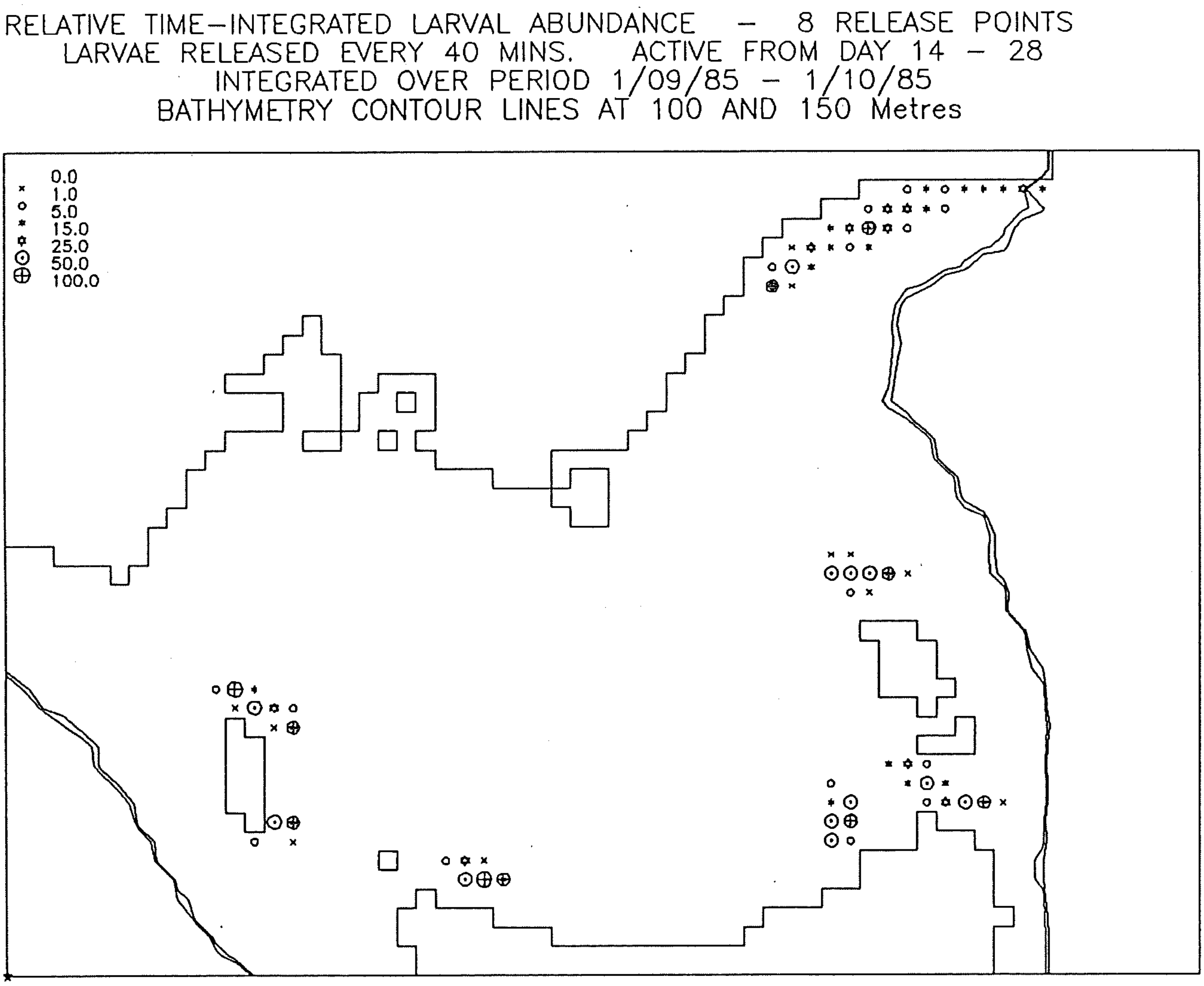

Fig. 4.6a Relative integrated larval abundances over the 14-28 day viable period for larvae released on September 1, 1985 from the 8 modern scallop beds. The abundances are scaled as a percentage of the maximum abundance.

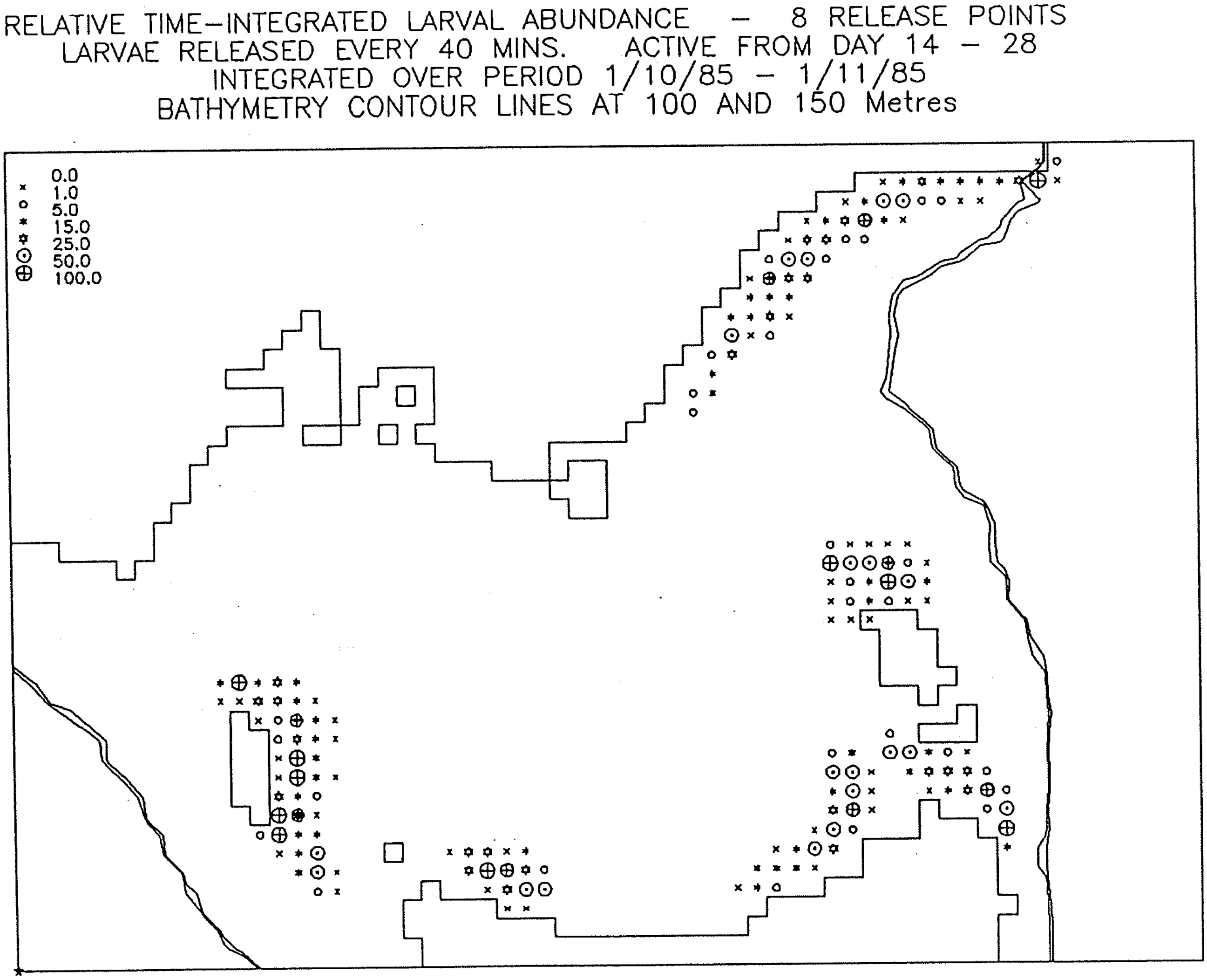

Fig. 4.6b Relative integrated larval abundances over the 14-28 day viable period for larvae released on October 1, 1985 from the 8 modern scallop beds. The abundances are scaled as a percentage of the maximum abundance.

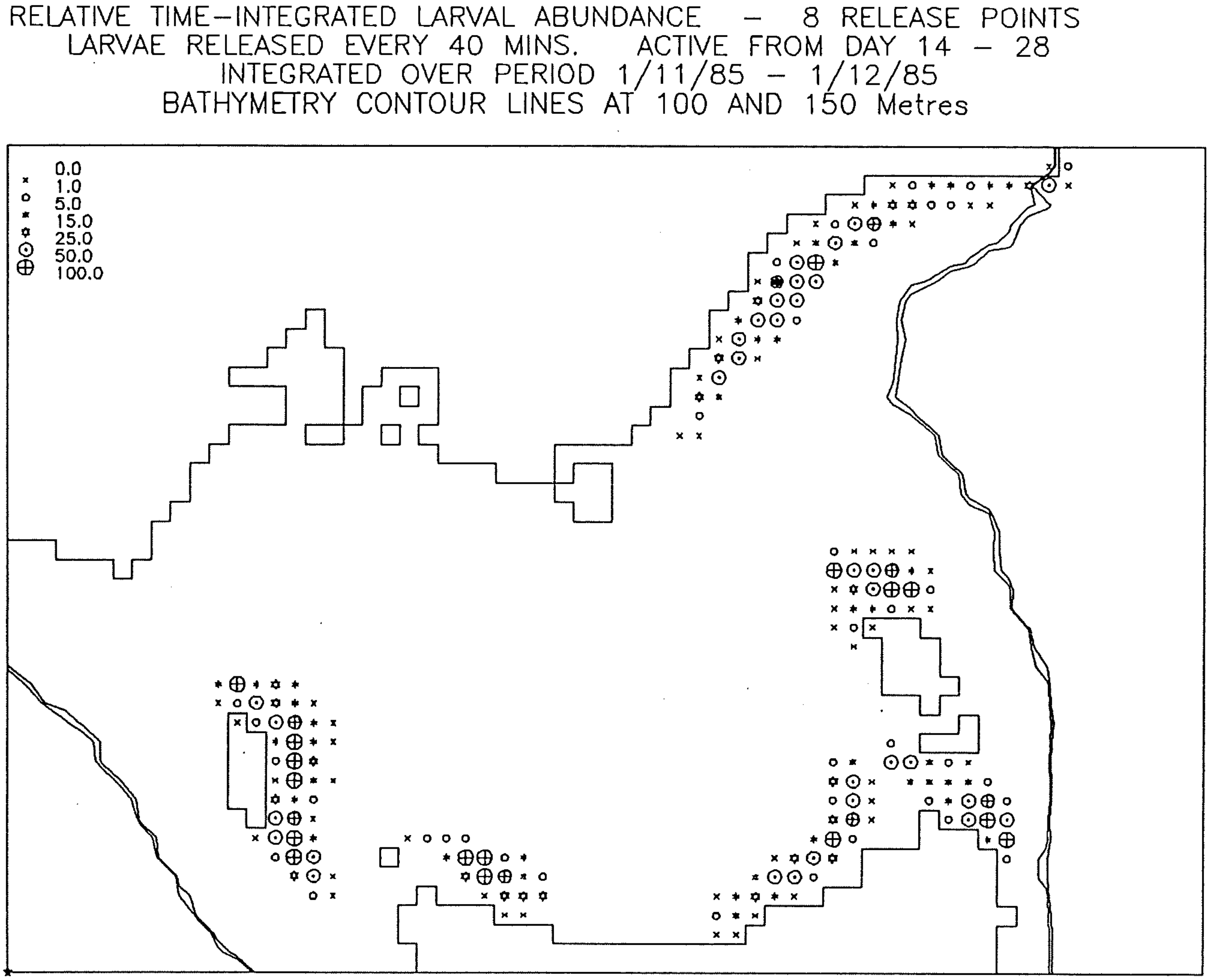

Fig. 4.6c Relative integrated larval abundances over the 14-28 day viable period for larvae released on November 1, 1985 from the 8 modern scallop beds. The abundances are scaled as a percentage of the maximum abundance.

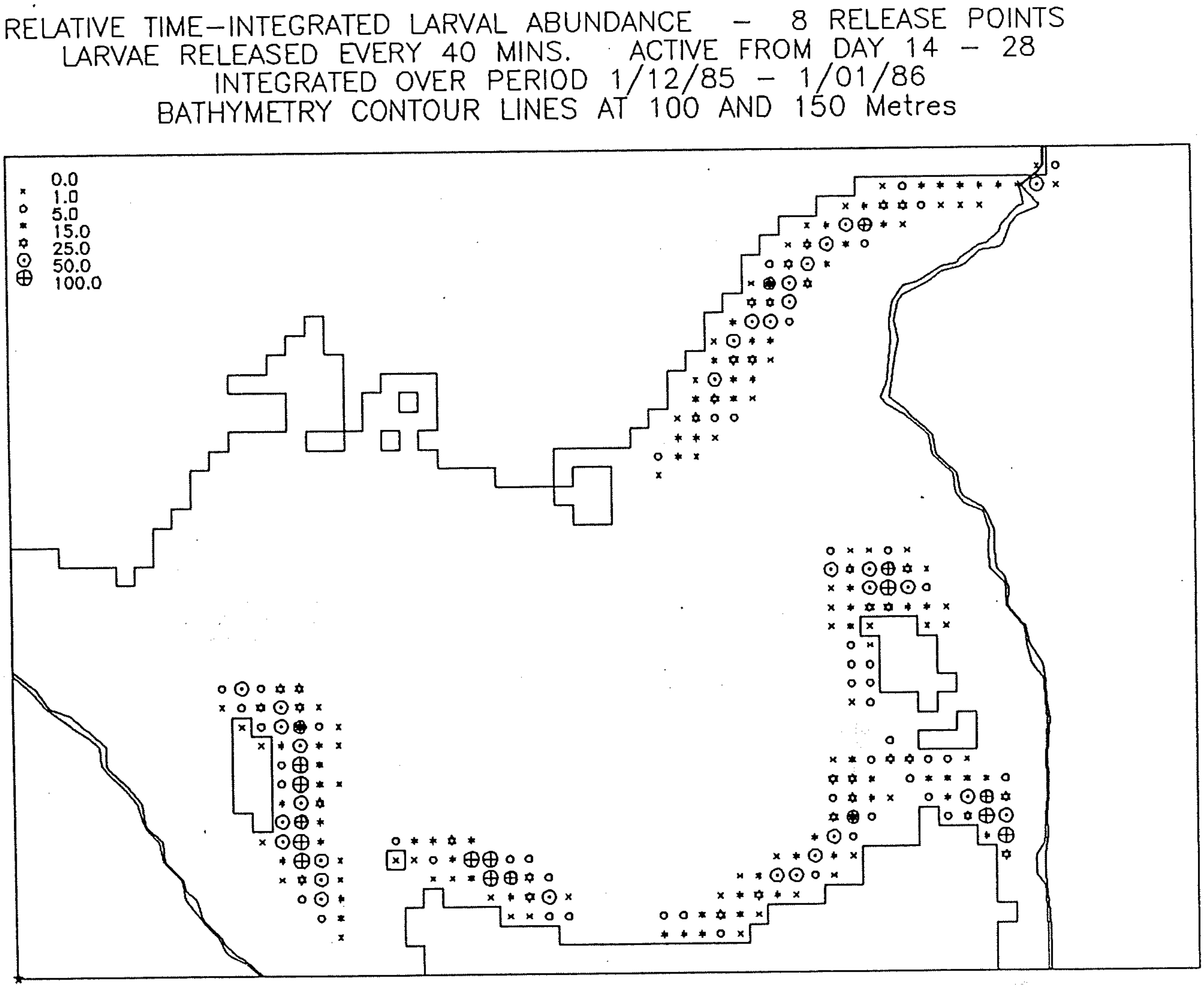

Fig. 4.6d Relative integrated larval abundances over the 14-28 day viable period for larvae released on December 1, 1985 from the 8 modern scallop beds. The abundances are scaled as a percentage of the maximum abundance.

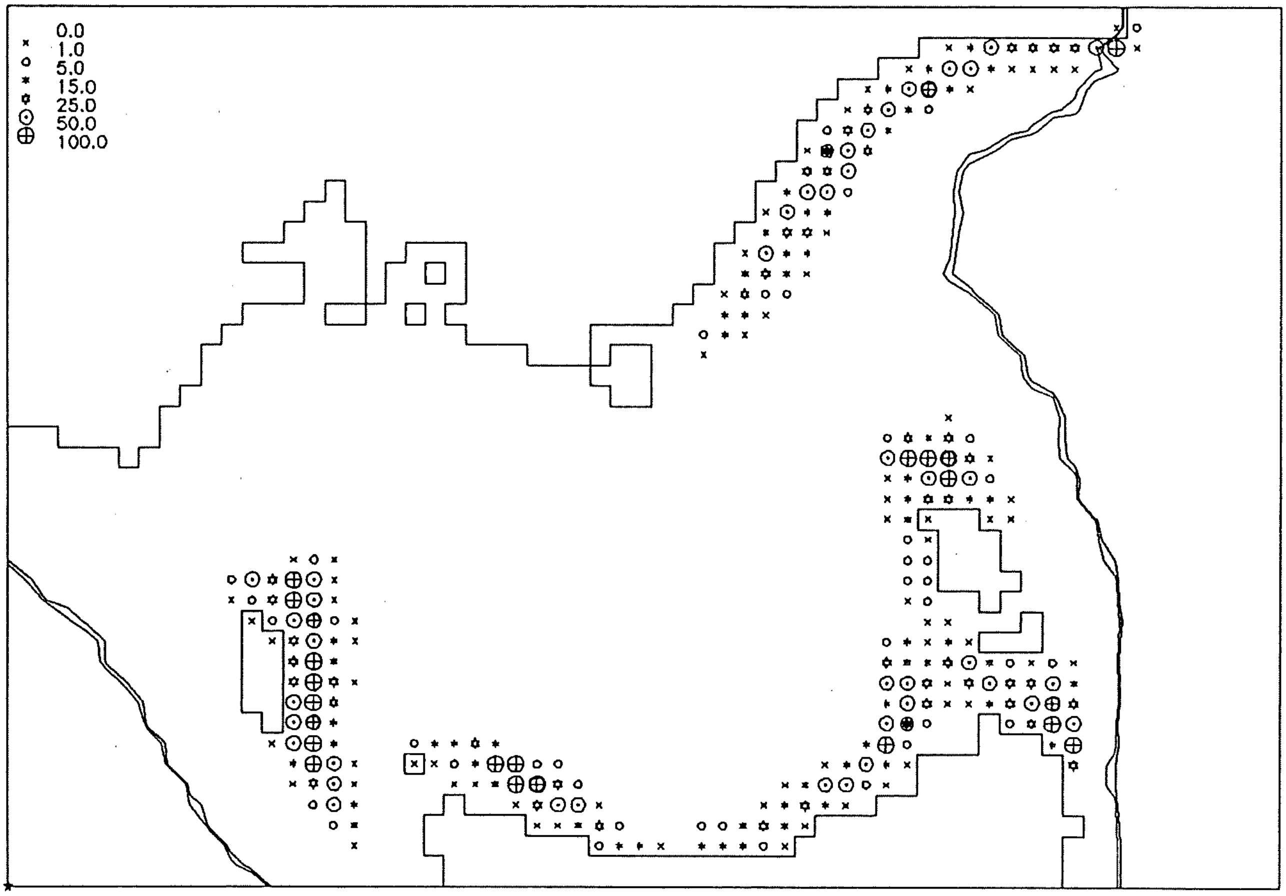
RELATIVE TIME-INTEGRATED LARVAL ABUNDANCE - 8 RELEASE POINTS
LARVAE RELEASED EVERY 40 MINS. ACTIVE FROM DAY 14 - 28
INTEGRATED OVER PERIOD 1/01/86 - 1/02/86
BATHYMETRY CONTOUR LINES AT 100 AND 150 Metres

Fig. 4.6e Relative integrated larval abundances over the 14-28 day viable period for larvae released on January 1, 1986 from the 8 modern scallop beds. The abundances are scaled as a percentage of the maximum abundance.

RELATIVE TIME-INTEGRATED LARVAL ABUNDANCE – 8 RELEASE POINTS
LARVAE RELEASED EVERY 40 MINS. ACTIVE FROM DAY 14 – 28
INTEGRATED OVER PERIOD 1/02/86 – 1/03/86
BATHYMETRY CONTOUR LINES AT 100 AND 150 Metres

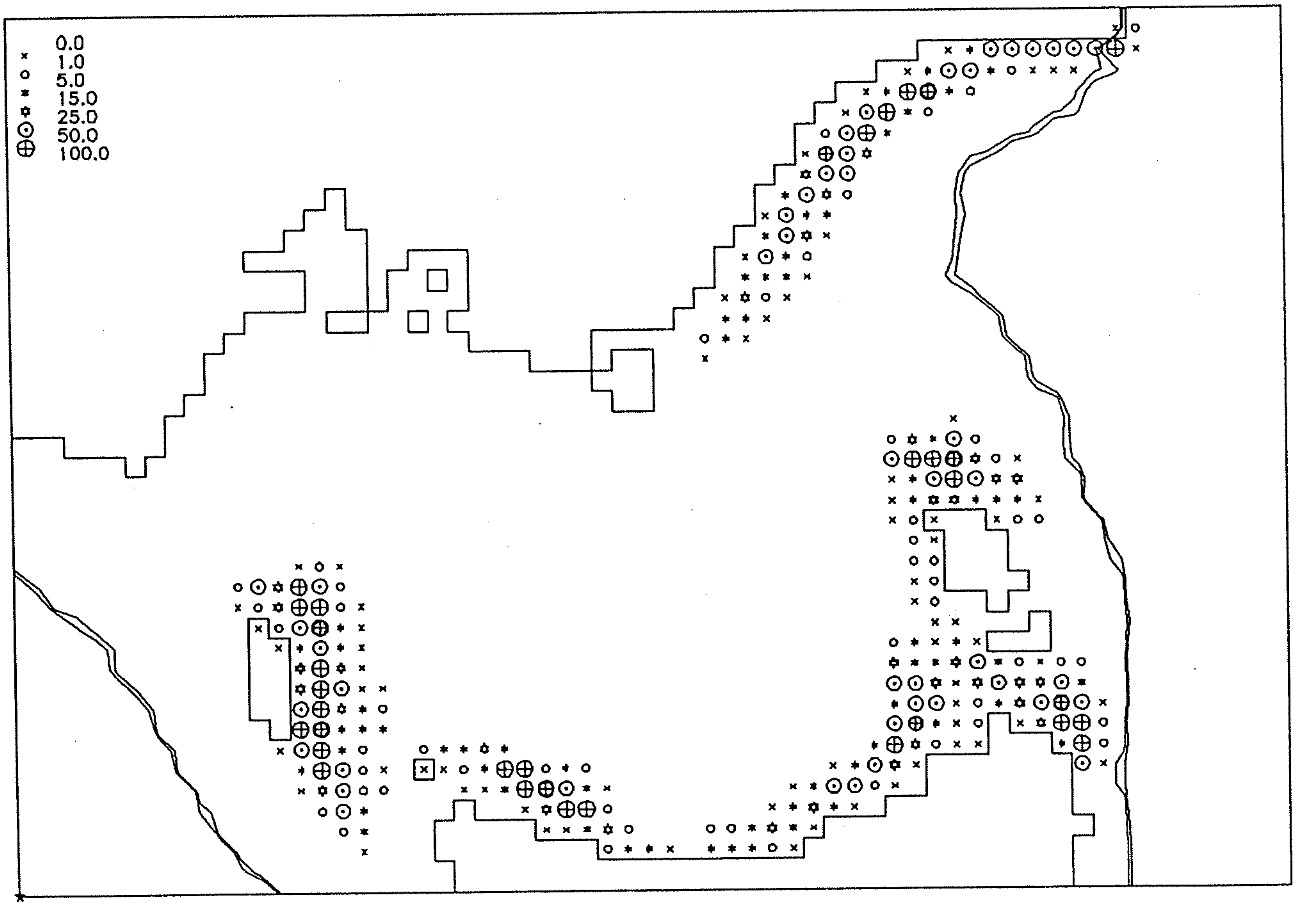

Fig. 4.6f Relative integrated larval abundances over the 14-28 day viable period for larvae released on February 1, 1986 from the 8 modern scallop beds. The abundances are scaled as a percentage of the maximum abundance.

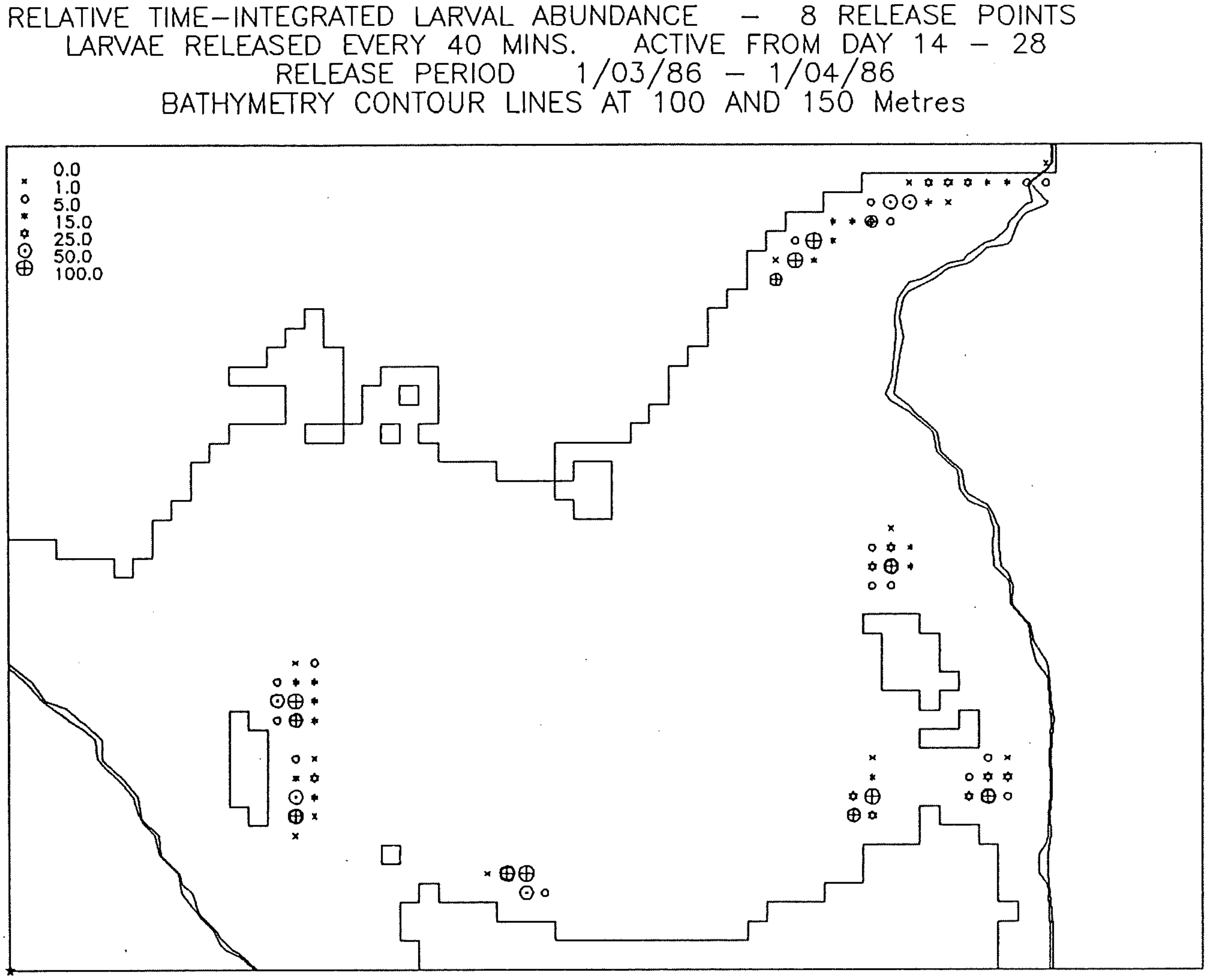

RELATIVE TIME-INTEGRATED LARVAL ABUNDANCE – 8 RELEASE POINTS
LARVAE RELEASED EVERY 40 MINS. ACTIVE FROM DAY 14 – 28
RELEASE PERIOD 1/03/86 – 1/04/86
BATHYMETRY CONTOUR LINES AT 100 AND 150 Metres

Fig. 4.6g Relative integrated larval abundances over the 14-28 day viable period for larvae released on March 1, 1986 from the 8 modern scallop beds. The abundances are scaled as a percentage of the maximum abundance.

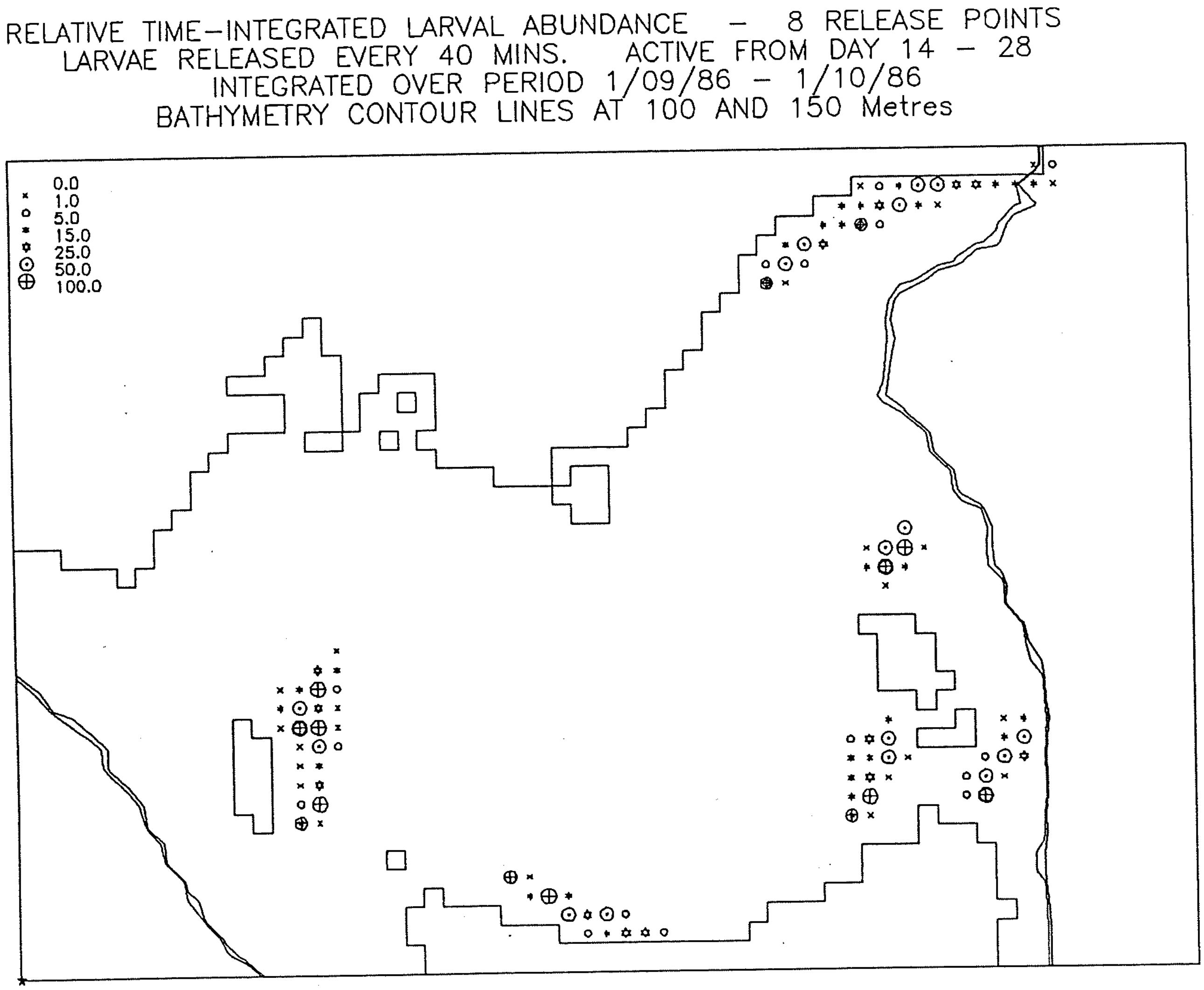

RELATIVE TIME-INTEGRATED LARVAL ABUNDANCE – 8 RELEASE POINTS
LARVAE RELEASED EVERY 40 MINS. ACTIVE FROM DAY 14 – 28
INTEGRATED OVER PERIOD 1/09/86 – 1/10/86
BATHYMETRY CONTOUR LINES AT 100 AND 150 Metres

Fig. 4.6h Relative integrated larval abundances over the 14-28 day viable period for larvae released on September 1, 1986 from the 8 modern scallop beds. The abundances are scaled as a percentage of the maximum abundance.

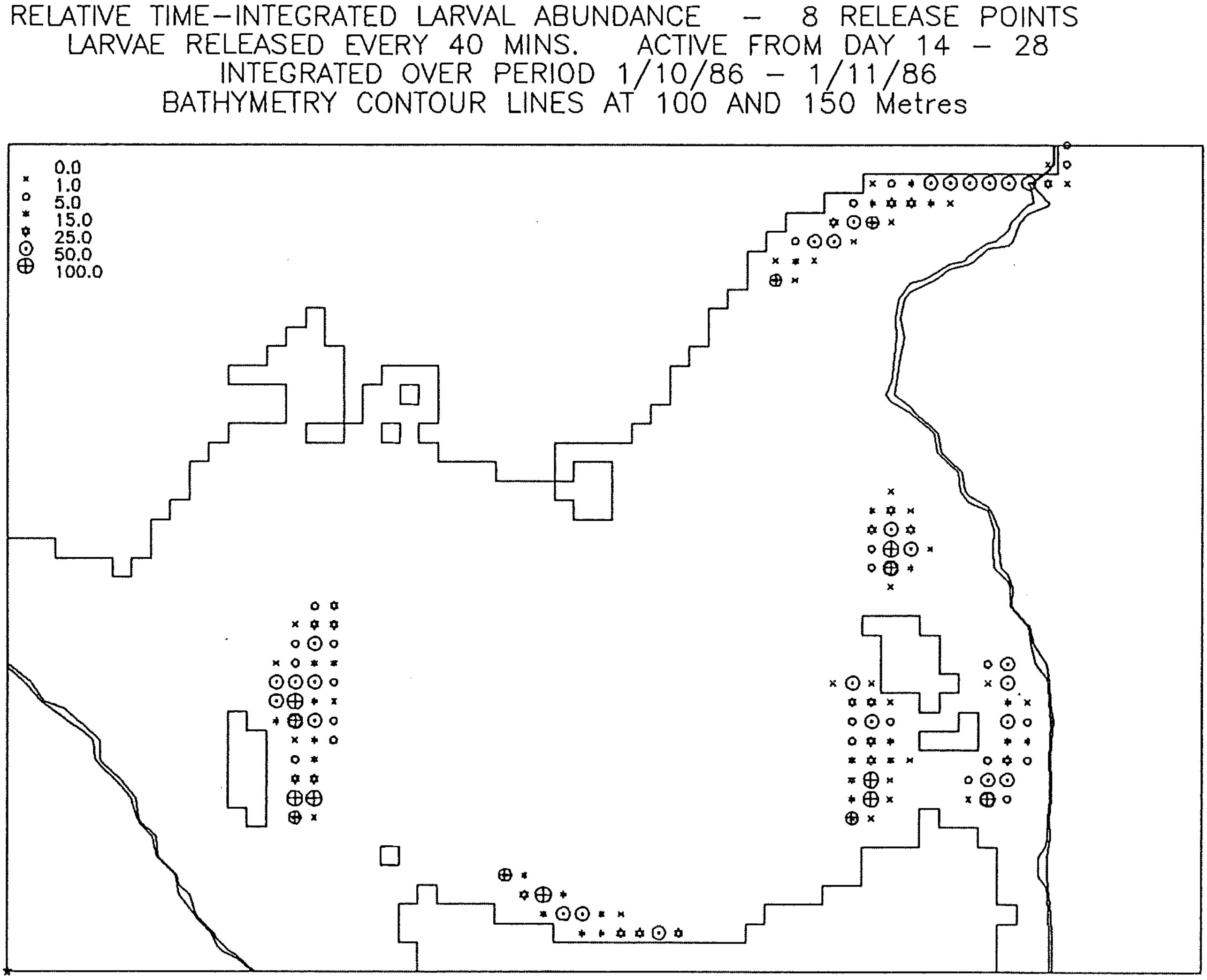

Fig. 4.6i Relative integrated larval abundances over the 14-28 day viable period for larvae released on October 1, 1986 from the 8 modern scallop beds. The abundances are scaled as a percentage of the maximum abundance.

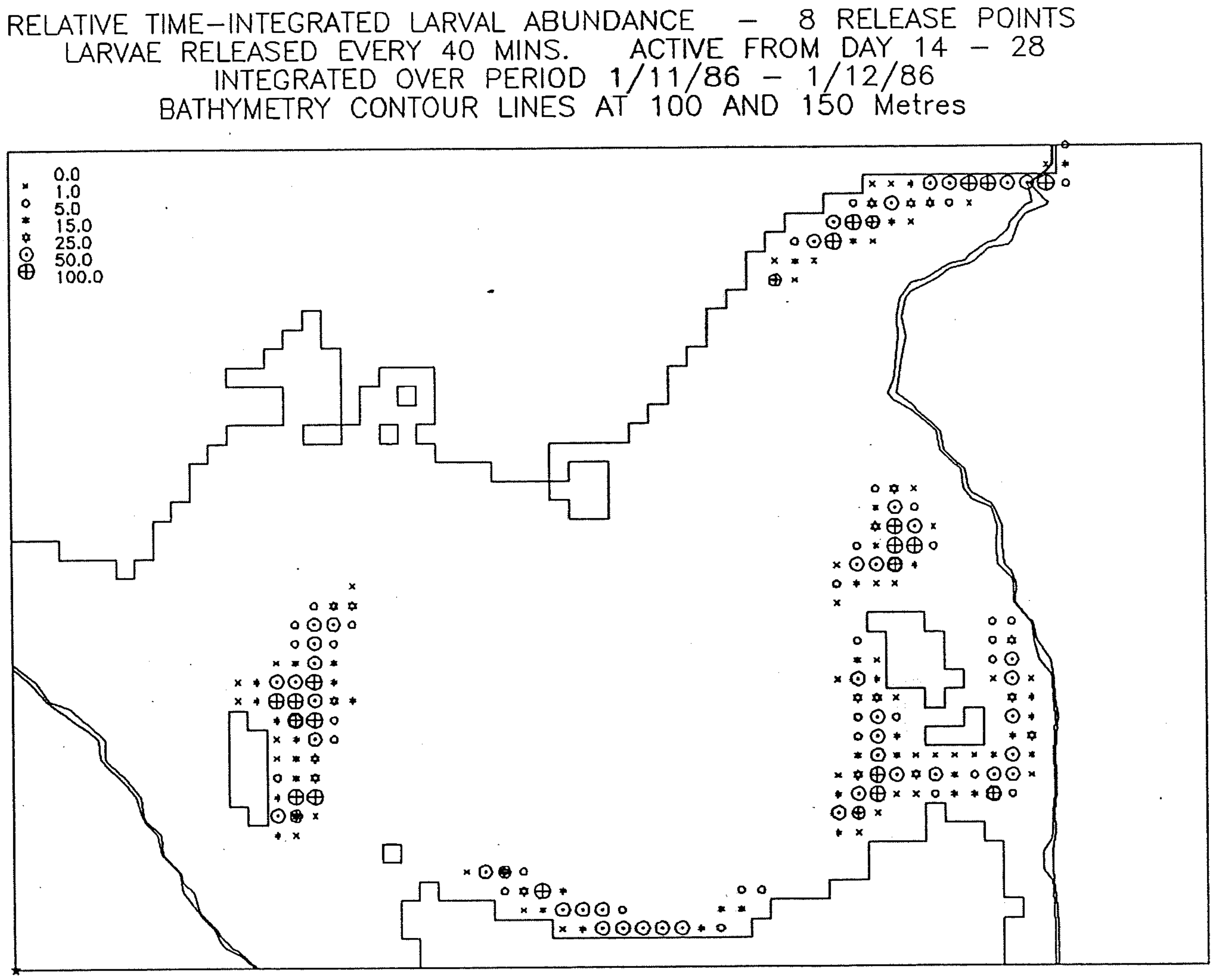

RELATIVE TIME-INTEGRATED LARVAL ABUNDANCE – 8 RELEASE POINTS
LARVAE RELEASED EVERY 40 MINS. ACTIVE FROM DAY 14 – 28
INTEGRATED OVER PERIOD 1/11/86 – 1/12/86
BATHYMETRY CONTOUR LINES AT 100 AND 150 Metres

Fig. 4.6j Relative integrated larval abundances over the 14-28 day viable period for larvae released on November 1, 1986 from the 8 modern scallop beds. The abundances are scaled as a percentage of the maximum abundance.

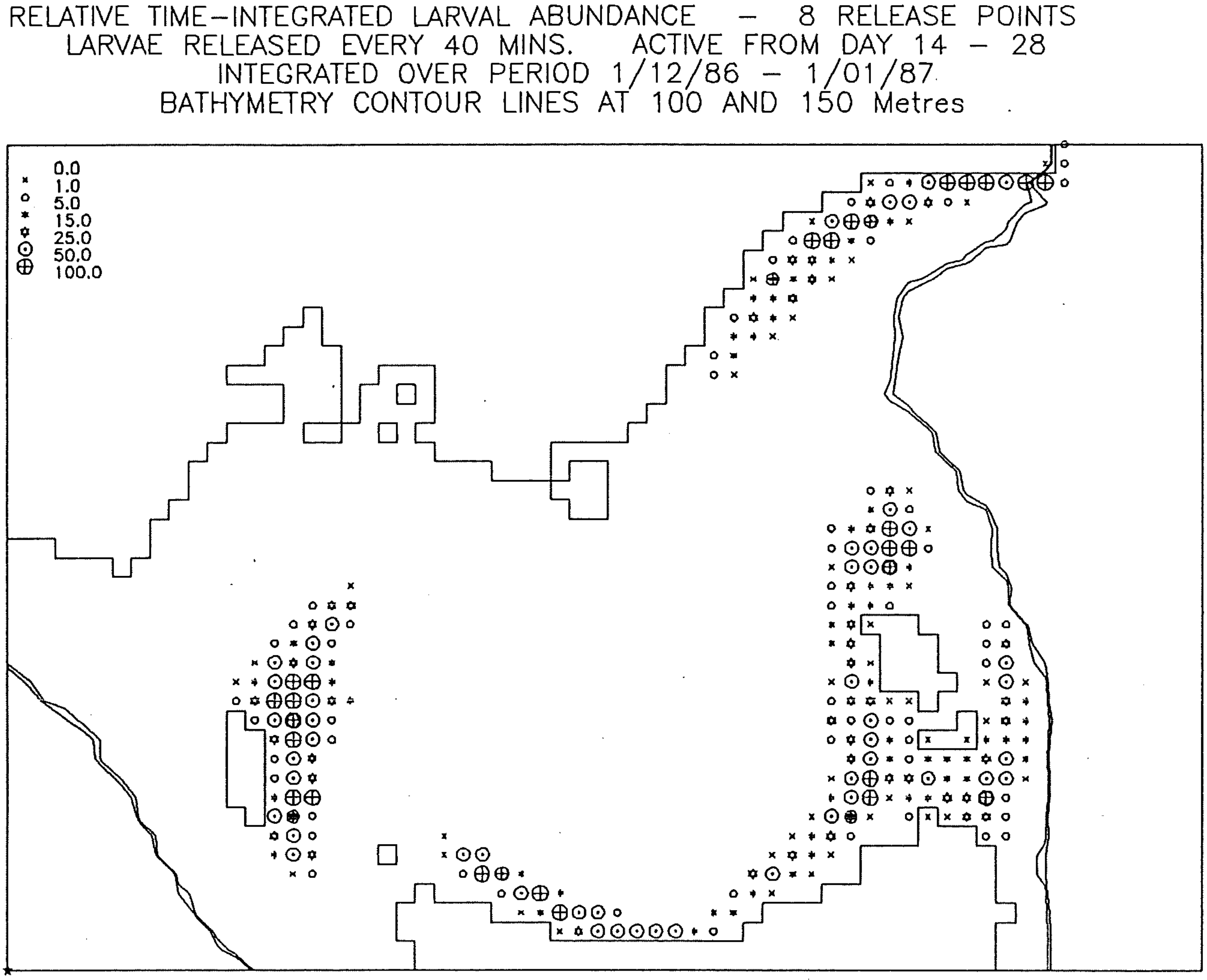

Fig. 4.6k Relative integrated larval abundances over the 14-28 day viable period for larvae released on December 1, 1986 from the 8 modern scallop beds. The abundances are scaled as a percentage of the maximum abundance.

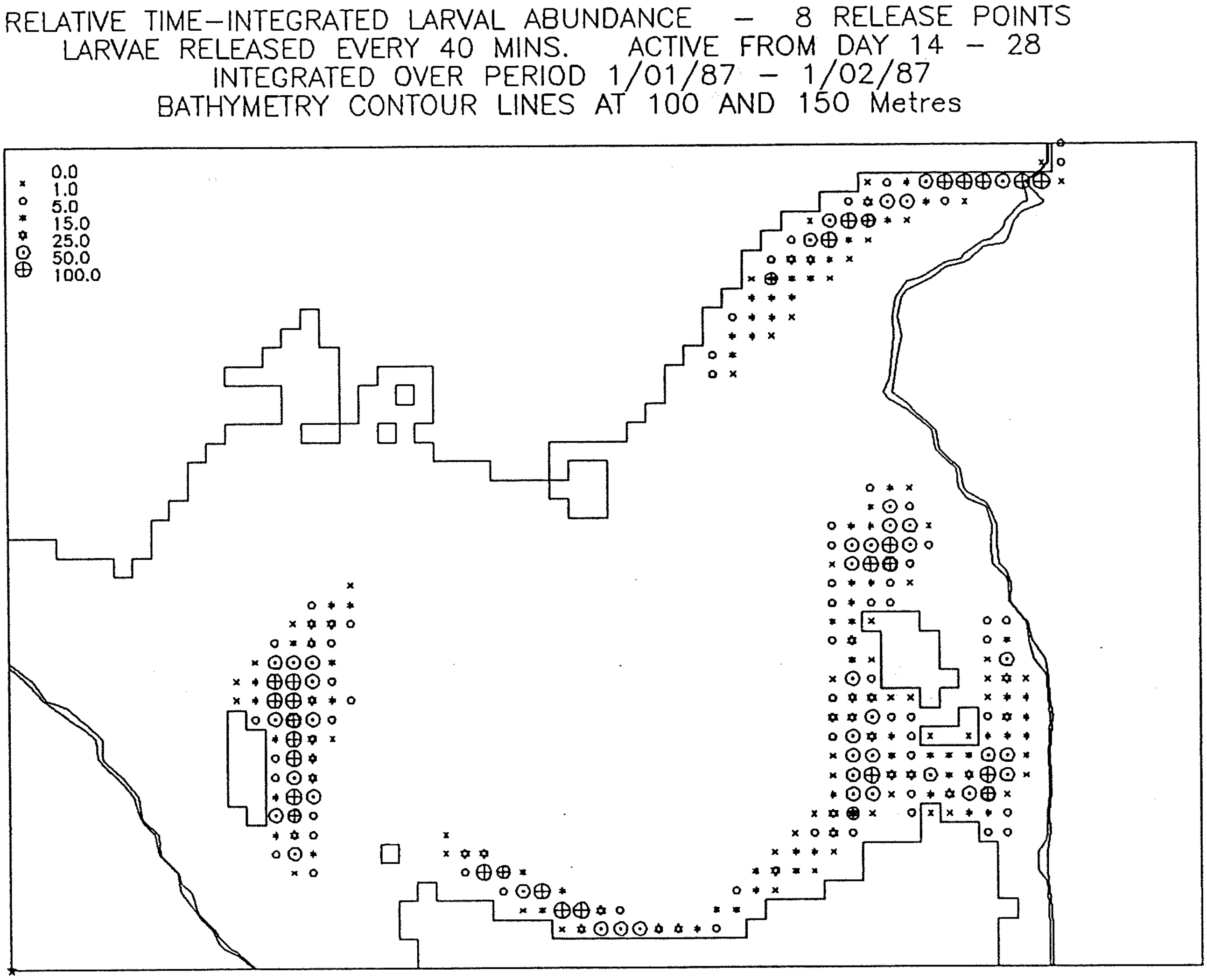

Fig. 4.61 Relative integrated larval abundances over the 14-28 day viable period for larvae released on January 1, 1987 from the 8 modern scallop beds. The abundances are scaled as a percentage of the maximum abundance.

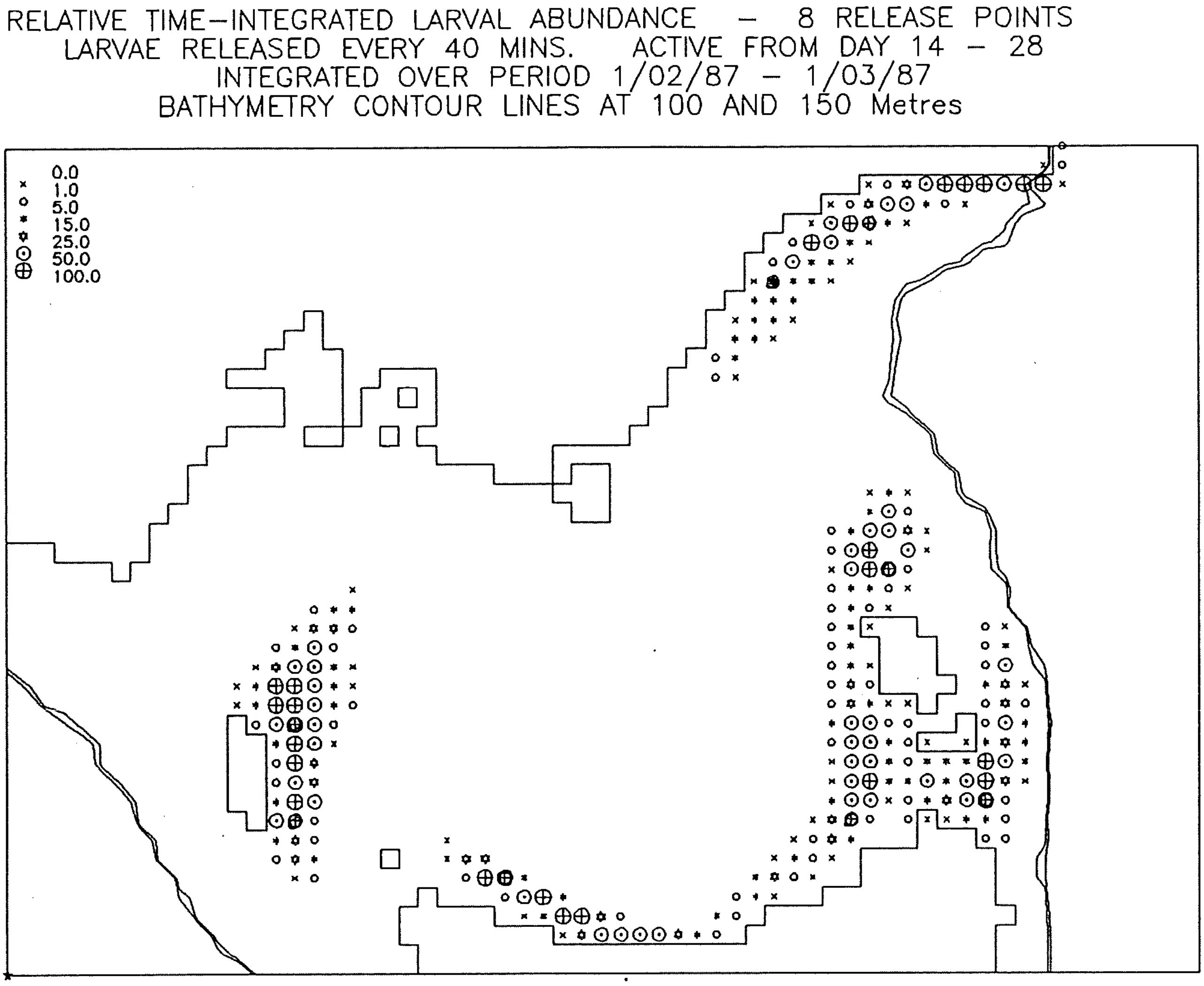

Fig. 4.6m Relative integrated larval abundances over the 14-28 day viable period for larvae released on February 1, 1987 from the 8 modern scallop beds. The abundances are scaled as a percentage of the maximum abundance.

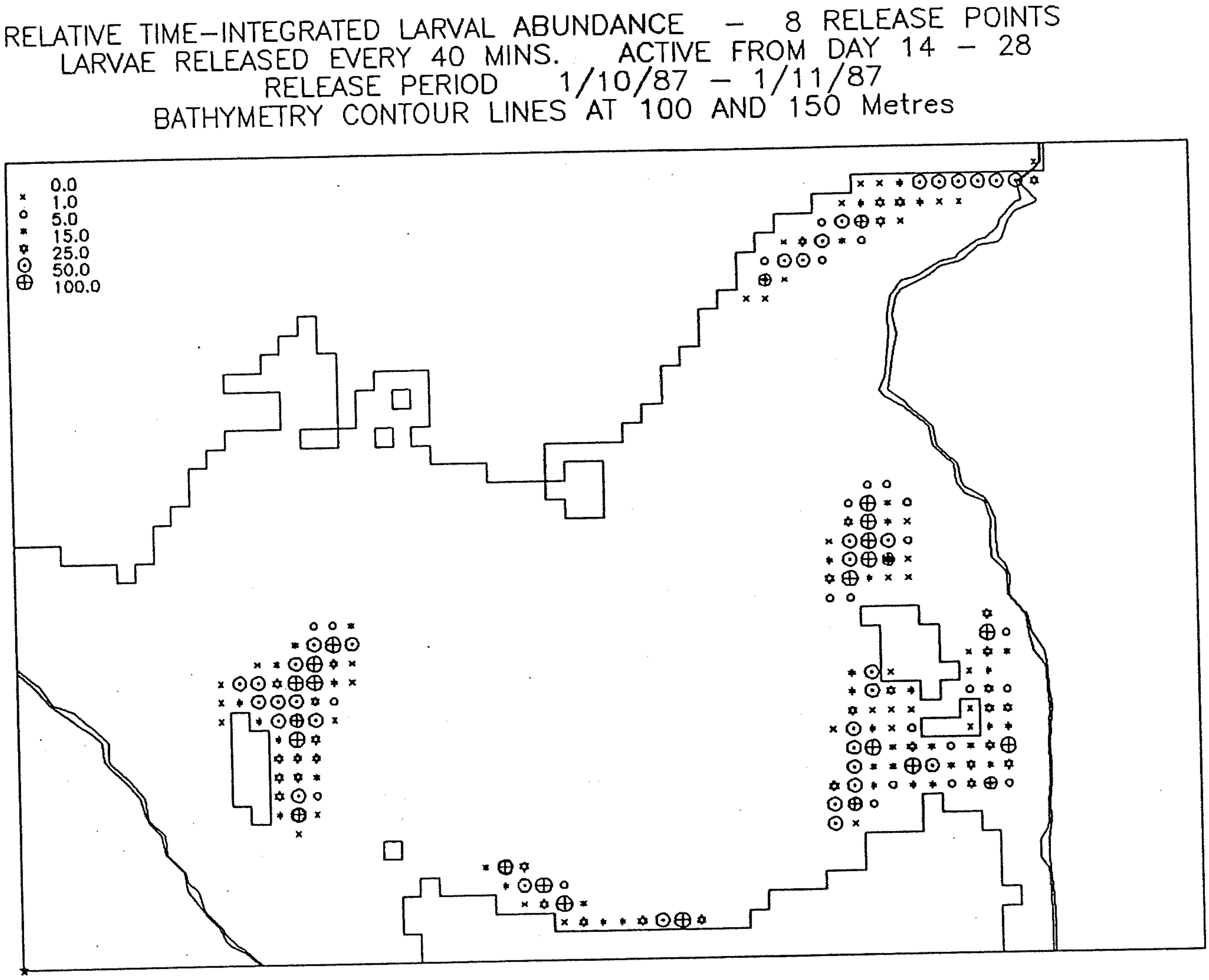

Fig. 4.6n Relative integrated larval abundances over the 14-28 day viable period for larvae released on October 1, 1987 from the 8 modern scallop beds. The abundances are scaled as a percentage of the maximum abundance.

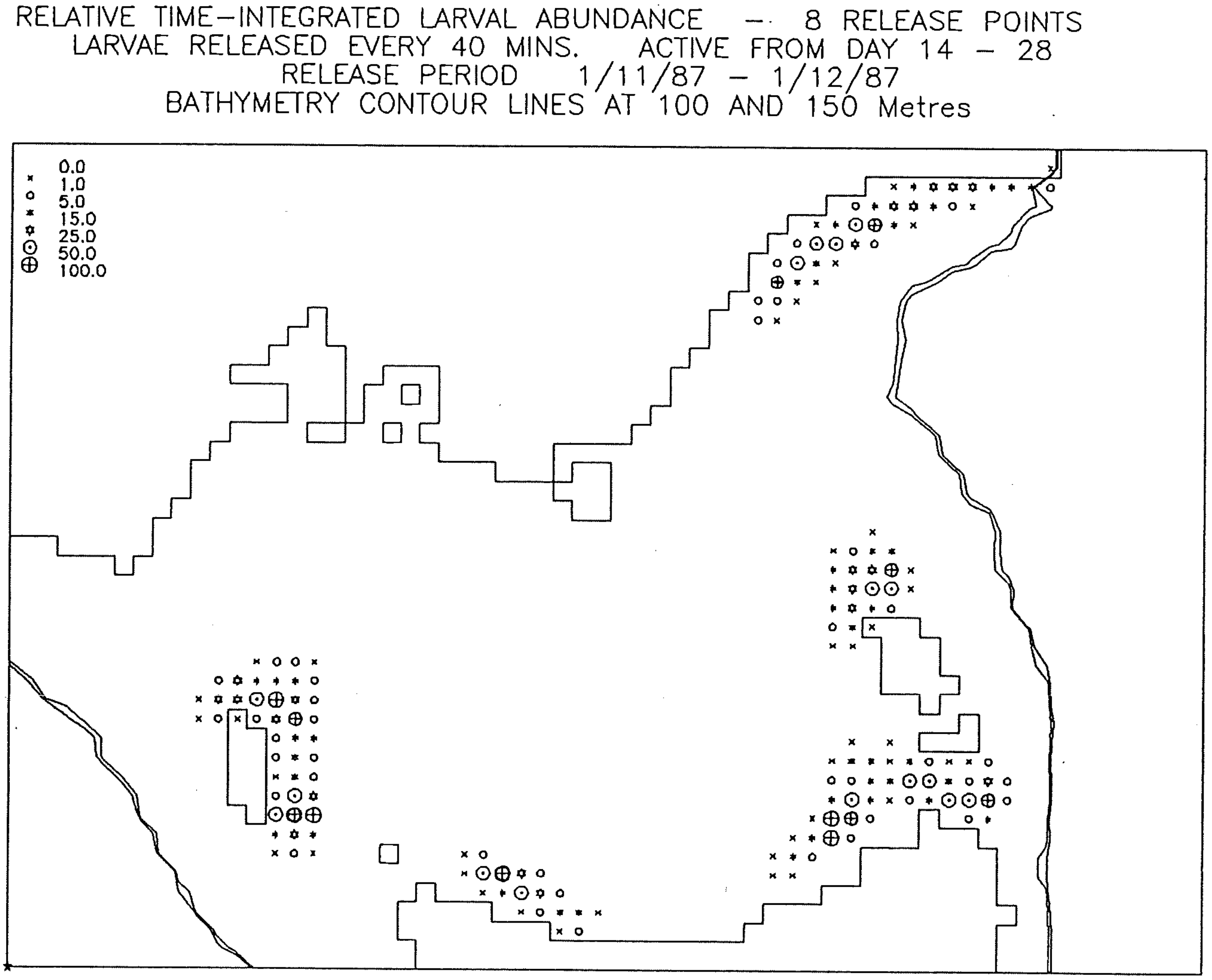

RELATIVE TIME-INTEGRATED LARVAL ABUNDANCE — 8 RELEASE POINTS
LARVAE RELEASED EVERY 40 MINS. ACTIVE FROM DAY 14 - 28
RELEASE PERIOD 1/11/87 - 1/12/87
BATHYMETRY CONTOUR LINES AT 100 AND 150 Metres

Fig. 4.6o Relative integrated larval abundances over the 14-28 day viable period for larvae released on November 1, 1987 from the 8 modern scallop beds. The abundances are scaled as a percentage of the maximum abundance.

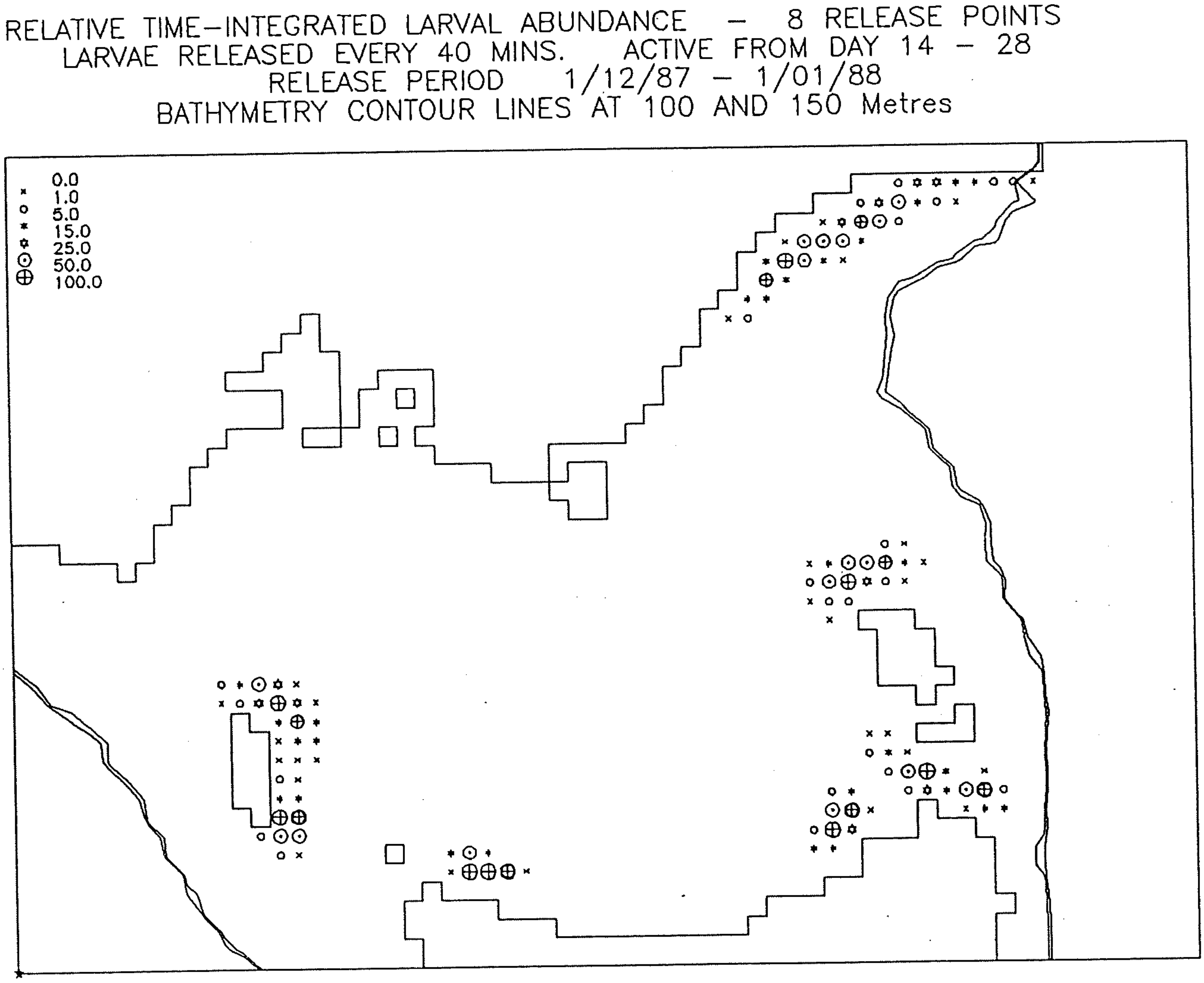

Fig. 4.6p Relative integrated larval abundances over the 14-28 day viable period for larvae released on December 1, 1987 from the 8 modern scallop beds. The abundances are scaled as a percentage of the maximum abundance.

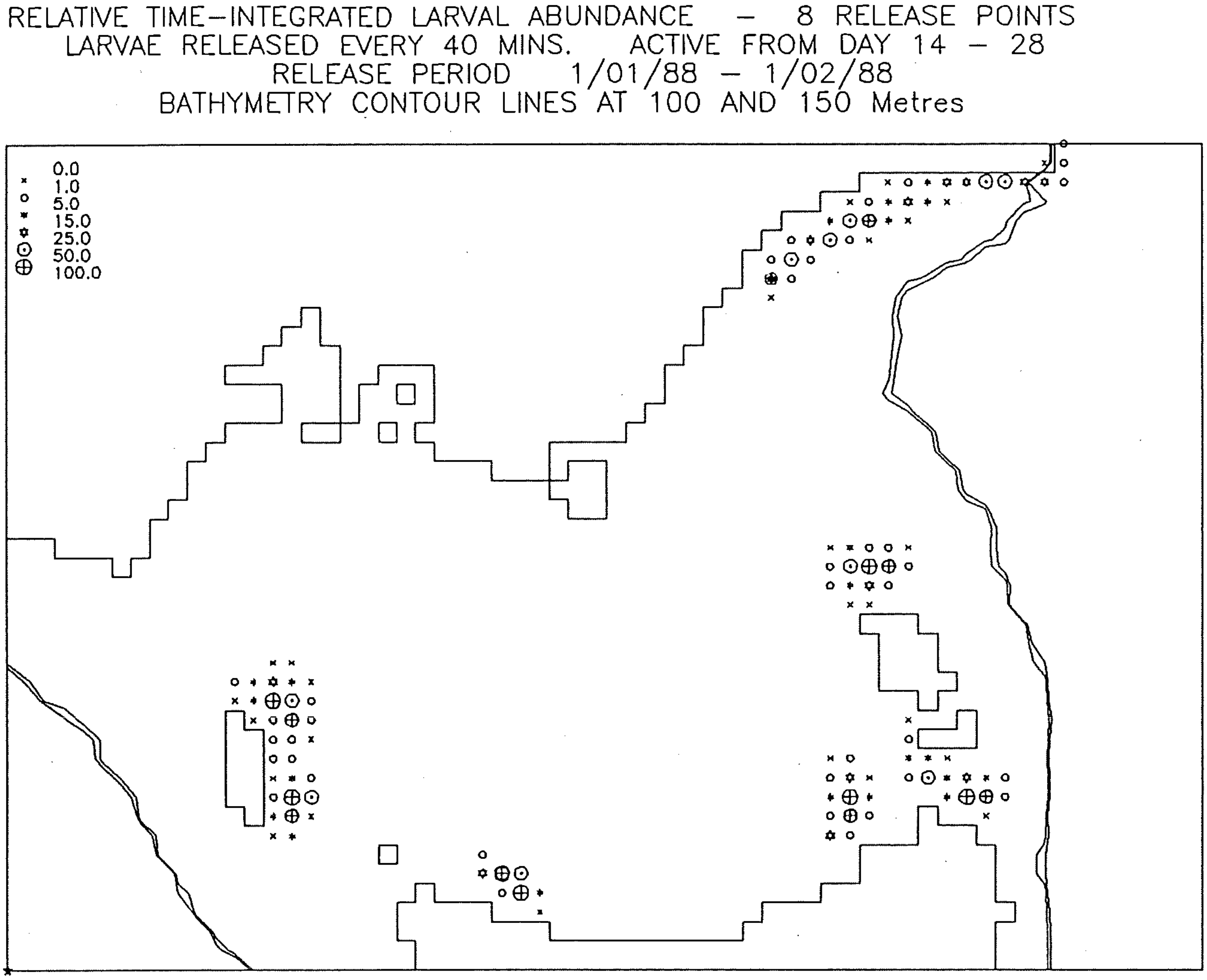

Fig. 4.6q Relative integrated larval abundances over the 14-28 day viable period for larvae released on January 1, 1988 from the 8 modern scallop beds. The abundances are scaled as a percentage of the maximum abundance.

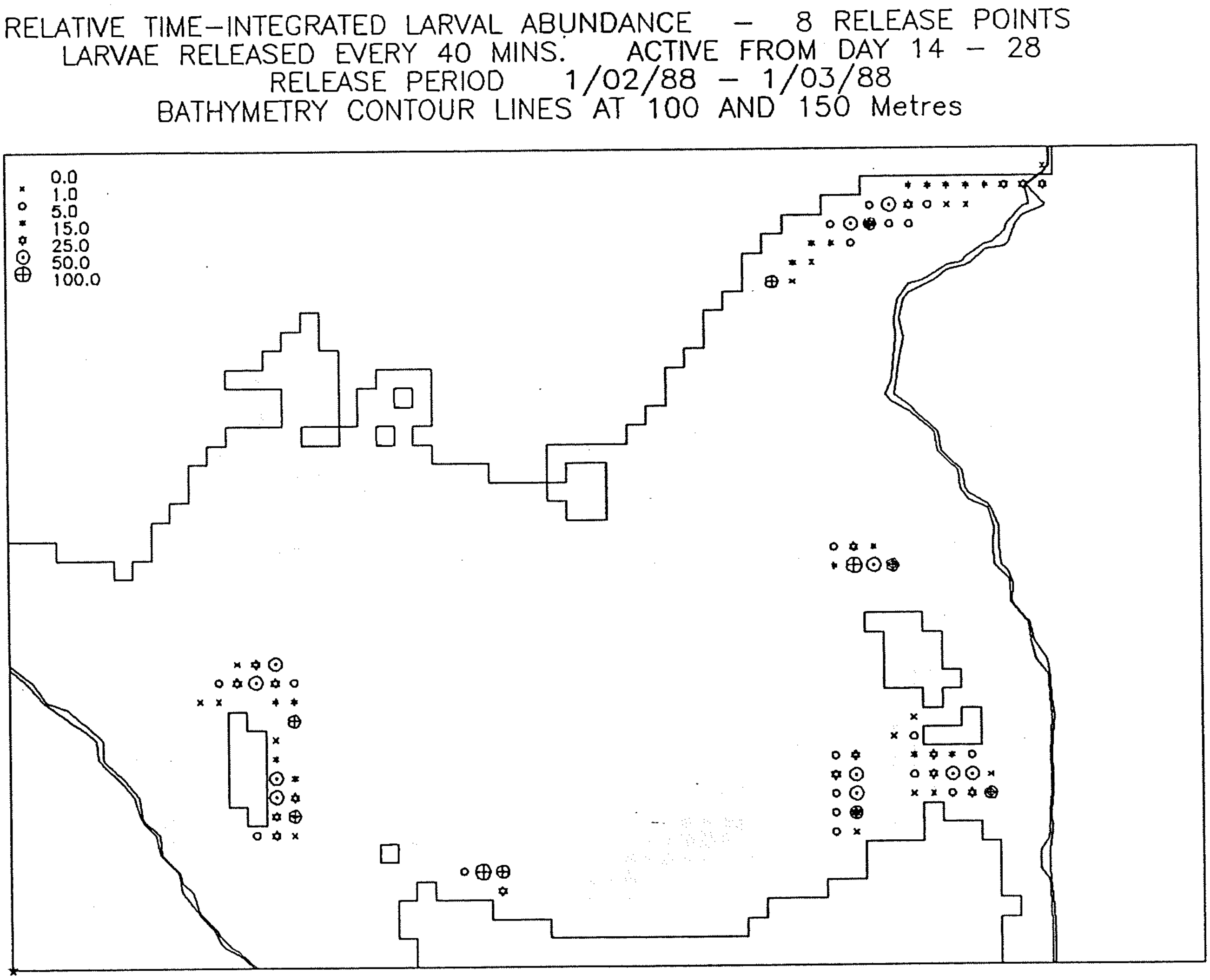

Fig. 4.6r Relative integrated larval abundances over the 14-28 day viable period for larvae released on February 1, 1988 from the 8 modern scallop beds. The abundances are scaled as a percentage of the maximum abundance.

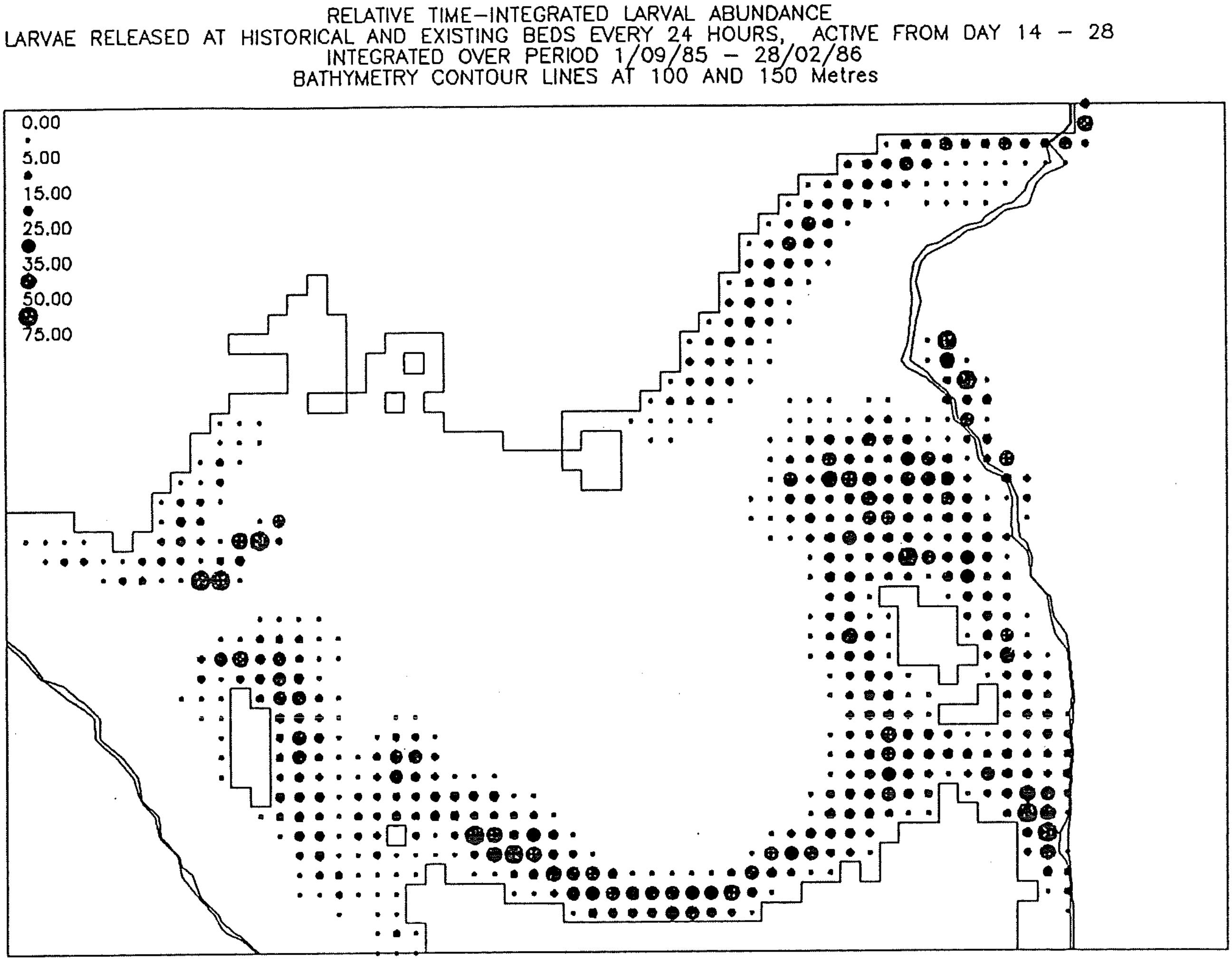

Fig. 4.7a Relative integrated larval abundances over the 14-28 day viable period for larvae released on September 1, 1985 from the modern and historical scallop beds. The abundances are scaled as a percentage of the maximum abundance.

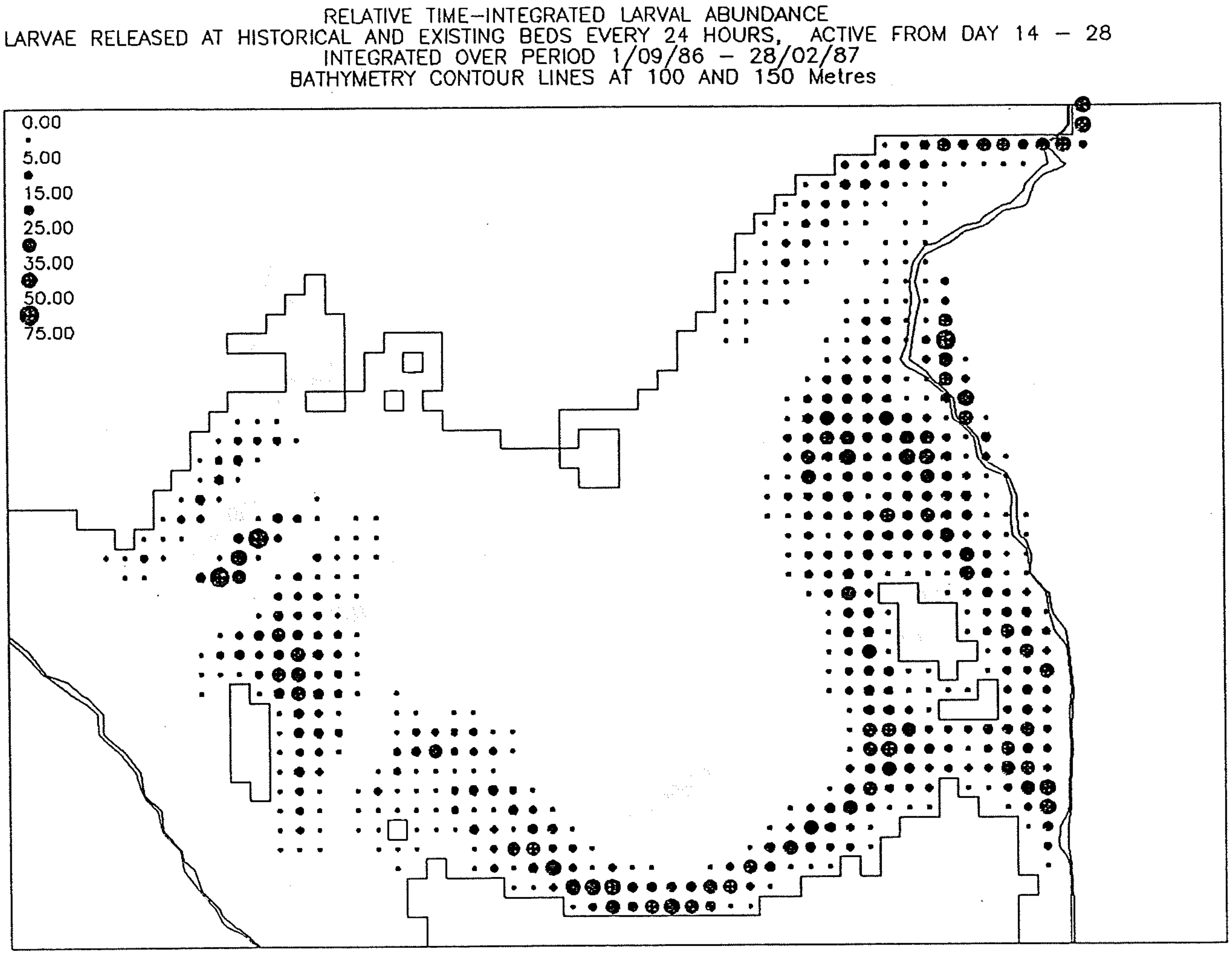

Fig. 4.7b Relative integrated larval abundances over the 14-28 day viable period for larvae released on September 1, 1986 from the modern and historical scallop beds. The abundances are scaled as a percentage of the maximum abundance.

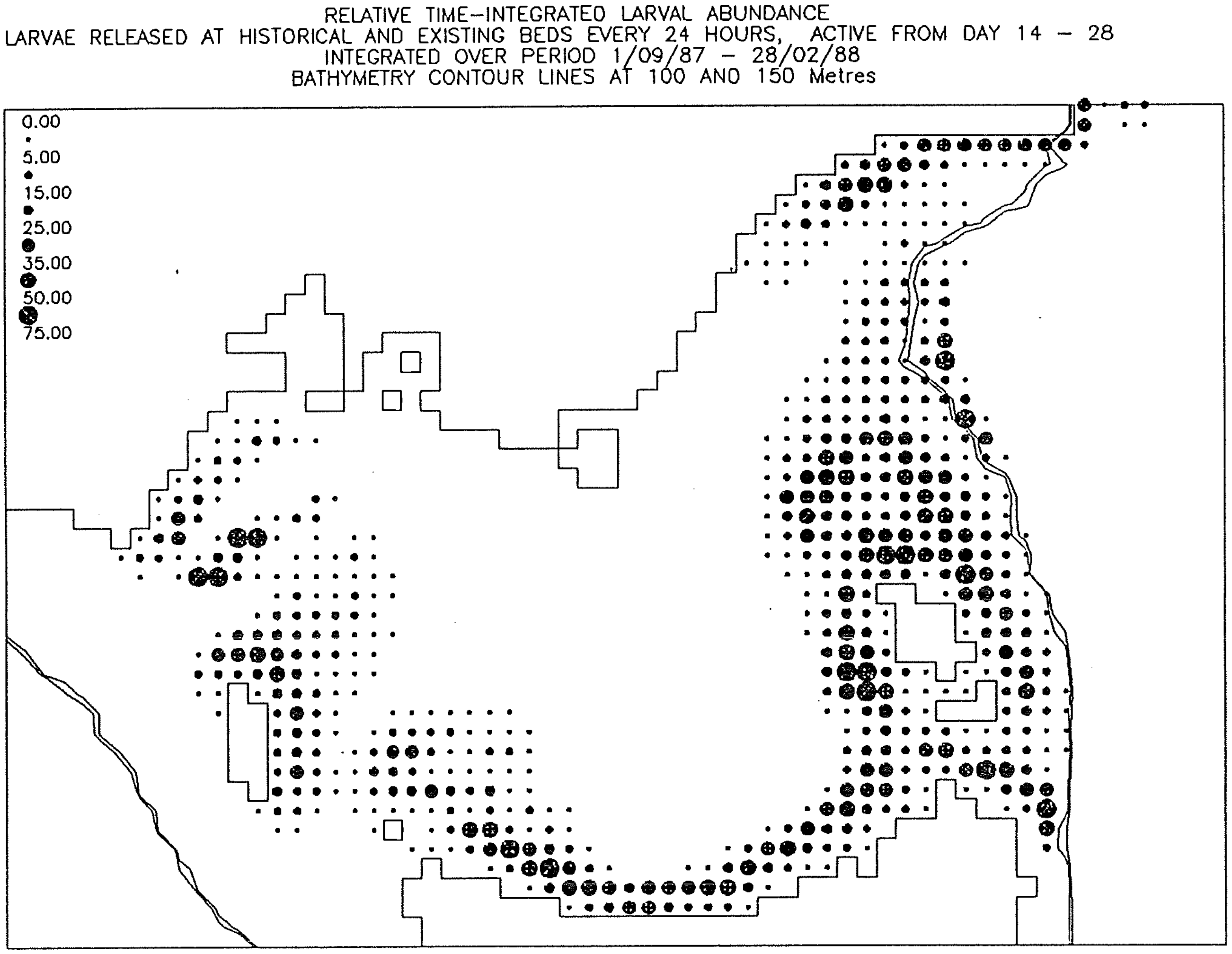

Fig. 4.7c Relative integrated larval abundances over the 14-28 day viable period for larvae released on September 1, 1987 from the modern and historical scallop beds. The abundances are scaled as a percentage of the maximum abundance.

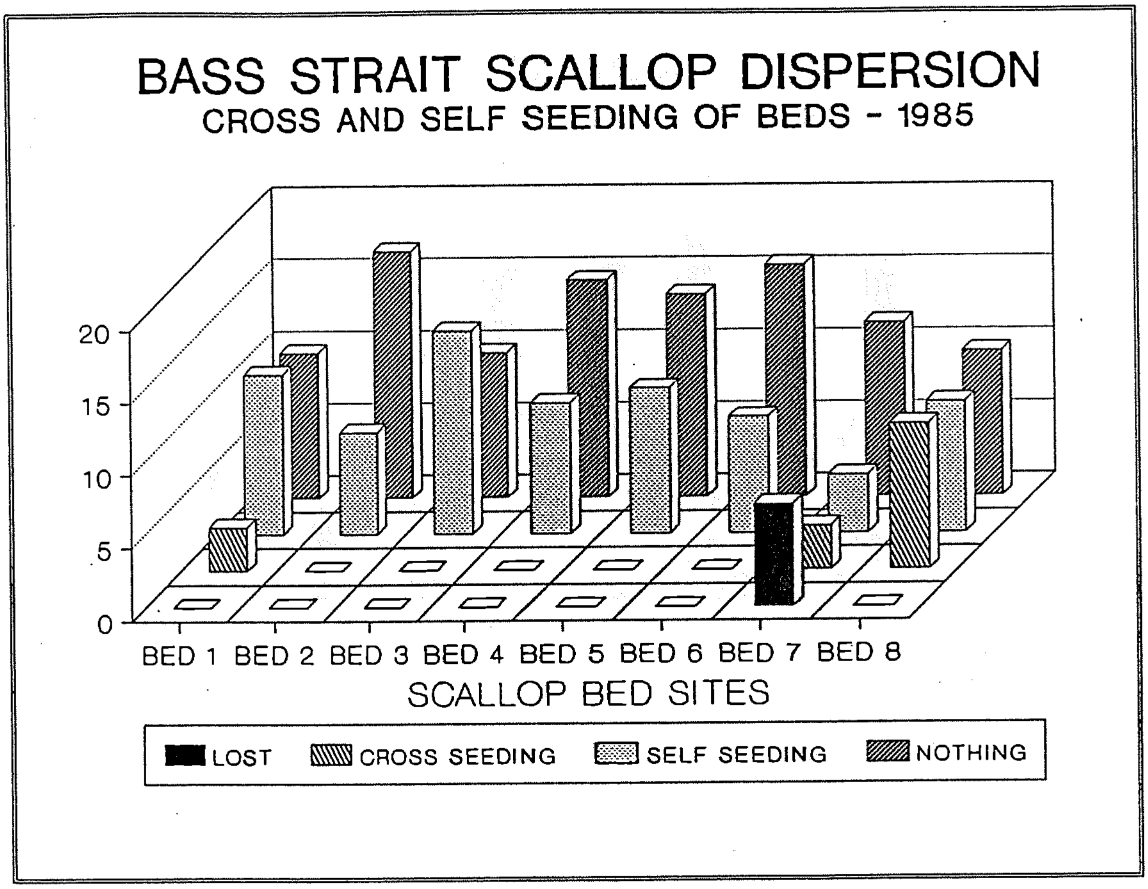

Fig. 4.8a Percentage probabilities for 1985 of larvae being; lost (off the continental shelf), cross-seeding (another known scallop bed), self-seeding (the same bed) or nothing (settling between known beds).

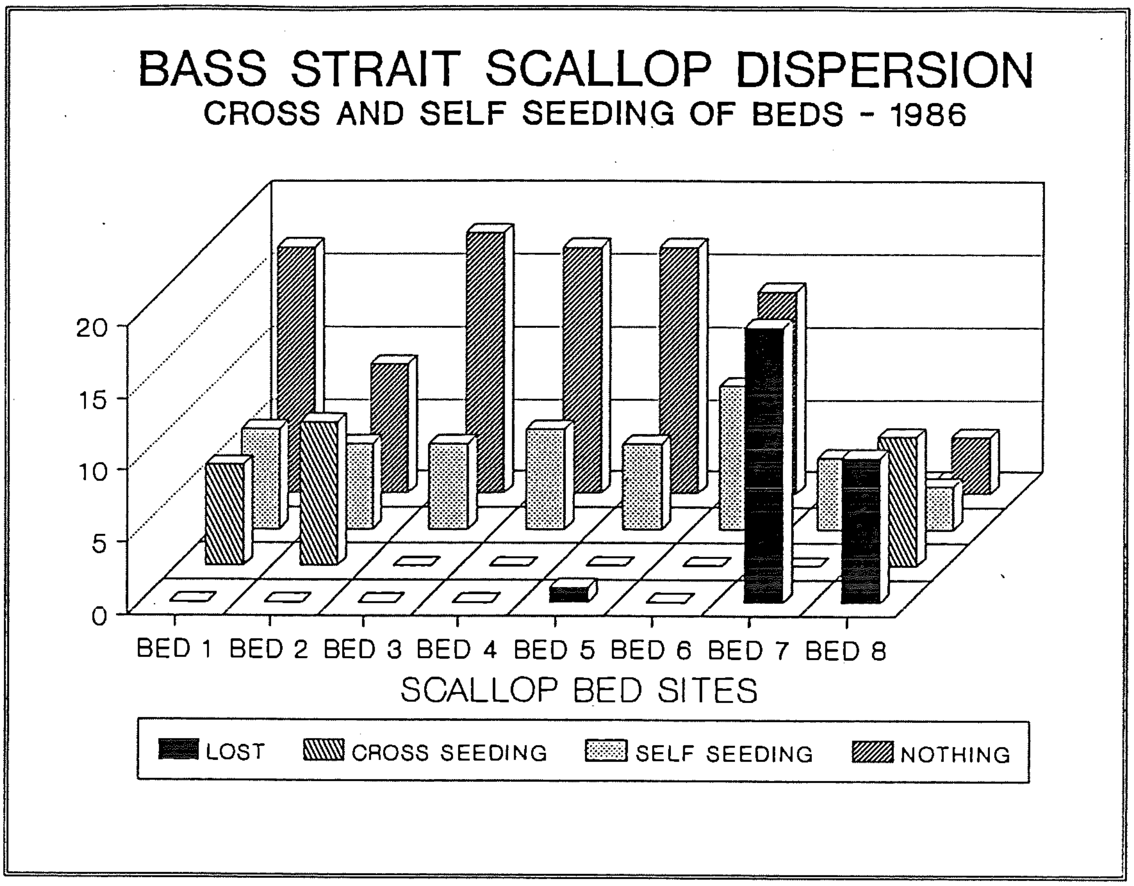

Fig. 4.8b Percentage probabilities for 1986 of larvae being; lost (off the continental shelf), cross-seeding (another known scallop bed), self-seeding (the same bed) or nothing (settling between known beds).

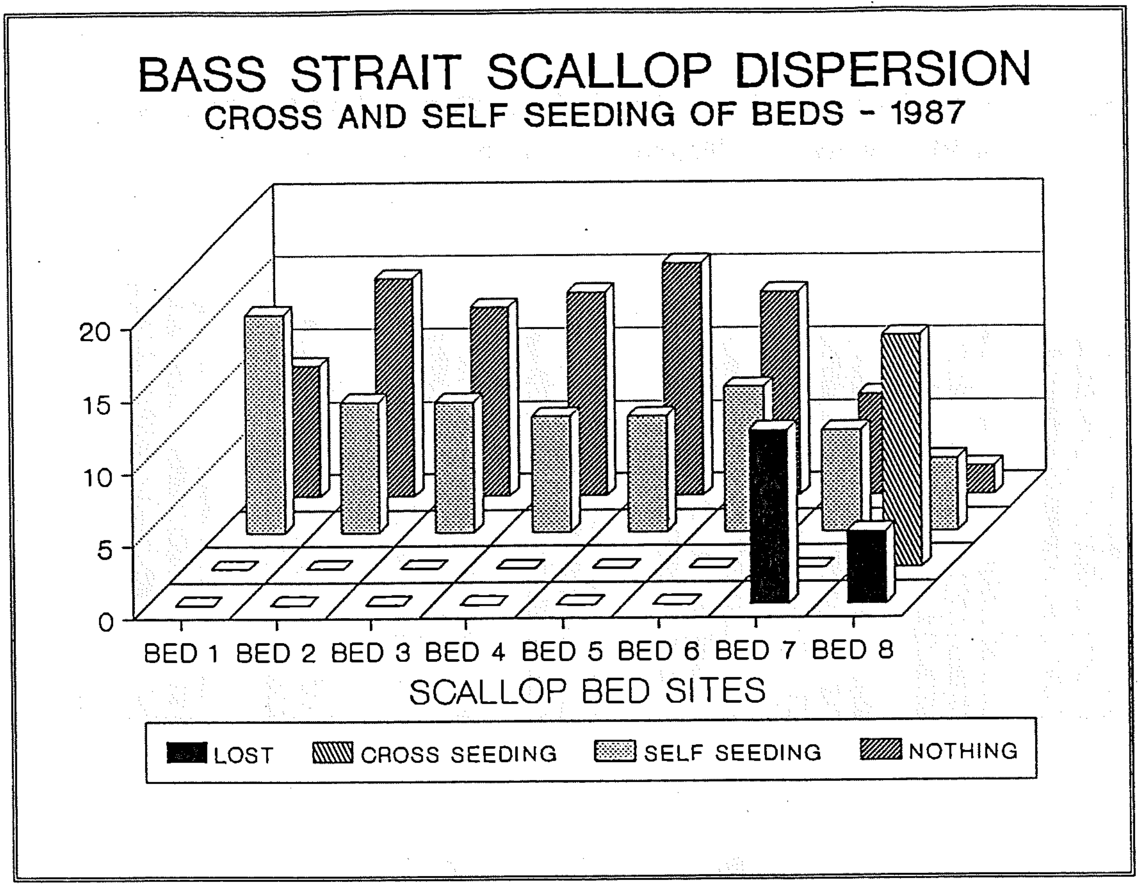

Fig. 4.8c Percentage probabilities for 1987 of larvae being; lost (off the continental shelf), cross-seeding (another known scallop bed), self-seeding (the same bed) or nothing (settling between known beds).

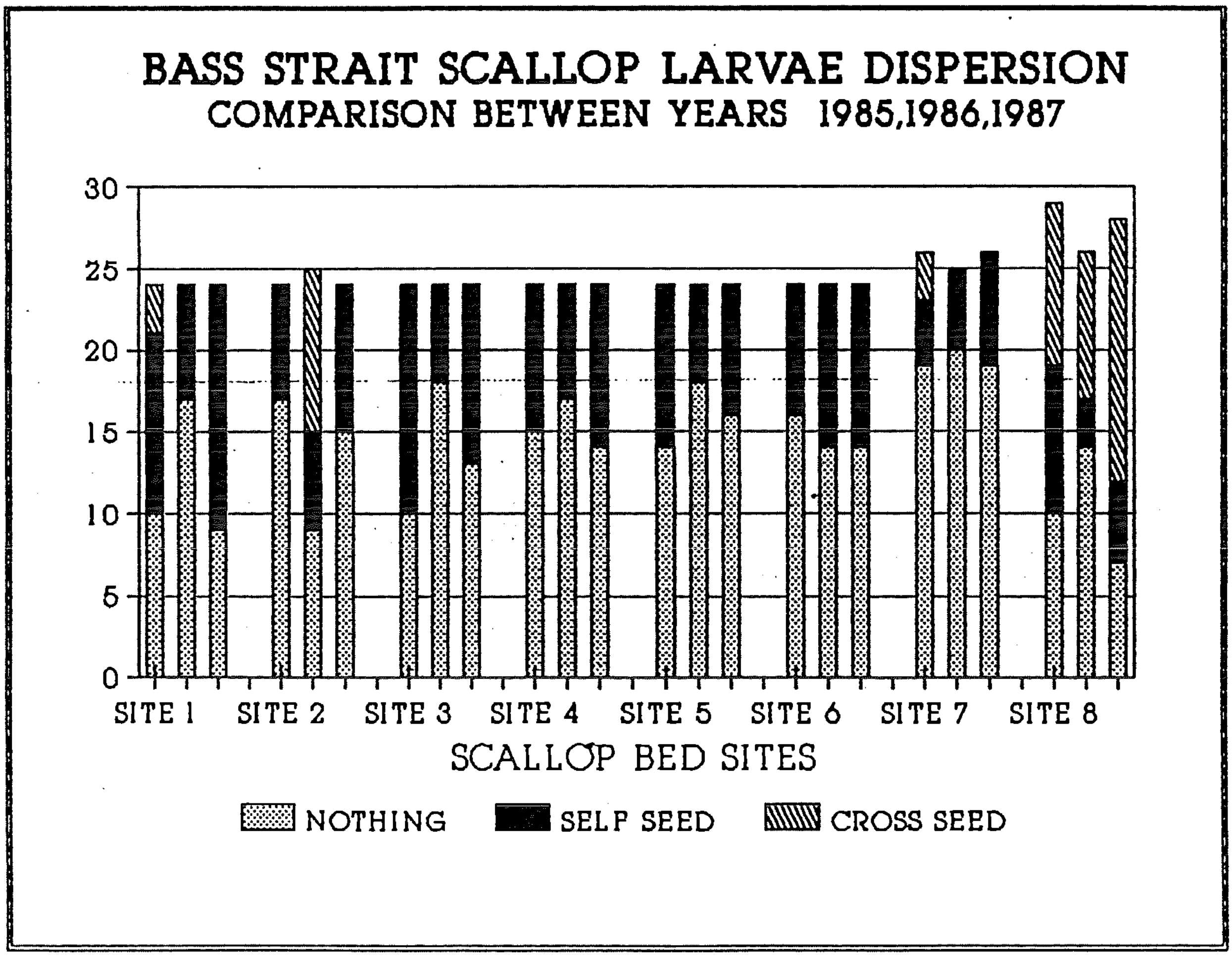

Fig. 4.8d Percentage probabilities comparing the years 1985, 1986 and 1987 of larvae cross-seeding (another known scallop bed), self-seeding (the same bed) or nothing (settling between known beds).

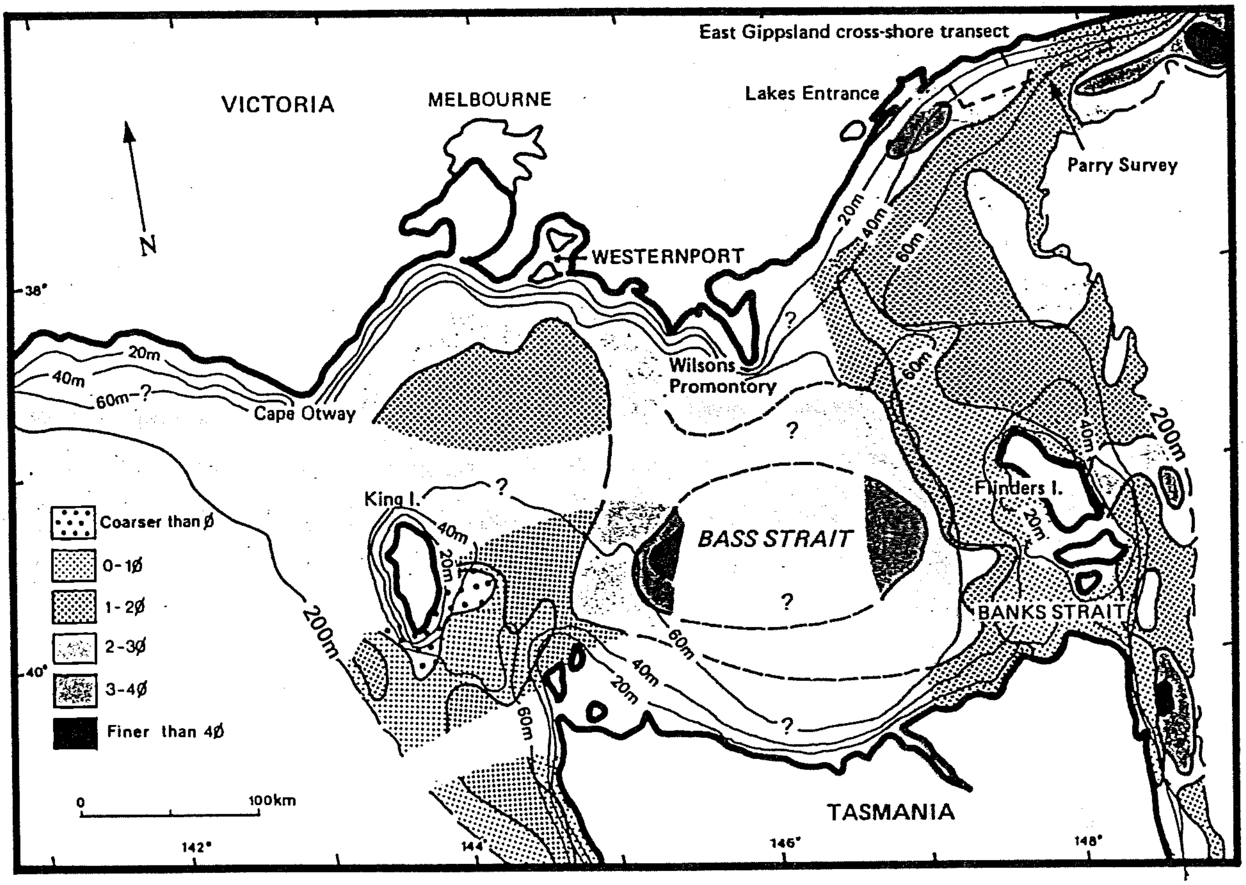

Fig. 5.1 Surface sediments in Bass Strait (after Jones and Davies, 1983)

APPENDICES

APPENDIX 1

The Link between Sediments and Hydrodynamics in Bass Strait

Sediment grain sizes in Bass Strait, southern Australia, vary widely across the strait. When compared to a calibrated numerical hydrodynamic model of the tidal circulation, the grain size variation was found to correspond with tidal current intensity. The velocity for sediment erosion coincided with the maximum tidal current. The results show that current strength is the dominant factor determining the nature of the modern sea bed throughout Bass Strait.

Background

As part of VIMS' sediment transport and hydrodynamic research programs, the Institute undertook to examine the link between sediment grain sizes and physical factors in Bass Strait. Several bed sediment sampling programs had been conducted in Bass Strait. However, the researchers had no information about the magnitude of the tidal currents, making it difficult to hypothesise about the mechanisms responsible for the differences in bed types.

A program of numerical modelling was initiated as part of a wider study to investigate the interaction of waves and currents on the continental shelf. An extended version of the VIMS' Bass Strait hydrodynamic model was developed.

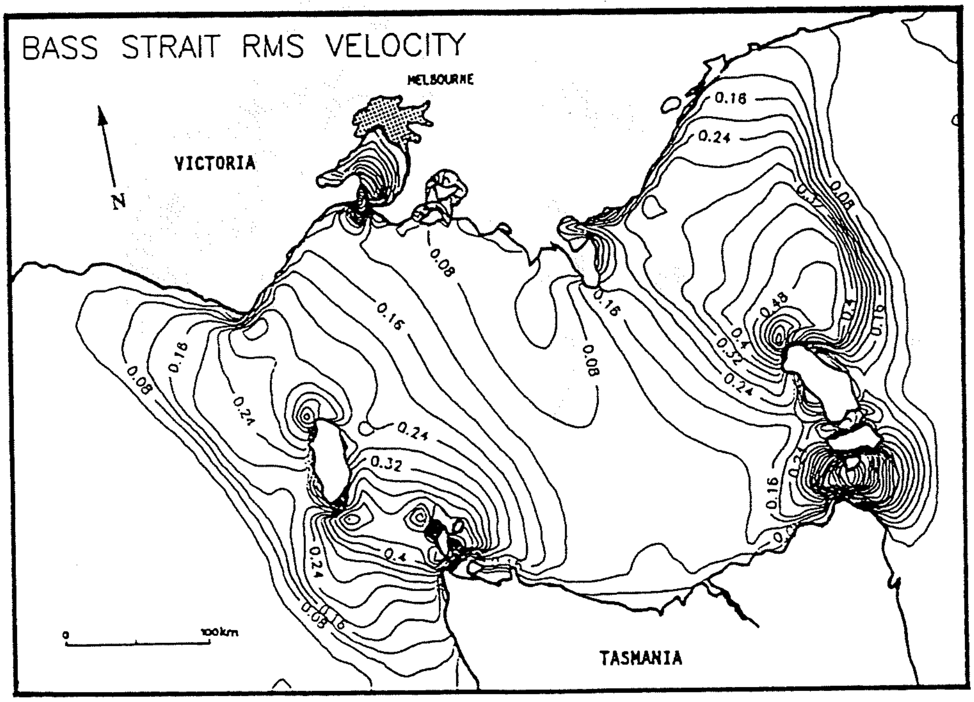

Figure 1: Root-mean-square M2 vertically averaged tidal current speeds in Bass Strait

Results

A wide range of tidal current speeds was depicted by the model. Figure 1 shows the root-mean-square current speeds for the dominant M_2 tidal constituent. The tides flood into both sides of Bass Strait simultaneously and then ebb from both sides about 6 hours later. Thus, fast currents occur in the two entrances to the strait where the constriction and the tidal prism is largest. The two incoming streams meet near central Bass Strait and the current intensities are small in the central regions.

While there are some exceptions, the nature of the sea bed (Fig. 2) exhibits a clear correspondence to the tidal currents across Bass Strait. First the north/south transects through King and Flinders Islands are characterised by the coarsest sediments and fastest currents. Second, central Bass Strait is muddy where RMS currents are slow. Third, finer sediments along the Gippsland shoreline reflect a reducing current strength to the east. Fourth, grain size contours and current contours are approximately aligned on the eastern side of Bass Strait.

Notably, measurements by VIMS in east Gippsland show the expected result that waves play a much larger role in depths under about 40 m. The wave effect would go deeper on the exposed west coast where longer period and larger waves characterise the local wave climate.

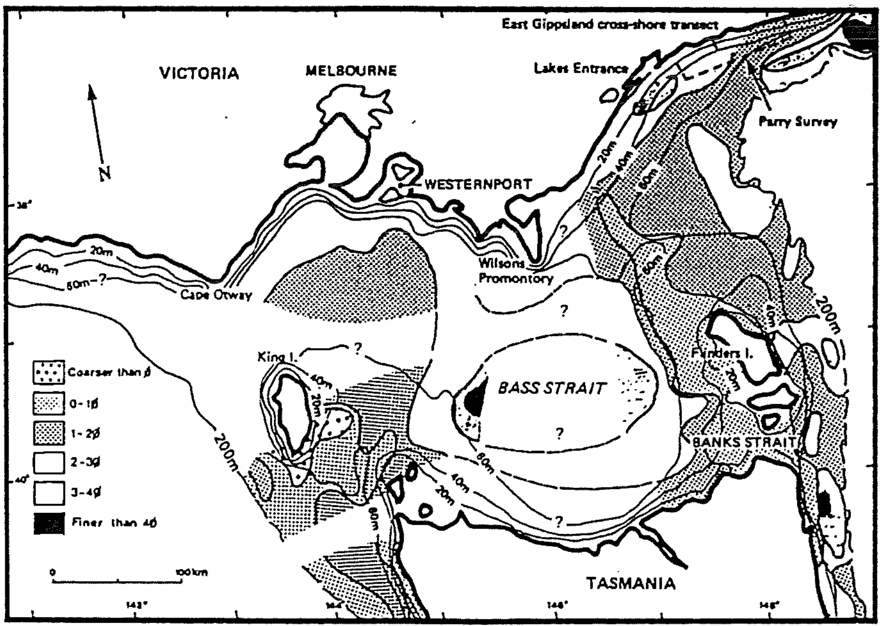

Figure 2: Distribution of mean grain size in Bass Strait

For further information contact:
Dr Kerry Black, Head of the Research and Consulting Division
Victorian Institute of Marine Sciences
23 St. Andrews Place, East Melbourne, Victoria, 3002
Telephone (03) 651 1998, Facsimile (03) 651 1702, Email vims@peg.apc.org

APPENDIX 2

MODEL EQUATIONS

The model 3DD is a layered extension, to include the vertical dimension, of the mean-vertically averaged model 2DD (Black, 1983). The 3-dimensional equations are,

$$\frac{\partial u}{\partial t}+\frac{u\partial u}{\partial x}+\frac{v\partial u}{\partial y}+\frac{w\partial u}{\partial z}-fv=-\frac{g\partial \varsigma}{\partial x}-\frac{1\partial p}{\rho\partial x} \qquad \text{(A2.1)}$$

$$+A_H\left(\frac{\partial^2 u}{\partial x^2}+\frac{\partial^2 u}{\partial y^2}\right)+\frac{\partial}{\partial z}\left(N_z\frac{\partial u}{\partial z}\right)$$

$$\frac{\partial v}{\partial t}+\frac{u\partial v}{\partial x}+\frac{v\partial v}{\partial y}+\frac{w\partial v}{\partial z}+fu=-\frac{g\partial \varsigma}{\partial y}-\frac{1\partial p}{\rho\partial y} \qquad \text{(A2.2)}$$

$$+A_H\left(\frac{\partial^2 v}{\partial x^2}+\frac{\partial^2 v}{\partial y^2}\right)+\frac{\partial}{\partial z}\left(N_z\frac{\partial v}{\partial z}\right)$$

$$w=-\frac{\partial}{\partial x}\int_{-h}^{z} u\,dz-\frac{\partial}{\partial y}\int_{-h}^{z} v\,dz \qquad \text{(A2.3)}$$

t is the time, u, v are velocities in the x,y directions respectively, w the vertical velocity in the z direction (positive upward) at the top of each layer, h the depth, g the gravitational acceleration, ε the sea level above a horizontal datum, f the Coriolis parameter, P the pressure, A_H the horizontal eddy viscosity coefficient, and N_z the vertical eddy viscosity coefficient.

The pressure at depth z is

$$P=P_{atm}+g\int_{z}^{0}\rho\,dz \qquad \text{(A2.4)}$$

where P_{atm} is the atmospheric pressure. The conservation equations for temperature and salinity may be written as

$$\frac{\partial T}{\partial t}+\frac{u\,\partial T}{\partial x}+\frac{v\partial T}{\partial y}+\frac{w\partial T}{\partial z}=\frac{\partial}{\partial z}\left(K_z\frac{\partial T}{\partial z}\right) \qquad \text{(A2.5)}$$

$$+K_H\left(\frac{\partial^2 T}{\partial x^2}+\frac{\partial^2 T}{\partial y^2}\right)$$

$$\frac{\partial S}{\partial t}+\frac{u\,\partial S}{\partial x}+\frac{v\,\partial S}{\partial y}+\frac{w\,\partial S}{\partial z}=\frac{\partial}{\partial z}\left(K_z\frac{\partial S}{\partial z}\right) \qquad \text{(A2.6)}$$

$$+\left(K_H\frac{\partial^2 S}{\partial x^2}+\frac{\partial^2 S}{\partial y^2}\right)$$

where T is temperature, S is salinity, and K_H, K_Z are the horizontal and vertical coefficients of eddy diffusivity.

Using the temperature and salinity, the density is computed according to an equation of state of the form,

$$\rho=\rho(T,S,z) \qquad \text{(A2.7)}$$

Surface boundary conditions at z=0 are

$$\rho N_z\frac{\partial u}{\partial z}=\tau^s_x \qquad \rho N_z\frac{\partial v}{\partial z}=\tau^s_y \qquad \frac{\partial \varepsilon}{\partial t}+u\frac{\partial \varepsilon}{\partial x}+v\frac{\partial \varepsilon}{\partial y}=w^s \ \text{(A2.8)}$$

where τ^s_x, τ^s_y denotes the components of wind stress and

$$\tau^s_x=\rho_a\,\gamma\,|W|\,W_x/\rho \qquad \tau^s_y=\rho_a\,\gamma\,|W|\,W_y/\rho \qquad \text{(A2.9)}$$

ρ is the water density, W the wind speed at 10 m above sea level while W_x and W_y are the x and y components, γ is the wind drag coefficient, ρ_a the density of air.

Surface boundary conditions for temperature and salinity are,

$$\rho N_z\frac{\partial S}{\partial z}=S_1 \qquad \rho N_z\frac{\partial T}{\partial z}=T_1 \qquad \text{(A2.10)}$$

where

$$S_1=S(0)\,(E_1-P_1)/\rho \qquad \text{(A2.11)}$$

$$T_1=Q/c$$

and S(0) is the surface salinity, E_1 is the net evaporation, P_1 is the net precipitation mass flux of fresh water, Q is the net ocean heat flux and c is the water heat capacity.

At the sea bed, z = -h, we have

$$\rho N_z \frac{\partial u}{\partial z} = \tau_x^h \qquad \rho N_z \frac{\partial v}{\partial z} = \tau_y^h \qquad \text{(A2.12)}$$

where τ_x^h, τ_y^h denotes the components of bottom stress. Applying a quadratic law at the sea bed,

$$\tau_x^h = g u_h (u_h^2 + v_h^2)^{1/2} / C^2 \qquad \text{(A2.13)}$$

$$\tau_y^h = g v_h (u_h^2 + v_h^2)^{1/2} / C^2$$

with u_h, v_h being the bottom currents and C is Chezy's C. For a logarithmic profile,

$$C = 18 \log_{10}(0.37\, h/z_o) \qquad \text{(A2.14)}$$

where z_o is the roughness length.

Also,

$$\frac{\partial S}{\partial z} = 0 \qquad \frac{\partial T}{\partial z} = 0 \qquad w_h = -u_h \frac{\partial h}{\partial x} - v_h \frac{\partial h}{\partial y} \qquad \text{(A2.15)}$$

The form of the horizontal eddy viscosity term results when the depth is presumed constant before taking the derivative of the horizontal shear stresses. The term, as presented, behaves as a velocity smoothing algorithm. The horizontal eddy viscosity coefficient is a variable in space in the model.

A staggered finite difference grid is utilised similar to that applied by Leendertse and Liu (1975) which places the v and u components on "north and south" walls respectively. w is located in the centre of the "top" wall. The sea level replaces w in the top layer. The solution is found by time stepping with an explicit scheme.

APPENDIX 3

MODEL DESCRIPTION

A general description of the model's capabilities follows.

Model output

The model outputs,

- current speeds and directions,
- sea levels, and,
- density, temperature and salinity structure.

Model features

Portability and applicability to new locations is achieved by,

- including all of the important terms in the momentum equation for both deep and shallow water cases,
- including a flooding and drying capability for simulation of inter-tidal zones such as sand banks in estuaries, and,
- providing a wide range of open boundary options, e.g. currents, sea levels, volumes, radiation conditions and sponges.

The model is easy to use while retaining a broad range of options. For example,

- 3DD can be operated in 2 or 3 dimensions using the same input files in both cases, thereby ensuring an effortless transition,
- the procedures to specify the open boundaries are both simple to use and comprehensive,
- continuity of style is maintained throughout the model and the support software,
- 3DD is fully coupled to a dispersal, sediment transport, oil spill and wave refraction model, and,
- the model is supported by a range of software tools for data input, model output manipulation and graphical presentation.

Enhanced characteristics of the model are,

- a boundary slip parameter eliminates the problem of excessive damping of currents in narrow channels due to horizontal diffusion,
- third-order accurate derivative approximations eliminate grid-scale zig-zagging,
- the inter-tidal flooding and drying scheme prevents the development of velocity spikes on the sand banks when flooding first occurs,
- an effective depth formulation prevents excessive frictional resistance in very shallow water,
- a body force can be applied to simulate large-scale pressure gradients associated with coastal trapped waves, other continental shelf waves or geostrophic gradients, for example,
- a variety of vertical eddy viscosity formulations are selectable including a level 2 1/2 turbulence closure scheme and Richardson Number dependant eddy viscosities and diffusivities,
- barometric pressure and wind conditions, entered as time series from a number of locations, will be interpolated by the model,
- enhanced bed friction due to wave/current interaction can be selected,
- hot starts are possible so that new runs can commence at any time during a prior simulation,
- provides for nested simulations,
- bathymetry can be represented on the cell walls (rather than cell mid-points) thereby maximising bathymetric resolution without increasing CPU requirements,
- advection/diffusion can be treated by 3DD using a Eulerian scheme and/or these simulations can be undertaken with a coupled Lagrangian scheme,
- presents model results to the screen at run-time as a diagnostic aid to allow rapid assessment of model behaviour, the
- the model is operated by an information file which is structured for easy assimilation in a menu format.

APPENDIX 4

MODEL SUPPORT SOFTWARE

3DD has a range of support software routines for preparation of input files, extraction of results from the model output file and for graphics. Described here is a group of programs which are used commonly. Program operation is specified at run time, so only their purpose is given here.

Input support routines

BATH is used to generate the bathymetry, friction, eddy viscosity or boundary slip files for input to 3DD. Options for data manipulation as well as data entry are provided.

BNDGEN assists with the generation of boundary files. Time series or sinusoidal boundary conditions can be expressed in arbitrary or actual time from tidal constituent amplitudes and phases. The boundary phases can be linearly interpolated between known locations or the model will calculate phases from the grid of depths generated for 3DD. BNDGEN is sufficiently general to cover most practical applications.

Nested model simulations

2DDBND is the key "nested grid" program which extracts boundary information from a coarse grid run and places the information in formatted boundary files for finer grid simulations. Boundary sea levels or velocities can be treated.

Manipulation of model output files

3DBACK will extract and manipulate selected sections of the model output file. For example, it can be used to link two model output files together after removing the header information from the second file. Alternatively, 3DBACK will extract a section from a long model output file.

3DASCI converts the binary model output files to ASCII and vice versa. The program is mostly used to transmit files between computers which have different FORTRAN compilers and binary codes.

Extraction of information from the model output file

3DFORM will generate time series and plot files from the model output file. The routine will extract (a) time series of sea level, velocity and flow direction, or of sea gradients; (b) files for contouring of sea level etc.; (c) files for vector plotting of velocity maps; or (d) time series of the terms in the momentum equation for careful scrutiny.

DDFORM extracts bathymetry contours from a model bathymetry file. With program CONEXT, the contours can be added to vector plots created with 3DDVEC.

3DDPRT generates a printable ASCII file of sea levels etc. for model output inspection. This routine creates a neatly formatted file for inspection at the terminal or for printing. The user can select specific regions or times from the model output and information contained in the file is optional.

Graphics support

3DD_SUPPORT is a full supporting, interactive graphics package written specifically for 3DD within the MATLAB environment. Projections, contours, vector plots and surfaces can be plotted for all model variables. Movies can be generated to view a full simulation.

3DDVEC creates vector plots of flow patterns. This program gives options on scaling of both the map size and the vectors and includes bar and numerical scales. Land may be optionally shaded and up to 6 heading lines can be entered. Bathymetry contours may also be added to the plot.

CONTOURS and 3-dimensional projections are produced with the software package GOLDEN SOFTWARE (copyright), P.O. Box 281, Golden, Colorado, 80402, USA, or with the more sophisticated menu-driven package "TECPLOT - Interactive plotting for scientists and engineers" when very high quality output is required.

LINPLT and **MULPLT** are used to graph model output time series, when rapid output is needed. More sophisticated graphs are created with TECPLOT using the program 3DFORM to create input time series with the appropriate format.

Analysis of model results

ELRESI analyses the model output to calculate residual velocities, residual distances, time-averaged kinetic energy levels and root mean square speeds over selected averaging periods. Results are written to output files with formats identical to the model output file for direct application in the support software.

3DPERC performs vector subtraction or addition of model output files. This may be used for comparison of flows after changing model inputs such as bathymetry. For example, the currents around various port designs may be tested and compared using 3DPERC.

3DDAVG extracts averages and extreme values of model output variables including salinity, temperature and density.

APPENDIX 5

A NUMERICAL SCHEME FOR DETERMINING TRAJECTORIES IN PARTICLE MODELS

Source: Bradbury, R.H. (ed.) (1988) Lecture Notes in Biomathematics 88. Acanthaster and the Coral Reef: A Theoretical Perspective. Proceedings of a Workshop held at the Australian Institute of Marine Science, Townsville, Aug. 6-7, 1988. Springer-Verlag.

KERRY P. BLACK
Victorian Institute of Marine Sciences, Melbourne, Victoria 3002

AND

STEPHEN L. GAY
Australian Institute of Marine Science, Townsville, Queensland 4810

Abstract. A scheme for modelling of trajectories of particles in Lagrangian advection/dispersion models is presented. The second-order accurate method is numerically tractable and eliminates the tendency for particles to spiral outwards on curved streamlines. The method is compared with Euler and Taylor series solutions.

INTRODUCTION

With the increase in modern computing capacity (e.g. faster and/or parallel processors), a resurgence in interest in particle tracking techniques in oceanography is evident. The particle models operate by tracking a large number of individual particles as they traverse a velocity grid associated with a finite difference hydrodynamic model. These Lagrangian particle models have been applied recently to diverse phenomena such as the dispersion of sewage and larvae on Australia's Great Barrier Reef (Black, 1988; Dight *et al.*, 1988), abalone larval dispersal (McShane *et al.*, 1988) and estuarine circulation problems (Hunter, 1987).

Lagrangian particle methods, although requiring a greater computer capacity, eliminate the smearing of concentrations (numerical viscosity) throughout the grid which occurs with an Eulerian scheme, particularly at sharp concentration gradients. This important advantage will often be more important than the cost of extra computer time (Hunter, 1987).

For tracking particles in a grid-cell (where orthogonal velocities U and V are known and derivatives U_x, U_y, V_x, and V_y can be easily calculated) it was found that for circular orbits the use of a second order Taylor's scheme resulted in the trajectories slowly spiralling away from the centre. By slightly varying this simple scheme the problem was overcome. This paper presents a method to track particles which is truly second-order accurate, in the sense that particles will remain on the arc of a circle indefinitely, excluding round-off error.

NUMERICAL SCHEME FOR DETERMINING TRAJECTORIES

Consider the following ordinary differential equation:

$$\frac{dx}{dt} = u(x,t) \tag{1}$$

Starting at x_0, t_0 the first-order estimate of the next value of x after a time step δt is:

$$x = x_0 + u(x_0,t_0)\,\delta t \tag{2}$$

This scheme is known as Euler's method.

Higher order methods take account of the fact that u(x,t) varies during the length of the trajectory. There are numerous higher order schemes used to track trajectories, some of the more well known are Runge-Kutta, Taylor, Midpoint, Trapezoidal and Milne's (Atkinson, 1978). The scheme chosen by a modeller depends on the desired accuracy of the trajectories, the type of equations and computational constraints. Of the schemes which presently exist, the most suitable for our purposes appeared to be Taylor's scheme.

To second-order, Taylor's scheme finds $\delta x/\delta t$ as the average of the initial and final values of u. Putting $h=\delta t$, the equation for tracking a particle may be written as:

$$\frac{\delta x}{\delta t} = 1/2\,(u(x_0,t_0) + u(x_0 + h\frac{\delta x}{\delta t}, t_0 + h)) \tag{3}$$

Using Taylor's Theorem $u(x_0 + h\,\delta x/\delta t, t_0 + h)$ can be approximated as:

$$u(x_0,t_0) + h\,\frac{\delta u}{\delta t}\,(x_0 + h\frac{\delta x}{\delta t}, t_0 + h) \tag{3a}$$

$$= u + h\frac{\delta x}{\delta t}u_x + h\,u_t \tag{3b}$$

where u implies $u(x_0,t_0)$

Hence, Eqn (1) becomes:

$$\frac{\delta x}{\delta t} = u + 1/2\,h\left(\frac{\delta x}{\delta t}u_x + u_t\right) \qquad (4)$$

In the standard Taylor's scheme, Eqn (1) is used to replace $\delta x/\delta t$ on the right hand side of the above equation with $u(x_o, t_o)$. Hence, Eqn (4) becomes:

$$\frac{\delta x}{\delta t} = u + 1/2\,h\,(u_t + u\,u_x) \qquad (5)$$

In our scheme however, $\delta x/\delta t$ of the right hand side of Eqn (3) is assumed to be the same as the left hand side. In this way $\delta x/\delta t$ is taken as being the slope of the trajectory rather than the slope at the start of the trajectory. Therefore, it is slightly more accurate.

Rearrangement of Eqn (4) now yields:

$$\frac{\delta x}{\delta t} = \frac{u + 1/2\,h\,u_t}{1 - 1/2\,h\,u_x}$$

For tracking of particles in 2-dimensions, the equations are slightly more complicated.

$$\frac{\delta x}{\delta t} = u(x,y,t) \qquad (6)$$

$$\frac{\delta y}{\delta t} = v(x,y,t) \qquad (7)$$

Applying Taylor's Theorem causes the tracking equations to become:

$$\frac{\delta x}{\delta t} = u + 1/2\,h\left(\frac{\delta x}{\delta t}u_x + \frac{\delta y}{\delta t}u_y + u_t\right) \qquad (8)$$

$$\frac{\delta y}{\delta t} = v + 1/2\,h\left(\frac{\delta x}{\delta t}v_x + \frac{\delta y}{\delta t}v_y + v_t\right) \qquad (9)$$

substituting $\delta x/\delta t$ with u and $\delta y/\delta t$ with v under the standard Taylor Scheme yields:

$$\delta x = (u + 1/2\,h\,(u\,u_x + v\,u_y + u_t))\,h \qquad (10)$$

$$\delta y = (v + 1/2\,h\,(u\,v_x + v\,v_y + v_t))\,h \qquad (11)$$

Using our scheme and denoting $\delta x/\delta t$ by $\bar{u}$, $\delta y/\delta t$ by $\bar{v}$, and $u + \frac{hu_t}{2}$ by u', causes Eqns (8) and (9) to become:

$$\bar{u} = u' + 1/2\, h\, (\bar{u}\, u_x + \bar{v}\, u_y)$$

$$\bar{v} = v' + 1/2\, h\, (\bar{u}\, v_x + \bar{v}\, v_y)$$

Solving these equations simultaneously for $\bar{u}$ and $\bar{v}$ and replacing $\bar{u}$ and $\bar{v}$ gives the changes in x and y as:

$$\delta x = \frac{(\, u' + (u_y v' - v_y u')\, h/2\,)\, h}{(1 - u_x h/2)\, (1 - v_y h/2) - u_y\, v_x\, h^2/4} \tag{12}$$

$$\delta y = \frac{(\, v' + (v_x u' - u_x v')\, h/2\,)\, h}{(1 - u_x h/2)\, (1 - v_y h/2) - u_y\, v_x\, h^2/4} \tag{13}$$

The reasons for adopting this scheme as compared to Euler's scheme and Taylor's scheme will now be considered.

Consider what would happen if u and v were known to satisfy:

$$u = \Omega y$$
$$v = -\Omega x$$

A particular trajectory of a particle has a solution

$$x = \sin\, (\Omega\, t)$$
$$y = \cos\, (\Omega\, t)$$

Hence, this trajectory defines a circle of radius 1 and angular frequency Ω

If Euler's scheme is adopted starting at (0,1) then

$$u = \Omega$$
$$v = 0$$

after time step h,

$$\delta x = \Omega h$$
$$\delta y = 0$$

Therefore, $x = \Omega h$
$y = 1$

The value of x^2+y^2 at $[(x_0+\delta x),(y_0+\delta y)]$ is $1+\Omega^2 h^2$. So the trajectory spirals away from the centre.

Furthermore, it can be shown that by using this method on the above equations, all of the trajectories will spiral away from the centre in a similar manner to this example. Clearly then, Euler's method is not adequate, particularly if the purpose of monitoring trajectories is to determine whether particles can be retained near the same area.

Consider now what happens if Taylor's scheme is adopted.

Again $u=\Omega$, $v=\Omega$ but also $u_x=0$, $u_y=\Omega$, $v_x=-\Omega$, $v_y=0$, $u_t=0$, $v_t=0$.

Hence, Eqns (10) and (11) become:

$$\Omega x = \Omega h$$

$$\Omega y = -1/2\,\Omega^2 h^2$$

So, the new value of x^2+y^2 is:

$$(\Omega h)^2 + (1 - 1/2\,\Omega^2 h^2)^2$$

$$= 1 + 1/4\,\Omega^4 h^4$$

So, in this case, the particle again spirals away from the centre. However, if $\Omega h < 1$, which is normally the case, the rate of spiralling is much slower than for Euler's scheme.

Using Eqns (12) and (13) however gives:

$$\delta x = \frac{\Omega h}{1 + \Omega^2 h^2/4}$$

$$\delta y = \frac{-\Omega^2 h^2/2}{1 + \Omega^2 h^2/4}$$

x^2+y^2 now equals 1.

In this case, no spiralling occurs.

CONCLUSIONS

An accurate solution to second-order is presented for application to particle models which utilize velocities from the finite difference grid of a hydrodynamic model. The method eliminates the outward spiral error on curved streamlines which occurs in Euler's or Taylor's scheme solutions.

Acknowledgements. The authors would like to thank John Hunter and Lance Bode for their comments on this manuscript. The work was jointly funded by the Crown-of-Thorns Starfish Advisory Committee and the Victorian Institute of Marine Sciences.

REFERENCES

Atkinson, K.E. (1978) An Introduction to Numerical Analysis, Publisher; John Wiley and Sons, New York.

Black, K.P. (1988) The relationship of reef hydrodynamics to variations in numbers of planktonic larvae on and around coral reefs. Proceedings 6th International Coral Reef Symposium 2, 125-130.

Dight, I.J., James, M.K. & Bode, L. (1988) Models of larval dispersal within the central Great Barrier Reef: patterns of connectivity and their implications for species distributions.
Proceedings 6th International Coral Reef Symposium 3, 217-224.

Hunter, J.R. (1977) The application of Lagrangian particle-tracking techniques to modelling of dispersion in the sea. In: J. Noye (ed) Numerical Modelling: Applications to Marine Systems. Elsevier Science Pub. pp 257-270.

McShane, P.D., Black, K.P., & Smith, M.G. (1988) Recruitment processes in *Haliotis rubra* (Mollusca: Gastropoda) and regional hydrodynamics in south-eastern Australia imply localised dispersal of larvae. Journal of Experimental Marine Biology and Ecology 124, 175-203.